

BINAPHTHOLATE AND OCTAHYDROBINAPHTHOLATE
RARE-EARTH METAL CATALYSTS FOR
ASYMMETRIC HYDROAMINATION OF ALKENES

by

HIEP NHU NGUYEN

A dissertation submitted to the

School of Graduate Studies

Rutgers, The State University of New Jersey

In partial fulfillment of the requirements

For the degree of

Doctor of Philosophy

Graduate Program in Chemistry and Chemical Biology

Written under the direction of

Professor Alan Goldman

And approved by

New Brunswick, New Jersey

OCTOBER 2018

Abstract of Dissertation

Binaphtholate and octahydrobinaphtholate rare-earth metal catalysts for
asymmetric hydroamination of alkenes

By Hiep Nhu Nguyen

Dissertation Director: Professor Alan Goldman

In this thesis we summarize our efforts towards the development of binaphtholate and octahydrobinaphtholate rare-earth metal complexes for asymmetric hydroamination of aminoalkenes, as well as kinetic resolution of chiral aminoalkenes *via* hydroamination. These complexes were also found to be efficient catalysts for the asymmetric intermolecular hydroamination of unactivated alkenes with simple amines. Catalytic screening results indicated that increasing steric bulk of the silyl-substituents in the ligand and decreasing ionic radius of the rare earth metal helped increase catalytic activity and enantioselectivity of the hydroamination product. Consistent with our previous findings, the hydroamination reaction catalyzed by these complexes showed zero order rate dependence on substrate concentration and first order rate dependence on catalyst concentration. In most cases, octahydrobinaphtholate complexes (*R*)-[Ln{L}(*o*-C₆H₄-CH₂NMe₂)(Me₂NCH₂Ph)] (Ln = Y, Lu; L = 3,3'-bis(triphenylsilyl)-5,5',6,6',7,7', 8,8'-octahydro-1,1'-binaphthyl-2,2'-diolate (**50a-Ln**); L = 3,3'-bis(*tert*-butyldiphenyl silyl)-5,5',6,6',7,7',8,8'-octahydro-1,1'-binaphthyl-2,2'-diolate (**50b-Ln**); and L = 3,3'-bis(cyclohexyldiphenylsilyl)-5,5',6,6',7,7',8,8'-octahydro-1,1'-binaphthyl-2,2'-diolate

(**50c-Ln**) were shown to be more reactive and more enantioselective catalysts for asymmetric hydroamination than their related binaphtholate complexes (*R*)-[Ln{L}(*o*-C₆H₄CH₂NMe₂)(Me₂NCH₂Ph)] (Ln = Y, Lu; L = 3,3'-bis(triphenylsilyl)-1,1'-binaphthyl-2,2'-diolate (**19a-Ln**); L = 3,3'-bis(*tert*-butyldiphenylsilyl)-1,1'-binaphthyl-2,2'-diolate (**39b-Ln**); and L = 3,3'-bis(cyclohexyldiphenylsilyl)-1,1'-binaphthyl-2,2'-diolate (**39c-Ln**)). Turnover frequencies as high as 2400 h⁻¹ were achieved for 2,2-diphenyl-pent-4-enylamine using (*R*)-**50c-Y** and enantiomeric excess of up to 98% could be obtained in the cyclization of *C*-(1-allylcyclohexyl)-methylamine using (*R*)-**50c-Lu** at room temperature. The stability of binaphtholate and octahydrobinaphtholate rare earth metal catalysts at elevated temperature of up to 150 °C extended their usages for asymmetric intermolecular hydroamination of simple amines and unactivated alkenes, forming exclusively Markovnikov amine products. (*R*)-**50a-Y** displayed the high efficiency for catalytic addition of benzylamine to 4-phenyl-1-butene at 110 °C, affording (*R*)-*N*-benzyl-4-phenylbutan-2-amine, with enantiomeric excess of up to 67%. The complexes were also suitable for kinetic resolution of chiral α -substituted aminoalkenes *via* catalytic asymmetric hydroamination. Kinetic resolution factors *f* of up to 90 and equilibrium constant K^{dias} of up to 5.1, indicating a Curtin-Hammett pre-equilibrium favoring the matching combination of substrate and complex, were observed for 1-methylpent-4-enylamine using (*R*)-**39c-Y** at 25 °C. The 2,5-disubstituted pyrrolidines were formed in 7:1 to \geq 50:1 *trans* diastereoselectivity, depending on the size of the α -substituent of the aminoalkene. Kinetic studies of (*S*)-1-methylpent-4-enylamine provided an access to activation parameters for matching pair (using (*R*)-**39c-Y**), $\Delta H^\ddagger = 43(5)$ kJ mol⁻¹, $\Delta S^\ddagger = -136(17)$ J K⁻¹ mol⁻¹) and for mismatching pair (using (*S*)-**39c-Y**), *trans* diastereomer,

$\Delta H^\ddagger = 45(2) \text{ kJ mol}^{-1}$, $\Delta S^\ddagger = -160(7) \text{ J K}^{-1} \text{ mol}^{-1}$; *cis* diastereomer, $\Delta H^\ddagger = 54(4) \text{ kJ mol}^{-1}$, $\Delta S^\ddagger = -130(14) \text{ J K}^{-1} \text{ mol}^{-1}$).

Dedication

To my parents, Viet Nguyen and Ty Huyen, for their constant and unconditional support

and

To my dear wife, Linh Huynh, for her encouragement and endless love.

Acknowledgements

I would like to thank Professor Kai Hultzsich for allowing me to join his research group and to work on very exciting projects. His endless patience and generous support have made my life in graduate school much easier and more enjoyable. In the Hultzsich group, I have gained both knowledge and skills to be an independent research chemist as well as to be a better teacher.

I would also like to thank Professor Alan Goldman, Professor Ralf Warmuth, and Professor Lawrence Williams for being on my thesis defense committee and providing very helpful comments over my research.

Dr. Nagarajan Murali and Dr. Seho Kim are acknowledged for assisting with NMR studies.

I want to express my warm thanks to current and former members of the Hultzsich group: Hyeunjo Lee, Dr. Anandarup Goswami, Dr. Lisa Hurd, John Soltys, particularly Dr. Alexander Reznichenko and Boyan Lazarov for their friendly help over the years at Rutgers. I also thank Dr. Agnieszka Nawara-Hultzsich for correcting the experimental section.

I would like to thank my brothers, sisters, and parents for their continuous support. Last but not least, a special thanks to my wife for her encouragement and endless love.

Table of Contents

	Page
Abstract of the Dissertation	ii
Dedication	v
Acknowledgement	vi
Table of Contents	vii
List of Tables	xi
List of Figures	xiii
List of Schemes	xvi
List of Abbreviation	xix
Chapter 1: Introduction to the Catalytic Hydroamination of Alkenes	1
1.1 General Introduction	1
1.2 Intramolecular Hydroamination of Aminoalkenes	3
1.2.1 Rare-Earth Metals Catalyzed Hydroamination	3
1.2.1.1 Lanthanocene Catalyzed Hydroamination	3
1.2.1.2 Non-Metallocene Catalyzed Asymmetric Hydroamination	11
1.2.2 Group 4 Metals Catalyzed Hydroamination	18
1.2.3 Late Transition Metals Catalyzed Hydroamination	22
1.2.4 Kinetic Resolution of Chiral Aminoalkenes via Asymmetric Hydroamination	25
1.3 Intermolecular Hydroamination	27
1.3.1 Intermolecular Hydroamination with Rare-Earth Metals	27
1.3.2 Intermolecular Hydroamination with Late Transition Metals	28

1.4 Significance and Aim of the Study	34
Chapter 2: Binaphtholate Rare Earth Metal Complexes	36
2.1 Introduction	36
2.2 Synthesis of 3,3'-Bis(alkylarylsilyl)-Substituted Binaphtholate Ligands	38
2.3 Synthesis and Characterization of Binaphtholate Rare Earth Metal Complexes	41
Chapter 3: Octahydrobinaphtholate Rare Earth Metal Complexes.....	47
3.1 Introduction	47
3.2 Synthesis of 3,3'-Bis(alkylarylsilyl)-Substituted Octahydrobinaphthol Ligands	48
3.3 Synthesis and Characterization of Octahydrobinaphtholate Rare Earth Metal Complexes.....	52
Chapter 4: Asymmetric Intramolecular Hydroamination of Aminoalkenes	56
4.1 Introduction	56
4.2 Catalytic Results and Discussion	57
4.2.1 Asymmetric Intramolecular Hydroamination of Primary Amines	57
4.2.2 Asymmetric Intramolecular Hydroamination of Secondary Amines..	73
4.2.3 Kinetic Studies of Hydroamination/Cyclization	75
4.3 Summary	78
Chapter 5: Asymmetric Intermolecular Hydroamination of Unactivated Alkenes with Simple Amines	79
5.1 Introduction	79

5.2 Catalytic Results and Discussion	80
5.2.1 Binaphtholate Rare-Earth Metal Catalyst Evaluation.....	80
5.2.2 Octahydrobinaphtholate Rare-Earth Metal Catalyst Evaluation..	85
5.2.3 Mechanistic Studies	89
5.3 Summary	92
Chapter 6: Kinetic Resolution of Chiral Aminoalkenes <i>via</i> Hydroamination	93
6.1 Introduction	93
6.2 Kinetic Resolution of α -Substituted Aminopentenes	95
6.3 Stereomodel for the Kinetic Resolution of α -Substituted Aminopentenes....	
.....	109
6.4 Conclusions	112
Chapter 7: Experimental Section	114
7.1 Synthesis of Chlorosilanes	115
7.2 Synthesis of Binaphthol Ligands	120
7.3 Synthesis of Octahydrobinaphthol Ligands	127
7.4 Synthesis of Rare Earth Metal Complexes	131
7.5 Synthesis of Substrates	148
7.6 Procedures for Catalytic Hydroamination and Kinetic Resolution	152
7.7 Procedures for Kinetic Resolution of α -Substituted Aminopentenes <i>via</i>	
Asymmetric Hydroamination	154
7.8 Procedures for Asymmetric Intermolecular Hydroamination.....	156
Chapter 8: References	162
Chapter 9: Appendix	168

Appendix A: ^1H , ^{13}C , and ^{19}F NMR Spectra	168
Appendix B: Kinetic Resolution of Aminoalkenes	207
Appendix C: Structures of Binaphtholate and Octahydrobinaphtholate Rare-Earth Metal Complexes	209
Appendix D: Substrates and Hydroamination/Cyclization Products.....	210

List of Tables

	Page
Table 1-1. Rate dependence on ionic radius, steric demand of the ancillary ligand, and ring size of hydroamination product, in the rare-earth metal catalyzed cyclization of aminoalkenes.....	5
Table 1-2. Lanthanocene-catalyzed asymmetric hydroamination/cyclization of aminoalkenes.....	9
Table 1-3. Non-metallocene-catalyzed asymmetric hydroamination of 2,2-dimethylpent-4-enylamine	14
Table 1-4. Binaphtholate- and aminodiolate-based rare-earth metal-catalyzed asymmetric hydroamination	16
Table 1-5. Catalytic kinetic resolution of aminoalkenes using binaphtholate rare-earth metal complexes	26
Table 1-6. Kinetic resolution parameters of aryl- and alkyl-substituted aminopentenes determined with (<i>R</i>)- 19a-Y	26
Table 2-1. ¹³ C NMR chemical shifts and ¹ J(Y,C) coupling constants of yttrium complexes.....	45
Table 3-1. Comparison of BINOL and H ₈ BINOL-based titanium catalysts in the asymmetric addition of alkylzinc and alkylaluminum reagents to aldehydes.....	48
Table 3-2. ¹³ C NMR chemical shifts and ¹ J(Y,C) coupling constants of yttrium complexes.....	55
Table 4-1. Asymmetric hydroamination of 51 catalyzed by the binaphtholate and octahydrobinaphtholate rare-earth metal complexes	59

Table 4-2. Catalytic evaluation of the hydroamination/cyclization of 53	62
Table 4-3. Catalytic evaluation of the hydroamination/cyclization of 55	65
Table 4-4. Catalytic evaluation for hydroamination/cyclization of 57	69
Table 4-5. Catalytic evaluation of the hydroamination/cyclization of aminohexene 59 and aminoheptene 61	71
Table 4-6. Catalytic evaluation of the hydroamination/cyclization of the 1,2- disubstituted alkene 63	73
Table 4-7. Catalytic evaluation for hydroamination/cyclization of secondary amines 65 and 67	74
Table 5-1. Asymmetric intermolecular hydroamination of unactivated alkenes with a primary amine using binaphtholate catalysts	82
Table 5-2. Asymmetric intermolecular hydroamination of unactivated alkene with primary amines using octahydrobinaphtholate catalysts	87
Table 6-1. Catalytic kinetic resolution of α -substituted 1-aminopent-4-enes....	97
Table 6-2. Large-scale preparation of enantiopure α -substituted aminopentenes <i>via</i> kinetic resolution using binaphtholate catalyst 39c-Y	103
Table 6-3. Kinetic resolution parameters of α -substituted aminopentenes.....	107

List of Figures

	Page
Figure 1-1. Dependence of rare-earth metals catalyzed hydroamination reaction rate on steric demand of the catalyst ligand framework	5
Figure 1-2. Chiral <i>ansa</i> -lanthanocene precatalysts for asymmetric hydroamination	7
Figure 1-3. Chiral lanthanocene complexes with extended “wing-span” and nonlinked chiral ytrocenes	8
Figure 1-4. Stereomodel for the observed absolute product configuration of pent-4-enylamine	10
Figure 1-5. Chiral biarylamido, amino(thio)phenylate and bisoxazolinato catalysts for asymmetric hydroamination	11
Figure 1-6. Binaphtholate and aminodiolate catalysts for asymmetric hydroamination	15
Figure 2-1. ¹ H NMR spectra of (<i>R</i>)- 39a -Y in C ₆ D ₆ at 25 °C and (<i>R</i>)- 39b -Y in C ₇ D ₈ at 0 °C	44
Figure 3-1. ¹ H NMR spectra of (<i>R</i>)- 50a -Y in C ₆ D ₆ at 6 °C.....	53
Figure 4-1. Binaphtholate and octahydrobinaphtholate rare-earth metal catalysts for asymmetric hydroamination	57
Figure 4-2. Turnover frequency (scatter chart) and enantioselectivity (column chart) profiles for the hydroamination of aminoalkene 51 catalyzed by binaphtholate and octahydrobinaphtholate rare-earth metal complexes	61

Figure 4-3. Turnover frequency (scatter chart) and enantioselectivity (column chart) profiles for the hydroamination of aminoalkene 53 catalyzed by binaphtholate and octahydrobinaphtholate rare-earth metal complexes	64
Figure 4-4. Temperature dependence of enantioselectivity in cyclization of 55 using (<i>R</i>)- 39c-Lu	66
Figure 4-5. Concentration of aminopentene 55 (0.2 mol L ⁻¹) versus time for the hydroamination/cyclization using (<i>R</i>)- 39c-Y (0.004 mol L ⁻¹) at variable temperatures in C ₆ D ₆ . The lines are drawn as a guide for the eyes	76
Figure 4-6. Rate versus catalyst concentration for the hydroamination of 55 ([subst.] ₀ = 0.2 mol L ⁻¹) using (<i>R</i>)- 39c-Y in C ₆ D ₆ at 25 °C.....	77
Figure 5-1. First order plot for the addition of benzylamine (0.33-0.42 mol L ⁻¹) to 4-phenyl-1-butene (5.0-6.3 mol L ⁻¹) using varying catalyst concentrations of (<i>R</i>)- 19a-Y [0.009 M (♦), 0.018 M (●), 0.025 M (×)] in tol-d ₈ at 150 °C	89
Figure 5-2. Dependency of <i>k</i> _{obs} on the concentration of (<i>R</i>)- 19a-Y in the addition of benzylamine to 4-phenyl-1-butene	90
Figure 5-3. Observed pseudo-first order rate constant vs. alkene concentration for the reaction of benzylamine [C ₀ = 0.17 M] with 4-phenyl-1-butene in the presence of (<i>R</i>)- 19a-Y [0.032 M] at 150 °C in C ₆ D ₆ . Linear correlation illustrates effective first order in alkene.....	90
Figure 6-1. Rare-earth metal complexes based on 3,3'-bis(alkylarylsilyl)-binaphtholate ligands	95
Figure 6-2. Plot of ln[(1- <i>C</i>)(1- <i>ee</i>) versus ln[(1- <i>C</i>)(1+ <i>ee</i>) for the kinetic resolution of 25a using the binaphtholate catalyst (<i>R</i>)- 39c-Y at 25 °C	101

Figure 6-3. Dependence of enantiomeric excess of recovered starting material on conversion in the kinetic resolution of **25a** with (*R*)-**39c-Y** at 25 °C. The line was fitted to a resolution factor $f = 89.7$ 102

Figure 6-4. Time dependence of the substrate concentration in the hydroamination of (*S*)-**25a** using (*R*)-**39c-Y** (matching pair; $[(S)\text{-}25a]_0 = 0.140$ mol L⁻¹, $[(R)\text{-}39c\text{-Y}] = 2.73$ mmol L⁻¹). The straight lines represent the least square linear regression 103

Figure 6-5. Time dependence of the substrate concentration in the hydroamination of (*S*)-**25a** using (*S*)-**39c-Y** (mismatching pair; $[(S)\text{-}25a]_0 = 0.140$ mol L⁻¹, $[(S)\text{-}39c\text{-Y}] = 2.73$ mmol L⁻¹). The straight lines represent the least square linear regression 104

Figure 6-6. A stack plot of ¹H NMR spectra of hydroamination products obtained with matching pair of (*S*)-**25a** and (*R*)-**39c-Y** and with mismatching pair of (*S*)-**25a** and (*S*)-**39c-Y**..... 105

Figure 6-7. *Trans/cis* ratio of the cyclization product of *rac*-**25a** using 2 mol% of (*R*)-**39c-Y** as a function of conversion 106

Figure 6-8. Eyring plot for the hydroamination/cyclization of (*S*)-**25a** using (*R*)-**39c-Y** (matching) and (*S*)-**39c-Y** (mismatching) 109

List of Schemes

	Page
Scheme 1-1. Proposed mechanism for the hydroamination/cyclization using rare-earth metal catalysts	6
Scheme 1-2. Epimerization of chiral lanthanocene complexes during the hydroamination reaction	8
Scheme 1-3. Zwitterionic oxazolinylborato yttrium catalyzed asymmetric hydroamination	17
Scheme 1-4. Hydroamination/cyclization of aminoalkenes using ionic and neutral zirconium catalysts	19
Scheme 1-5. Proposed mechanism for hydroamination/cyclization of primary aminoalkenes using group 4 metal catalysts	20
Scheme 1-6. Group 4 metal-mediated asymmetric hydroamination of primary aminoalkenes.....	21
Scheme 1-7. The activation modes of the substrate in the late transition metal-catalyzed hydroamination	22
Scheme 1-8. Rhodium catalyzed intramolecular hydroamination of primary and secondary aminoalkenes.....	23
Scheme 1-9. Rhodium-catalyzed asymmetric intramolecular hydroamination of aminoalkenes	24
Scheme 1-10. Catalytic cycle for hydroamination of vinyl arenes catalyzed by palladium-diphosphine complexes.....	29

Scheme 1-11. Nucleophilic attack of the aniline at the η^3 -aryl palladium intermediate.....	30
Scheme 1-12. Proposed mechanism for intermolecular hydroamination catalyzed by iridium.....	31
Scheme 1-13. Asymmetric hydroamination of aniline and norbornene catalyzed by Ir-diphosphine complexes.....	32
Scheme 1-14. Ir-catalyzed enantioselective intermolecular hydroamination of amides and sulfonamides with bicycloalkenes	33
Scheme 1-15. Ir-catalyzed intermolecular hydroamination of amides and sulfonamides with unactivated alkenes.....	33
Scheme 1-16. Ir-Catalyzed addition of indoles to unactivated alkenes	34
Scheme 2-1. Asymmetric hydroamination of aminoalkenes catalyzed by rare-earth metal complexes based on binaphtholate ligands	36
Scheme 2-2. Two synthetic routes for preparing 3,3'-bis(triarylsilyl)-substituted binaphthols.....	38
Scheme 2-3. Synthesis of 3,3'-disilyl-substituted binaphthol using an one-pot procedure.....	39
Scheme 2-4. Synthesis of 3,3'-disilyl-substituted binaphthols using optimized reaction conditions	40
Scheme 2-5. Synthesis of di- <i>tert</i> -butyl(bromo)phenylsilane	41
Scheme 2-6. Synthesis of binaphtholate complexes utilizing [Ln(<i>o</i> -C ₆ H ₄ CH ₂ NMe ₂) ₃]	43
Scheme 3-1. Synthesis of (<i>R</i>)-3,3'-dibromo-H ₈ BINOL from (<i>R</i>)-BINOL	49

Scheme 3-2. Synthesis of 3,3'-disilyl-substituted octahydrobinaphthols	50
Scheme 3-3. Synthesis of (<i>R</i>)-3,3'-di(triphenylsilyl)-H ₈ BINOL using one-pot procedure.....	51
Scheme 3-4. Attempted synthesis of the unsymmetrically (<i>R</i>)-3,3'-disubstituted H ₈ BINOL proligand 49	52
Scheme 3-5. Synthesis of octahydrobinaphthol rare-earth metal complexes	53
Scheme 4-1. Catalytic cycle of intramolecular hydroamination of aminoalkenes.....	67
Scheme 5-1. Mechanistic scenarios for intermolecular hydroamination.....	91
Scheme 6-1. General scheme for the kinetic resolution of aminoalkenes.....	94
Scheme 6-2. The general model for the kinetic resolution of aminoalkenes.....	99
Scheme 6-3. Proposed stereomodel for the kinetic resolution of α -substituted aminopentenes.....	110

List of Abbreviation

BINAP	2,2-Bis(diphenylphosphino)-1,1'-binaphthyl
BINOL	1,1'-Binaphthyl-2,2'-diol
H ₈ -BINOL	5,5',6,6',7,7',8,8'-Octahydro-1,1'-binaphthyl-2,2'-diol
<i>n</i> Bu	<i>n</i> -Butyl
<i>t</i> Bu	<i>tert</i> -Butyl
Bn	Benzyl
cat.	Catalyst
Cy	Cyclohexyl
Cp	η^5 -Cyclopentadienyl
Cp [*]	η^5 -Pentamethylcyclopentadienyl
DCM	Dichloromethane
DMF	<i>N,N</i> -Dimethylformamide
δ	Chemical shift
d	Doublet
Et	Ethyl
HMPA	Hexamethylphosphoramide
L	Ligand
Ln	Rare Earth metals (Sc, Y, La-Lu)
M	Metal
Me	Methyl
m	multiplet

MOM	Methoxymethyl
NOBIN	2-amino-2'-hydroxy-1,1'-binaphthyl
<i>i</i> Pr	Isopropyl
Ph	Phenyl
s	Singlet
THF	Tetrahydrofurane

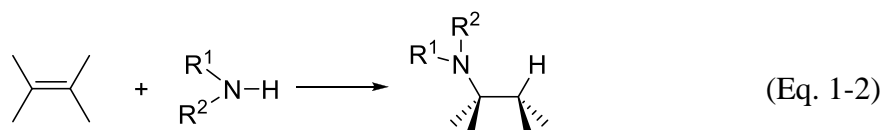
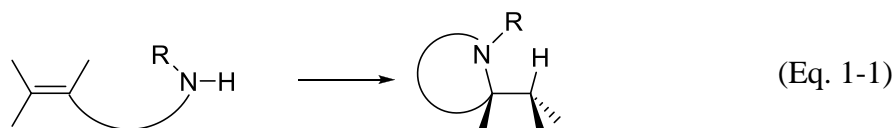
Chapter 1

Introduction to the Catalytic Hydroamination of Alkenes

1.1 General Introduction

Nitrogen-containing compounds, such as amines, enamines, and imines, play vital roles in almost all fields of chemistry, bulk and fine chemicals, as well as pharmaceuticals, particularly naturally occurring products.¹⁻⁴ The high importance of amines and their derivatives have attracted great attention of organic chemists in searching for efficient synthetic processes. Amines can be approached through many organic synthetic pathways, which are nucleophilic substitution with nitriles or azides, reductive amination of carbonyl compounds followed by reduction, amination of organic halides or alcohols, and reduction of nitro compounds.^{5,6} These traditional organic reactions are well-known and widely used in organic laboratories, but not preferential if there are other synthetic routes available, due to their relatively low atom efficiency (EA = 26-87%).⁷ One of the simplest methods that release amine products with 100% atom efficiency is the hydroamination, reaction which has been studied in the past 60 years using a wide range of catalysts including alkali bases, alkaline earth metals, rare earth metals (scandium, yttrium, and lanthanides), actinides, early and late transition metals, and organocatalysts. Notably the last decade has seen an increasing amount of publications reporting many catalytic systems for stereoselective hydroamination.⁷⁻¹⁶ The hydroamination reaction can be achieved by direct addition of an amine to an unsaturated

carbon-carbon bond to form a new carbon-nitrogen bond. Significant research efforts on the development of catalysts for intramolecular hydroamination reactions (Eq. 1-1) as well as intermolecular hydroamination (Eq. 1-2) have been reported.



The lower reactivity and electron density of alkene functionality make the hydroamination of alkenes more difficult than that of alkynes. The addition of ammonia to acetylene is estimated to be about 63 kJ mol^{-1} more favorable than the addition to ethylene.¹⁷ However, considering the possibility for applications, the hydroamination of alkenes is more attractive, because the starting materials, alkenes, are cheaper and more readily available than alkynes.¹⁸ Moreover, the hydroamination of alkenes forms amine products directly, without requirement of reduction of imines and enamines, which are the products of hydroamination of alkynes.

The hydroamination reaction of alkenes is a thermodynamically feasible process, with slightly positive reaction enthalpy and highly negative reaction entropy. However the direct addition of amine to a C-C multiple bond is very challenging due to a high reaction barrier.^{19,20} Because of the highly negative reaction entropy, the high reaction barrier cannot be overcome by increasing the reaction temperature. Electrostatic repulsion of the lone pair electrons of the amine nitrogen and the π -electrons of multiple

bonds also makes the addition of an amine to an alkene difficult.^{21,22} Therefore, the direct nucleophilic addition of amines only occurs to a limited set of electron-deficient (activated) alkenes containing neighboring electron-withdrawing groups, such as esters, nitriles, nitro, or keto groups.^{6,23,24} Moreover, the thermal [2+2] cycloaddition of the N-H bond and the alkene is forbidden due to the intrinsically high energy difference between π (C=C) and σ (N-H) orbitals.

The metal catalyzed asymmetric hydroamination reaction has been one of the highly challenging and competitive topics in chemical research.^{8-10,25-29} Despite of numerous investigations in recent years, the issue is not completely solved. While rare-earth and Group 4 metals are very efficient for promoting hydroamination in term of activity and enantioselectivity, their uses are limited due to high air and moisture sensitivity and low functional group tolerance. These groups of metals are remarkably utilized for intramolecular hydroamination of various simple and unactivated alkenes.³⁰⁻³⁸ However, intermolecular hydroamination of alkenes using rare-earth metal complexes is still far from ideal for practical applications, because they generally show slow reactions. Though late transition metals are less sensitive to air and moisture and they are also more functional group compatible compared to rare-earth metals, their limitations lie in the substrate range of amines and alkenes. The amines involved in this type of transformation ideally should have low basicity, such as anilines, carboxamides, sulfonamides, and other protected amines. In most cases, only activated and strained alkenes, such as vinylarenes, 1,3-dienes, or norbornene, can undergo intermolecular hydroamination catalyzed by late transition metal complexes under normal conditions.^{8,9,39}

1.2 Intramolecular Hydroamination of Aminoalkenes

1.2.1 Rare-Earth Metal Catalyzed Hydroamination

Despite of high air and moisture sensitivity and low functional group compatibility, intramolecular hydroamination reactions of aminoalkenes catalyzed by rare-earth metal complexes were first reported by Marks⁴⁰ more than two decades ago and has been extensively studied in the last two decades.⁹ The intramolecular addition of an N-H bond across a C-C double bond of an alkene in the presence of rare-earth metal catalysts can be achieved with very high turnover numbers in general and excellent stereoselectivities in some cases.

1.2.1.1 Lanthanocene Catalyzed Hydroamination

In 1989, Marks and coworkers first reported the intramolecular hydroamination of aminoalkenes catalyzed by the lanthanocenes $\text{Me}_2\text{Si}(\text{Me}_5\text{C}_5)_2\text{LnH}$ and Cp^*LnH ($\text{Cp}^* = \eta^5\text{-Me}_5\text{C}_5$; $\text{Ln} = \text{La-Lu}$). The lanthanocene-based catalysts for this type of reaction were expanded to the use of other ligands that provided different degrees of steric demands at the metal centers. In general, the reaction rate increases with more open lanthanocene precatalyst systems, which can be obtained with larger ionic radii of Ln^{3+} ($\text{La} > \text{Sm} > \text{Lu}$) (Table 1-1, entries 1–3) and/or less sterically demanding ligands (Figure 1-1 and Table 1-1, entries 3 and 4). Moreover, the rate of cyclization generally decreases with increasing ring size ($5 > 6 >> 7$) (Table 1-1, entries 5–7).⁴⁰⁻⁴²

Figure 1-1 Dependence of rare-earth metals catalyzed hydroamination reaction rate on steric demand of the catalyst ligand framework.

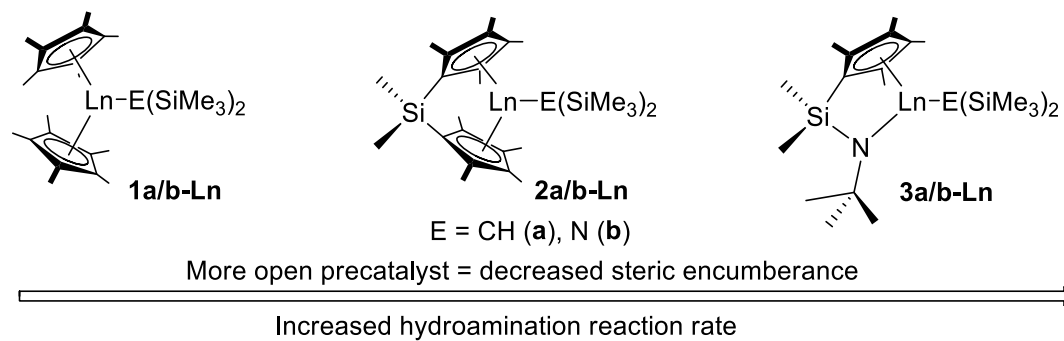
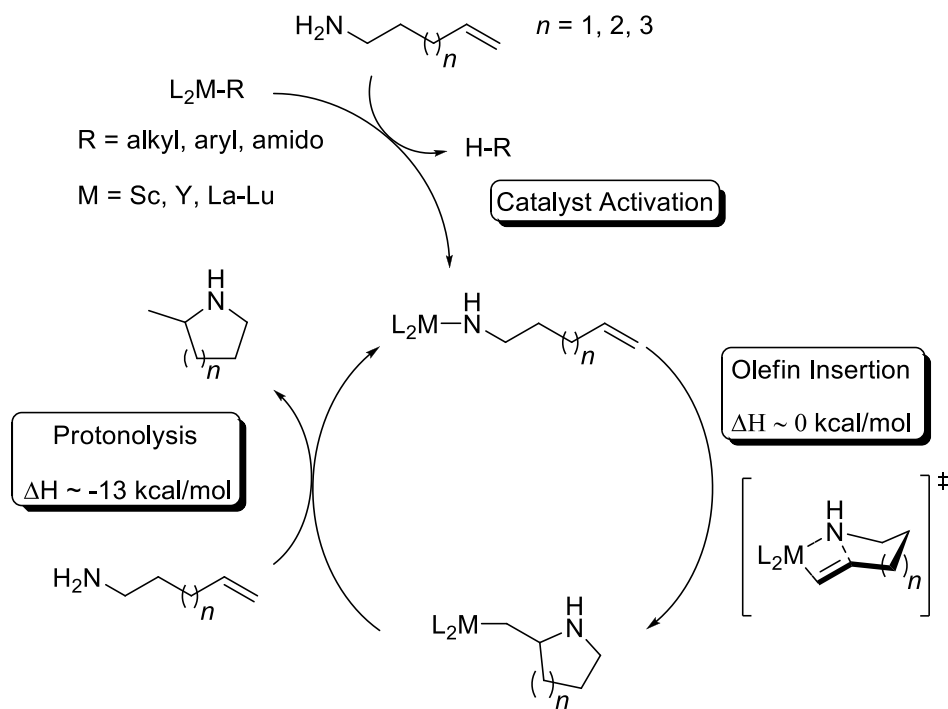


Table 1-1. Rate dependence on ionic radius, steric demand of the ancillary ligand, and ring size of hydroamination product, in the rare-earth metal catalyzed cyclization of aminoalkenes.

Entry	Substrate	Product	Catalyst	T, °C	TOF, h ⁻¹
1			1a-La	25	95
2			1a-Sm	60	48
3			1a-Lu	80	< 1
4			2a-Lu	80	75
5			1b-La	60	140
6			1b-La	60	5
7			2a-Nd	60	0.3

The hydroamination/cyclization mechanism proposed by Marks⁴² indicates that the catalytic cycle is initiated by activation of the amine substrate *via* fast protonolysis of a metal amido, metal alkyl, or metal aryl bond in the precatalyst, forming a metal amido species. The reaction proceeds by undergoing olefin insertion into the metal amido bond, *via* a four-centered transition state. This presumably irreversible olefin insertion process is shown to be approximately thermoneutral. The resulting metal alkyl species undergoes rapid exothermic protonolysis in the presence of excess of amine substrate, generating the catalytically active species and releasing the hydroamination/cyclization product (Scheme 1-1). The extensive kinetic and mechanistic studies indicate that the reaction rate is zero order in aminoalkene substrate concentration and first order in catalyst concentration. The olefin insertion into the metal amide bond is the rate limiting step.



Scheme 1-1. Proposed mechanism for the hydroamination/cyclization using rare-earth metal catalysts.

The first asymmetric hydroamination/cyclization of aminoalkenes using C_1 -symmetric chiral *ansa*-lanthanocene complexes in which one of the cyclopentadienyl ligands was attached with (+)-neomenthyl, (-)-menthyl, or (-)-phenylmenthyl, was reported by Marks and coworkers in 1992 (Figure 1-2).⁴³⁻⁴⁵ The chiral substituent on the cyclopentadienyl ligand results in the formation of two separable diastereomeric *ansa*-lanthanocene complexes, because cyclopentadienyl ligands can coordinate to the lanthanide metal center with either diastereotopic face. Fractional crystallization usually can be applied to successfully obtain diastereomerically pure complexes if one of the two diastereomers is not predominantly formed.

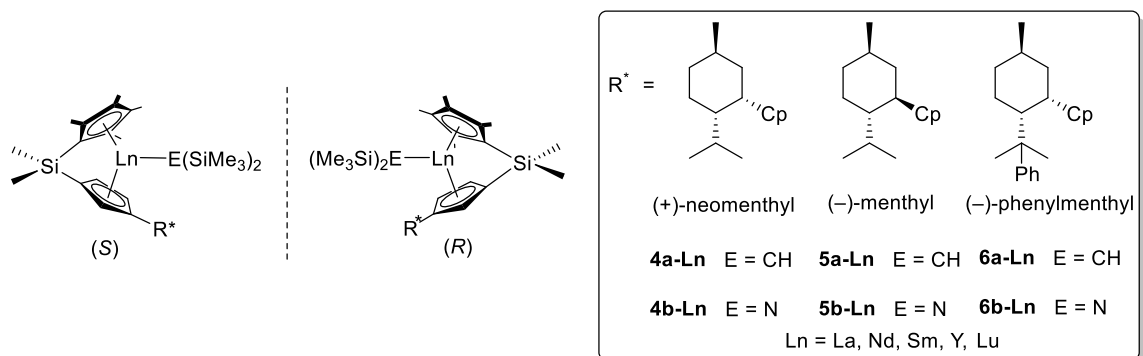
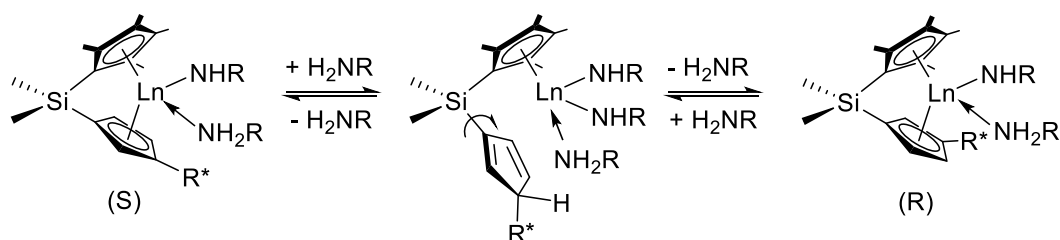


Figure 1-2. Chiral *ansa*-lanthanocene precatalysts for asymmetric hydroamination

Unfortunately the rare-earth metal-cyclopentadienyl bond in the chiral lanthanocenes undergoes reversible protolytic cleavage under the catalytic conditions of the hydroamination reaction, facilitating epimerization (Scheme 1-2).⁴³⁻⁴⁶



Scheme 1-2. Epimerization of chiral lanthanocene complexes during the hydroamination reaction.

Lanthanocene complexes **4–6** possess the same high catalytic activity for hydroamination of aminoalkenes as their counterpart **2**, shown above in Table 1-1. Catalytic results for traditional substrates, such as 2,2-dimethyl-pent-4-enylamine and pent-4-enylamine, displayed moderate to good enantioselectivity of the cyclization products (Table 1-2). Despite the occurrence of the epimerization process of lanthanocene complexes during the hydroamination reaction, cyclization of aminopentenes furnished pyrrolidine derivatives with up to 74% ee at $-30\text{ }^{\circ}\text{C}$ (Table 1-2, entry 5).

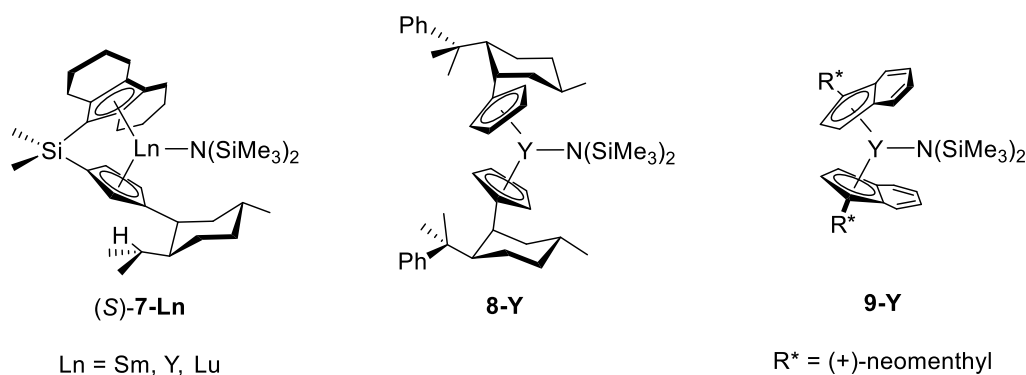
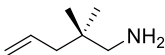
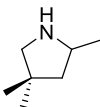
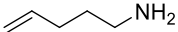
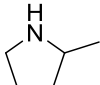
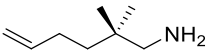
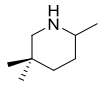
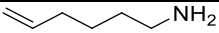
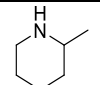


Figure 1-3. Chiral lanthanocene complexes with extended “wing-span” and nonlinked chiral ytrocenes.

Table 1-2. Lanthanocene-catalyzed asymmetric hydroamination/cyclization of aminoalkenes

Entry	Substrate	Product	Catalyst	<i>T</i> , °C	TOF, h ⁻¹	% ee	Ref.
1			(<i>R</i>)- 4b-La	25		14 (<i>R</i>)	32, 44
2			(<i>R</i>)- 4b-Y	25	21	40 (<i>R</i>)	32
3			(<i>R</i>)- 4b-Lu	25		40 (<i>S</i>)	32
4			(<i>S</i>)- 5b-Sm	25	84	53 (<i>S</i>)	32, 44
5			(<i>S</i>)- 5b-Sm	-30		74 (<i>S</i>)	32, 44
6			(<i>R</i>)- 6a-Y	25	8	56 (<i>S</i>)	32
7			(<i>R</i>)- 4b-La	25		31 (<i>R</i>)	32, 44
8			(<i>R</i>)- 4b-Y	25		50 (<i>R</i>)	32
9			(<i>S</i>)- 4b-Sm	25	33	55 (<i>R</i>)	32
10			(<i>S</i>)- 5b-Sm	0		72 (<i>S</i>)	32, 44
11			(<i>R</i>)- 6a-Y	25		64 (<i>S</i>)	32
12			(<i>S</i>)- 7-Sm	60	28.4	37 (<i>S</i>)	47
13			8-Y	100	0.8	35 (<i>S</i>)	48
14			(<i>S</i>)- 5b-Sm	25	2	15 (<i>R</i>)	32, 44
15			(<i>S</i>)- 7-Sm	60	89.4	43 (<i>S</i>)	47
16			(<i>S</i>)- 7-Y	25	2.1	67 (<i>S</i>)	47
17			(<i>S</i>)- 7-Y	60	86	54 (<i>S</i>)	47
18			(<i>S</i>)- 7-Lu	60		15 (<i>S</i>)	47
19			(<i>S</i>)- 7-Sm	60	6.6	10 (<i>S</i>)	47
20			(<i>S</i>)- 7-Y	60	3.6	3.2 (<i>S</i>)	47

Cyclization of 2,2-dimethyl-hex-5-enylamine and hex-5-enylamine yielded piperidines with disappointing low enantioselectivity compared to pyrrolidine products (Table 1-2, entries 4 and 14, and entries 12 and 19). Chiral lanthanocene complexes (*S*)-**7-Sm** and (*S*)-**7-Y** with the extended “wing-span” octahydrofluorenyl ligand (Figure 1-3) generated some piperidines with better enantioselectivities (Table 1-2, entries 15–17).

However, lower enantioselectivities were obtained if (*S*)-**7-Ln** was applied to the unsubstituted aminopentene and aminohexene (Table 1-2, entries 12, 19, and 20). The sterically more encumbered ytrocene **9-Y** (Figure 1-3) predominantly formed the *p-S,p-S* diastereomer, but the bond of yttrium and an indenyl ligand underwent protolytic cleavage.⁴⁸

Based on the observed absolute configuration of the cyclization products of aminoalkenes, it is believed that the irreversible insertion of olefin into the Ln-N bond through a seven-membered chair-like transition state is the stereo-determining step. A stereomodel built for the cyclization of pent-4-enylamine helps to rationalize the stereoselectivity (Figure 1-4). Steric interactions between either the C₅Me₄-ring (see frontal approach) or the chiral auxiliary R* (see lateral approach) and an axial substituent of the metallacycle inhibits the formation of the unfavorable transition state.⁴⁴ Both frontal and lateral approach modes lead to the same product configuration.

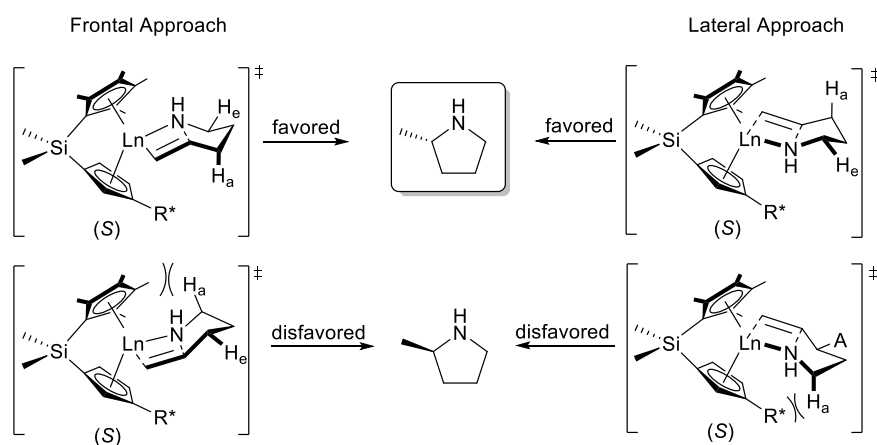


Figure 1-4. Stereomodel for the observed absolute product configuration of pent-4-enylamine.

1.2.1.2 Non-Metallocene Catalyzed Asymmetric Hydroamination

The lanthanocenes displayed promising results in the catalytic intramolecular hydroamination of unactivated alkenes.^{42,44,49} However, the cyclopentadienyl-based catalyst systems cannot be relied on for development of asymmetric hydroamination catalysts, due to the reversible protolytic cleavage of the rare-earth metal-cyclopentadienyl bond under the catalytic conditions of hydroamination reaction,^{42,44-46} consequently diminishing stereoselectivities. Therefore, the scientific community turned its research efforts onto non-cyclopentadienyl-based catalysts for asymmetric hydroamination, in hope for better catalytic systems with high activity and improved enantioselectivities.

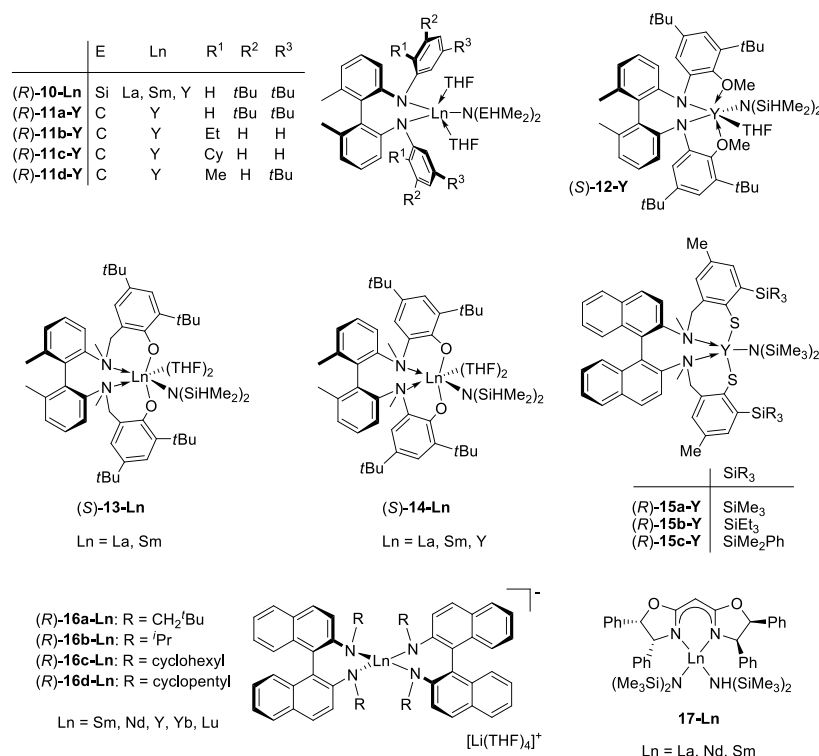


Figure 1-5. Chiral biarylamido, amino(thio)phenylate and bisoxazolinato catalysts for asymmetric hydroamination

Non-metallocene catalysts for the hydroamination/cyclization of aminoalkenes, mainly based on C_2 -symmetric ligands, have been intensively studied over the last decade. Significant progress in the area of rare-earth metal hydroamination catalysts have been made by the groups of Scott,^{32,33,36} Livinghouse,^{34,37} Collin and Trifonov,⁵⁰⁻⁵⁵ Marks,^{56,57} and Hultsch.^{30,31,38,58,59}

Scott and coworkers showed one of the first studies involving the application of enantiopure biaryl diamido precatalysts (*R*)-**10-Ln** (Ln = Y, Sm, La) and (*R*)-**11-Y** (Figure 1-5).³³ The diamido-based complexes exhibited moderate success in asymmetric hydroamination reactions of *gem*-dimethyl aminopentene with disappointingly low catalytic activity even at 60 °C (Table 1-3, entries 1-3). The more basic diisopropylamido ligand increased the catalytic activity of complex (*R*)-**11-Y** in comparison to complex (*R*)-**10-Ln** containing the less basic (bis(dimethylsilyl)amido ligand, but unfortunately lower enantioselectivities for the cyclization products were observed (Table 1-3, entries 1 and entries 4–7).³³ Another effort for better hydroamination catalysts involved modification of the biaryl diamine ligand by introducing additional *O*-donors (Figure 1-5, complex (*S*)-**12-Y**). The anisole oxygen, fluxionally coordinated to the rare-earth metal, did not improve enantioselectivity (Table 1-3, entry 8).³²

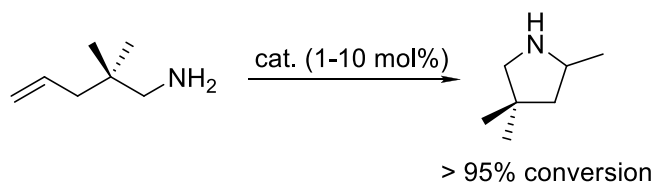
The group of Scott also designed aminophenolate complexes (*S*)-**13-Ln** and (*S*)-**14-Ln** in search for more efficient catalyst systems for hydroamination (Figure 1-5).³⁶ The lanthanum catalyst (*S*)-**13**, with an improved “reach around” chiral chelating ligand framework, could release hydroamination products with enantioselectivities of up to 61% ee, but the catalytic activity was rather slow (Table 1-3, entry 10). Complex (*S*)-**14** with

aminophenolate ligand without methylene linker between the phenol unit and the biaryl amine gave almost racemic pyrrolidine (Table 1-3, entry 11).

The aminothiophenolate catalysts (*R*)-**15-Y** developed by Livinghouse³⁷ and coworkers displayed significantly higher enantioselectivities, though catalytic activity remained low (Table 1-3, entries 12-15). Selectivities of up to 89% ee were observed, but the cyclization required 552 hours to reach >95% conversion at 30 °C (Table 1-3, entry 12).

Diamidobinaphthyl-based complexes (*R*)-**16-Ln** were applied for cyclization of *gem*-dimethyl aminopentene to give hydroamination product with good enantioselectivities of up to 73% ee (Table 1-3, entries 16–17). Highest selectivities of up to 87% ee could be obtained using (*R*)-**16-Yb** in the asymmetric hydroamination of *C*-(1-allylcyclohexyl)-methylaniline.⁵⁵ However, (*R*)-**16-Ln** generally exhibited only moderate activity.

Bisoxazoline ligands are very versatile and modular ligands in asymmetric catalysis.⁶⁰ The bisoxazolinato catalyst system **17** was reported by Marks for hydroamination/cyclization of a wide range of aminoalkenes as well as aminodienes, generating pyrrolidine and piperidine derivatives in good stereoselectivities. The highest turnover frequency (25 h⁻¹) and highest enantioselectivity (67% ee) in the cyclization of 2,2-dimethylpent-4-enylaniline were observed for (*R*)-**17-La**. A variety of bisoxazoline ligands were applied in the screening study, revealing that a combination of good enantioselectivities and high catalytic activity is determined by the presences of stereodirecting groups at 4 position (aryl) and 5 position (geminal dimethyl or aryl) of the oxazoline ring.⁵⁶

Table 1-3. Non-metallocene-catalyzed asymmetric hydroamination of 2,2-dimethylpent-4-enylamine

Entry	Catalyst	<i>T</i> , °C	<i>t</i> , h	TOF, h ⁻¹	% ee	Ref.
1	(<i>R</i>)- 10-Y	60	336		50	33
2	(<i>R</i>)- 10-Sm	60	168		33	33
3	(<i>R</i>)- 10-La	60	168		18	33
4	(<i>R</i>)- 11a-Y	35	120		45	33
5	(<i>R</i>)- 11b-Y	35	120		20	33
6	(<i>R</i>)- 11c-Y	35	120		21	33
7	(<i>R</i>)- 11d-Y	35	120		23	33
8	(<i>S</i>)- 12-Y	60	192		21	32
9	(<i>S</i>)- 13-Sm	70	30		27	36
10	(<i>S</i>)- 13-La	70	40		61	36
11	(<i>S</i>)- 14-Y	70	24		11	36
12	(<i>R</i>)- 15a-Y	30	552		89	37
13	(<i>R</i>)- 15a-Y	60	15		78	37
14	(<i>R</i>)- 15b-Y	60	12		83	37
15	(<i>R</i>)- 15c-Y	60	9		87	37
16	(<i>R</i>)- 16b-Yb	25	168 ^a		69	51
17	(<i>R</i>)- 16c-Yb	25	168 ^b		73	51
18	(<i>R</i>)- 17-La	23		25	67	56
19	(<i>R</i>)- 17-Nd	23		~10	61	56
20	(<i>R</i>)- 17-Sm	23		13	55	56

^a 49% conversion, ^b 77% conversion.

Binaphtholate catalysts were first reported by the group of Hultzs, ^{31,58} showing not only excellent stereoselectivities but also high reactivity compared to those of lanthanocene catalysts for hydroamination of aminoalkenes. Sterically demanding tris(aryl)silyl substituents in the 3 and 3' positions of the binaphtholate ligand play a vital role in stereoselectivities, catalytic activity, as well as catalyst stability. The post-lanthanocene complexes (*R*)-**19-Ln** displayed the highest enantioselectivities of up to 95% ee in hydroamination/cyclization of aminoalkenes, in less than 30 minutes using (*R*)-**19-Sc** at room temperature (Table 1-4, entry 11). Higher catalytic activity could be achieved (highest turnover frequency of up to 840 h⁻¹) by using rare-earth metals with larger ionic radii, at the expense of selectivities.³¹

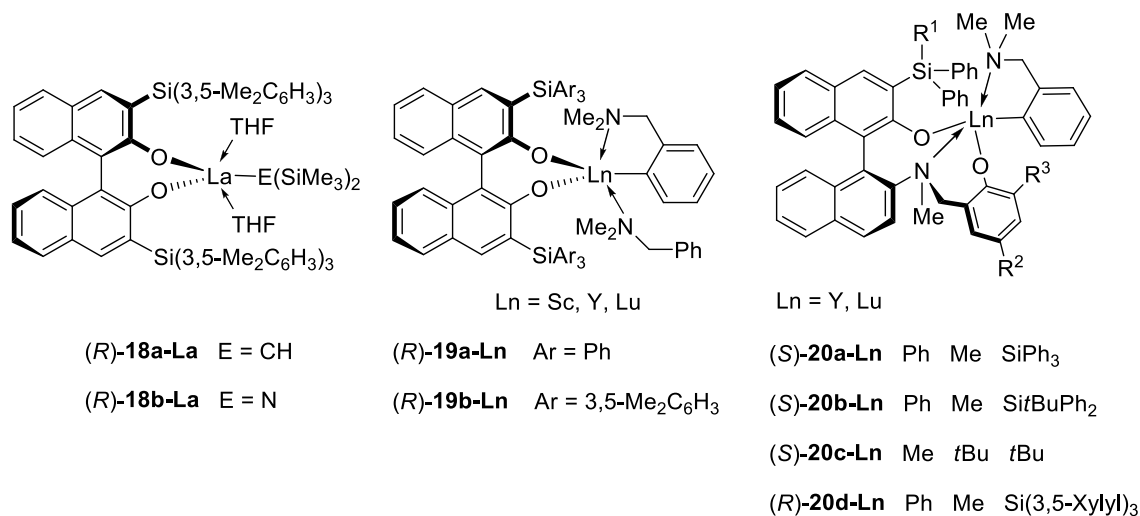
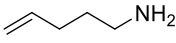
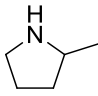
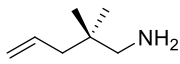
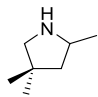
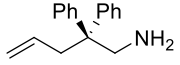
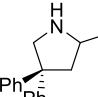
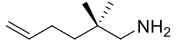
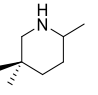
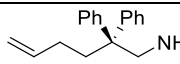
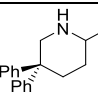
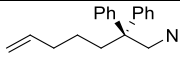
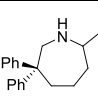


Figure 1-6. Binaphtholate and aminodiolate catalysts for asymmetric hydroamination.^{31,59}

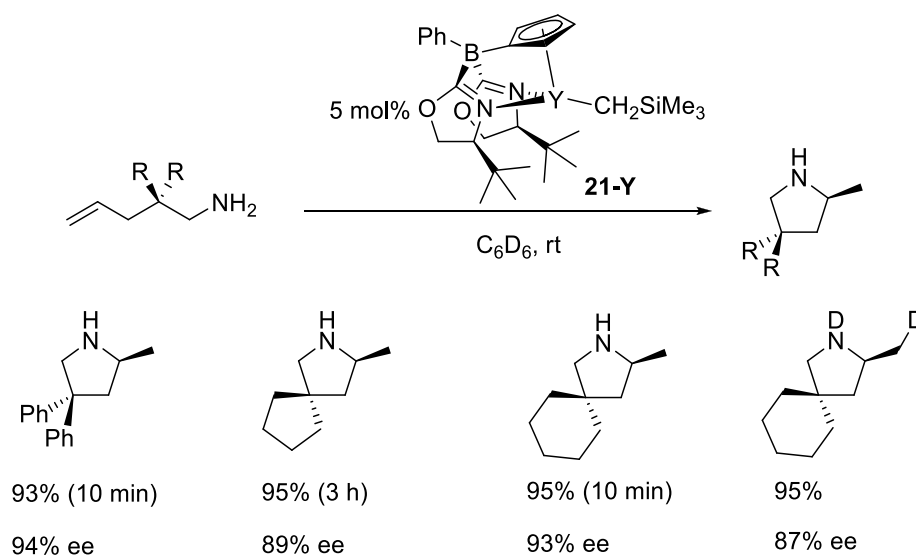
Table 1-4 Binaphtholate- and aminodiolate-based rare-earth metal-catalyzed asymmetric hydroamination

Entry	Substrate	Product	Catalyst	<i>T</i> , °C	TOF, h ⁻¹	% ee (config.)	Ref.
1			(<i>R</i>)- 18a-La	22	37	72 (<i>S</i>)	31
2			(<i>R</i>)- 18b-La	22	≥33	71 (<i>S</i>)	31
3			(<i>R</i>)- 19a-Lu	60	18	72 (<i>S</i>)	31
4			(<i>R</i>)- 19b-Lu	22	1.7	90 (<i>S</i>)	31
5			(<i>R</i>)- 19b-Lu	0	0.13	92 (<i>S</i>)	31
6			(<i>S</i>)- 20a-Lu	80	15	59 (<i>S</i>)	59
7			(<i>R</i>)- 19a-Y	60	480	65 (<i>S</i>)	31
8			(<i>R</i>)- 19b-Lu	22	3.1	68 (<i>S</i>)	31
9			(<i>R</i>)- 20a-Lu	40	12	62 (<i>S</i>)	59
10			(<i>R</i>)- 20a-Y	40	15	35 (<i>S</i>)	59
11			(<i>R</i>)- 19a-Sc	25	110	95 (<i>S</i>)	31
12			(<i>R</i>)- 19a-Y	25	≥840	84 (<i>S</i>)	31
13			(<i>S</i>)- 20a-Lu	25	200	92 (<i>S</i>)	59
14			(<i>S</i>)- 20c-Y	25	50	48 (<i>R</i>)	59
15			(<i>R</i>)- 20d-Y	25	150	8 (<i>R</i>)	59
16			(<i>R</i>)- 19a-Sc	60	4.1	40	31
17			(<i>R</i>)- 19b-Sc	60	0.9	61	31
18			(<i>R</i>)- 19b-Y	60	2.9	36	31
19			(<i>S</i>)- 20a-Lu	25	20	73	59
20			(<i>R</i>)- 20d-Y	60	150	37	59
21			(<i>S</i>)- 20a-Lu	90	0.5	27	59

Hultzs ch recently reported a new catalytic system for the asymmetric hydroamination of aminoalkenes. Chiral *C*₁-symmetric NOBIN-derived aminodiolate

complexes of the rare-earth metals with multiple tunable sites (Figure 1-6, **20-Ln** complexes)⁵⁹ were efficient for hydroamination/cyclization of aminopentenes and aminohexenes with enantioselectivities of up to 92 and 73% ee, respectively. This novel catalytic system displayed some success in asymmetric hydroamination of unactivated alkenes; however, it was found to be slightly less reactive and selective than the binaphtholate rare-earth metal catalysts (*R*)-**19-Ln** (Table 1-4).

Another major contribution to the area of rare-earth metals-catalyzed hydroamination was published by the group of Sadow in 2011.⁶¹ The *C*₁-symmetric zwitterionic oxazolinylborato yttrium complex **21-Y** exhibited high activity and excellent stereoselectivities for hydroamination of a limited set of *gem*-disubstituted aminoalkenes (Scheme 1-3). The experimental data showed isotopic effects on the enantioselectivity, suggesting that an N-H bond was not only involved in the rate-determining step, but also in the stereochemistry-discriminating step.



Scheme 1-3. Zwitterionic oxazolinylborato yttrium catalyzed asymmetric hydroamination

1.2.2 Group 4 Metal Catalyzed Hydroamination

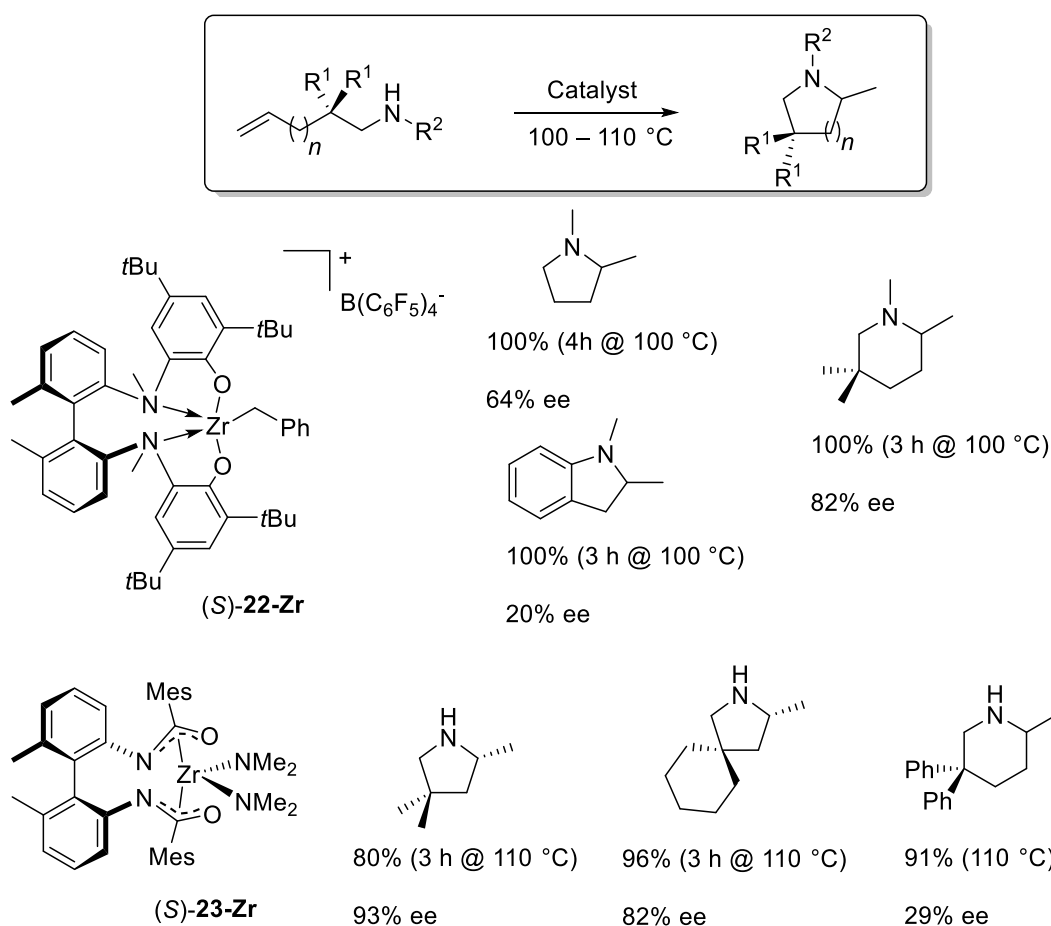
Groups 4 metal catalysts are well developed and widely used for olefin polymerization;^{62,63} therefore, their application in asymmetric hydroamination is particularly attractive. Group 4 metal compounds are well known for their low cost, high activity with commonly low sensitivity, easy handling and preparation, and commercial availability.

Studies on catalytic hydroamination by Group 4 metal catalysts were reported in the early 1990's; however, the catalysts were limited to alkyne and allene substrates.^{11,14,64-66} There have been several significant studies on the catalytic hydroamination of aminoalkenes published recently, involving the uses of titanium, zirconium, and hafnium complexes.⁶⁷⁻⁷²

The group of Scott reported the first chiral Group 4 metal catalysts for asymmetric hydroamination/cyclization of aminoalkenes in 2004.⁷⁰ The cationic zirconium complex (*S*)-**22-Zr** was based on the chiral aminophenolate ligand (Scheme 1-4). The cyclization reaction required reaction temperatures of up to 100 °C to obtain full conversion in reasonable reaction time due to low solubility of the catalyst in bromobenzene. The highest observable enantioselectivities of up to 82% ee were encouraging; however, the efficiency for hydroamination using this Group 4 catalyst was confined to secondary aminoalkenes (Scheme 1-4). It is believed that primary aminoalkenes did not react, because the catalytic active cationic metal-imido species underwent facile α -deprotonation, leading to an unreactive metal-imido species.^{67,70,73} In other words, the catalytic cycle involving cationic Group 4 metals is thought to involve

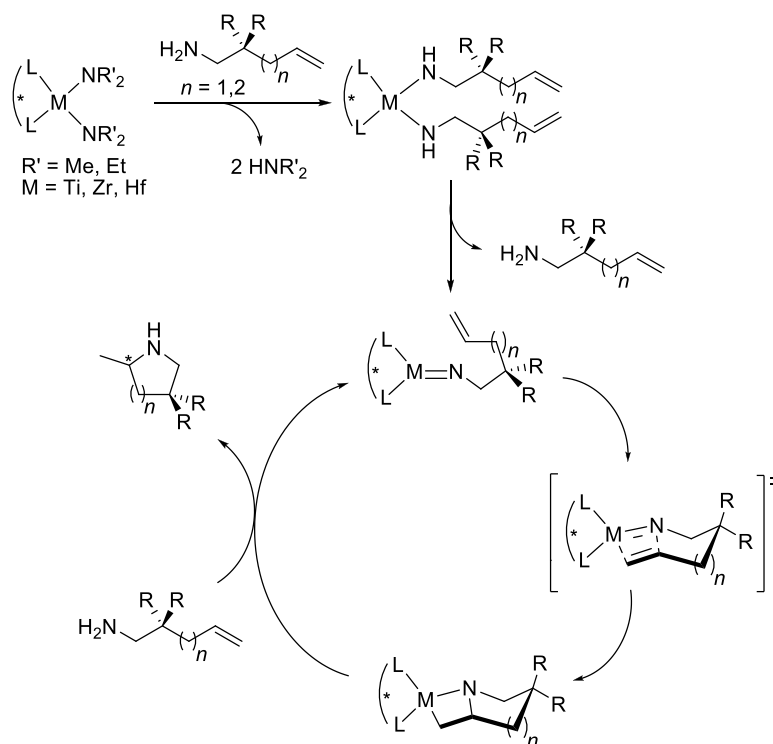
the olefin insertion into the metal amido bond, *via* a four-centered transition state, similar to the mechanism of rare-earth metal-based catalysts (Scheme 1-1).

Neutral Group 4 metal catalysts cyclized aminoalkenes with enantioselectivities of up to 93% ee, as first reported by Schafer^{68,74} and soon after by Scott.⁷¹ The studies indicated that the chiral bis(amidate) zirconium complex was not active for hydroamination/cyclization of secondary aminoalkenes.



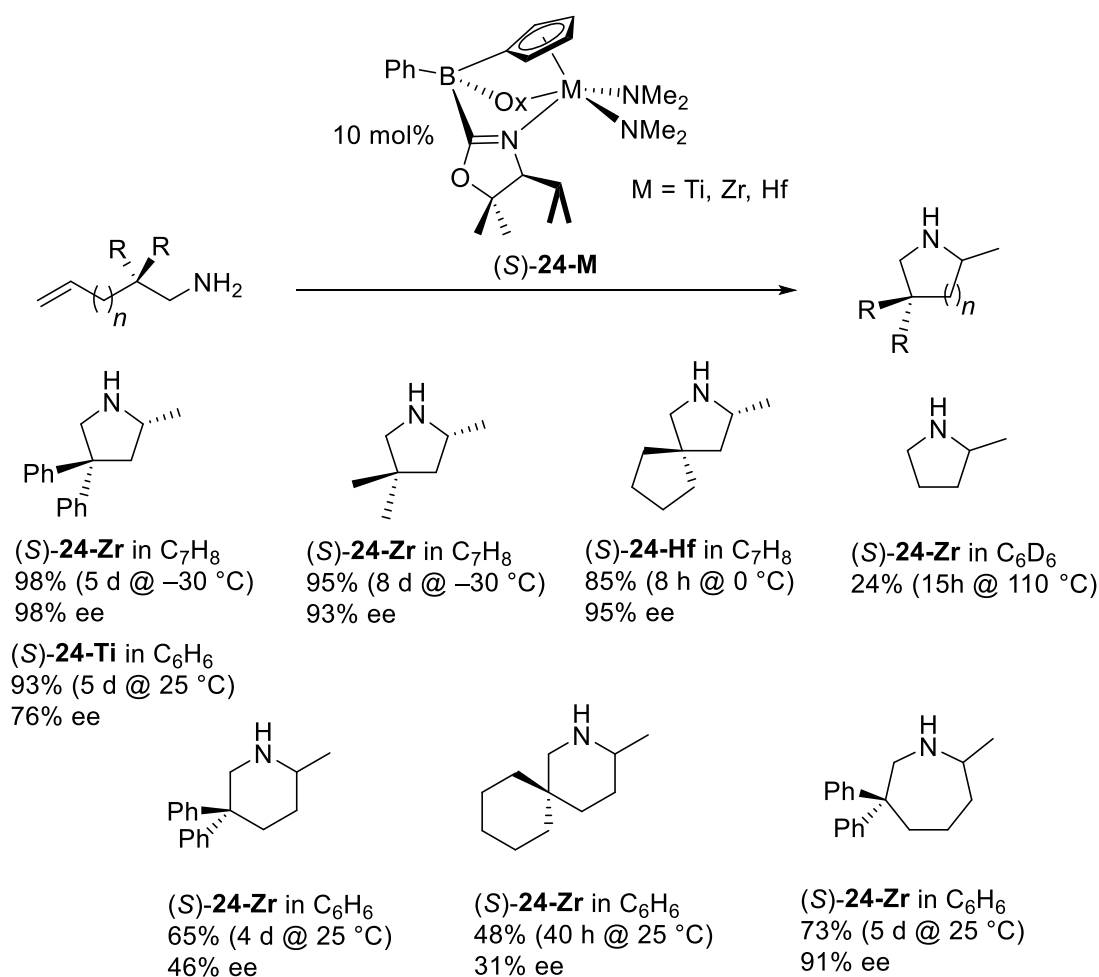
Scheme 1-4 Hydroamination/cyclization of aminoalkenes using ionic and neutral zirconium catalysts.

A mechanism similar to that of alkyne and allene hydroamination⁷⁵⁻⁸¹ was proposed for the hydroamination/cyclization of aminoalkenes catalyzed by neutral Group 4 metal catalysts, which involved metal imido species as catalytically active species. This proposed mechanism (Scheme 1-5) is based on the observation that neutral Group 4 metal catalysts are only efficient for asymmetric hydroamination/cyclization of primary aminoalkenes. The bis(amido) precursor undergoes α -elimination of an amine, generating metal imido species, which cyclizes to form an azametallacyclobutane *via* a [2+2] cycloaddition transition state. The resulting azametallacyclobutane is protolytically cleaved to regenerate the metal imido species concomitant with the release of the hydroamination product.^{68,69,74,82,83}



Scheme 1-5. Proposed mechanism for hydroamination/cyclization of primary aminoalkenes using Group 4 metal catalysts.

Recently Sadow^{84,85} reported a highly active Group 4 metal catalyst system containing a cyclopentadienyl bis(oxazolinyl)borate ligand, which catalyzed the hydroamination reaction of aminoalkenes at room temperature with excellent enantioselectivities. The highest selectivities of up to 98% ee could be obtained at $-30\text{ }^{\circ}\text{C}$ in the cyclization of *gem*-diphenyl aminopentene. The application of (*R*)-**M-24** (M = Ti, Zr, Hf), however, seemed to be confined to *gem*-disubstituted aminoalkenes, evidenced by the reaction in which only 24% cyclization of the non-substituted aminopentene was obtained after 15 h even at high temperature of up to $110\text{ }^{\circ}\text{C}$ (Scheme 1-5).⁸⁴

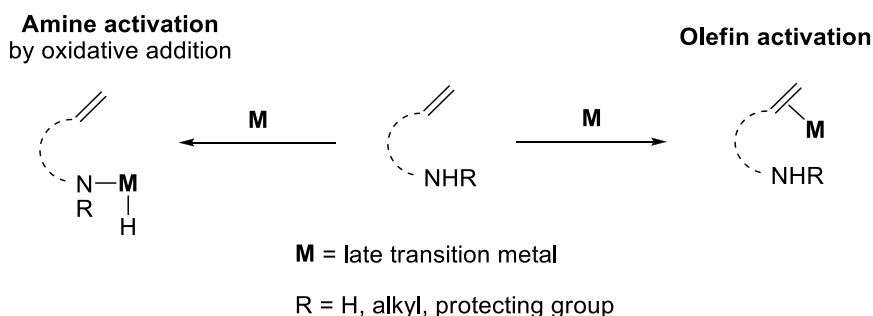


Scheme 1-6. Group 4 metal-mediated asymmetric hydroamination of primary aminoalkenes.

1.2.3 Late Transition Metal Catalyzed Hydroamination

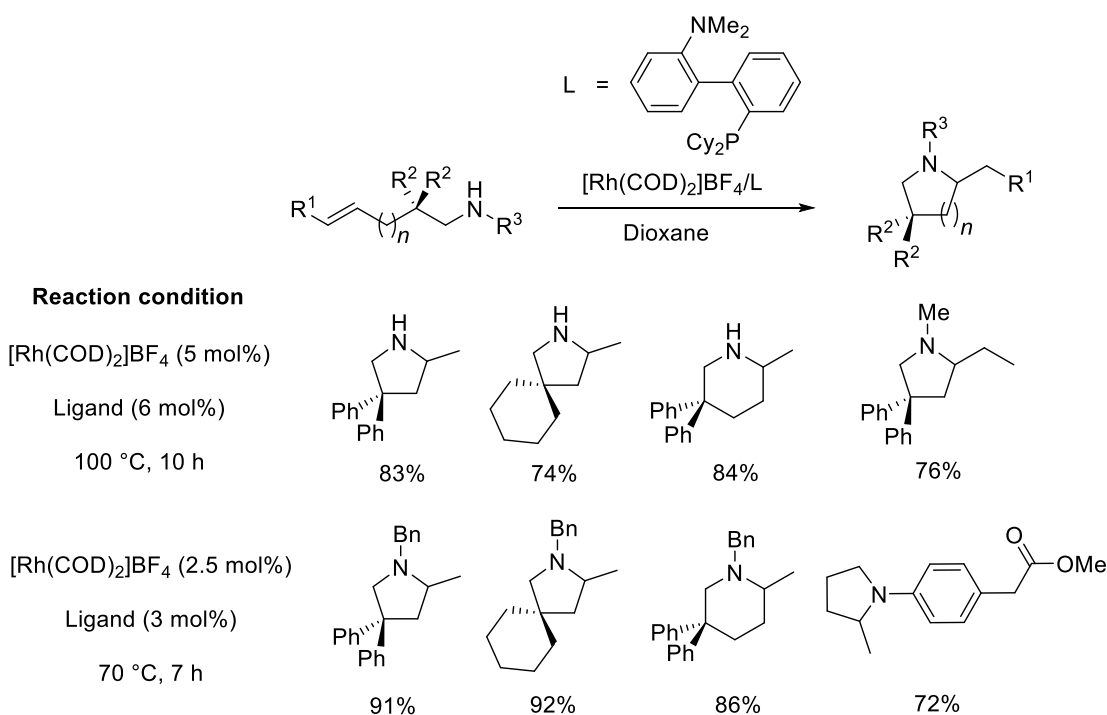
The well-developed rare-earth metal catalyst systems have shown to be excellent catalysts for asymmetric hydroamination/cyclization of aminoalkenes, providing a combination of high activity and enantioselectivities. However, their applications are limited to a set of substrates with limited functional group tolerance. Though late transition metals do not potentially possess the limitation of low functional group compatibility, there are only few reports on the intramolecular hydroamination of alkenes catalyzed by these metal complexes.

The proposed mechanisms of rare-earth metal- and Group 4 metal-catalyzed hydroamination indicate that the catalytic cycles are initiated by activation of amine, generating amido^{12,40,42,86,87} or imido^{75-81,88} species, respectively. In contrast, alkene or alkyne activation by coordination to the metal is often believed to take place in hydroaminations using late transition metal catalysts.⁸⁹⁻⁹¹ However, amine activation by oxidative addition to a coordinatively unsaturated late transition metal in low oxidation state, giving a metal hydride complex, is also discussed as an alternative pathway for hydroamination.⁹²⁻⁹⁹



Scheme 1-7. The activation modes of the substrate in the late transition metal-catalyzed hydroamination.

Late transition metal catalyst systems for the hydroamination/cyclization of aminoalkenes are less active than rare-earth metal catalysts; higher temperatures and longer reaction times are generally required to achieve high conversion. For instance, the group of Widenhoefer¹⁰⁰ reported an efficient platinum catalyst, $[\text{PtCl}_2(\text{H}_2\text{C}=\text{CH}_2)]_2/\text{PPh}_3$, for cyclization of secondary amines at temperatures as high as 120 °C. Reactions involving primary amines or internal olefins do not proceed using this catalyst system.

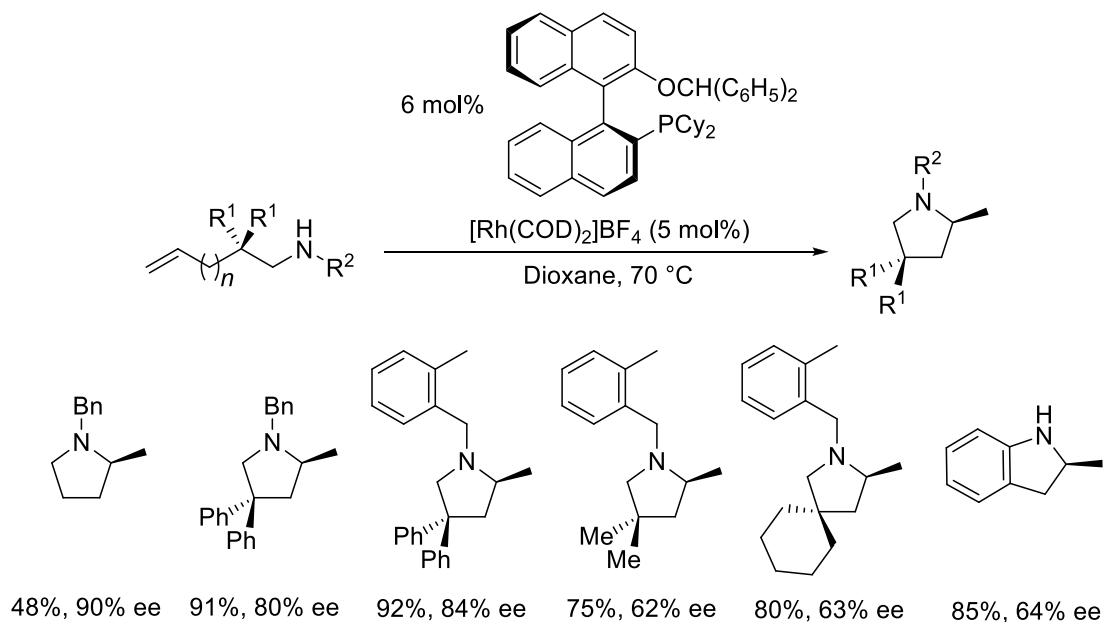


Scheme 1-8. Rhodium catalyzed intramolecular hydroamination of primary and secondary aminoalkenes

A major contribution from Hartwig¹⁰¹ and coworkers shows the use of a rhodium catalyst in the presence of an amino analogue to the biarylphosphine ligand developed in the Buchwald laboratory for cross-coupling.¹⁰² The cyclization of primary and secondary

aminoalkenes as well as internal olefins are observed; however, primary amines require higher temperature (100 °C) and catalyst loading (5 mol%), and longer reaction time (10 h) to give the same high conversions compared to the corresponding secondary amines (Scheme 1-8).

Following the seminal work of Liu and Hartwig,¹⁰¹ the group of Buchwald turned its attention to the development of an enantioselective rhodium catalyst using chiral cyclohexyl-MOP-type ligands. The selectivity of the hydroamination reaction improves with increasing size of the oxygen substituent on the ligand. Amine protecting groups and *gem*-disubstituted groups have significant effects on stereoselectivities of the hydroamination/cyclization products, as well as reaction yield. A primary amine cyclized with lower selectivity (Scheme 1-9).¹⁰³

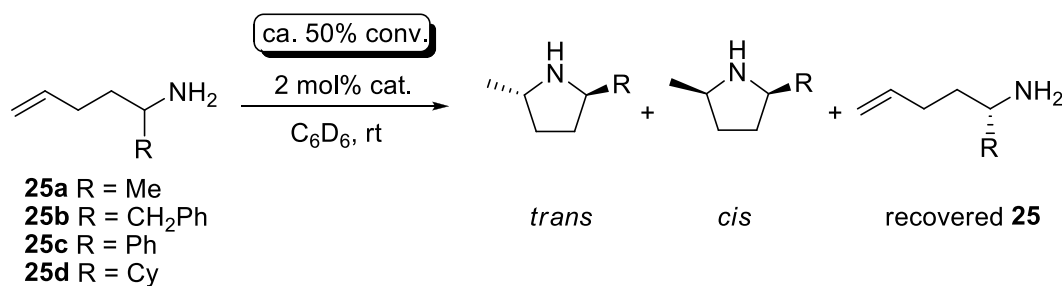


Scheme 1-9. Rhodium-catalyzed asymmetric intramolecular hydroamination of aminoalkenes.

1.2.4 Kinetic Resolution of Chiral Aminoalkenes via Asymmetric Hydroamination

Enantiomeric forms of an organic compound can have different potency, toxicity, and behavior in biological systems. Therefore, the asymmetric syntheses of enantiomers of chiral molecules, particularly bioactive compounds, are major research areas of interest. Kinetic resolution has provided an alternatively useful method to prepare stereochemically-enriched compounds *via* separation of enantiomers.

Table 1-5. Catalytic kinetic resolution of aminoalkenes using binaphtholate rare-earth metal complexes.^{31,104}



Entry	Catalyst	Subs.	<i>t</i> , h	conv. (%)	<i>trans:cis</i>	% ee of recovered 25	<i>f</i>
1	(<i>R</i>)- 19a-Y	25a	25.5	53	11:1	72	9.5
2	(<i>R</i>)- 19b-Y	25a	26	52	13:1	80	16
3	(<i>R</i>)- 19a-Y	25b	9	50	20:1	42	3.6
4	(<i>R</i>)- 19a-Lu	25c	15 ^a	52	≥50:1	83	19
5	(<i>R</i>)- 19a-Y	25c	95	50	≥50:1	74	15
6	(<i>R</i>)- 19a-Y	25d	8	56		49	3.5
7	(<i>R</i>)- 19a-Lu	25d	23	47		51	6.0

^a At 40 °C

The Hultsch group first reported binaphtholate rare-earth metal complexes as efficient catalysts for kinetic resolution of racemic α -substituted 1-aminopent-4-ene.^{31,58,104} The catalysts were applied to kinetically resolve chiral aminopentenes with various sterically demanding substituents at α -position, giving a kinetic resolution factor of up to 19. The sterically more encumbered binaphtholate complex (*R*)-**19b-Y** kinetically resolved substrate **25a** more efficiently than triphenylsilyl-substituted binaphtholate catalyst (*R*)-**19a-Y**, with a kinetic factor as high as 16 (Table 1-5, entries 1 and 2).

Table 1-6. Kinetic resolution parameters of aryl- and alkyl-substituted aminopentenes determined with (*R*)-**19a-Y**.¹⁰⁴

Entry	Subs.	<i>T</i> , °C	<i>f</i>	$k_{\text{fast}}/k_{\text{slow}}$	K^{dias}	<i>trans:cis</i> Fast (slow)
1	25a	30	6.4	7.6	0.84	>30:1 (2.8:1)
2	25b	30	2.6	9.6	0.27	>30:1 (>30:1)
3	25c	50	12.8	6.6	1.9	>50:1 (9.2:1)
4	25c	60	11.5	7.1	1.6	>50:1 (8.8:1)
5	25d	30	2.7	8.5	0.32	9:1 (1.4:1)

The kinetic resolution factor *f* is defined as $f = K^{\text{dias}} \times k_{\text{fast}}/k_{\text{slow}}$; where K^{dias} is the Curtin-Hammett equilibrium constant between the two diastomeric substrate/catalyst-complexes and $k_{\text{fast}}/k_{\text{slow}}$ is the ratio of faster and slower reaction rate constant. The aryl-substituted aminoalkene **25c** behaves differently from the alkyl- and benzyl-substituted aminoalkenes **25a**, **25b**, and **25d**. The Curtin-Hammett preequilibrium favored the matching pair of substrate **25c** and catalyst ($K^{\text{dias}} > 1$), thus, effectively enhancing the

efficiency of the kinetic resolution process (Table 1-6, entries 3 and 4).¹⁰⁴ The other substrates (**25a**, **25b**, **25d**) on the other hand exhibited Curtin-Hammett pre-equilibrium constants favoring the mismatching substrate/catalyst pair ($K^{\text{dias}} < 1$); thus, reducing the overall kinetic resolution efficiency (Table 1-6, entries 1, 2, and 5).

1.3 Intermolecular Hydroamination

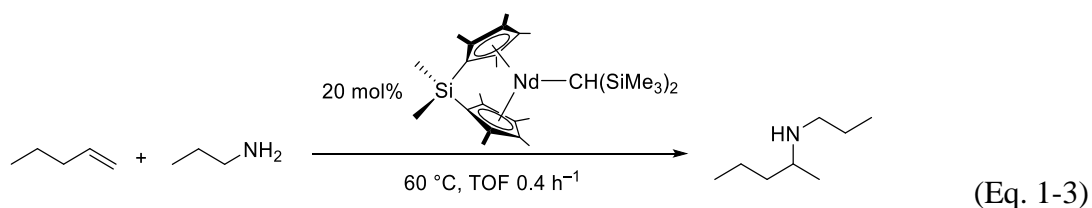
The hydroamination provides a direct method to synthesize nitrogen-containing compounds which are important in biological systems as well as industrially relevant basic and fine chemicals. Intramolecular hydroamination of alkenes can be approached effectively using rare-earth and Group 4 metal complexes as catalysts, in terms of high activity and excellent enantioselectivities. However, these catalysts show to be less efficient for intermolecular hydroamination of alkenes, which is a highly desired and difficult process. Many research efforts have focused on the development of late transition metal catalysts for the intermolecular hydroamination of alkenes, but most of the successful examples are limited to activated or strained alkenes, such as vinylarenes, 1,3-dienes, and norbornene, or amines with low basicity, such as anilines, carboxamides, sulfonamides, and other protected amines.^{8,9,13}

1.3.1 Intermolecular Hydroamination with Rare-Earth Metals

The intermolecular hydroamination of alkenes are generally slow compared to the intramolecular reaction. High catalyst loading and a large excess of the olefin are

required to achieve considerable reaction conversion due to weak coordination of olefins and strong binding of amines to rare-earth metals.

The *ansa*-lanthanocene $\text{Me}_2\text{Si}(\text{C}_5\text{H}_4)_2\text{NdCH}(\text{SiMe}_3)_2$ is an efficient catalyst for the hydroamination of a simple amine and 1-pentene, in which up to 70 equiv. of 1-pentene is added to obtain 90% conversion (Eq. 1-3).¹⁰⁵

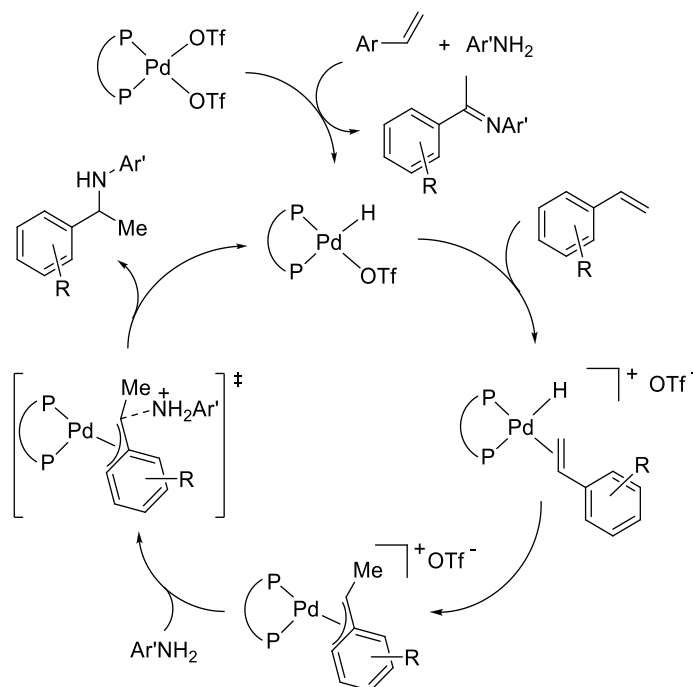


1.3.2 Intermolecular Hydroamination with Late Transition Metals

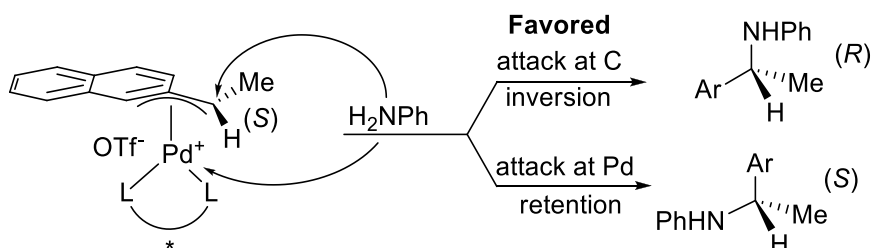
While there are only limited reports on the intramolecular hydroamination of alkenes using late transition metal catalysts, many reports on intermolecular hydroamination are available⁹ using various metals, such as Pd,^{13,106} Ru,¹⁰⁷ Ir,¹⁰⁸⁻¹¹¹ Pt,^{112,113} Au,^{114,115} and inexpensive metals like Cu¹¹⁶ and Fe.¹¹⁷ However, most of the catalyst systems reported for this type of reaction are achiral; only a few enantioselective versions of this process have been discovered. The most important chiral transition metal catalysts for intermolecular hydroamination will be discussed below.

Pd(II) and Pt(II) are generally found to catalyze hydroamination of alkenes and alkynes through a mechanism in which a C-C multiple bond coordinated to the metal center is attacked by an amine nucleophile, followed by protonolysis or β -hydride elimination, releasing the hydroamination product or an oxidative amination product,

respectively. However, the intermolecular hydroamination of vinyl arenes with arylamines catalyzed by palladium-diphosphine complexes can proceed *via* a different mechanism, proposed by the group of Hartwig.¹⁰⁶ The catalytic cycle involves the vinyl arene inserting into the catalytic active palladium hydride species, forming a η^3 -benzyl palladium intermediate. The intermediate undergoes externally nucleophilic attack by an amine, releasing the hydroamination product and regenerating the catalytically active palladium hydride species. External attack describes the direct attack of an amine on the benzylic carbon, forming the C-N bond, which should be differentiated from internal attack, where the amine may coordinate to palladium first, and then internally attack the benzylic carbon. The external nucleophilic attack is favorable, based on mechanistic studies, leading to formation of the hydroamination product with inversion of configuration (Scheme 1-11).

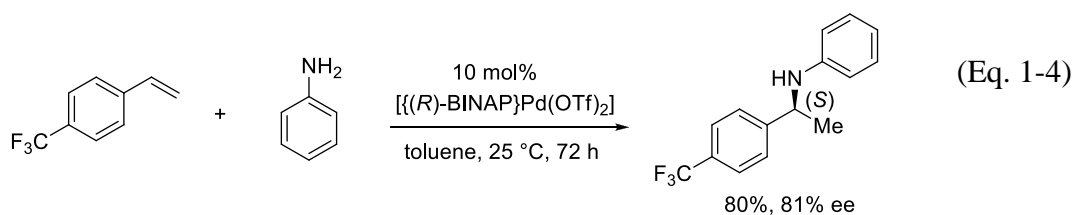


Scheme 1-10 Catalytic cycle for hydroamination of vinyl arenes catalyzed by palladium-diphosphine complexes



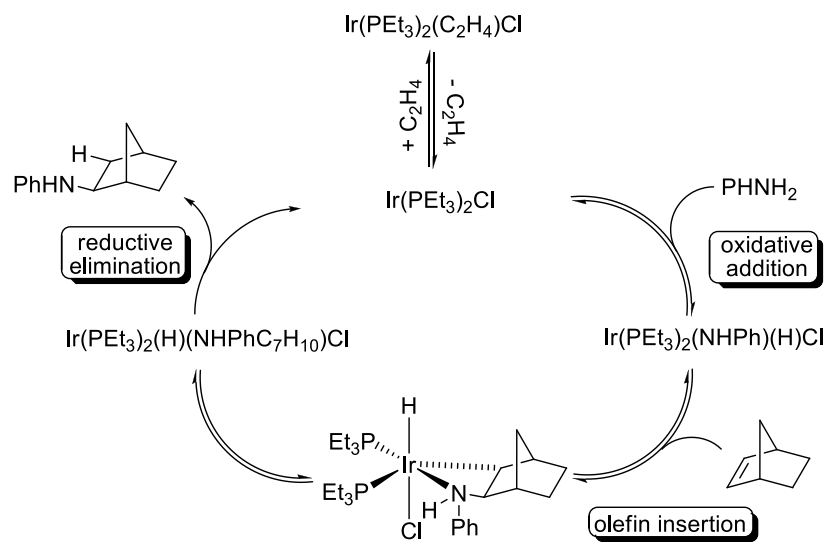
Scheme 1-11 Nucleophilic attack of the aniline at the η^3 -aryl palladium intermediate

The asymmetric hydroamination of weakly basic aniline and vinyl arenes in the presence of $[(R)\text{-BINAP}]\text{Pd}(\text{OTf})_2$ as catalyst can be performed under mild condition, giving the Markovnikov addition product in good yield and high enantioselectivity of up to 81% ee (Eq. 1-4).⁹⁴

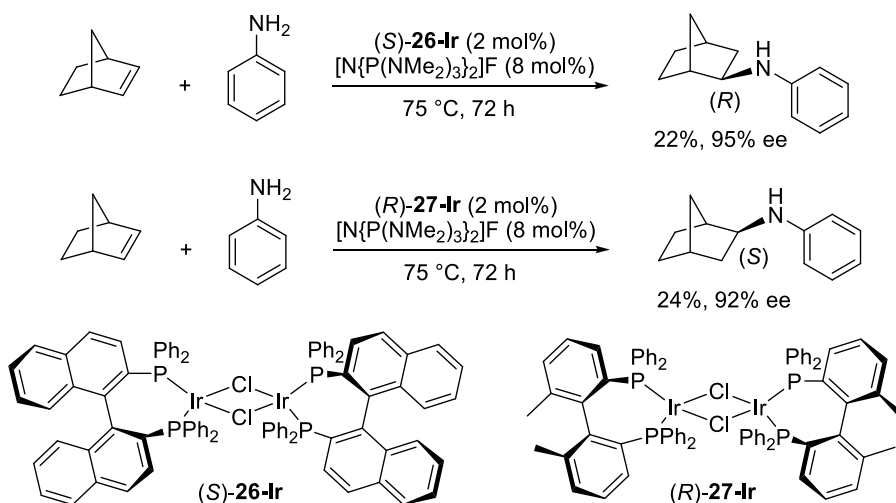


Hydroamination reaction catalyzed by late transition metals can also proceed *via* amine activation. This mechanism pathway is mostly observed for late transition metals in low oxidation states such as Ir(I) and Rh(I). The iridium-catalyzed hydroamination of norbornene with aniline *via* amine activation was reported by Milstein and coworkers in 1988.¹¹⁸ Aniline undergoes oxidative addition to the Ir(I) complex $[\text{Ir}(\text{PET}_3)_2(\text{C}_2\text{H}_4)\text{Cl}]$, leading to formation of an Ir(III) hydrido amido species, followed by insertion of norbornene into the amido bond. The resulting alkylamino Ir(III) complex releases the hydroamination product upon reductive elimination (Scheme 1-12).¹¹⁸

In 1997 the group of Togni reported the first asymmetric intermolecular hydroamination of alkenes using a chiral iridium catalyst,¹⁰⁸ analogous to achiral $[\text{Ir}(\text{PET}_3)_2(\text{C}_2\text{H}_4)\text{Cl}]$. The hydroamination of aniline and norbornene catalyzed by $[\{(S)\text{-BINAP}\}\text{IrCl}]_2$, (*S*)-**26-Ir**, afforded secondary amine product in low yield (12%) and modest enantioselectivity (57%). The addition of fluoride (8 mol%) significantly enhanced both activity and selectivity of the catalyst, raising the enantiomeric excess to 95%. Under the same reaction condition, $[\{(R)\text{-Biphemp}\}\text{Ir}(\mu\text{-Cl})]_2$, (*S*)-**27-Ir**, delivered hydroamination products with similar yield and slightly lower enantioselectivity (92% ee) (Scheme 1-13).¹⁰⁸

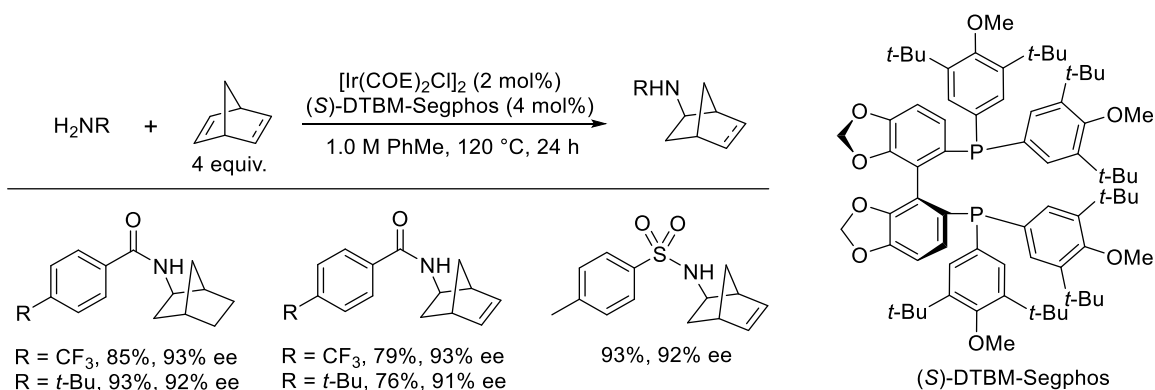


Scheme 1-12. Proposed mechanism for intermolecular hydroamination catalyzed by iridium.¹¹⁸

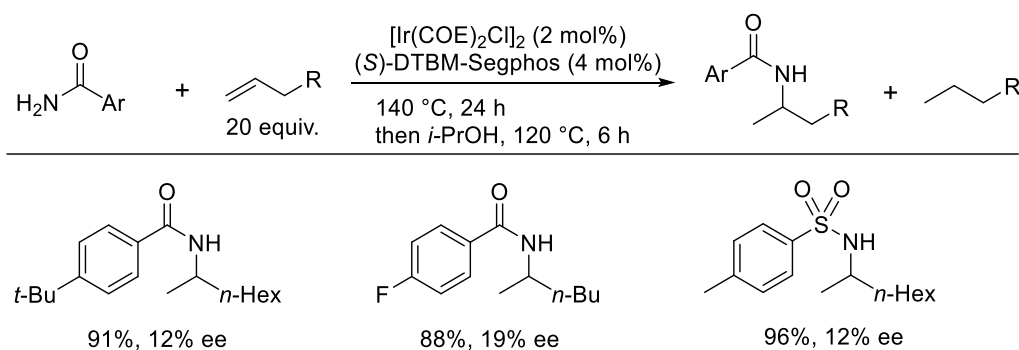


Scheme 1-13. Asymmetric hydroamination of aniline and norbornene catalyzed by Ir-diphosphine complexes.¹⁰⁸

The intermolecular hydroamination is not restricted to aniline. Enantioselective addition of amides and sulfonamides to norbornene and norbornadiene can be achieved under catalytic condition using $[\text{Ir}(\text{COE})_2\text{Cl}]_2$ and the commercially available ligand (*S*)-DTBM-Segphos (DTBM = 3,5-di-*tert*-butyl-4-methoxy), generating products in high yield and excellent enantioselectivities (Scheme 1-14). This iridium complex was also efficient for hydroamination of amides and sulfonamides and unactivated alkenes; however, negligible stereoselectivities were observed (Scheme 1-15).¹¹⁰



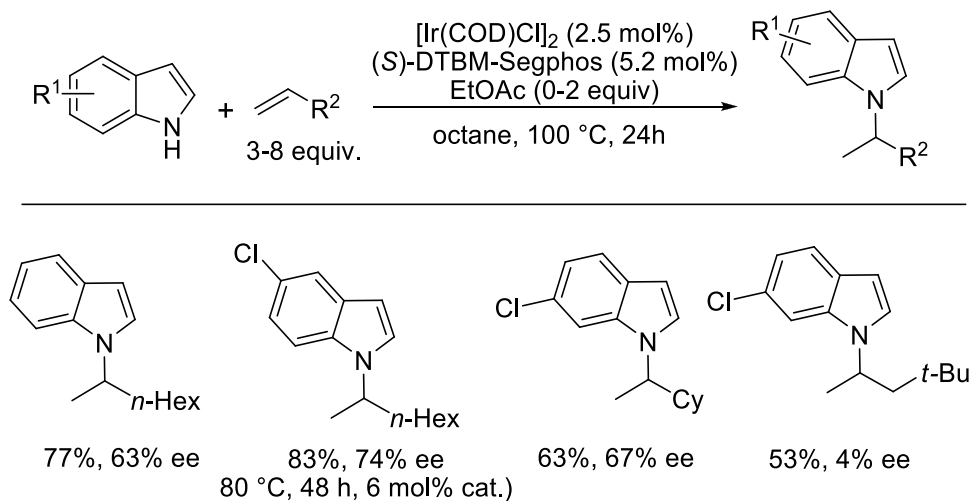
Scheme 1-14. Ir-catalyzed enantioselective intermolecular hydroamination of amides and sulfonamides with bicycloalkenes.¹¹⁰



Scheme 1-15. Ir-catalyzed intermolecular hydroamination of amides and sulfonamides with unactivated alkenes.¹¹⁰

Instead of using $[\text{Ir}(\text{COE})_2\text{Cl}]_2$, Hartwig utilized $[\text{Ir}(\text{COD})\text{Cl}]_2$ as an iridium source in the presence of (S)-DTBM-Segphos, to add indoles to unactivated alkenes, yielding hydroamination products with enantioselectivities as high as 74% ee.¹¹¹ The highest reaction conversion could be achieved by adding EtOAc (1 equiv. with respect to

indole). However, the origin of its positive effect on the reaction rate is unknown. Noticeably, the added EtOAc was not consumed during the reaction. Moreover, the substituents on indoles and the alkene chains displayed significant effects on activity as well as enantioselectivities of the hydroamination reaction (Scheme 1-16).



Scheme 1-16. Ir-Catalyzed addition of indoles to unactivated alkenes.¹¹¹

1.4 Significance and Aim of the Study

The catalytic asymmetric hydroamination of alkenes provides a useful method for the synthesis of chiral nitrogen-containing compounds, which are particularly important in pharmaceuticals as well as in industrial chemistry. This research area has been explored extensively in the last ten years, and many catalyst systems efficient for asymmetric addition of amines to alkenes have been developed. Despite of their high air and moisture sensitivity and low functional group compatibility, rare-earth and Group 4 metals have made dramatic progress in the area of asymmetric hydroamination of

aminoalkenes. High activity and excellent enantioselectivities can be obtained for intramolecular hydroamination of alkenes; however, asymmetric intermolecular hydroamination of alkenes using rare-earth metals remains a difficult process. The late transition metals, with their advantages of easy handling and highly functional group tolerance, have been proven to be effective in catalytic intermolecular hydroaminations of alkenes, particularly asymmetric transformations. These catalyst systems, unfortunately, only display high yield and stereoselectivities for intermolecular addition of amines with low basicity, such as anilines, carboxamides, sulfonamides, and other protected amines, to activated or strained alkenes, such as vinylarenes, 1,3-dienes, and norbornene. The metal-catalyzed asymmetric intermolecular hydroamination of simple amines and unactivated alkenes is of interest, but very challenging.

Our work has been focused on development of rare-earth metal complexes based on binaphtholate as well as octahydrobinaphtholate ligands as catalysts for the asymmetric hydroamination of alkenes.

Chapter 2

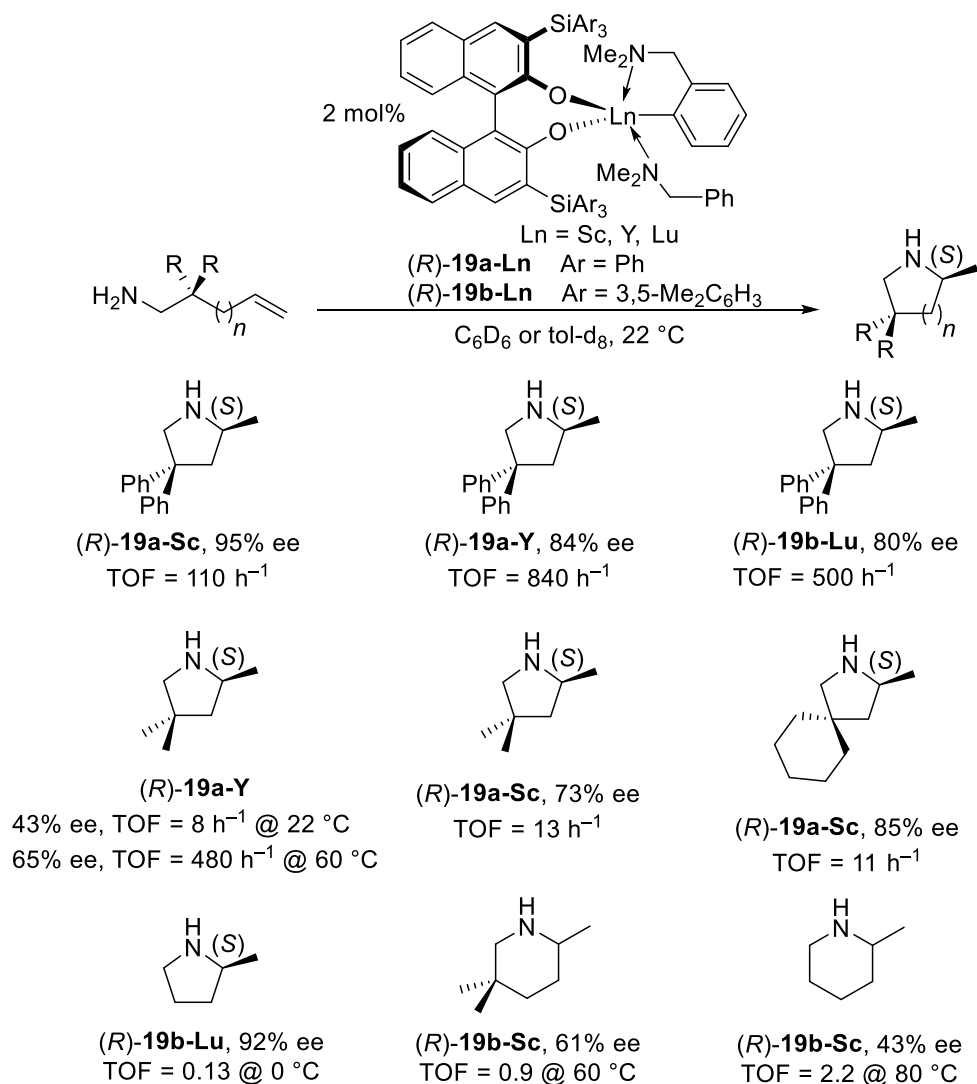
Binaphtholate Rare Earth Metal Complexes

2.1 Introduction

Syntheses of nitrogen based molecules are of great interest because they are found in the majority of naturally occurring products and particularly biological active substances. Therefore, a method that allows preparing chiral compounds containing amine functionality, without the involvement of stoichiometrically chiral auxiliaries or enantiomerically pure starting materials, is highly desired. Hydroamination of alkenes is a perfect solution in which a new carbon-nitrogen bond with chirality was formed by direct addition of an amine to an olefin. This atom economic transformation has been studied intensively and many efficient transition metal catalyst systems have been discovered.^{8,9,28}

Research in the Hultzsch group has been focused on the development of rare-earth metal complexes based on biphenolate and binaphtholate ligands as catalysts for the asymmetric hydroamination of alkenes.^{30,31,38,58} Our important findings were that the steric bulk in the 3 and 3' positions of the binaphtholate ligand played a crucial role in preventing the formation of higher aggregates and the stability of the rare-earth metal precatalysts. More importantly, highly sterically demanding silyl-substituents in these positions would significantly enhance catalytic activity and/or enantioselectivities. While the highest enantioselectivity was observed with (*R*)-**19a-Sc**, the catalyst with a larger

ionic radius metal, (*R*)-**19a-Y**, cyclized aminopentenes with high turnover frequency of up to 840 h⁻¹ at the expense of selectivity (Scheme 2-1).^{31,119}

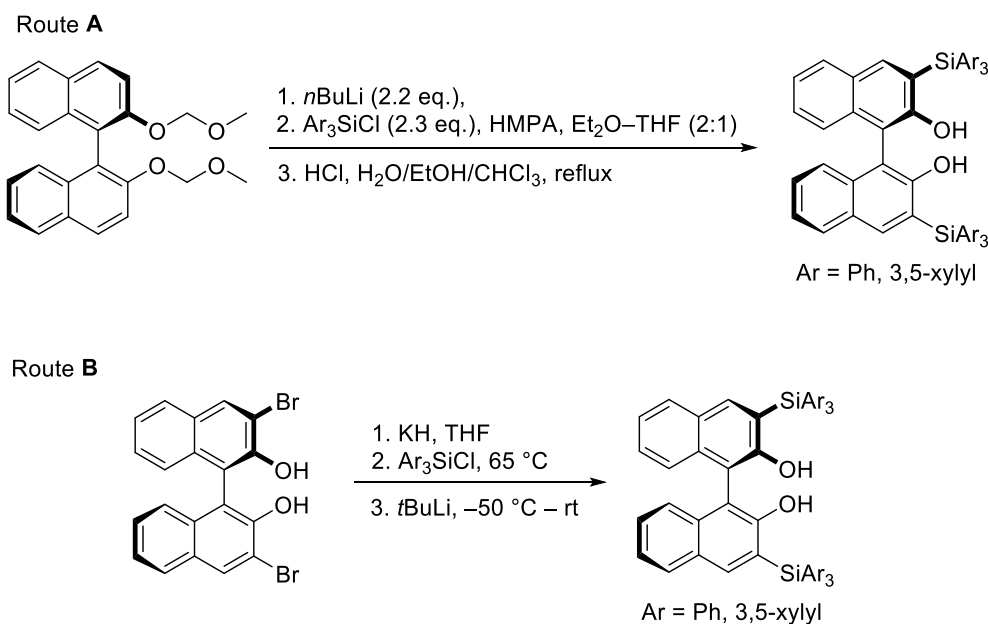


Scheme 2-1. Asymmetric hydroamination of aminoalkenes catalyzed by rare-earth metal complexes based on binaphtholate ligands.

In the extended studies focusing on catalysts for asymmetric hydroamination of alkenes, we synthesized rare-earth metal complexes based on binaphtholate ligands bearing a variety of sterically demanding silyl-substituents at the 3 and 3' position.

2.2 Synthesis of 3,3'-Bis(alkylarylsilyl)-Substituted Binaphtholate Ligands

In general, the silyl-substituents can be introduced to binaphthol at 3 and 3' positions *via* two synthetic routes (Scheme 2-2). The method which involves an nucleophilic substitution at silicon by 3,3'-dilithiated MOM-protected binaphthol in the presence of HMPA is straight forward;^{120,121} however, this reaction is only efficient for sterically less hindered silanes such as triphenylchlorosilane, delivering (*R*)-3,3'-bis(triphenylsilyl)-1,1'-binaphthalene-2,2'-diol ((*R*)-**28**) in good yield of up to 61% after MOM-deprotection with HCl. The substitution reaction involving the sterically more hindered tris(3,5-xylyl)chlorosilane gives significantly lower yield (< 15%).¹¹⁹

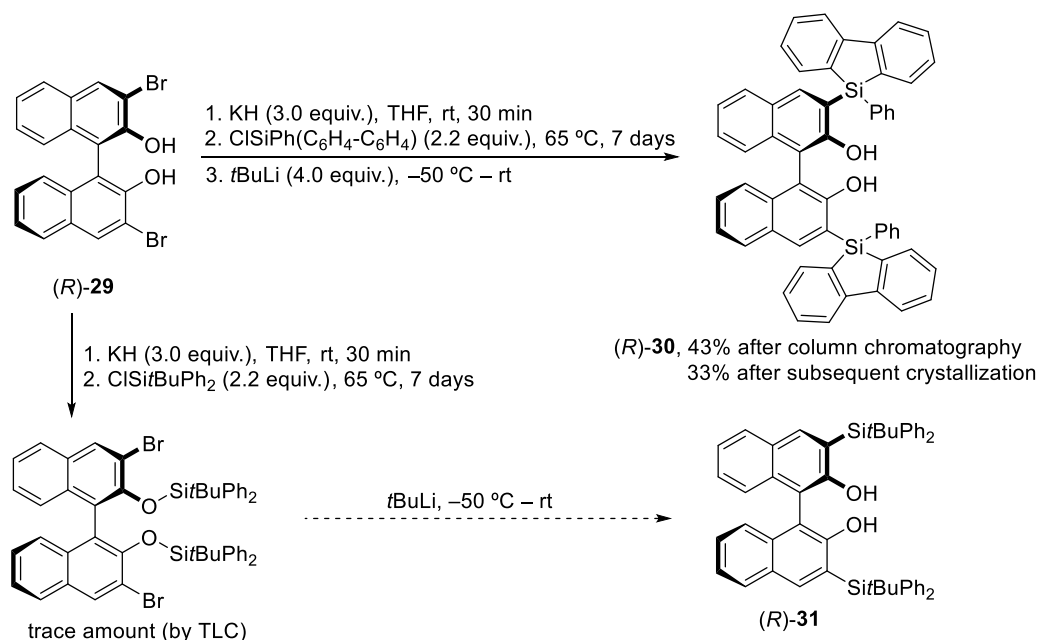


Scheme 2-2. Two synthetic routes for preparing 3,3'-bis(triarylsilyl)-substituted binaphthols.

Therefore, in our efforts to synthesize binaphtholate ligands with different sterically demanding silyl-substituents, this synthetic approach was not utilized. An

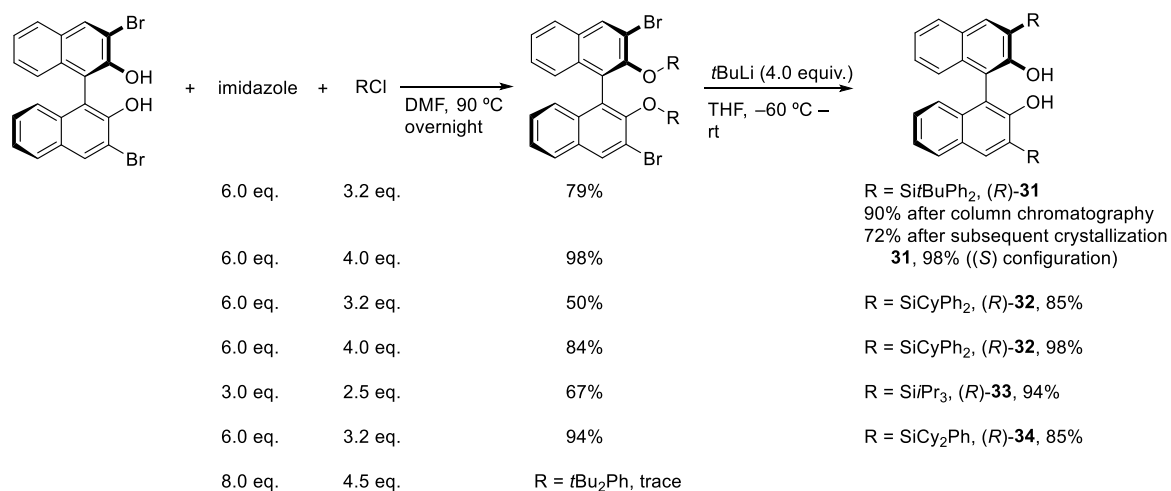
alternative and more favorable pathway to approach 3,3'-disilyl-substituted binaphthol is based on the retro-Brook-rearrangement of bis(tris(aryl)silyl ethers of (*R*)-3,3'-dibromo-1,1'-binaphthalene-2,2'-diol ((*R*)-**29**), generally leading to the desired products in moderate to good yields (39-69% after 2 steps).^{89,119}

Ligand (*R*)-**30** has a more rigid structure than (*R*)-**28**. It could be obtained from (*R*)-**29** in one pot with moderate yield using a modified literature procedure.⁸⁹ To the potassium phenolate, generated from deprotonation of (*R*)-**29** with KH in THF, was added 5-chloro-5-phenyldibenzosilole. The resulting silyl ether was treated with *t*BuLi to form the desired product (*R*)-**30**. However, the reaction condition was unsuccessful in the transformation of (*R*)-**29** to the 3,3'-bis(*tert*-butyl(diphenyl)silyl)-substituted binaphthol ((*R*)-**31**) due to low yield of the corresponding silyl ether intermediate (Scheme 2-3).



Scheme 2-3. Synthesis of 3,3'-disilyl-substituted binaphthol using an one-pot procedure.

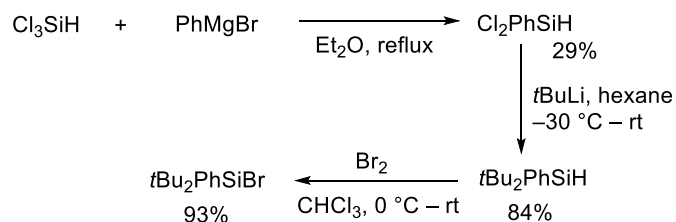
Although a high yield in the silylation reaction utilizing chloro[tris(3,5-xylyl)]silane had been observed, it was noted that this high yield was not reproducible in several experiments¹¹⁹ when using the classical silyl ether synthesis involving imidazole in DMF. We have successfully optimized the reaction conditions for a variety of sterically demanding chlorosilanes. Excess of imidazole (6 equiv.) and chlorosilane (4 equiv.) as well as prolonged heating at temperatures of up to 90 °C were generally required in order to achieve high yields of silyl ethers (Scheme 2-4).



Scheme 2-4. Synthesis of 3,3'-disilyl-substituted binaphthols using optimized reaction conditions.

Di-*tert*-butylphenylbromosilane¹²² could be prepared in three steps from commercially available trichlorosilane (Scheme 2-5). Dichloro(phenyl)silane was obtained by refluxing a mixture of trichlorosilane (1 equiv.) and the Grignard reagent PhMgBr in Et₂O in low yield (29%). Besides the mono-phenyl substituted product, di- and tri-substituted silanes were also formed in considerable amounts. An attempt to improve the yield of dichloro(phenyl)silane product by increasing the amount of

trichlorosilane (1.9 equiv) was not successful. Dichloro(phenyl)silane was then treated with *t*BuLi to give di-*tert*-butyl(phenyl)silane¹²³ in good yield (84%). Bromination of di-*tert*-butyl(phenyl)silane was carried out smoothly in CHCl₃ at 0 °C to obtain di-*tert*-butyl(bromo)phenylsilane in excellent yield (93%). However, attempts to synthesize the binaphthol ligand with this highly bulky silyl group have been unsuccessful so far. While a considerable amount of the mono-silylation intermediate was observed, only a trace amount of the desired di-silylation product was formed even when the reaction was heated to 90 °C for 7 days (Scheme 2-3). Moreover, it was difficult to separate the product from the unreacted starting material, (*R*)-3,3'-dibromo-1,1'-binaphthalene-2,2'-diol.



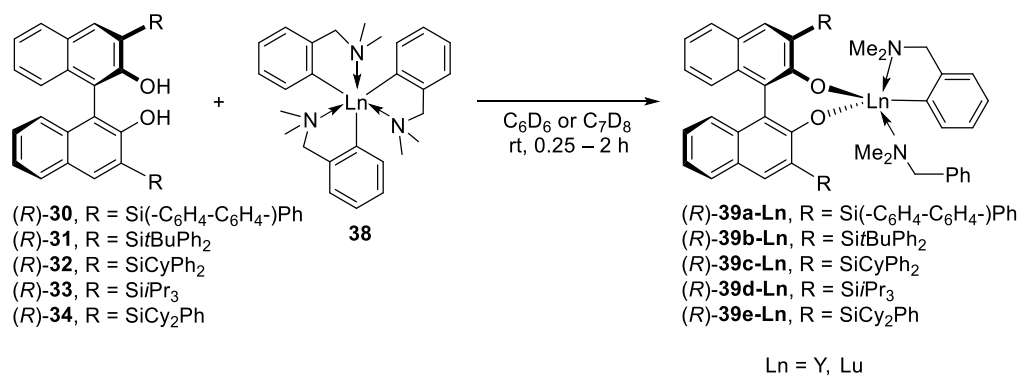
Scheme 2-5. Synthesis of di-*tert*-butyl(bromo)phenylsilane.

2.3 Synthesis and Characterization of Binaphtholate Rare Earth Metal Complexes

Prospective rare-earth metal complexes for efficient hydroamination catalysis generally possess at least one protonolytically cleavable Ln-C or Ln-N bond to allow catalyst activation to occur. A number of suitable precursors for the synthesis of binaphtholate rare-earth metal complexes are available, including [Ln{N(SiHMe₂)₂}₃(THF)₂] (**35**), [Ln{N(SiMe₃)₂}₃] (**36**), [Ln{CH(SiMe₃)₂}₃] (**37**) (Ln =

Y, La), and $[\text{Ln}(o\text{-C}_6\text{H}_4\text{CH}_2\text{NMe}_2)_3]$ (**38**, Ln = Y, Lu). Diolate complexes formed from **35** displayed poor catalytic activity and required elevated temperatures for hydroamination/cyclization of aminoalkenes.³⁰ Incomplete protonolysis of the Ln-N bond by the aminoalkene substrate due to the low basicity of the bis(dimethylsilyl)amido ligand was believed to be the origin of the low reactivity of binaphtholate complexes utilizing **35**.^{31,119} Higher reactivity was observed with complexes originating from **36**, which contained the more basic bis(trimethylsilyl)amido ligand. Binaphtholate lanthanum complexes utilizing **37** were also examined in a previous study,³¹ because rare-earth metals with larger ionic radius generally display higher catalytic activity. However, a combination of high activity and excellent enantioselectivities was not achieved with the complexes using these types of precursors.^{31,119} Inspired by the tremendous success in asymmetric hydroamination/cyclization of aminoalkenes achieved with (*R*)-**19a-Ln** and (*R*)-**19b-Ln** (Chapter 1, Table 1-4), we focused on syntheses of binaphtholate complexes utilizing $[\text{Ln}(o\text{-C}_6\text{H}_4\text{CH}_2\text{NMe}_2)_3]$ (Ln = Y, Lu).

Reaction of the highly bulky binaphthols **30–34** with **38** resulted in clean formation of rare-earth metal complexes **39a–e** in quantitative yields (by ^1H NMR spectroscopy) at room temperature in less than 2 hours. The formation of yttrium complexes was generally completed faster than that of corresponding lutetium complexes (Scheme 2-6). While $[\text{Y}(o\text{-C}_6\text{H}_4\text{CH}_2\text{NMe}_2)_3]$ ¹²⁴ and $[\text{Lu}(o\text{-C}_6\text{H}_4\text{CH}_2\text{NMe}_2)_3]$ ¹²⁵ could be prepared using literature procedures, $[\text{Sc}(o\text{-C}_6\text{H}_4\text{CH}_2\text{NMe}_2)_3]$ ^{119,126} could not be obtained in pure form. Attempts to purify the scandium precursor through crystallization in Et_2O were not successful.



Scheme 2-6. Synthesis of binaphtholate complexes utilizing [Ln(*o*-C₆H₄CH₂NMe₂)₃].

Complexes **39a–e** were prepared either in benzene or toluene and stored at room temperature for 7 days without decomposition. Attempts to crystallize the yttrium complexes from toluene, hexanes/toluene, and pentane/toluene mixtures yielded finely powdery materials, which were not suitable for X-ray crystallography analysis. After solvents were removed in vacuum, white or pale yellow solids were generally obtained in quantitative yields. Based on ¹H and ¹³C NMR spectra, the observation of methylene and methyl groups of *N,N*-dimethylbenzylamine suggests that the complexes retain one equivalent of *N,N*-dimethylbenzylamine.

The ¹H NMR spectrum of complex (R) -**39a-Y** can be obtained with good resolution at 25 °C (Figure 2-1, upper spectrum); however, at this temperature signals for CH₂ groups of *o*-C₆H₄CH₂NMe₂ ligand and those of coordinated and free *N,N*-dimethylbenzylamine of complex (R) -**39b-Y** coalesce to a broad peak. Upon cooling the solution of complex (R) -**39b-Y** to 0 °C, the signals decoalesce to separate peaks (Figure 2-1, lower spectrum).

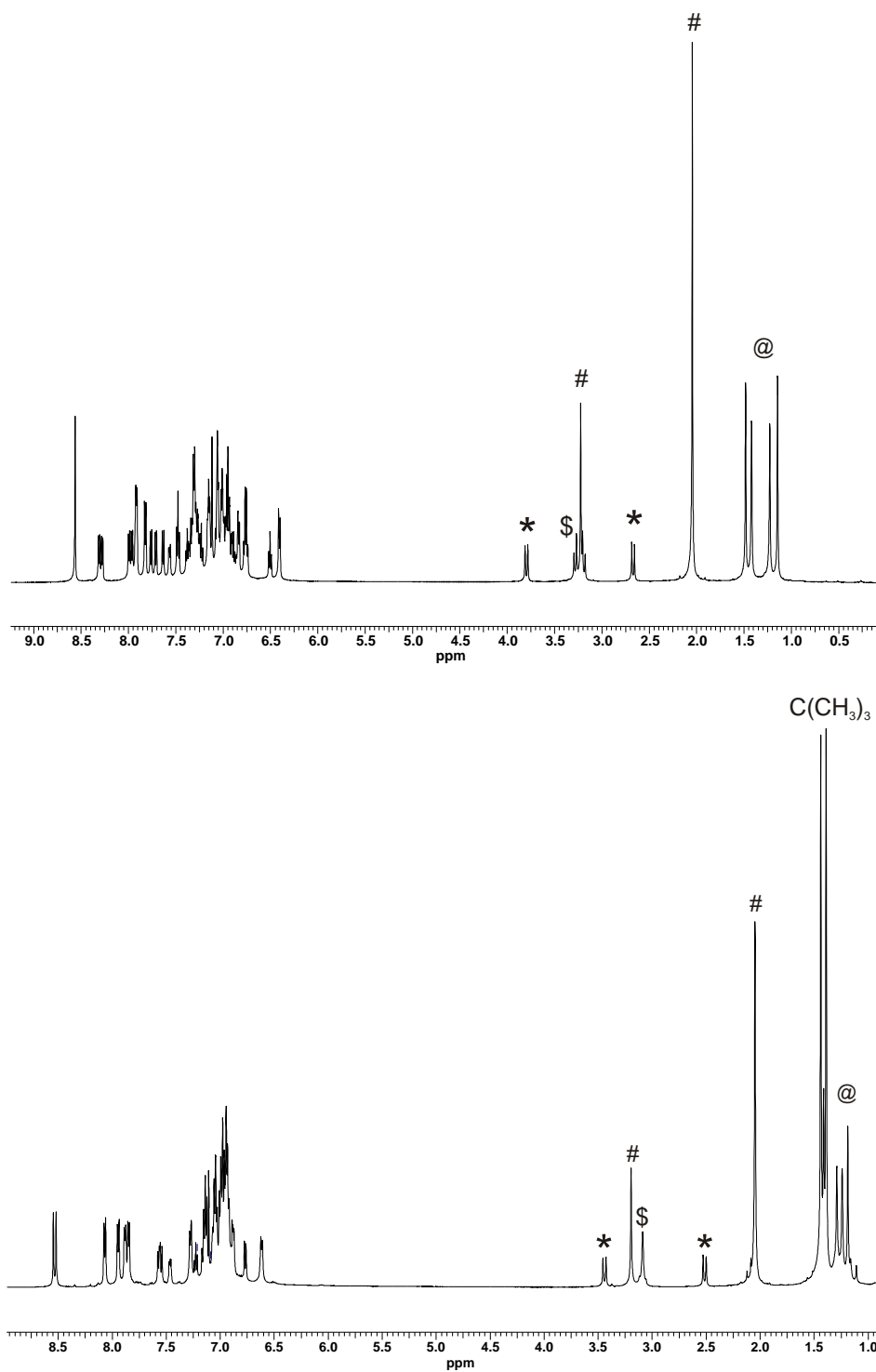
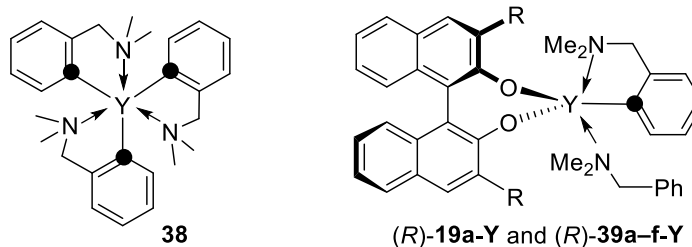


Figure 2-1. ^1H NMR spectra of (*R*)-**39a-Y** in C_6D_6 at 25°C (upper spectrum) and (*R*)-**39b-Y** in toluene-d_8 at 0°C (lower spectrum). * = CH_2 group of $o\text{-C}_6\text{H}_4\text{CH}_2\text{NMe}_2$ ligand; \$ = CH_2 group of coordinated *N,N*-dimethylbenzylamine; # = free *N,N*-dimethylbenzylamine; @ = $\text{N}(\text{CH}_3)_2$ moieties of $o\text{-C}_6\text{H}_4\text{CH}_2\text{NMe}_2$ ligand and coordinated *N,N*-dimethylbenzylamine.

Table 2-1. ^{13}C NMR chemical shifts and $^1J(\text{Y,C})$ coupling constants of yttrium complexes.

Entry	Complex	Solvent	T (°C)	^{13}C Chemical shift (ppm)	$^1J(\text{Y,C})$ Coupling constant (Hz)
1	38	C_6D_6	25	186.7	43.3
2	(R)-19a-Y ³¹	C_6D_6	6	182.0	52.7
3	(R)-39a-Y	C_6D_6	25	182.2	53.5
4	(R)-39b-Y	Tol- d_8	0	181.9	52.6
5	(R)-39c-Y	C_6D_6	25	181.5	53.5
6	(R)-39d-Y	C_6D_6	25	181.6	53.1
7	(R)-39e-Y	C_6D_6	6	181.5	53.5
8	(R)-39f-Y [*]	C_6D_6	25	181.6	52.3

We were also interested in ^{13}C NMR chemical shifts of carbons (labeled as black ●) on amide ligand, as well as $^1J(\text{Y,C})$ coupling constants (Table 2-1). Precursor $[\text{Y}(o\text{-C}_6\text{H}_4\text{CH}_2\text{NMe}_2)_3]$, **38**, is a known compound;¹²⁴ however, $^1J(\text{Y,C})$ coupling constant was not reported. The complex **38** was prepared using the literature procedure¹²⁴ and was spectroscopically characterized in C_6D_6 at 25 °C. It should be noted that the ^{13}C NMR spectra of the BINOL complexes **(R)-19a-Y** and **(R)-39a-f-Y** were acquired using

^{*} This complex was prepared by Dr. Alexander Reznichenko, a former Ph.D. candidate in the Hultsch group.

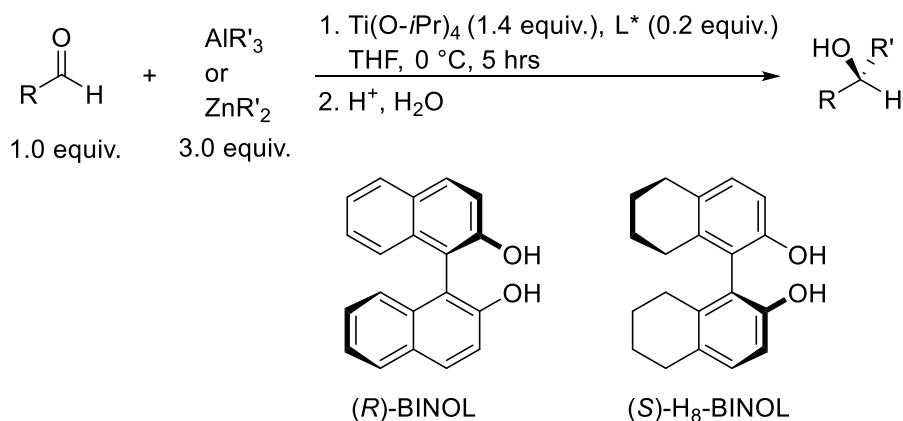
various deuterated solvents and temperatures, for their best resolutions. Because the ^{13}C NMR spectra are solvent-dependent, data in Table 2-1, entry 4 will not be included in the discussion. The ^{13}C NMR chemical shift of the labeled carbon of **38** and $^1J(\text{Y-C})$ coupling constant were 186.7 ppm and 43.3 Hz, respectively (Table 2-1, entry 1). The ^{13}C NMR chemical shifts moving upfield and increases in $^1J(\text{Y-C})$ coupling constants were observed for binaphtholate complexes (Table 2-1, entries 2, 3 and 5-8). So far, we have not found any correlation between ^{13}C NMR chemical shifts and $^1J(\text{Y,C})$ coupling constants of yttrium complexes and their catalytic activities and/or enantioselectivity in asymmetric hydroamination of alkenes (see Chapters 4 and 5).

Chapter 3

Octahydrobinaphtholate Rare Earth Metal Complexes

3.1 Introduction

Inspired by the results of the asymmetric hydroamination of alkenes catalyzed by binaphtholate rare earth metal complexes (reported earlier^{31,119} and discussed in chapters 4, 5, and 6), our attempts to increase the enantioselectivity and catalytic activity of the catalysts were focused on 3,3'-bis(alkylarylsilyl)-substituted octahydrobinaphtholate (H₈BINOL) ligands. While BINOL and its substituted derivatives have been extensively studied and have been applied in many chiral catalysts for asymmetric synthesis, studies involving H₈BINOL have been also reported in recent years.¹²⁷⁻¹³⁶ H₈BINOL contains sp³ hybridized carbons leading to an increase in steric bulkiness and also an increase in dihedral angle. ChemDraw 3D calculation (MM2) estimates the dihedral angles of the axial biaryl groups of BINOL to be 72.3°, while it is 94.3° for H₈BINOL.¹²⁷ And in many cases, these structural modifications result in improvements of enantioselectivity of the catalysts.¹²⁷ For examples, higher enantioselective products were achieved with titanium-H₈BINOL catalysts in comparison to (BINOL)Ti complexes in the asymmetric addition of alkylzinc and alkylaluminum reagents to aldehydes (Table 3-1).^{137,138}



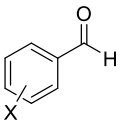
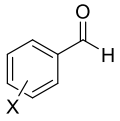
		Enantioselectivity, % ee		
Reagent	Aldehyde	L* = (<i>R</i>)-BINOL	(<i>S</i>)-H ₈ BINOL	
ZnEt ₂		X = H	92	98
		X = <i>ortho</i> -Br	59	85
		X = <i>para</i> -OMe	79	95
AlEt ₃		X = H	81	96
		X = <i>ortho</i> -Cl	62	91
		X = <i>para</i> -OMe	67	93

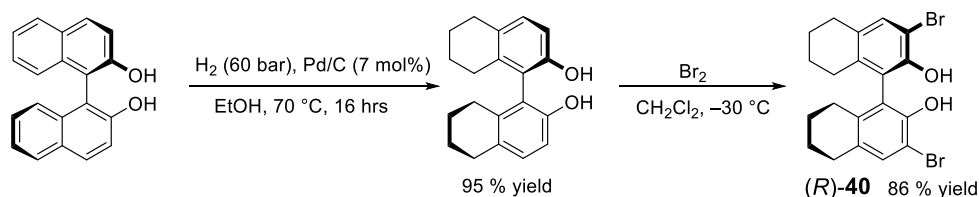
Table 3-1. Comparison of BINOL and H₈BINOL-based titanium catalysts in the asymmetric addition of alkylzinc and alkylaluminum reagents to aldehydes.^{137,138}

3.2 Synthesis of 3,3'-Bis(alkylarylsilyl)-Substituted Octahydrobinaphthol Ligands

While (*R*)-H₈BINOL is commercially available, it can be prepared easily using literature procedure,¹³⁹ by reducing the corresponding BINOL under high pressure of

hydrogen gas in the presence of Pd/C as a catalyst. Heating was required to facilitate the hydrogenation. Moreover, stirring the reaction overnight was essential to achieve complete conversion. Shorter reaction times led to a mixture of the intermediate H₄BINOL and H₈BINOL.

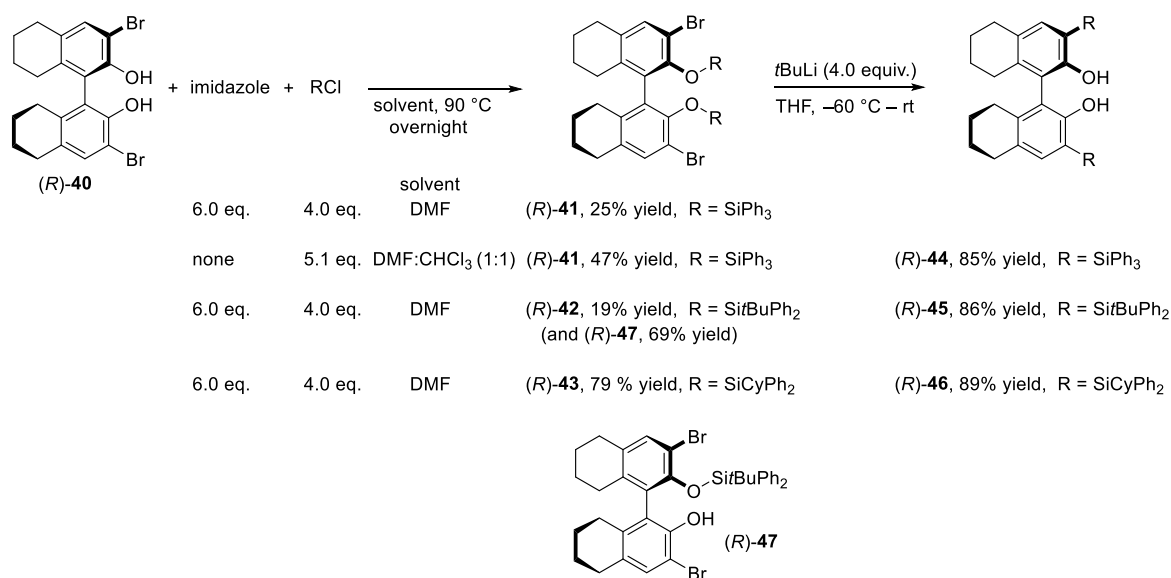
H₈BINOL displays different reactivity from BINOL in the electrophilic aromatic substitution. When BINOL is treated with bromine, the bromination occurs preferentially at the 6,6'-positions and then at 4,4'-positions.¹⁴⁰ The preparation of 3,3'-dibromo-1,1'-binaphthalene-2,2'-diol **29** from BINOL requires methyl- or MOM-protection of the hydroxyl groups, then ortho-lithiation, followed by bromination, and finally deprotection.^{121,141} However, bromination of (*R*)-H₈BINOL at the *ortho*-positions was achieved directly to generate (*R*)-3,3'-dibromo-H₈BINOL¹⁴² (*R*)-**40** in 86% yield (Scheme 3-1).



Scheme 3-1. Synthesis of (*R*)-3,3'-dibromo-H₈BINOL from (*R*)-BINOL

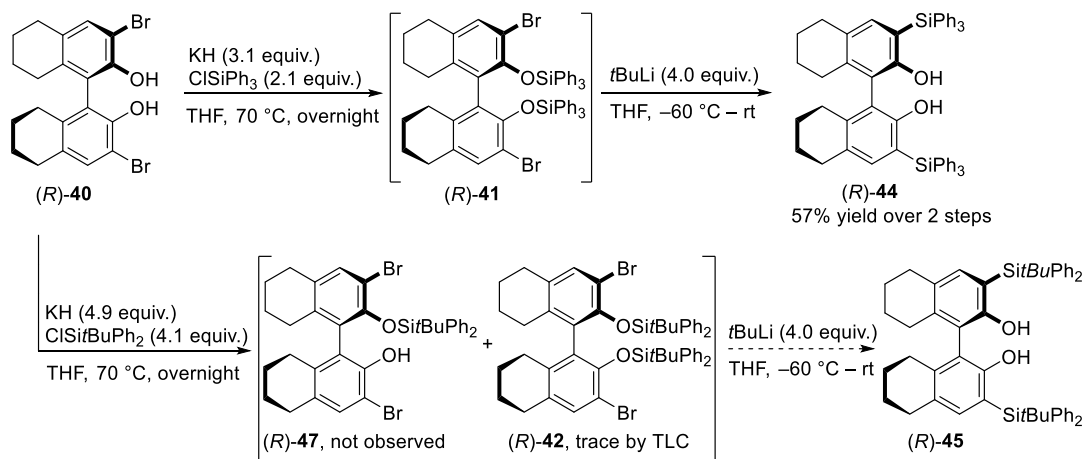
The successful syntheses of 3,3'-bis(arylalkylsilyl)-2,2'-dihydroxy-1,1'-binaphthylene from 3,3'-dibromo-2,2'-dihydroxy-1,1'-binaphthylene *via* retro-Brook rearrangement of the silyl ether (discussed in Chapter 2), have encouraged us to utilize the same synthetic route to prepare the corresponding 3,3'-bis(arylalkylsilyl)-5,5',6,6',7,7',8,8'-2,2'-dihydroxy-1,1'-binaphthylene. Unfortunately the silylation of (*R*)-

40 under forcing conditions (heated to 90 °C overnight in the presences of excessive imidazole and chlorosilane) gave (*R*)-**41** in 25% yield (Scheme 3-2) when triphenylchlorosilane was used. We also applied a literature procedure¹⁴³ to prepare (*R*)-**41**, in which a 1:1 solvent mixture of DMF and CHCl₃ was used in the absence of imidazole. We could not reproduce the reported high yield of up to 89%; however, the yield increased from 25% to 47%. The synthesis of (*R*)-**45** from (*R*)-**40** gave only 16% yield over 2 steps, due to the difficulty in the formation of disilyl ether (*R*)-**42** described in Scheme 3-2. It is worth noting that the mono-silylated H₈BINOL (*R*)-**47** was the main product, 69% yield, in the silylation reaction of (*R*)-**40** with *tert*-butyldiphenylchlorosilane. Cyclohexyldiphenylchlorosilane gave a better yield of the silyl ether (*R*)-**43** (79%) under the same reaction conditions. In all cases, the silyl ethers were smoothly transformed to the desired 3,3'-disilyl-substituted octahydrobinaphthol derivatives *via* retro-Brook rearrangement in high yields (Scheme 3-2).



Scheme 3-2. Synthesis of 3,3'-disilyl-substituted octahydrobinaphthols.

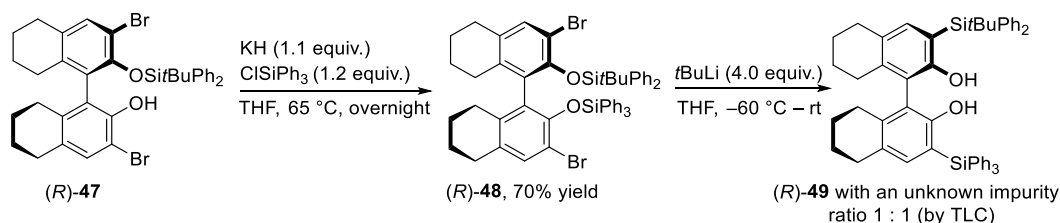
(*R*)-**44** was also synthesized using a one pot reaction procedure as described in Scheme 3-3. The silylation reaction proceeded cleanly as indicated by thin layer chromatography (TLC). 3,3'-Dibromo- H_8 BINOL ((*R*)-**40**) was consumed completely to form di-silylation product (*R*)-**41** and no mono-silylation product was observed. The overall yield, however, was only 57% due to formation of an unidentified side product during the retro-Brook rearrangement. The same reaction conditions were applied in the synthesis of (*R*)-**45**. Unfortunately, only trace amounts of (*R*)-**42** were detected by TLC, because *tert*-butyldiphenylchlorosilane is sterically more hindered than triphenylchlorosilane, thus making the silylation reaction harder to proceed (Scheme 3-3).



Scheme 3-3. Synthesis of (*R*)-3,3'-di(triphenylsilyl)- H_8 BINOL using one-pot procedure.

We were also interested in preparing the unsymmetrically (*R*)-3,3'-disubstituted H_8 BINOL proligand (*R*)-**49**. Mono-silylated compound (*R*)-**47** (prepared from (*R*)-**40**, described in Scheme 3-2) was deprotonated by KH before it was treated with triphenylchlorosilane, yielding (*R*)-**48** in 70% yield (Scheme 3-4). Unfortunately the retro-Brook rearrangement of (*R*)-**48** led to the desired unsymmetrically (*R*)-3,3'-

disubstituted H₈BINOL proligand (*R*)-**49** with an unknown impurity which could not be separated through column chromatography. An attempt to isolate (*R*)-**49** by crystallization in pentane was not successful.



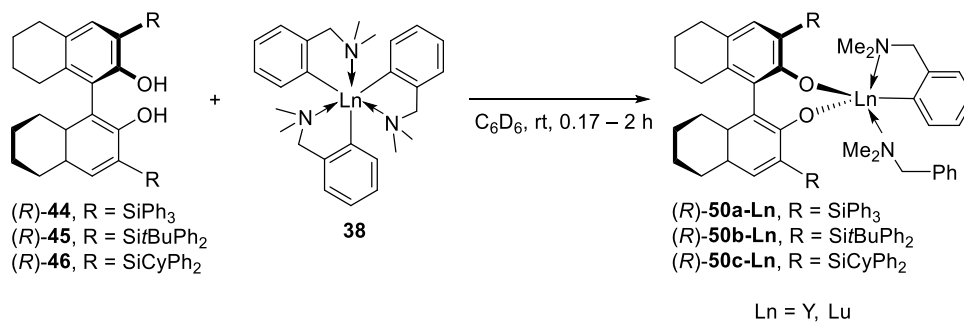
Scheme 3-4. Attempted synthesis of the unsymmetrically (*R*)-3,3'-disubstituted H₈BINOL proligand **49**.

3.3 Synthesis and Characterization of Octahydrobinaphtholate Rare-Earth Metal Complexes

Binaphtholate rare-earth metal complexes (*R*)-**19a–b** (Chapter 1, Table 1-4) and (*R*)-**39a–e** (Chapters 4-6) display high reactivity and excellent enantioselectivities in the asymmetric hydroamination of alkenes. Inspired by those promising results, we focused on the synthesis of octahydrobinaphtholate complexes utilizing [Ln(*o*-C₆H₄CH₂NMe₂)₃] (**38**) (Ln = Y, Lu).

Reactions of the highly bulky (*R*)-3,3'-disubstituted H₈BINOL proligands (*R*)-**44**, (*R*)-**45**, and (*R*)-**46** with **38** resulted in the clean formation of rare-earth metal complexes (*R*)-**50a–Ln**, (*R*)-**50b–Ln**, and (*R*)-**50c–Ln**, respectively, in quantitative yields (by ¹H NMR spectroscopy, see Figure 3-1) at room temperature in less than 2 hours (Scheme 3-5). While [Y(*o*-C₆H₄CH₂NMe₂)₃] generally took less than 10 minutes to complete

formation of the complexes, $[\text{Lu}(o\text{-C}_6\text{H}_4\text{CH}_2\text{NMe}_2)_3]$ was less reactive and required up to 2 hours.



Scheme 3-5. Synthesis of octahydrobinaphtholate rare-earth metal complexes.

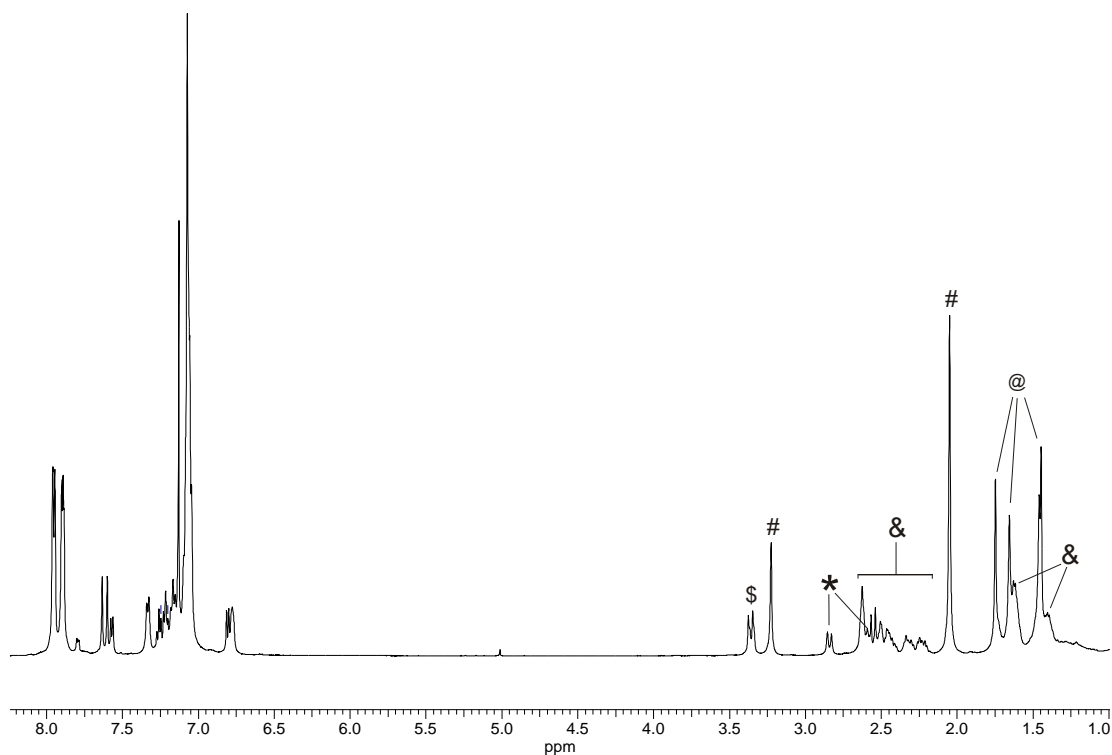


Figure 3-1. ^1H NMR spectra of $(R)\text{-50a-Y}$ in C_6D_6 at 6°C . \$ = CH_2 group of coordinated N,N -dimethylbenzylamine; # = free N,N -dimethylbenzylamine; * = CH_2 group of $o\text{-C}_6\text{H}_4\text{CH}_2\text{NMe}_2$ ligand; & = CH_2 groups of octahydrobinaphtholate ligand; @ = $\text{N}(\text{CH}_3)_2$ moieties of $o\text{-C}_6\text{H}_4\text{CH}_2\text{NMe}_2$ ligand and coordinated N,N -dimethylbenzylamine.

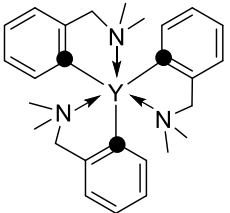
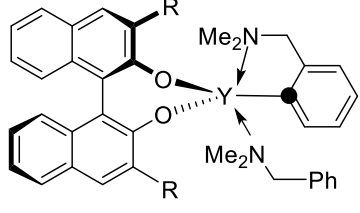
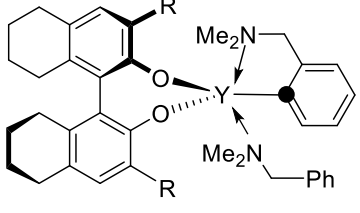
The ^1H NMR spectra of complex (*R*)-**50a-Y**, (*R*)-**50b-Y**, and (*R*)-**50c-Y** were acquired at 6 °C in C_6D_6 for good spectral resolutions. At 25 °C, signals for CH_2 group of *o*- $\text{C}_6\text{H}_4\text{CH}_2\text{NMe}_2$ ligand and those of coordinated and free *N,N*-dimethylbenzylamine of octahydrobinaphtholate complexes coalesce to a broad peak. Upon cooling the solutions of complexes to 6 °C, the signals decoalesce to separate peaks (see Figure 3-1 for the ^1H NMR spectra of complex (*R*)-**50a-Y**).

Complexes **50a-c** were prepared in benzene and stored at room temperature for 7 days without decomposition. Attempts to crystallize the yttrium complexes from toluene, hexanes/toluene, and pentane/toluene mixtures, for X-ray crystallography analysis were not successful. Based on ^1H and ^{13}C NMR spectra, the observation of methylene and methyl groups of *N,N*-dimethylbenzylamine suggests that the complexes retain one equivalent of *N,N*-dimethylbenzylamine.

^{13}C NMR chemical shifts of carbons (labeled as black ●) on amide ligands of octahydrobinaphtholate yttrium complexes (*R*)-**50a-c-Y** were almost the same (Table 3-2, entries 5–7), and similar to those of their corresponding binaphtholate yttrium complexes (*R*)-**19a-Y** and (*R*)-**39b-c-Y** (Table 3-2, entries 2–4). The ^{13}C NMR chemical shifts of octahydrobinaphtholate yttrium complexes moved slightly upfield in comparison to yttrium complex **38** (Table 3-2, entries 5–7 versus entry 1). Increases in $^1J(\text{Y,C})$ coupling constants of (*R*)-**50a-c-Y** were observed when two *N,N'*-dimethylbenzylamine ligands on yttrium complex **38** were replaced by octahydrobinaphthol ligands (Table 3-2, entries 5–7 vs. entry 1). $^1J(\text{Y,C})$ coupling constants of octahydrobinaphtholate yttrium complexes (*R*)-**50a-b-Y** were similar to those of their corresponding binaphtholate yttrium complexes (*R*)-**19a-Y** and (*R*)-**39b-Y**. So far, we have not found any correlation

between ^{13}C NMR chemical shifts and $^1J(\text{Y},\text{C})$ coupling constants of yttrium complexes and their catalytic activities and/or enantioselectivity in asymmetric hydroamination of alkenes (see Chapters 4 and 5).

Table 3-2. ^{13}C NMR chemical shifts and $^1J(\text{Y},\text{C})$ coupling constants of yttrium complexes.

<div style="display: flex; justify-content: space-around; align-items: center;"> <div style="text-align: center;">  <p>38</p> </div> <div style="text-align: center;">  <p>(R)-19a-Y and (R)-39b-c-Y</p> </div> <div style="text-align: center;">  <p>(R)-50a-c-Y</p> </div> </div>					
Entry	Complex	Solvent	T (°C)	^{13}C Chemical shift (ppm)	$^1J(\text{Y},\text{C})$ Coupling constant (Hz)
1	38	C_6D_6	25	186.7	43.3
2	(R)-19-Y ³¹	C_6D_6	6	182.0	52.7
3	(R)-39b-Y	Tol-d8	0	181.9	52.6
4	(R)-39c-Y	C_6D_6	25	181.5	53.5
5	(R)-50a-Y	C_6D_6	6	182.1	52.6
6	(R)-50b-Y	C_6D_6	6	182.2	52.6
7	(R)-50c-Y	C_6D_6	6	181.7	52.5

Chapter 4

Asymmetric Intramolecular Hydroamination of Aminoalkenes

4.1 Introduction

Nitrogen-containing compounds play an important role in natural products and biologically active molecules.¹⁻⁴ The metal-catalyzed asymmetric intramolecular hydroamination of alkenes, in which an amine N-H functionality is added to an unsaturated carbon-carbon bond, is one of the most atom-economic and simplest processes to generate enantioenriched nitrogen heterocycles.^{9,12,25,26,29,144,145} The last two decades have seen significant developments of catalytic systems for this challenging transformation, but only a limited number of metal complexes for the efficient and highly enantioselective formation of cyclic amines have been reported.^{31,68,71,84} Despite of the high sensitivity toward air and moisture and low functional group tolerance, rare-earth metal complexes are among the most reactive catalysts for asymmetric intramolecular hydroamination of alkenes.³¹ The Hultsch research group first reported chiral binaphtholate catalysts based on rare-earth metals for the hydroamination of aminoalkenes, displaying the same high catalytic activity as the lanthanocene catalysts and excellent enantioselectivities of up to 95% ee.^{31,58} However these inspiring catalytic results were only observed for a limited range of aminoalkene substrates. Therefore, the

development of new catalysts for the asymmetric hydroamination of alkenes is still an important problem.

In this chapter we will report our extended study of the asymmetric intramolecular hydroamination of aminoalkenes catalyzed by a series of binaphtholate and octahydrobinaphtholate rare-earth metal complexes (Figure 4-1).

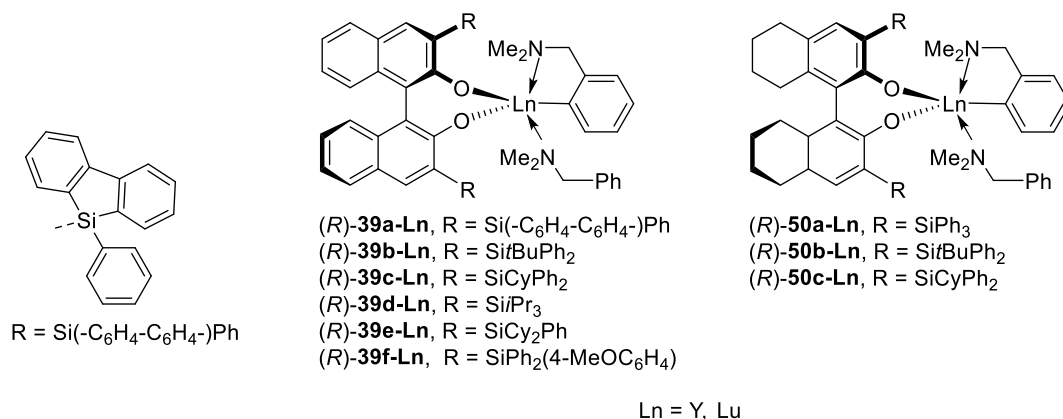


Figure 4-1. Binaphtholate and octahydrobinaphtholate rare-earth metal catalysts for asymmetric hydroamination.

4.2 Catalytic Results and Discussion

4.2.1 Asymmetric Intramolecular Hydroamination of Primary Amines

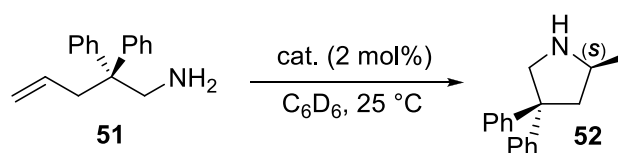
The binaphtholate and octahydrobinaphtholate rare-earth metal complexes were evaluated with a wide range of selective aminoalkenes for the asymmetric intramolecular hydroamination/cyclization. While aminopentenes **51**, **53**, **55**, and **57** and aminohexene **59** were cyclized smoothly at room temperature, aminoheptene **61** required high catalytic loading at elevated temperature to generate azepane **62** (Tables 4-1 – 4-5). In general, the

hydroamination/cyclization reaction rates decreased with increasing sizes of heterocyclic rings, $5 > 6 \gg 7$. For example, the turnover frequencies in the hydroamination using (*R*)-**39c-Y** decreased in the following sequence: aminopentene **51** (746 h^{-1} @ 25°C) $>$ aminohexene **59** (6.5 h^{-1} @ 25°C) \gg aminoheptene **61** (0.17 h^{-1} @ 80°C) (Tables 4-1 and 4-5).

We started the catalytic evaluation with one of the most reactive substrate, the *gem*-diphenyl-substituted aminopentene **51**. Our previous study³¹ showed that the cyclization of **51** proceeded with rates as high as 840 h^{-1} using the triphenylsilyl-substituted binaphtholate complex (*R*)-**19a-Y**. We believe that the sterically demanding tris(aryl)silyl substituents in the 3 and 3' positions of the binaphtholate ligand play a vital role in catalytic activity and stereoselectivities, as well as catalyst stability. As expected, (*R*)-**39a-Ln** ($\text{Ln} = \text{Y, Lu}$) with a more rigid, but less bulky structure in the silyl-substituent compared to (*R*)-**19a-Ln**, exhibited decreased reaction rates as well as selectivities (Table 4-1, entries 1, 2 and 4, 5).

The binaphtholate complexes (*R*)-**39b-Lu** and (*R*)-**39c-Lu**, containing sterically more hindered *tert*-butyldiphenylsilyl and cyclohexyldiphenylsilyl groups, respectively, displayed significantly increased catalytic activity in the hydroamination/cyclization of **51** compared to (*R*)-**19a-Lu** (Table 4-1, entries 2, 7, and 9). Moreover, higher enantioselectivities of up to 95% ee were also achieved with these highly bulky binaphtholate complexes (Table 4-1, entries 7, 9).

Table 4-1. Asymmetric hydroamination of **51** catalyzed by the binaphtholate and octahydrobinaphtholate rare-earth metal complexes



Entry	Catalyst ^a	<i>t</i> (h) ^b	<i>TOF</i> (h ⁻¹)	ee (%) ^c
1	(<i>R</i>)- 19a-Y	0.06	≥ 840	84 ^d
2	(<i>R</i>)- 19a-Lu	0.25	≥ 180	93 ^d
3	(<i>R</i>)- 19a-Sc	0.6	110	95 ^d
4	(<i>R</i>)- 39a-Y	0.27	185	66
5	(<i>R</i>)- 39a-Lu	0.30	167	82
6	(<i>R</i>)- 39b-Y	0.067	764	87
7	(<i>R</i>)- 39b-Lu	0.071	704	95
8	(<i>R</i>)- 39c-Y	0.067	746	85
9	(<i>R</i>)- 39c-Lu	0.067	724	95
10	(<i>R</i>)- 39d-Y	0.18	273	78
11	(<i>R</i>)- 39d-Lu	0.33	152	81
12	(<i>R</i>)- 39e-Y	0.16	316	77
13	(<i>R</i>)- 39e-Lu	0.083	600	86
14	(<i>R</i>)- 39f-Y	0.046	1090	73
15	(<i>R</i>)- 39f-Lu	0.050	1000	82
16	(<i>R</i>)- 50a-Y	0.033	1500	88
17	(<i>R</i>)- 50a-Lu	0.033	1500	91
18	(<i>R</i>)- 50b-Y	0.042	1200	91
19	(<i>R</i>)- 50b-Lu	0.033	1500	97
20	(<i>R</i>)- 50c-Y	0.021	2400	83
21	(<i>R</i>)- 50c-Lu	0.033	1500	96

^a Reaction condition: 0.1 M solution of substrate **51** in C₆D₆, Ar atm, at 25 °C.

^b At which at least 95% NMR conversion was obtained relative to ferrocene internal standard. ^c Enantiomeric excess determined by ¹⁹F NMR of the Mosher amides. ^d From ref. 31.

However, (*R*)-**39e-Ln**, containing dicyclohexylphenylsilyl-substituted binaphtholate ligand, which can be considered as the most sterically demanding binaphtholate complex we have prepared so far, displayed no improved catalytic results (Table 4-1, entries 12, 13). It is noteworthy that **51** was cyclized using (*R*)-**39e-Lu** (TOF = 600 h⁻¹) at a rate about twice as fast as (*R*)-**39e-Y** (TOF = 316 h⁻¹). This observation is in contrast to the general trend for substrate **51**, in which the catalytic activity decreases with decreasing ionic radius for most other binaphtholate catalysts (Table 4-1).

Substitution of one phenyl substituent in (*R*)-**19a-Ln** by a *para*-methoxyphenyl group represents a small modification to the steric demand of the trisarylsilyl substituent, but the resulting complexes (*R*)-**39f-Ln** showed improved turnover frequencies of up to 1090 h⁻¹ (Table 4-1, entry 14). However, at the same time the enantioselectivities were diminished in comparison to (*R*)-**19a-Ln** (compare Table 4-1, entries 1, 2 with entries 14, 15).

The sterically more demanding octahydrobinaphtholate complexes (*R*)-**50a-Ln**, (*R*)-**50b-Ln**, and (*R*)-**50c-Ln** with larger biaryl dihedral angles compared to the corresponding binaphtholate complexes (*R*)-**19a-Ln**, (*R*)-**39b-Ln**, and (*R*)-**39c-Ln** generally exhibited improved activities and enantioselectivities in the catalytic hydroamination/cyclization of **51** (Table 4-1, entries 1, 2, 4–9 and 16–21). While enantioselectivity of up to 97% ee for pyrrolidine **52** was achieved with (*R*)-**50b-Lu**, the fastest rate of cyclization of **51** was observed with (*R*)-**50c-Y** (turnover frequency of up to 2400 h⁻¹; Table 4-1, entries 19, 20).

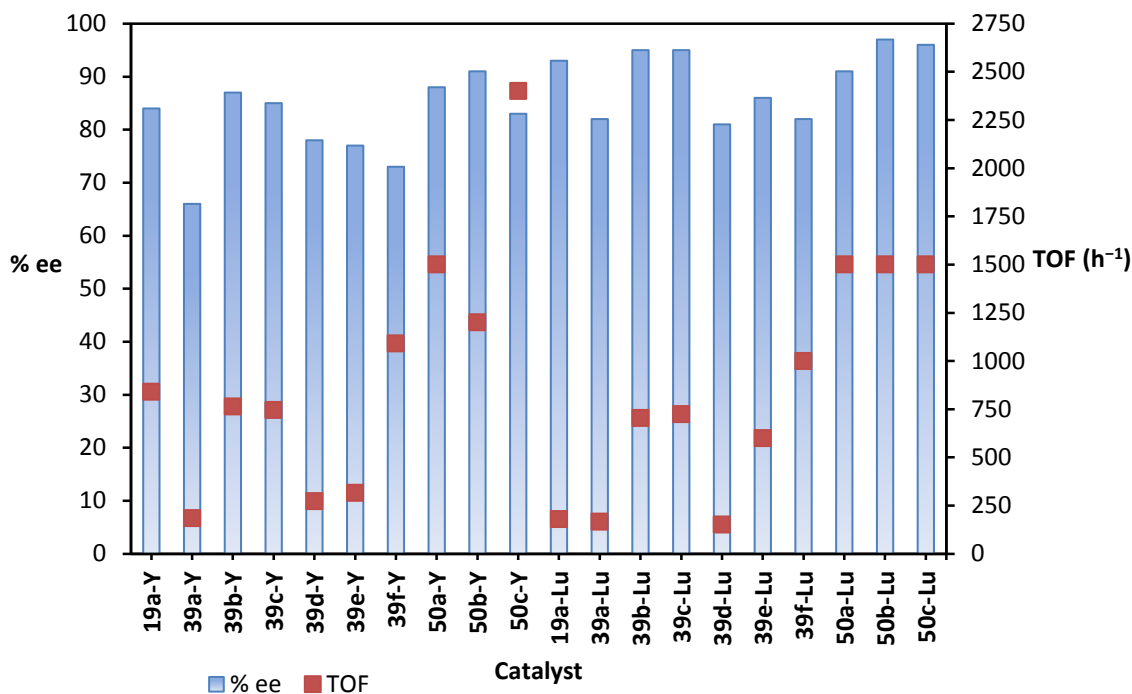
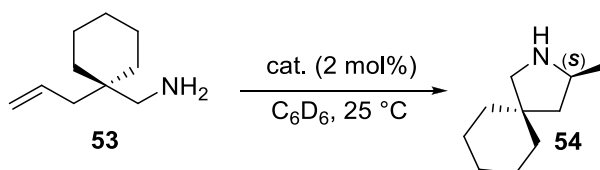


Figure 4-2. Turnover frequency (scatter chart) and enantioselectivity (column chart) profiles for the hydroamination of aminoalkene **51** catalyzed by binaphtholate and octahydrobinaphtholate rare-earth metal complexes.

The catalytic data of the hydroamination of aminoalkene **51** catalyzed by the binaphtholate and octahydrobinaphtholate rare-earth metal complexes, which were discussed in Table 4-1, could be summarized in Figure 4-2 above. It clearly shows that the cyclization proceeds most efficiently using the octahydrobinaphtholate complexes (*R*)-**50b-Lu** and (*R*)-**50c-Lu**, giving a combination of the fastest rates and the highest enantioselectivities (Figure 4-2).

Table 4-2. Catalytic evaluation of the hydroamination/cyclization of **53**

Entry	Catalyst ^a	<i>t</i> (h) ^b	<i>TOF</i> (h ⁻¹)	ee (%) ^c
1	(<i>R</i>)- 19a-Lu	0.11	460	83 ^d
2	(<i>R</i>)- 39a-Y	0.50	98	49
3	(<i>R</i>)- 39a-Lu	0.58	84	75
4	(<i>R</i>)- 39b-Y	0.075	640	69
5	(<i>R</i>)- 39b-Lu	0.14	340	86
6	(<i>R</i>)- 39c-Y	0.083	602	80
7	(<i>R</i>)- 39c-Lu	0.083	590	89
8	(<i>R</i>)- 39d-Y	0.22	223	43
9	(<i>R</i>)- 39d-Lu	0.50	97	59
10	(<i>R</i>)- 39e-Y	0.18	273	73
11	(<i>R</i>)- 39e-Lu	0.23	214	87
12	(<i>R</i>)- 39f-Y	0.13	375	65
13	(<i>R</i>)- 39f-Lu	0.23	214	81
14	(<i>R</i>)- 50a-Y	0.058	840	85
15	(<i>R</i>)- 50a-Lu	0.083	588	91
16	(<i>R</i>)- 50b-Y	0.075	667	84
17	(<i>R</i>)- 50b-Lu	0.12	429	90
18	(<i>R</i>)- 50c-Y	0.058	857	85
19	(<i>R</i>)- 50c-Lu	0.042	1200	98

^a Reaction condition: 0.1 M solution of substrate **53** in C₆D₆, Ar atm. ^b At which at least 95% NMR conversion was obtained relative to ferrocene internal standard. ^c Enantiomeric excess determined by ¹⁹F NMR of the Mosher amides. ^d From ref. 31.

The cyclization of **53** proceeded smoothly at room temperature within a period of minutes to half an hour generating pyrrolidine **54** with moderate to excellent enantioselectivities (43–98% ee) (Table 4-2). Similar to the *gem*-diphenyl-substituted aminopentene **51**, substrate **53** displayed lower activity and lower selectivities for (*R*)-**39a-Ln** and (*R*)-**39d-Ln**, in comparison to other binaphtholate catalysts (Table 4-2, entries 2, 3, 8, 9). Among the binaphtholate complexes, the highest enantioselectivity of 89% ee was achieved with (*R*)-**39c-Lu** (Table 4-2, entry 7), whereas the fastest reaction rate was observed with (*R*)-**39b-Y** (TOF = 640 h⁻¹, Table 4-2, entry 4). In contrast to the results observed with **51**, (*R*)-**39f-Lu** exhibited lower activity in the cyclization of **53** compared to (*R*)-**19a-Lu** (Table 4-2, entries 1 and 13).

Significant improvements in activity and stereoselectivities were observed in the cyclization of **53** using the octahydrobinaphtholate complexes (*R*)-**50a-Ln**, (*R*)-**50b-Ln**, and (*R*)-**50c-Ln**, in comparison to the corresponding binaphtholate complexes (*R*)-**19a-Ln**, (*R*)-**39b-Ln**, and (*R*)-**39c-Ln** (Table 4-2, entries 14–19 and 1, 4–7). Interestingly, the most active catalyst (*R*)-**50c-Lu** for the hydroamination of **53** generated the pyrrolidine **54** with the highest selectivity of 98% ee (Table 4-2, entry 19).

The catalytic results of the hydroamination of aminoalkene **53** catalyzed by the binaphtholate and octahydrobinaphtholate rare-earth metal complexes is summarized in Figure 4-3 below.

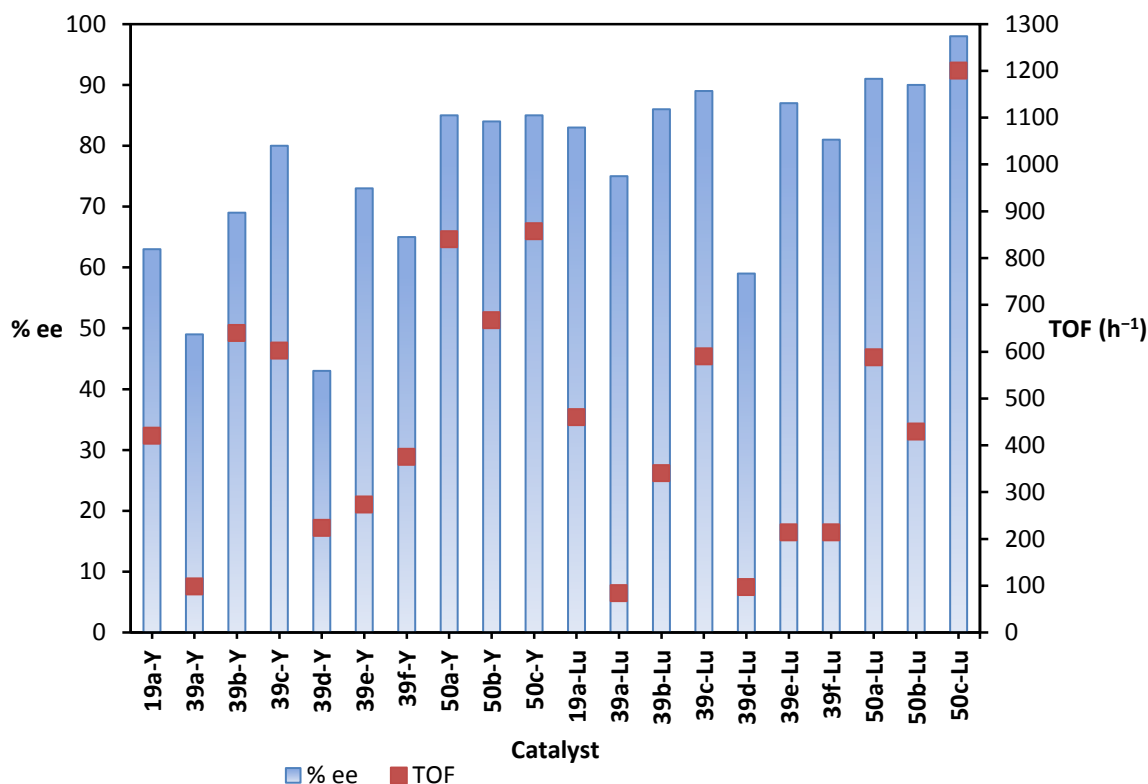
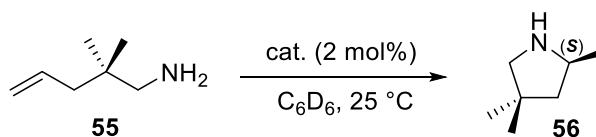


Figure 4-3. Turnover frequency (scatter chart) and enantioselectivity (column chart) profiles for the hydroamination of aminoalkene **53** catalyzed by binaphtholate and octahydrobinaphtholate rare-earth metal complexes.

The *gem*-dimethyl-substituted aminopentene **55** could be cyclized by the binaphtholate and octahydrobinaphtholate rare-earth metal complexes at room temperature within a reasonable period of time; however, the substrate showed significantly reduced reactivity toward the catalysts compared to substrates **51** and **53** (Table 4-3). For example, the cyclization of **51** and **53** proceeded with rates as high as 764 h⁻¹ and 340 h⁻¹ at the room temperature using (*R*)-**39b-Y** (Table 4-1, entry 6 and Table 4-2, entry 5, respectively) while a much lower reaction rate (20 h⁻¹) was observed for the cyclization of **55** under the same catalytic reaction condition (Table 4-3, entry 4).

Table 4-3. Catalytic evaluation of the hydroamination/cyclization of **55**

Entry	Catalyst ^a	<i>t</i> (h) ^b	<i>TOF</i> (h ⁻¹)	ee (%) ^c
1	(<i>R</i>)- 19a-Lu	27.5	2.4	69 ^d
2	(<i>R</i>)- 39a-Y	13.5	4	26
3	(<i>R</i>)- 39a-Lu	17.0	3	60
4	(<i>R</i>)- 39b-Y	2.5	20	50
5	(<i>R</i>)- 39b-Lu	23.0	2.2	78
6	(<i>R</i>)- 39c-Y	3.75	13	59
7	(<i>R</i>)- 39c-Lu	5.25	10	84
8	(<i>R</i>)- 39c-Lu ^e	0.67	75	87
9	(<i>R</i>)- 39c-Lu ^f	0.17	294	89
10	(<i>R</i>)- 39c-Lu ^g	< 0.025	> 2000	90
11	(<i>R</i>)- 39d-Y	4.0	12.3	22
12	(<i>R</i>)- 39d-Lu	10.0	4.8	39
13	(<i>R</i>)- 39e-Y	7.0	7	59
14	(<i>R</i>)- 39e-Lu	9.0	5.4	73
15	(<i>R</i>)- 39f-Y	8.5	5.8	41
16	(<i>R</i>)- 39f-Lu	20.5	2.5	59
17	(<i>R</i>)- 50a-Y	5.5	8.9	63
18	(<i>R</i>)- 50a-Lu	8.0	6.3	86
19	(<i>R</i>)- 50b-Y	2.0	24	69
20	(<i>R</i>)- 50b-Lu	6.0	8.3	83
21	(<i>R</i>)- 50c-Y	1.75	28.6	72
22	(<i>R</i>)- 50c-Lu	1.75	28.6	88

^a Reaction condition: 0.2 M solution of substrate **55** in C₆D₆, Ar atm. ^b At which at least 95% NMR conversion was obtained relative to ferrocene internal standard. ^c Enantiomeric excess determined by ¹⁹F NMR of the Mosher amides. ^d From ref. 31. ^e At 40 °C. ^f At 60 °C. ^g In toluene-*d*₈ at 110 °C.

While binaphtholate catalysts (*R*)-**39a–f** exhibit comparable catalytic activity in the hydroamination of **55** at room temperature in the range of 2.2–20 h⁻¹, the enantioselectivities vary over a broad range (Table 4-3, entries 2–16). The highest enantioselectivity of up to 84% ee was achieved at the room temperature using (*R*)-**39c-Lu**, whereas the sterically less demanding complex (*R*)-**39d-Y** furnished pyrrolidine **56** with an enantioselectivity of 22% ee. In general, the sterically more hindered binaphtholate complexes (*R*)-**39b-Lu**, (*R*)-**39c-Lu**, and (*R*)-**39e-Lu** were the more enantioselective catalysts for the catalytic hydroamination of **55** than other binaphtholate complexes (Table 4-3, entries 5, 7, and 14).

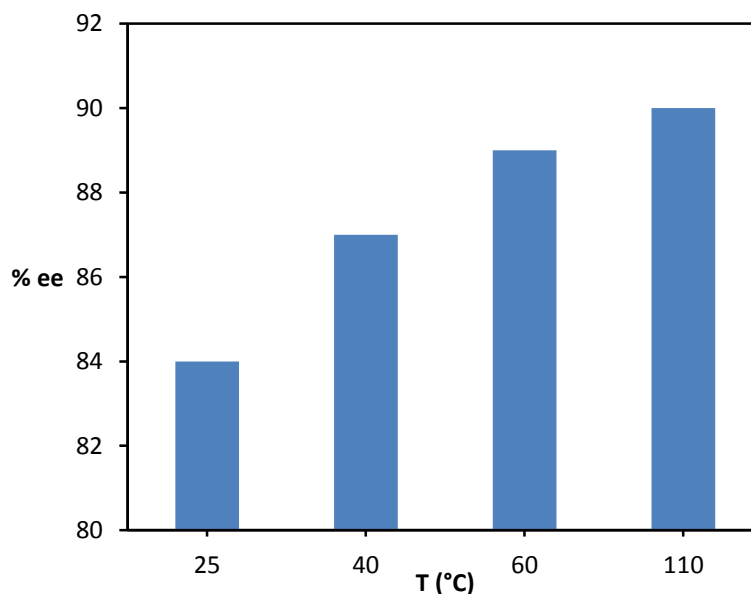
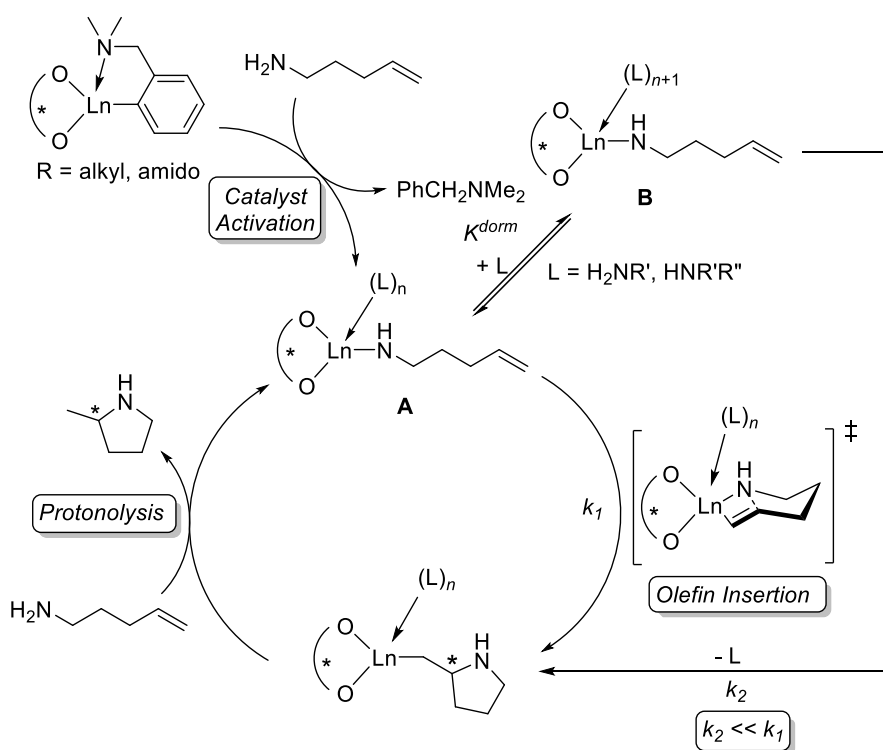


Figure 4-4. Temperature dependence of enantioselectivity in cyclization of **55** using (*R*)-**39c-Lu**.

It is noteworthy that increased selectivities were observed in the cyclization of **55** using (*R*)-**39c-Lu** as the temperature was raised, reaching the maximum enantioselectivity of up to 90% ee at 110 °C (Table 4-3, entries 7–10). The unusual

observation can be explained with an equilibrium between two species **A** and species **B**, as depicted in Scheme 4-1.⁴² The lower coordinate species **A** is catalytically more active and more selective than the sterically more crowded species **B**.³¹ As the temperature increases, the equilibrium between species **A** and species **B** is shifted toward the entropically favored lower coordinate species **A**, which is presumed to be catalytically more active and more selective.



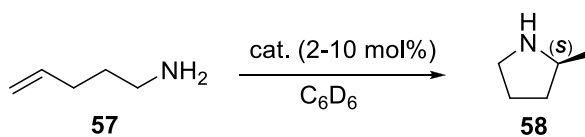
Scheme 4-1. Catalytic cycle of intramolecular hydroamination of aminoalkenes.⁴²

The octahydrobinaphtholate rare-earth metal complexes (*R*)-**50a-Ln**, (*R*)-**50b-Ln**, and (*R*)-**50c-Ln** displayed faster rates and higher enantioselectivities in the hydroamination of the *gem*-dimethyl-substituted aminopentene **55**, compared to the corresponding binaphtholate complexes (*R*)-**19a-Ln**, (*R*)-**50b-Ln**, and (*R*)-**50c-Ln** (Table

4-3, entries 1, 4–7 and 17–22). Interestingly, (*R*)-**50c-Lu** catalyzed the cyclization of **55** at the fastest rate at room temperature (turnover frequency of 28.6 h⁻¹), also forming pyrrolidine **56** with the highest selectivity (88% ee) under these conditions (Table 4-3, entry 22).

The Thorpe-Ingold effect¹⁴⁶ of the *gem*-diaryl/alkyl substituents plays a significant role in enhancing the cyclization rates of the di-substituted aminopentenes **51**, **53**, and **55** in comparison to that of the un-substituted aminopentene **57**. As a result, the rates of the hydroamination reactions decrease with decreasing size of the substituents in the order, **51** > **53** > **55** > **57** (Tables 4-1–4-4). While ring-closing of the *gem*-diphenyl-substituted aminopentene **51** proceeded at room temperature using 2 mol% of the catalysts with the highest turnover frequency of up to 2400 h⁻¹ (Table 4-1, entry 20), the un-substituted aminopentene **57** required either elevated reaction temperatures or higher catalytic loadings to achieve complete cyclization in a reasonable period of time in most cases (Table 4-4, entries 4–14).

The structurally more rigid binaphtholate complex (*R*)-**39a-Y** displayed significantly decreased activity as well as enantioselectivity in the hydroamination of **57** in comparison to (*R*)-**19a-Y**, (Table 4-4, entries 1, 4). High catalytic loading of (*R*)-**39a-Lu** (up to 10 mol%) was required for complete cyclization of **57** within 46 hours at the room temperature. As expected, the lutetium catalyst (*R*)-**39a-Lu** afforded pyrrolidine product **58** with higher enantioselectivity than the corresponding yttrium catalyst (Table 4-4, entries 4, 5).

Table 4-4. Catalytic evaluation for hydroamination/cyclization of **57**

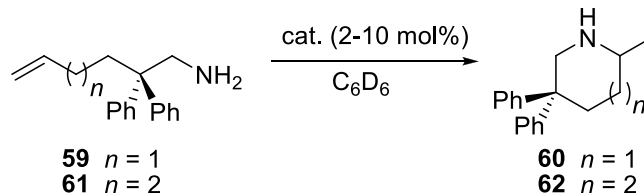
Entry	Catalyst ^a	[cat.]/[subs.] (%)	<i>T</i> (°C)	<i>t</i> (h) ^b	<i>TOF</i> (h ⁻¹)	<i>ee</i> (%) ^c
1	(<i>R</i>)- 19a-Y	2.0	25	24.0	2.6	70 ^d
2	(<i>R</i>)- 19a-Y	2.0	60	0.8	93	66 ^d
3	(<i>R</i>)- 19a-Lu	2.0	60	4	18	72 ^d
4	(<i>R</i>)- 39a-Y	5.0	25	31.0	0.65	49
5	(<i>R</i>)- 39a-Lu	10.0	25	46.0	0.22	67
6	(<i>R</i>)- 39b-Y	5.0	25	10.0	2	71
7	(<i>R</i>)- 39b-Lu	5.0	25	35.0	0.57	75
8	(<i>R</i>)- 39c-Y	2.0	60	1.5	32	70
9	(<i>R</i>)- 39c-Lu	2.0	60	1.6	31	87
10	(<i>R</i>)- 39c-Lu	5.0	25	27.0	0.73	83
11	(<i>R</i>)- 39d-Y	10.0	25	46.0	0.22	31
12	(<i>R</i>)- 39d-Lu	10.0	25	140.0	0.07	46
13	(<i>R</i>)- 39e-Y	5.0	25	11.5	1.7	59
14	(<i>R</i>)- 39e-Lu	5.0	25	49.0	0.41	75
15	(<i>R</i>)- 50a-Y	2.0	25	10.5	4.7	79
16	(<i>R</i>)- 50b-Y	2.0	25	20.0	2.5	77
17	(<i>R</i>)- 50c-Y	2.0	25	27.0	1.8	69

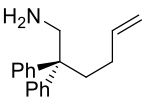
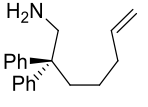
^a Reaction condition: 0.25 M solution of substrate **57** in C₆D₆, Ar atm. ^b At which at least 95% NMR conversion was obtained relative to ferrocene internal standard. ^c Enantiomeric excess determined by ¹⁹F NMR of the Mosher amides. ^d From ref. 31.

The sterically more demanding binaphtholate complexes (*R*)-**39b-Ln**, (*R*)-**39c-Lu**, and (*R*)-**39e-Ln** exhibited the same low activity at room temperature as other binaphtholate complexes (Table 4-4, entries 6, 7, 10, 13, 14); however, high enantioselectivities of up to 83% ee was observed in the ring-closing of **57** using (*R*)-**39c-Lu** (Table 4-4, entry 10). Catalytic evaluations of the cyclohexyldiphenylsilyl-substituted binaphtholate complexes (*R*)-**39c-Ln** were also performed at 60 °C, but noticeably higher activities were observed in the cyclization of **57** (Table 4-4, entries 8, 9). Interestingly, the hydroamination product **58** was obtained in 87% ee with catalyst (*R*)-**39c-Lu** at 60 °C (Table 4-4, entry 9).

The triisopropylsilyl-substituted binaphtholate complex (*R*)-**39d-Y** was the least efficient catalyst for the cyclization of the un-substituted aminopentene **57**, affording the hydroamination product **58** in only 31% ee (Table 4-4, entry 11).

Better cyclization rates for **57** were observed with the octahydrobinaphtholate rare-earth metal catalysts; the reactions were performed at room temperature and lower catalytic loadings could be used (Table 4-4, entries 15–17). The cyclization of **57** proceeded two times faster using the triphenylsilyl-substituted octahydrobinaphtholate complex (*R*)-**50a-Y** than when using the corresponding binaphtholate complex (*R*)-**19a-Y**. Additionally, the enantioselectivity increased to 79% ee for (*R*)-**50a-Y** in comparison to its binaphtholate analogue (*R*)-**19a-Y** (Table 4-4, entries 1 and 15).

Table 4-5. Catalytic evaluation of the hydroamination/cyclization of aminohexene **59** and aminoheptene **61**

Entry	Substrate	Catalyst ^a	[cat.]/[subs.] (%)	<i>T</i> (°C)	<i>t</i> (h) ^b	<i>TOF</i> (h ⁻¹)	<i>ee</i> (%) ^c
1	 59	(<i>R</i>)- 39a-Y	5.0	25	29	0.68	51
2		(<i>R</i>)- 39a-Lu	5.0	25	36.2	0.55	21
3		(<i>R</i>)- 39b-Y	5.0	25	25	0.78	36
4		(<i>R</i>)- 39b-Lu	5.0	25	44.5	0.44	33
5		(<i>R</i>)- 39c-Y	2.0	25	7.5	6.5	46
6		(<i>R</i>)- 39c-Y	2.0	60	0.58	85	43
7		(<i>R</i>)- 39c-Lu	2.0	25	38	1.3	9
8		(<i>R</i>)- 39c-Lu	2.0	60	1.2	41	5
9	 61	(<i>R</i>)- 39a-Y	10.0	80	169	0.06	44
10		(<i>R</i>)- 39c-Y	5.0	80	116	0.17	50
11		(<i>R</i>)- 39c-Lu	10.0	80	124	0.08	8
12		(<i>R</i>)- 39d-Y	10.0	90	165	0.06	8 ^d

^a Reaction condition: 0.1 M solution of substrate in C₆D₆, Ar atm. ^b At which at least 95% NMR conversion was obtained relative to ferrocene internal standard. ^c Enantiomeric excess determined by ¹⁹F NMR of the Mosher amides. ^d Inverse configuration was observed.

The less reactive *gem*-diphenyl-substituted aminohexene **59** was cyclized with low to moderate selectivities (Table 4-5, entries 1–8). The binaphtholate complex (*R*)-**39a-Y** displayed the same low activity as the sterically more hindered binaphtholate complex (*R*)-**39b-Ln**; however, (*R*)-**39a-Y** afforded piperidine **60** with the highest enantioselectivity of 51% ee (Table 4-5, entry 1). The cyclohexyldiphenylsilyl-

substituted binaphtholate complex (*R*)-**39c-Y** exhibited the highest activity, as indicated by the cyclization of **59** at low catalyst loading (2 mol%) at room temperature (Table 4-5, entry 5). The enantiomeric excess of the hydroamination product **60** depended only slightly on the reaction temperature (Table 4-5, entries 5 and 6; 7 and 8). Interestingly, the enantioselectivity of the formation of piperidine **60** significantly decreased with decreasing ionic radius of the metal (Table 4-5, entries 1–8). This observation contrasts the trend observed in the cyclization of aminopentenes **51**, **53**, **55**, and **57** (Tables 4-1–4-4).

Cyclization of the *gem*-diphenyl-substituted aminoheptene **61** required harsher reaction conditions. Prolonged heating to 80–90 °C and high catalyst loadings were required to achieve complete cyclization of **61**. Again, the smaller lutetium catalyst (*R*)-**39c-Lu** produced the azepane **61** with significantly lower enantioselectivity than its yttrium congener (Table 4-5, entries 10, 11). More interestingly, the triisopropylsilyl-substituted binaphtholate complex (*R*)-**39d-Y** catalyzed the ring-closing of **61** with only 8% ee, and the inverse configuration was observed (Table 4-5, entry 12).

Much difference in activity between the *gem*-diphenyl-substituted aminopentene **51** and 1,2-disubstituted olefin **63** was observed. In general, the cyclization of aminoalkene **63** (Table 4-6) proceeded with significantly lower rates in comparison to that of the terminal alkene analogue **51** (Table 4-1). The observation is in agreement with the generally accepted mechanism of hydroamination/cyclization,⁴² in which the olefin insertion step is rate determining. The binaphtholate rare-earth metal complexes furnished the pyrrolidine product **64** with good to excellent enantioselectivities. It should be noted that ring-closing of **63** was achieved with higher selectivities than that of the

gem-diphenyl-substituted aminopentene analogue **51**, with the exception of (*R*)-**39c-Ln** (Table 4-1, entries 4–11, and Table 4-6).

Table 4-6. Catalytic evaluation of the hydroamination/cyclization of the 1,2-disubstituted alkene **63**

Entry	Catalyst ^a	<i>t</i> (h) ^b	TOF (h ⁻¹)	ee (%) ^c
1	(<i>R</i>)- 39a-Y	3	17	93
2	(<i>R</i>)- 39a-Lu	7.5	6.4	96
3	(<i>R</i>)- 39b-Y	1	50	92
4	(<i>R</i>)- 39b-Lu	1.75	28	96
5	(<i>R</i>)- 39c-Y	0.3	167	83
6	(<i>R</i>)- 39c-Lu	0.75	67	88
7	(<i>R</i>)- 39d-Y	3.5	14.3	93 ^d
8	(<i>R</i>)- 39d-Lu	7.75	6.4	91

^a Reaction condition: 0.1 M solution of substrate **63** in C₆D₆, Ar atm, at 25 °C.

^b At which at least 95% NMR conversion was obtained relative to ferrocene internal standard. ^c Determined by ¹⁹F NMR of the Mosher amides. ^d Determined by chiral HPLC of the corresponding 2-naphthoyl amide.

4.2.2 Asymmetric Intramolecular Hydroamination of Secondary Amines

A dramatic increase in catalytic activity was observed in the cyclization of the secondary aminoalkene **65** using the *tert*-butyldiphenylsilyl-substituted binaphtholate complexes (*R*)-**39b-Ln** in comparison to the primary aminoalkene analogue **55** (Table 4-7, entries 1, 2 vs. Table 4-3, entries 4, 5). While the cyclization of **65** proceeded more selective (71% ee) than that of **55** (50% ee) using (*R*)-**39b-Y** (Table 4-7, entry 1 vs. Table

4-3, entry 4), the opposite was true for the corresponding lutetium complex (Table 4-7, entry 2 vs. Table 4-3, entry 5).

Table 4-7. Catalytic evaluation for hydroamination/cyclization of secondary amines **65** and **67**

$\text{65 } R = \text{Me}$
 $\text{67 } R = \text{Ph}$

$\text{66 } R = \text{Me}$
 $\text{68 } R = \text{Ph}$

Entry	Substrate	Catalyst ^a	<i>T</i> (°C)	<i>t</i> (h) ^b	TOF (h ⁻¹)	ee (%) ^c (conf.)
1		(<i>R</i>)- 39b-Y	25	0.33	148	71 (<i>S</i>)
2		(<i>R</i>)- 39b-Lu	25	0.33	148	69 (<i>S</i>)
3		(<i>R</i>)- 39b-Y	25	16	3	37 (<i>R</i>)
4		(<i>R</i>)- 39b-Y	60	6.5	7.5	13 (<i>R</i>)
5		(<i>R</i>)- 39b-Lu	25	6	8	3 (<i>R</i>)
6		(<i>R</i>)- 39b-Lu	60	2	24.5	16 (<i>S</i>)
7		(<i>R</i>)- 39c-Y	25	15.8	3.1	52 (<i>S</i>)
8		(<i>R</i>)- 39c-Y	60	5.5	8.9	50 (<i>S</i>)
9		(<i>R</i>)- 39c-Lu	25	16	3	77 (<i>S</i>)

^a Reaction condition: 0.1 mol L⁻¹ solution of substrate in C₆D₆, Ar atm. ^b At which at least 95% NMR conversion relative to bis(trimethylsilyl)methane internal standard, was obtained. ^c Determined by ¹⁹F NMR of the Mosher amides after removal of *N*-benzyl group.

The enhanced activity and selectivity in the cyclization of the secondary amine **65** in comparison to the primary amine analogue **55** are in agreement with preferential formation of a catalytically more active and selective species **A**, facilitated by the bulkiness of the *N*-benzyl substituent (Scheme 4-1).

With the presence of the bulky *N*-benzyl, the equilibrium between the catalytically more active and lower coordinate species **A** and the less active and higher coordinate species **B** is shifted in favor of species **A** (Scheme 4-1). However, the *N*-benzyl *gem*-diphenyl-substituted aminopentene **67** is sterically more demanding than **65**, leading to high steric hindrance around the metal center. As a result, significantly lower activities and enantioselectivities were observed in the cyclization of the secondary amine **67** using (*R*)-**39b-Ln** and (*R*)-**39c-Ln** in comparison to those of the primary amine analogue **51** and the secondary amine **65** (Table 4-7, entries 3–9). Moreover, the hydroamination product **68** was obtained with inversed configuration using the *tert*-butyldiphenylsilyl-substituted binaphtholate complexes (*R*)-**39b-Ln** (Table 4-7, entries 3–5). Interestingly, the cyclization of **67** using (*R*)-**39b-Lu** furnished either (*R*) or (*S*) configured product **68**, depending on the reaction temperature (Table 4-7, entry 5 vs. entry 6). The other (*R*)-binaphtholate catalysts generally furnished the pyrrolidine products preferentially with (*S*)-configuration.

4.2.3 Kinetic Studies of Hydroamination/Cyclization

In agreement with the generally accepted mechanism of hydroamination, in which the olefin insertion step is rate determining, kinetic studies indicate that the hydroamination/cyclization using the binaphtholate rare-earth metal complexes is zero order in the aminoalkene substrate.

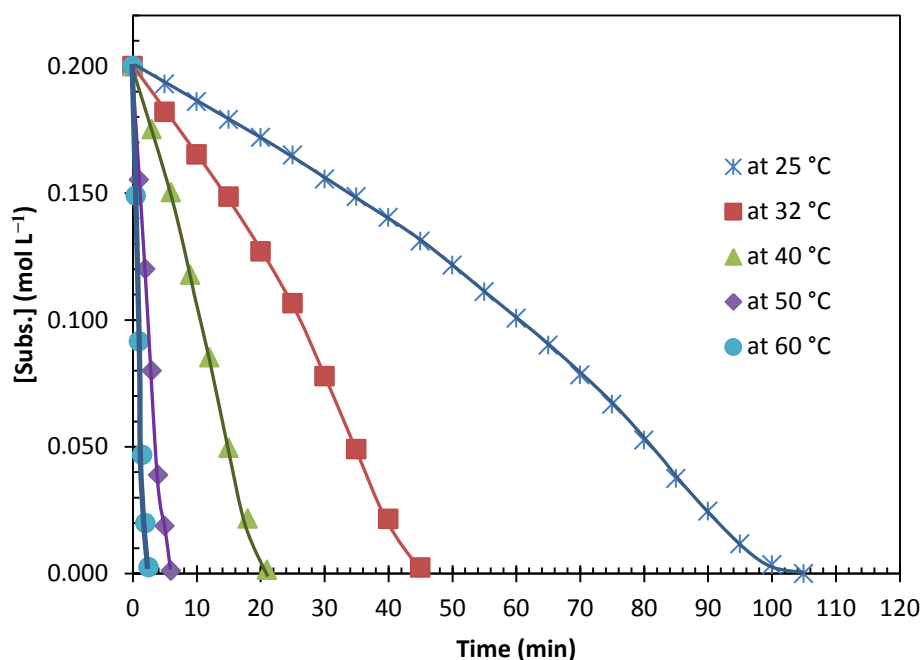


Figure 4-5. Concentration of aminopentene **55** (0.2 mol L^{-1}) versus time for the hydroamination/cyclization using (*R*)-**39c-Y** (0.004 mol L^{-1}) at variable temperatures in C_6D_6 . The lines are drawn as a guide for the eyes.

The kinetic studies were performed with the *gem*-dimethyl-substituted aminopentene **55** and (*R*)-**39c-Y** at variable temperatures in the range of 25–60 °C (Figure 4-5). The plots representing the data for the hydroamination of **55** at the temperatures of 25 and 32 °C showed a slight curvature, indicating slight rate acceleration during the catalytic reaction. This observation is due to a slight shift between the catalytically more active and selective species **A** and the less active and higher coordinate species **B**. Species **A** is slightly more favored at higher conversion, because the hydroamination product has a slightly smaller binding constant than the primary aminoalkene **55**. A decrease in the reaction rate was observed at about 90% conversion in the hydroamination of **55**, most obviously at 25 °C. Similar catalytic behavior was

previously reported for chiral lanthanocene complexes⁴⁴ and the triphenylsilyl-substituted binaphtholate complex (*R*)-**19a-Y**.^{31,119} It was proposed that catalyst inhibition by the hydroamination product, which competes with the aminoalkene substrate for empty coordination sites at the metal center, accounts for the decreased reaction rate at high conversion.

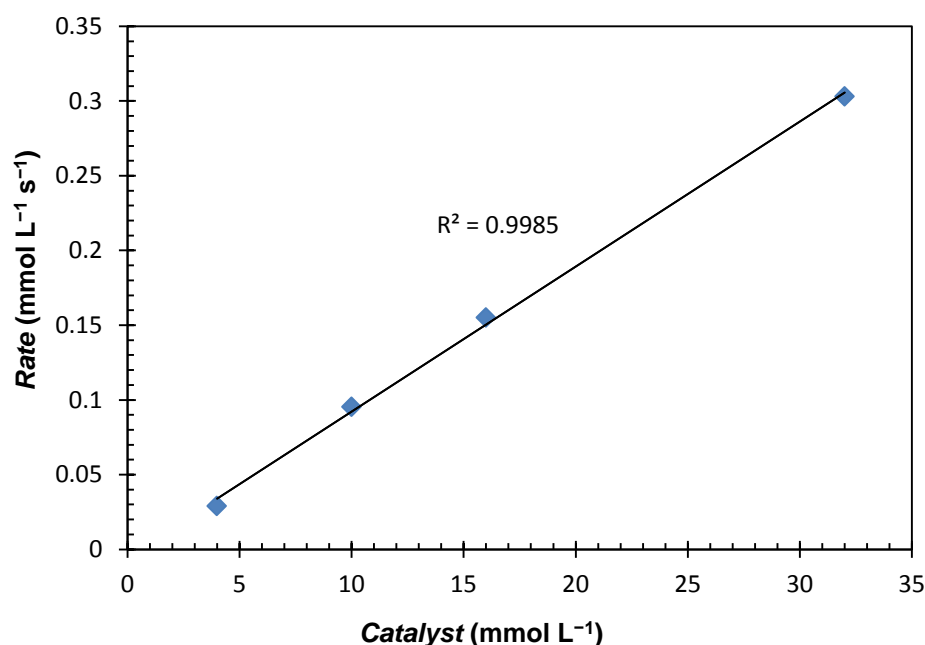


Figure 4-6. Rate versus catalyst concentration for the hydroamination of **55** ([subst.]₀ = 0.2 mol L⁻¹) using (*R*)-**39c-Y** in C₆D₆ at 25 °C.

The plot of the reaction rate versus catalyst concentration over an 8-fold range (4–32 mmol L⁻¹) (Figure 4-6) is a straight line, indicating that the rate of hydroamination/cyclization of **55** using (*R*)-**39c-Y** is first-order in catalyst concentration. This also suggests that the catalytically active species is monomeric.

4.3 Summary

The rare-earth metal complexes with the alkylarylsilyl-substituted binaphtholate and octahydrobinaphtholate ligands displayed high activity and excellent enantioselectivities in the asymmetric intramolecular hydroamination/cyclization of aminoalkenes. In most cases, sterically more demanding alkylarylsilyl-substituted octahydrobinaphtholate rare-earth metal complexes exhibited higher activity as well as selectivities in the ring-closure of aminopentenes in comparison to the corresponding binaphtholate complexes. While the highest turnover frequency of up to 2400 h^{-1} was achieved with the *gem*-diphenyl-substituted aminopentene **51** using the cyclohexyldiphenylsilyl-substituted octahydrobinaphtholate complex (*R*)-**50c-Y**, the cyclization of the less reactive aminopentene **53** produced the hydroamination product **54** with the highest selectivity of 98% ee using (*R*)-**50c-Lu**. The binaphtholate complexes were also efficient in the cyclization of aminohexene **59** at room temperature and aminoheptene **61** under harsher reaction conditions. The secondary amine **65** was more reactive and selective in the cyclization reaction than its primary amine analogue **55**. However, the sterically more demanding substrate **67** displayed significantly lower activities and selectivities in comparison to the primary amine **51** in the hydroamination using binaphtholate catalysts. In some cases, the cyclization product **68** was achieved with (*R*)-**39b-Ln** in inverse configuration. Kinetic studies were performed with the *gem*-dimethyl-substituted aminopentene **55** using (*R*)-**39c-Y**, indicating that the rate of hydroamination/cyclization is zero-order in substrate concentration and first-order in catalyst concentration.

Chapter 5

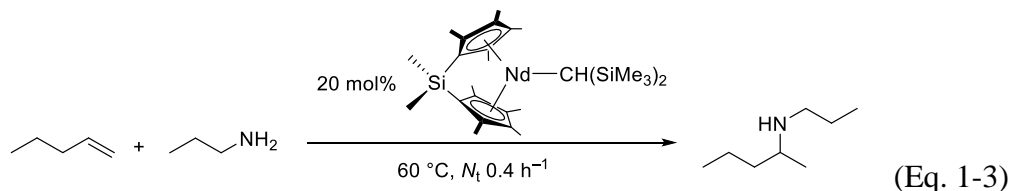
Asymmetric Intermolecular Hydroamination of Unactivated Alkenes with Simple Amines

5.1 Introduction

Nitrogen-containing compounds play a vital role in biological systems and pharmaceuticals; therefore, the development of efficient methods for the synthesis of this class of compounds has remained an important goal in chemical research.¹⁻⁴ The hydroamination with the advantages of generating amines directly from very simple starting materials and forming no byproducts, has been studied extensively in the last two decades.^{8,9,11,12,27,28,65,147,148} Although the development of novel catalyst systems for hydroamination has seen significant progress,^{7-9,11-14,28,31,59,65,149} the intermolecular hydroamination of unactivated alkenes with simple amines remains very challenging.^{105,150-152} Efficient catalysts for the intermolecular reaction have been reported,¹⁰⁶⁻¹¹⁷ but most of them are achiral. Moreover, those studies are limited to the involvement of activated or strained alkenes, such as vinylarenes, 1,3-dienes, and norbornene, or amines with low basicity, such as anilines, carboxamides, sulfonamides, and other protected amines.

Our studies focus on the development of rare-earth metal catalysts based on alkylarylsilyl-substituted binaphtholate and octahydrobinaphtholate ligands, which display high catalytic activity in the intramolecular hydroamination of aminoalkenes and

excellent selectivities of up to 98% ee (see Chapter 4 and ref. 31). Prior to our work, the Marks research group reported an example of a simple amine adding to 1-pentene in the presence of the *ansa*-lanthanocene $\text{Me}_2\text{Si}(\text{C}_5\text{H}_4)_2\text{NdCH}(\text{SiMe}_3)_2$.¹⁰⁵ It is noteworthy that more than 70 equiv. of 1-pentene was required to obtain 90% conversion (Eq. 1-3).



Indeed, the intermolecular hydroamination is much more difficult to achieve in comparison to the intramolecular reaction, due to the weak coordination of olefins to d^0 transition metals and the strong binding of amines.^{31,105,153,154} Therefore, in order to achieve a considerable conversion in the intermolecular hydroamination, a large excess of the olefin is generally required. In this chapter we report the stereoselective addition of simple amines to unactivated alkenes utilizing chiral rare-earth metal catalysts based on binaphtholate and octahydrobinaphtholate ligands.

5.2 Catalytic Results and Discussion

5.2.1 Binaphtholate Rare-Earth Metal Catalyst Evaluation

For the initial catalyst screening we chose the reaction of 1-heptene with benzyl amine (Table 5-1, entries 1–9). The reactions proceeded smoothly in the presence of 5 mol% binaphtholate catalyst, generating exclusively the Markovnikov hydroamination

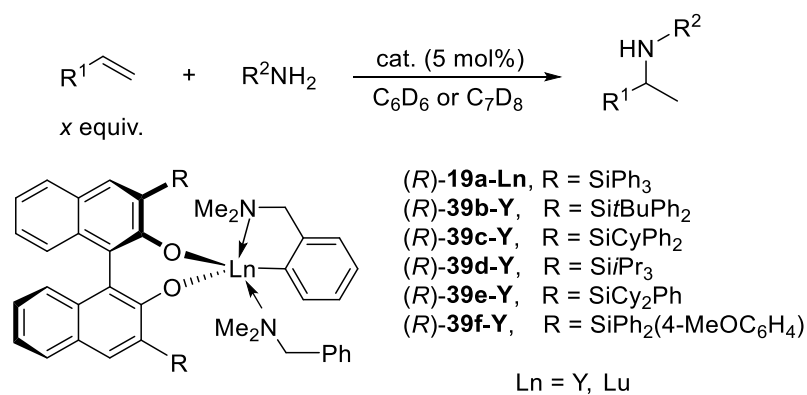
product **69**. The enantiomeric excess of the intermolecular hydroamination product **69** was determined by ^{19}F NMR spectroscopy after the removal of the *N*-benzyl group. The absolute configuration of the intermolecular hydroamination product **69** using the *R*-configured binaphtholate complexes was found to be *R*, which is opposite to that observed for the intramolecular hydroamination of aminopentenes (see Chapter 4 and ref. 31).

To achieve high conversions within a reasonable amount of time, the reactions were performed at temperature as high as 150 °C. Reactions performed at 110 °C required significantly longer reaction times (260 h) in order to achieve high conversion (Table 5-1, entries 1 and 2). It is noteworthy that the enantioselectivity improved from 58 to 65% ee when the reaction temperature was reduced from 150 to 110 °C.

A 15-fold excess of alkene was used to accelerate the reaction. While lower alkene/amine ratio resulted in lower conversion and longer reaction time (Table 5-1, entry 3), a slightly accelerated reaction was achieved in the presence of a large excess of alkene (Table 5-1, entry 4).

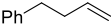
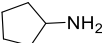
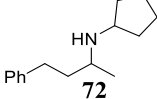
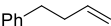
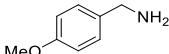
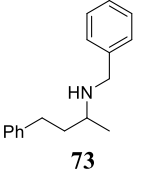
In contrast to observations for the intramolecular hydroamination of aminoalkenes,³¹ the triphenylsilyl-substituted binaphtholate complex with the smaller sized metal (*R*)-**19a-Lu** ($r(\text{Lu}^{3+}) = 0.86 \text{ \AA}$ vs. $r(\text{Y}^{3+}) = 0.90 \text{ \AA}$),¹⁵⁵ displayed slightly higher catalytic activity and significantly reduced selectivity than (*R*)-**19a-Y** (Table 5-1, entry 5 versus entry 1).

Table 5-1. Asymmetric intermolecular hydroamination of unactivated alkenes with a primary amine using binaphtholate catalysts.



Entry	Alkene	Amine	Product	Cat.	<i>x</i>	<i>T</i> (°C)	<i>t</i> (h)	% conv. ^a (% yield) ^b	% ee ^c (config.)
1 [†]				(<i>R</i>)- 19a-Y	15	150	36	90 (65)	58 (<i>R</i>)
2				(<i>R</i>)- 19a-Y	15	110	260	85 (51)	65 (<i>R</i>)
3 [*]				(<i>R</i>)- 19a-Y	7	150	48	85 (57)	57 (<i>R</i>)
4 [*]				(<i>R</i>)- 19a-Y ^d	50	150	18	95 (68)	54 (<i>R</i>)
5 [*]	<i>n</i> -C ₅ H ₁₁ CH=CH ₂	PhCH ₂ NH ₂		(<i>R</i>)- 19a-Lu	15	150	30	95 (62)	40 (<i>R</i>)
6 [*]			69	(<i>R</i>)- 39b-Y	15	150	48	85 (59)	46 (<i>R</i>)
7 [*]				(<i>R</i>)- 39c-Y	15	150	17	90	47 (<i>R</i>)
8 [*]				(<i>R</i>)- 39d-Y	15	150	72	60 (44)	38 (<i>R</i>)
9 [*]				(<i>R</i>)- 39f-Y	15	150	12	45	60 (<i>R</i>)
10 [*]	<i>n</i> -C ₆ H ₁₃ CH=CH ₂	PhCH ₂ NH ₂		(<i>R</i>)- 19a-Y	15	150	40	97 (72)	57 (<i>R</i>)
11			70	(<i>R</i>)- 39e-Y	15	150	36	100 (56)	40 (<i>R</i>)
12 [*]				(<i>S</i>)- 19a-Y ^e	10	150	11	100 (72)	56 (<i>S</i>)
13	PhCH ₂ CH=CHCH ₃	PhCH ₂ NH ₂		(<i>R</i>)- 19a-Y	15	110	212	68 (42)	66 (<i>R</i>)
14			71	(<i>R</i>)- 39e-Y ^e	10	150	33	100 (65)	44 (<i>R</i>)
15				(<i>R</i>)- 39f-Y	15	110	96	67 (40)	66 (<i>R</i>)

[†] The reactions were performed by Dr. Alexander L. Reznichenko, a former Ph.D. candidate in the Hultsch research group.

16*				(<i>S</i>)- 19a-Y ^c	9	150	39	90 (68)	54 ^f
17*				(<i>S</i>)- 19a-Y	10	150	48	85 (66)	56 (<i>S</i>) ^f
18*				(<i>R</i>)- 39b-Y	10	150	72	75 (61)	54 (<i>R</i>) ^f
19*				(<i>R</i>)- 39c-Y	10	150	48	80	44 (<i>R</i>) ^f

General reaction condition: 3.0 mmol alkene, 0.2 mmol amine, 10 μ mol cat. (0.1 mL of 0.1 M cat. solution in C₆D₆ or tol-*d*₈). ^a The conversion of amine was determined *via* ¹H NMR spectroscopy. ^b Isolated yield after column chromatography. ^c Determined by ¹⁹F NMR spectroscopy of the Mosher amide after debenzoylation. ^d 8 mol% cat. was used. ^e 4 mol% cat. was used. ^f Determined by ¹H NMR spectroscopy of the salt of *O*-acetyl mandelic acid.

The sterically more hindered *tert*-butyldiphenylsilyl- and cyclohexyldiphenylsilyl-substituted binaphtholate complexes (*R*)-**39b-Y** and (*R*)-**39c-Y**, respectively, exhibited similar high activity in the intramolecular hydroamination of aminopentenes in most cases (see Chapter 4, Tables 4-1–4-3), whereas the rate of the benzylamine addition to 1-heptene with (*R*)-**39c-Y** was about three times faster than that using (*R*)-**39b-Y** (Table 5-1, entries 6, 7). The selectivities of 46, respectively 47% ee achieved with (*R*)-**39b-Y** and (*R*)-**39c-Y** were slightly lower than that observed with (*R*)-**19a-Y** (Table 5-1, entries 6, 7 versus entry 1).

High conversions were observed in most cases without formation of other by-products, except the cases where complexes (*R*)-**39d-Y** and (*R*)-**39f-Y** were utilized (Table 5-1, entries 8, 9). The triisopropylsilyl-substituted binaphtholate complex (*R*)-**39d-Y** displayed low activity (60% conversion in 72 h) and selectivity (38% ee) in the intermolecular hydroamination reaction of benzylamine and 1-heptene. This result was expected because (*R*)-**39d-Y** was also the least efficient catalyst among our binaphtholate

catalysts for the intramolecular hydroamination of aminoalkenes (see Chapter 4). The *p*-methoxyphenyl(diphenyl)silyl-substituted complex (*R*)-**39f-Y** displayed the highest enantioselectivity of up to 60% ee at 150 °C; however, only 45% conversion was observed due to catalyst decomposition under these conditions (Table 5-1, entry 9).

Further investigations were conducted with other alkenes and amines (Table 5-1, entries 10–19). 1-Octene displayed similar activity and selectivity as 1-heptene in the reaction with benzylamine using (*R*)-**19a-Y** (Table 5-1, entry 10). The dicyclohexylphenylsilyl-substituted binaphtholate complex (*R*)-**39e-Y** catalyzed the intermolecular hydroamination of 1-octene with benzylamine at about the same rate as (*R*)-**19a-Y**; however, a significantly lower enantioselectivity was observed (Table 5-1, entry 11).

The addition of benzylamine to 4-phenyl-1-butene was achieved with alkene/amine ratio as low as 10:1 using the binaphtholate catalysts. The fastest rate was observed with (*S*)-**19a-Y** at 150 °C (Table 5-1, entry 12). At lower reaction temperature, a larger excess of alkene and longer reaction time was required to obtain considerable conversion. The highest enantioselectivity of 66% ee was observed using (*R*)-**19a-Y** at 110 °C (Table 5-1, entry 13). The *p*-methoxyphenyl(diphenyl)silyl-substituted binaphtholate complex (*R*)-**39f-Y** delivered the intermolecular hydroamination product **71** with the same high selectivity as that using (*R*)-**19a-Y** (Table 5-1, entry 15). A higher reaction rate was observed for (*R*)-**39f-Y** in comparison to (*R*)-**19a-Y**; however, full conversion was not achieved with (*R*)-**39f-Y** due to significant decomposition of the catalyst under the catalytic conditions.

The reaction of cyclopentylamine with 4-phenyl-1-butene proceeded with an enantioselectivity comparable to that of benzylamine, but diminished activity was observed (Table 5-1, entry 16). The decreased reactivity was also observed for *para*-methoxybenzylamine (Table 5-1, entries 17–19). The presence of the methoxy group, possibly leading to deactivation of the binaphtholate catalysts, accounts for the lower conversions and longer reaction times.

The binaphtholate complexes are apparently efficient catalysts for intermolecular hydroamination of unactivated alkenes with simple amines. However, the substrate scope is limited to primary amines and unbranched terminal alkenes. Attempts to perform the reactions involving di-substituted alkenes, such as cyclohexene and α -methylstyrene,¹⁵⁶ or secondary amines, such as piperidine¹⁵⁶ and pyrrolidine, were not successful. Moreover, the binaphtholate catalysts have a low functional group tolerance, thus they are prone to deactivation under the catalytic conditions, particularly in the presence of a methoxy group. The reaction of 1,3-benzodioxol-5-ylmethylamine, a derivative of benzylamine, with 1-octene did not lead to any conversion and significant decomposition of the catalyst was observed.

5.2.2 Octahydrobinaphtholate Rare-Earth Metal Catalyst Evaluation

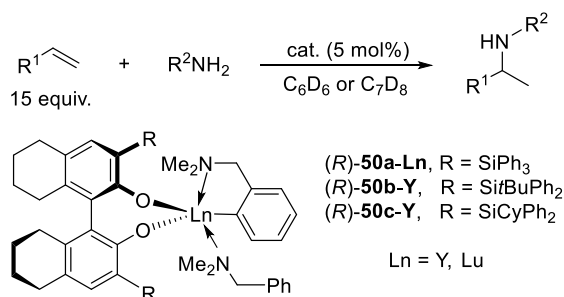
The rare-earth metal catalysts based on the alkylarylsilyl-substituted octahydrobinaphtholate ligands (*R*)-**50a–c** displayed high activity in the intramolecular hydroamination of aminopentenes (see Chapter 4, Table 4-1–4-4). Faster cyclization rates and slightly improved enantioselectivities were generally observed with the sterically

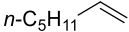
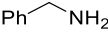
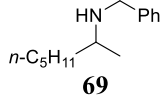
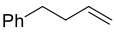
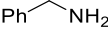
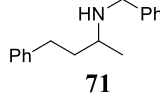
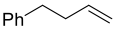
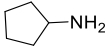
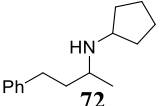
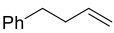
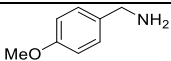
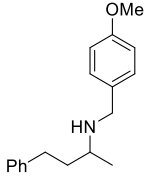
more demanding octahydrobinaphtholate catalysts in comparison to the corresponding binaphtholate catalysts. Herein we will discuss the catalytic performance of the octahydrobinaphtholate complexes in the asymmetric intermolecular hydroamination of unactivated alkenes with simple amines.

Although the intermolecular reactions of simple amines and unactivated alkenes was achieved in the presence of the binaphtholate catalysts with good turnover at 150 °C, the additions were also successful at temperatures as low as 110 °C, resulting in improved stereoselectivities. To maximize the efficiency of the octahydrobinaphtholate catalysts with respect to selectivities, the catalytic evaluations were performed mostly at 110 °C with long reaction times and a large excess of alkene (alkene/amine ratio 15:1) was used (Table 5-2).

Similar to the observation made with the binaphtholate catalysts, the *R*-configured octahydrobinaphtholate catalysts furnished the hydroamination products **69**, **71–73** with *R*-configuration and exclusive Markovnikov selectivity. The triphenylsilyl-substituted octahydrobinaphtholate complex (*R*)-**50a-Y** converted benzylamine to the secondary amine **69** quantitatively in 45 hrs at 150 °C, which is comparable to the reaction rate achieved with its corresponding binaphtholate complex (*R*)-**19a-Y** (Table 5-2, entry 1 versus Table 5-1, entry 1). A slower reaction rate and lower selectivity was observed with the smaller lutetium complex (*R*)-**19a-Lu** (Table 5-2, entry 2). The intermolecular reactions proceeded to full conversion at 110 °C with the novel catalysts (*R*)-**50b-Y** and (*R*)-**50c-Y**, generating product **69** with enantioselectivities of 53 and 42% ee, respectively; however, significantly longer reaction times were required (Table 5-2, entries 3, 4).

Table 5-2. Asymmetric intermolecular hydroamination of unactivated alkene with primary amines using octahydrobinaphtholate catalysts.



Entry	Alkene	Amine	Product	Cat.	<i>T</i> (°C)	<i>t</i> (h)	% conv. ^a	% ee ^c
								(% yield) ^b (config.)
1				(<i>R</i>)- 50a-Y	150	45	100 (62)	57 (<i>R</i>)
2			 69	(<i>R</i>)- 50a-Lu	150	73	100 (62)	42 (<i>R</i>)
3				(<i>R</i>)- 50b-Y	110	240	100 (67)	53 (<i>R</i>)
4				(<i>R</i>)- 50c-Y	110	240	100 (62)	42 (<i>R</i>)
5 ^d				(<i>R</i>)- 50a-Y ^d	150	23	58 (27)	52 (<i>R</i>)
6			 71	(<i>R</i>)- 50a-Y	110	96	100 (68)	67 (<i>R</i>)
7				(<i>R</i>)- 50a-Lu	110	190	39 (24)	52 (<i>R</i>)
8				(<i>R</i>)- 50b-Y	110	140	63 (41)	55 (<i>R</i>)
9				(<i>R</i>)- 50c-Y	110	212	66 (41)	49 (<i>R</i>)
10			 72	(<i>R</i>)- 50b-Y	110	260	58 (33)	50 ^e
11				(<i>R</i>)- 50c-Y	110	275	60 (37)	51 ^e
12			 73	(<i>R</i>)- 50b-Y	110	260	45 (31)	61 (<i>R</i>)

General reaction condition: 3.0 mmol alkene, 0.2 mmol amine, 10 μmol cat. (0.1 mL of 0.1 M cat. solution in C₆D₆ or tol-*d*₈). ^a The conversion of amine was determined *via* ¹H NMR spectroscopy. ^b Isolated yield

after column chromatography. ^c Determined by ¹⁹F NMR spectroscopy of the Mosher amide after debenzylation. ^d 4 mol% cat. was used, alkene/amine ratio 10:1. ^e Determined by ¹H NMR spectroscopy of the salt of *O*-acetyl mandelic acid.

While the intermolecular hydroamination product **71** was obtained with 52% ee using the triphenylsilyl-substituted octahydrobinaphtholate complex (*R*)-**50a-Y** at 150 °C, lowering the reaction temperature to 110 °C improved the enantioselectivity to 67% ee (Table 5-2, entries 5 versus 6). The smaller lutetium complex (*R*)-**50a-Lu** and the sterically more hindered *tert*-butyldiphenylsilyl-substituted and cyclohexyldiphenylsilyl-substituted octahydrobinaphtholate complexes (*R*)-**50b-Y** and (*R*)-**50c-Y**, respectively, displayed significantly lower catalytic activity, giving incomplete conversion (39–66%) even after prolonged heating at 110 °C. Moreover, the reactions with these three catalysts provided lower selectivities (in the range 49–55% ee; Table 5-2, entries 7–9) in comparison to (*R*)-**50a-Y**.

The addition of cyclopentylamine to 4-phenyl-1-butene to form the secondary amine **72** were sluggish using the octahydrobinaphtholate complexes (*R*)-**50b-Y** and (*R*)-**50c-Y**, giving incomplete conversion even after long reaction times of up to 275 hrs (Table 5-2, entries 10, 11). The enantioselectivities are comparable to those observed for benzylamine under the same catalytic reaction conditions. Incomplete conversion was also observed for *para*-methoxybenzylamine using (*R*)-**50b-Y** presumably due to catalyst deactivation from the coordinating methoxy group (Table 5-2, entry 12).

5.2.3 Mechanistic Studies

Mechanistic studies were performed with benzylamine and 4-phenyl-1-butene in the presence of the triphenylsilyl-substituted binaphtholate complex (*R*)-**19a-Y** at 150 °C. The initial kinetic data suggest that the reaction is first order with respect to amine*, alkene, and catalyst* concentration (Figures 5-1–5-3).

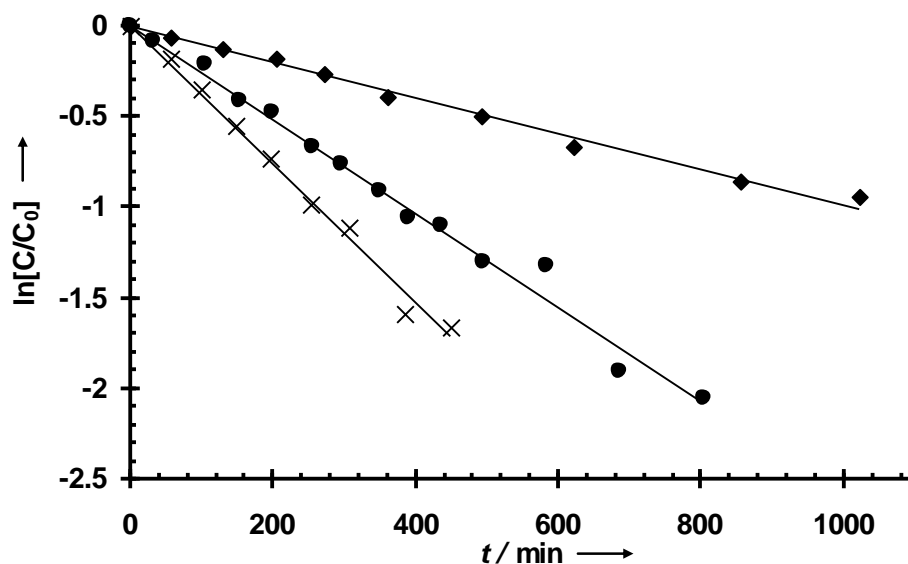


Figure 5-1. First order plot for the addition of benzylamine (0.33-0.42 mol L⁻¹) to 4-phenyl-1-butene (5.0-6.3 mol L⁻¹) using varying catalyst concentrations of (*R*)-**19a-Y** [0.009 M (♦), 0.018 M (●), 0.025 M (×)] in tol-d₈ at 150 °C.

(*) This study was performed by Dr. Alexander L. Reznichenko, a former Ph.D. candidate in the Hultsch group.

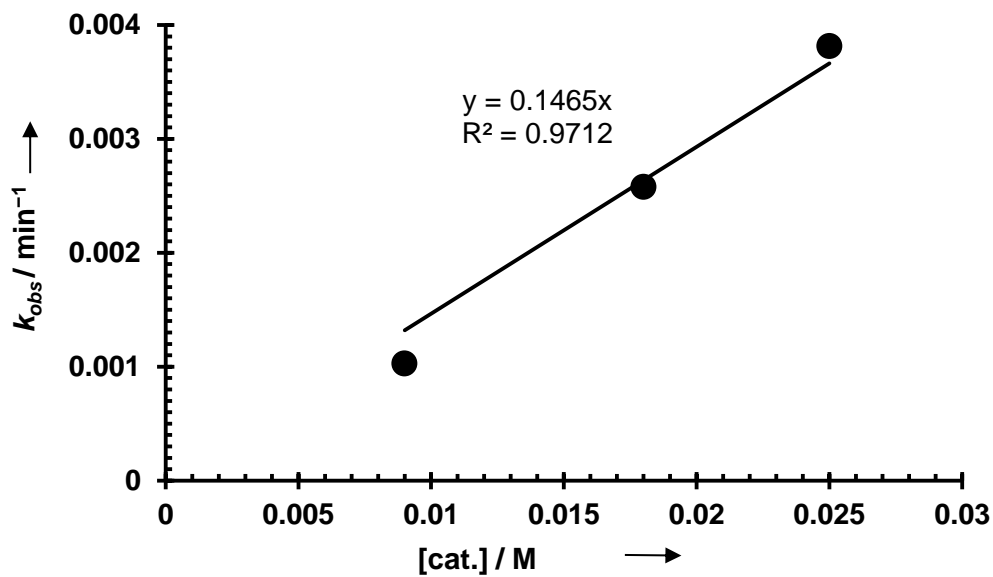


Figure 5-2. Dependency of k_{obs} on the concentration of (*R*)-**19a-Y** in the addition of benzylamine to 4-phenyl-1-butene.

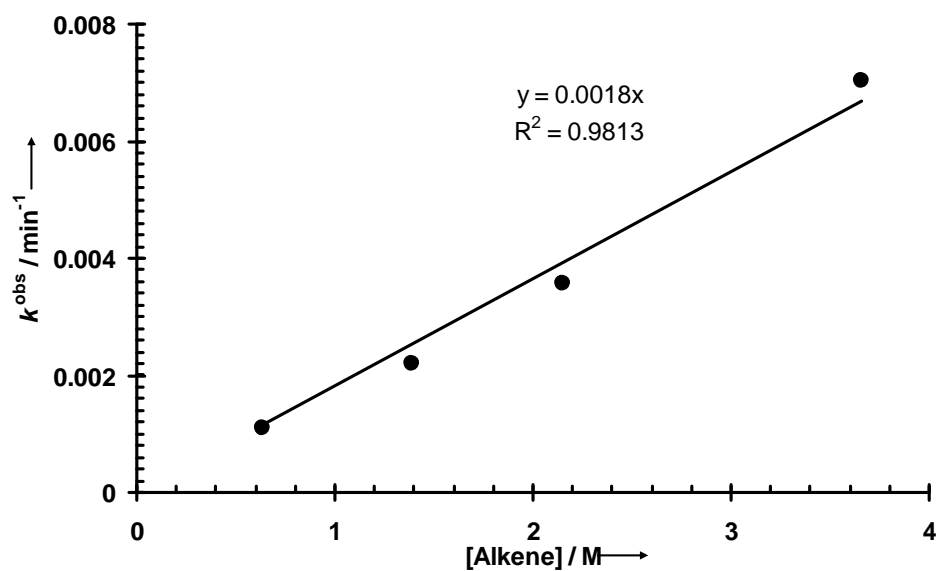
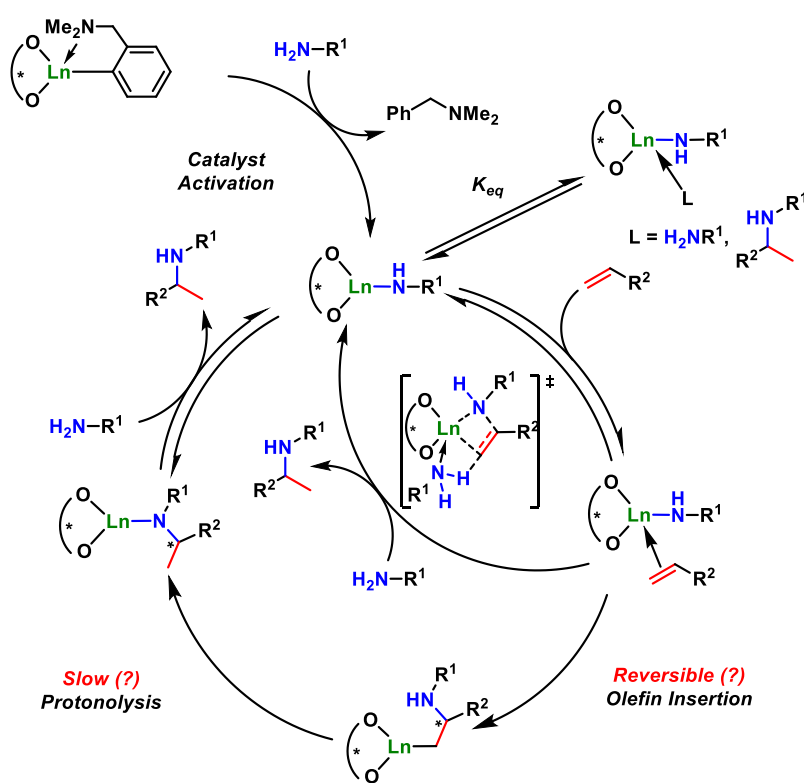


Figure 5-3. Observed pseudo-first order rate constant vs. alkene concentration for the reaction of benzylamine [$C_0 = 0.17 \text{ M}$] with 4-phenyl-1-butene in the presence of (*R*)-**19a-Y** [0.032 M] at 150°C in C_6D_6 . Linear correlation illustrates effective first order in alkene.

These preliminary data suggest the participation of the amine in the catalytic steps leading from the resting state of the catalyst to the presumably rate-determining alkene-insertion step. The amine possibly participates in slow concerted insertion/protonation, which is the rate-determining step. Another possibility is that reversible olefin insertion is taking place, followed by rate-determining protonolysis step (Scheme 5-1). Although kinetic data for these types of reactions are scarce, it should be noted that a zero-order rate dependence on the amine concentration was observed in the rare-earth-metal-catalyzed intermolecular hydroamination of alkynes.¹⁵⁰



Scheme 5-1. Mechanistic scenarios for intermolecular hydroamination

5.3 Summary

Rare-earth metal complexes based on binaphtholate and octahydrobinaphtholate ligands have been shown to be efficient catalysts for the asymmetric intermolecular hydroamination of unactivated alkenes with simple amines. The reactions occur at high temperatures (110–150 °C) in the presence of a large excess of alkenes (alkene/amine ratio 10–15:1), generating exclusively Markovnikov hydroamination products. The *R*-configured binaphtholate and octahydrobinaphtholate catalysts furnish the addition products with *R* configuration, which is opposite to the selectivity observed for the intramolecular hydroamination of aminopentenes with these catalysts. Generally increased enantioselectivities were observed at the lower reaction temperature (110 °C) at the expense of activity, sometimes resulting in incomplete conversion. The highest enantiomeric excess of 67% ee was observed for product **71** using the triphenylsilyl-substituted octahydrobinaphtholate catalyst (*R*)-**50a-Y**. Initial kinetic data suggest that the intermolecular reaction is first order with respect to amine, alkene, and catalyst concentration.

Chapter 6

Kinetic Resolution of

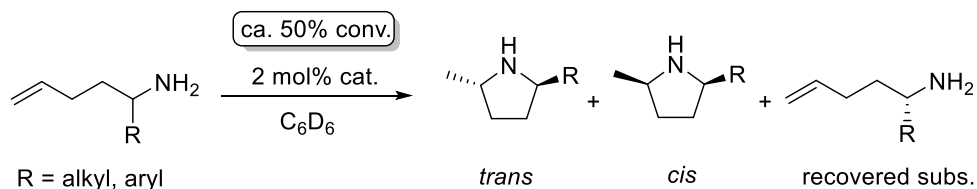
Chiral Aminoalkenes *via* Hydroamination

6.1 Introduction

Nitrogen-containing compounds are widely found in nature and biological systems; therefore, this class of organic compounds is of high importance in fundamental research, as well as pharmaceutical and chemical industry.¹⁻⁴ The metal-catalyzed hydroamination of olefins, in which an amine N-H functionality adds directly to an unsaturated carbon-carbon bond, provides one of the simplest routes to amine products with 100% atom efficiency.^{5,8,117-121} Despite of the development of a large variety of catalyst systems for the hydroamination of olefins over the last decade,^{7-9,11-14,28,31,59,65,149} this challenging transformation has remained an important goal in contemporary catalysis research, particularly with respect to asymmetric variants.^{25,26,29,157}

Binaphtholate catalysts for the asymmetric hydroamination of aminoalkenes were first reported by the Hultsch research group,³¹ displaying high activity comparable to that of lanthanocene catalysts reported by Marks.^{43,44,46} More importantly, high enantioselectivities of up to 95% ee were observed for the *gem*-diphenyl-substituted aminopentene **51** using the triphenylsilyl-substituted binaphtholate catalyst (*R*)-**19a-Sc**. Moreover, the rare-earth metal complexes based on tri(aryl)silyl-substituted binaphtholate ligands are also efficient catalysts for the catalytic kinetic resolution of

chiral aminoalkenes *via* the asymmetric hydroamination/cyclization (Scheme 6-1 and also see Chapter 1, Section 1.2.4 and ref. 31,104).



Scheme 6-1. General scheme of the kinetic resolution of aminoalkenes.

A widely used method for separating enantiomers in organic laboratories involves the uses of stoichiometric amounts of chiral resolving agents which associate with the racemates, forming a mixture of diastereomers. This mixture can be separated using available organic laboratory techniques. Chiral column chromatography is also useful for preparing enantioenriched compounds; however, high costs of the chiral stationary phases, the usages of large amounts of solvents, and low productivity of separation are some disadvantages of this method. The kinetic resolution provides an alternative pathway to prepare enantioenriched compounds other than classical resolution procedures.

Previous findings³¹ in our research group have shown that the resolution factor f as high as 19 can be achieved for the phenyl-substituted aminopentene **25c** using (*R*)-**19a-Lu** at 40 °C. The hydroamination products of aryl-substituted aminopentenenes using the binaphtholate catalysts **19a** and **19b** display high diastereoselectivity of up to 50:1 (*trans*:*cis* ratio). Moreover, the kinetic study of the kinetic resolution process indicates that the Curtin-Hammett pre-equilibrium favors the matching substrate/catalyst-complex

(pre-equilibrium constant $K^{\text{dias}} > 1$) for α -substituted aminopentene containing aryl substituents.

In this chapter we will report the kinetic resolution process using the rare-earth metal catalysts (*R*)-**39a–e-Ln** based on binaphtholate ligands with a variety of bulky alkylarylsilyl-substituents on the 3 and 3' positions (Figure 6-1). A detailed kinetic study of the kinetic resolution process will also be discussed.

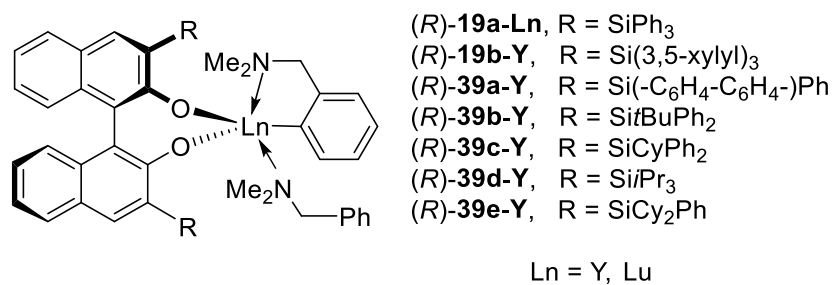


Figure 6-1. Rare-earth metal complexes based on 3,3'-bis(alkylarylsilyl)-binaphtholate ligands.

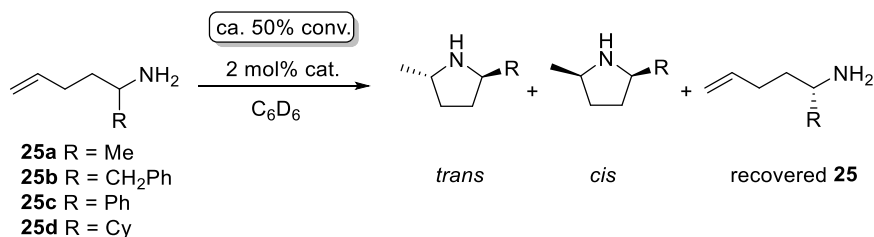
6.2 Kinetic Resolution of α -Substituted Aminopentenenes

Previously research in the Hultsch group has shown that the bis(triarylsilyl) substituted binaphtholate rare-earth metal complexes (*R*)-**19a-Ln** and (*R*)-**19b-Ln** (Ln = Y, Lu, Sc) are efficient catalysts for the kinetic resolution of some chiral aminoalkenes.^{31,119,156} It is believed that the sterically demanding silyl groups on the 3 and 3' positions of the binaphtholate ligands are responsible for catalyst stability as well as high catalytic activity and selectivity. In extension of the studies searching for catalysts with high activity and enantioselectivities in the hydroamination of alkenes, we successfully prepared 10 different rare-earth metal complexes (*R*)-**39a-Ln**–(*R*)-**39e-Ln**, based on binaphtholate ligands containing a variety of sterically hindered alkylarylsilyl-

substituents. Inspired by the high enantioselectivities observed for asymmetric hydroamination/cyclization of aminoalkenes catalyzed by our novel binaphtholate catalysts, our studies were focused on the kinetic resolution of racemic α -substituted 1-aminopent-4-enes **25a–25d** using these catalysts (Table 6-1).

In agreement with observations made in the asymmetric hydroamination of aminopentenes using binaphtholate catalysts, the cyclization rate of the methyl-substituted 1-aminopent-4-enes **25a** is about twice faster using the triphenylsilyl-substituted binaphtholate catalyst (*R*)-**19a-Y** than the rate for (*R*)-**19a-Lu**.³¹ Moreover, (*R*)-**19a-Y** displayed slightly higher efficiency in the kinetic resolution of the sterically less demanding substrate **25a** in comparison to the smaller ionic radius metal complex (*R*)-**19a-Lu** (Table 6-1, entries 1, 2).³¹ We therefore decided to focus our kinetic resolution studies using more active and more efficient yttrium catalysts.

Interestingly, the structurally more rigid complex (*R*)-**39a-Y** achieved an increased resolution factor for substrate **25a** (up to 14; Table 6-1, entry 3). While the cyclohexyldiphenylsilyl-substituted binaphtholate complex (*R*)-**39c-Y** exhibited the highest resolution factor of up to 89 for the methyl-substituted aminopentene **25a**, the sterically more demanding dicyclohexylphenylsilyl-substituted binaphtholate complex (*R*)-**39e-Y** showed significantly diminished kinetic resolution efficiency ($f = 2.8$; Table 6-1, entries 4, 5). The sterically bulky silyl groups in the 3 and 3' positions of the binaphtholate ligands produced remarkable effects on catalytic activity as well as the resolution factors in the cyclization of **25a**; however, the *trans:cis* selectivities were rather independent, showing consistently low ratios in the range of 7:1 to 11:1.

Table 6-1. Catalytic kinetic resolution of α -substituted 1-aminopent-4-enes.^a

Entry	Subs.	Cat.	T (°C)	t (h)	Conv. (%)	<i>trans/cis</i> ^b	ee (%) ^c	<i>f</i>
1		(<i>R</i>)- 19a-Y	22	25.5	53	11:1	72	9.5 ^d
2	 25a	(<i>R</i>)- 19a-Lu	22	42	55	10:1	73	8.4 ^d
3		(<i>R</i>)- 39a-Y	25	29.5	49	9:1	71	14
4		(<i>R</i>)- 39c-Y	25	13.0	48	7:1	86	89
5		(<i>R</i>)- 39e-Y	25	4	50	8:1	34.5	2.8
6	 25b	(<i>R</i>)- 19a-Y	22	9	50	20:1	42	3.6 ^d
7		(<i>R</i>)- 19b-Y	22	27	52	20:1	38	2.9 ^d
8		(<i>R</i>)- 39b-Y	25	42.3	50	20:1	64	8.6
9		(<i>R</i>)- 39c-Y	25	17.8	48	20:1	82	43
10		(<i>R</i>)- 19a-Y	22	95	50	≥50:1	74	15 ^d
11	 25c	(<i>R</i>)- 39a-Y	40	41.0	50	≥50:1	77	17.4
12		(<i>R</i>)- 39b-Y	40	39	54	≥50:1	86	16.6
13		(<i>R</i>)- 39c-Y	40	39	46	≥50:1	78	47
14		(<i>R</i>)- 39d-Y	40	82	50	≥50:1	30	2.4
15		(<i>R</i>)- 39e-Y	40	14	45	≥50:1	57.5	10
16		(<i>R</i>)- 19a-Y	22	8	56	---	49	3.5 ^e
17	 25d	(<i>R</i>)- 19b-Y	22	46	59	---	54	3.6 ^e
18		(<i>R</i>)- 39b-Y	25	3.3	54	5:1	56	4.7
19		(<i>R</i>)- 39c-Y	25	4.3	51	7:1	57	5.9
20		(<i>R</i>)- 39d-Y	25	16	58	---	79	8.5
21		(<i>R</i>)- 39e-Y	25	5.5	50	6:1	41	3.5

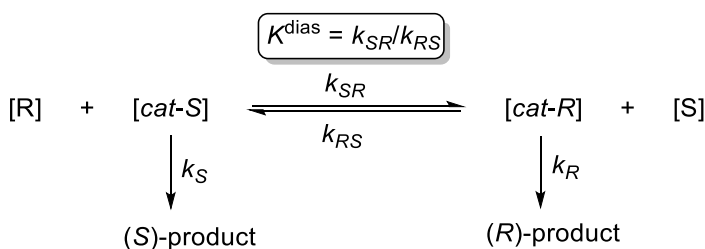
^a Reaction condition: 2 mol% cat., C₆D₆, Ar atm. ^b *Trans/cis* ratio of products. ^c Enantiomeric excess of recovered starting material **25**. ^d From ref. 31. ^e From ref. 104.

Higher *trans:cis* selectivities of up to 20:1 (Table 6-1, entries 6–9) were observed for the benzyl-substituted 1-aminopent-4-ene **25b**. However, the cyclization of **25b** proceeded at a much lower rate using the *tert*-butyldiphenylsilyl-substituted binaphtholate catalyst (*R*)-**39b-Y** in comparison to (*R*)-**19a-Y** (42.3 hrs at 25 °C and 9 hrs at 22 °C to obtain 50% conversion, respectively; Table 6-1, entry 8 versus entry 6). This is in contrast to our observation that (*R*)-**39b-Y** generally displayed similar catalytic activity as (*R*)-**19a-Y** in the cyclization of aminopentenes (see Chapter 4 and ref. ³¹). It is noteworthy that (*R*)-**39b-Y** resolved **25b** more efficiently than (*R*)-**19a-Y** (Table 6-1, entry 8 versus entry 6). Similar to the previous observation, the resolution of **25b** was generally less efficient than the resolution of **25a** with the same rare-earth metal binaphtholate catalyst (for example, compare Table 6-1, entry 4 and 9). Nevertheless, catalyst (*R*)-**39c-Y** resolved **25b** with a still impressive resolution factor of 43.

The kinetic resolution of the phenyl-substituted 1-aminopent-4-enes **25c** proceeded at 22 °C using (*R*)-**19a-Y**; however, a reaction time of 95 hrs was required for 50% conversion.³¹ The resolution of **25c** using our novel binaphtholate catalysts (*R*)-**39a-Y**–(*R*)-**39e-Y** was performed at 40 °C in this study with good turnover rates, giving consistently high *trans:cis* selectivities $\geq 50:1$ (Table 6-1, entries 11–15). Complexes (*R*)-**39a-Y**, (*R*)-**39b-Y**, and (*R*)-**39c-Y** displayed similar catalytic activity in the cyclization of **25c** (Table 6-1, entries 11–13), but the highest resolution factor of 47 was observed with (*R*)-**39c-Y**. As expected, the triisopropylsilyl-substituted binaphtholate catalyst (*R*)-**39d-Y** exhibited the lowest activity as well as the lowest efficiency in the resolution of **25c** (Table 6-1, entry 14) in agreement to its general performance. Although the hydroamination/cyclization of aminopentenes using (*R*)-**39c-Y** generally proceeded about

twice as fast as using the sterically more encumbered catalyst (*R*)-**39e-Y** (see Chapter 4, tables 4-1–4-3), (*R*)-**39e-Y** cyclized **25c** at three times the rate compared to (*R*)-**39c-Y** (Table 6-1, entry 13 versus entry 15). Unfortunately, catalyst (*R*)-**39e-Y** ($f = 10$) resolved **25c** much less efficiently than (*R*)-**39c-Y** ($f = 47$).

Previous studies in our group have shown that the sterically more demanding α -alkyl substrates, such as the benzyl-substituted **25b** and the cyclohexyl-substituted **25d** exhibit significantly diminished resolution factors using the bis(triarylsilyl)-substituted binaphtholate catalysts (*R*)-**19a-Ln** and (*R*)-**19b-Ln**.^{104,156} This observation is also true for **25d** using the cyclohexyldiphenylsilyl-substituted binaphtholate catalyst (*R*)-**39c-Y** (Table 6-1, entry 19). Interestingly, the least reactive catalyst (*R*)-**39d-Y** resolved **25d** most effectively among our available binaphtholate catalysts, with a resolution factor of 8.5 (Table 6-1, entry 20). The lowest diastereoselectivity was observed for the cyclohexyl-substituted **25d**, which gave *trans*:*cis* selectivities in the range of 5:1–7:1.



Scheme 6-2. The general model for the kinetic resolution of aminoalkenes.

According to the general model for the kinetic resolution of aminoalkenes (Scheme 6-2),³¹ the catalyst [*Ln*] is distributed between the two diastereomeric substrate/catalyst complexes [*cat-S*] and [*cat-R*] (Eq. 6-1).

$$[Ln] = [cat-S] + [cat-R] \quad (\text{Eq. 6-1})$$

NMR spectroscopic data indicate that the exchange rate between the two diastereomeric substrate/catalyst complexes is much faster than their rates k_S and k_R transforming to the products.³¹ The two diastereomeric substrate/catalyst complexes are in equilibrium with the equilibrium constant K^{dias} which is defined by Eq. 6-2.

$$K^{\text{dias}} = \frac{k_{SR}}{k_{RS}} = \frac{[\text{cat-R}][S]}{[\text{cat-S}][R]} \quad (\text{Eq. 6-2})$$

The rate of the hydroamination/cyclization of aminoalkene is first order in catalyst concentration; therefore, the rate law for each enantiomer can be written:

$$-\frac{d[R]}{dt} = k_R[\text{cat-R}] \quad (\text{Eq. 6-3})$$

$$-\frac{d[S]}{dt} = k_S[\text{cat-S}] \quad (\text{Eq. 6-4})$$

Combining equations 6-2–6-4, we obtain Eq. 6-5:

$$\frac{d[R]}{[R]} = K^{\text{dias}} \frac{k_R}{k_S} \frac{d[S]}{[S]} \quad (\text{Eq. 6-5})$$

$k_{\text{fast}}/k_{\text{slow}}$ now can be written as k_R/k_S . Integration of Eq. 6-5 leads to the resolution factor f :

$$f = K^{\text{dias}} \frac{k_R}{k_S} = \frac{\ln \frac{[R]}{[R]_0}}{\ln \frac{[S]}{[S]_0}} \quad (\text{Eq. 6-6})$$

The cyclization of the (*R*)-enantiomer is arbitrarily chosen as a faster reaction than that of the (*S*)-enantiomer during the kinetic resolution of a racemic aminoalkene. Assuming that the reaction starts with a racemic mixture ($[R]_0 = [S]_0 = 0.5$), the dependence of each enantiomer on conversion C and enantiomeric excess ee is defined by:

$$ee = \frac{[S] - [R]}{[S] + [R]} \quad (\text{Eq. 6-7})$$

$$[S] + [R] = 1 - C \quad (\text{Eq. 6-8})$$

Combination of Eq. 6-7 and 6-8 leads to:

$$[R] = \frac{(1-C)(1-ee)}{2} \quad (\text{Eq. 6-9})$$

$$[S] = \frac{(1-C)(1+ee)}{2} \quad (\text{Eq. 6-10})$$

Substitution of the Eqs. 6-9 and 6-10 into Eq. 6-6 leads to:

$$f = \frac{\ln[(1-C)(1-ee)]}{\ln[(1-C)(1+ee)]} \quad (\text{Eq. 6-11})$$

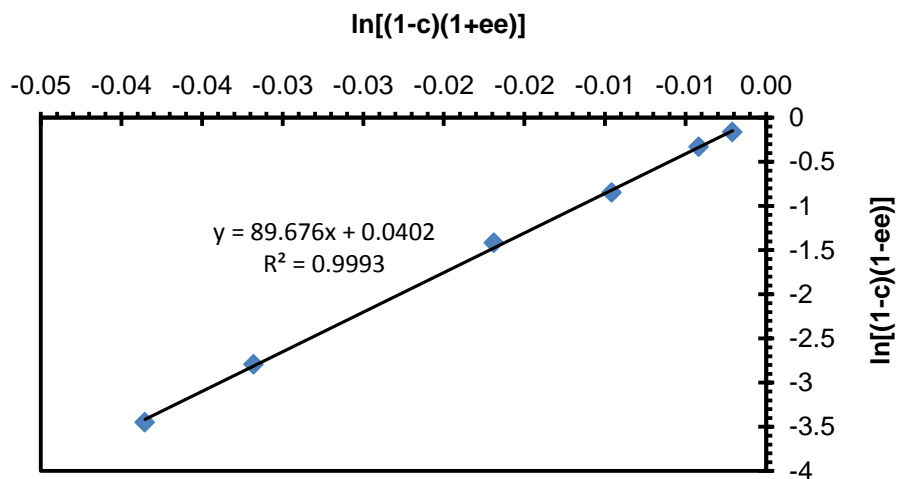


Figure 6-2. Plot of $\ln[(1-C)(1-ee)]$ versus $\ln[(1-C)(1+ee)]$ for the kinetic resolution of **25a** using binaphtholate catalyst (*R*)-**39c-Y** at 25 °C.

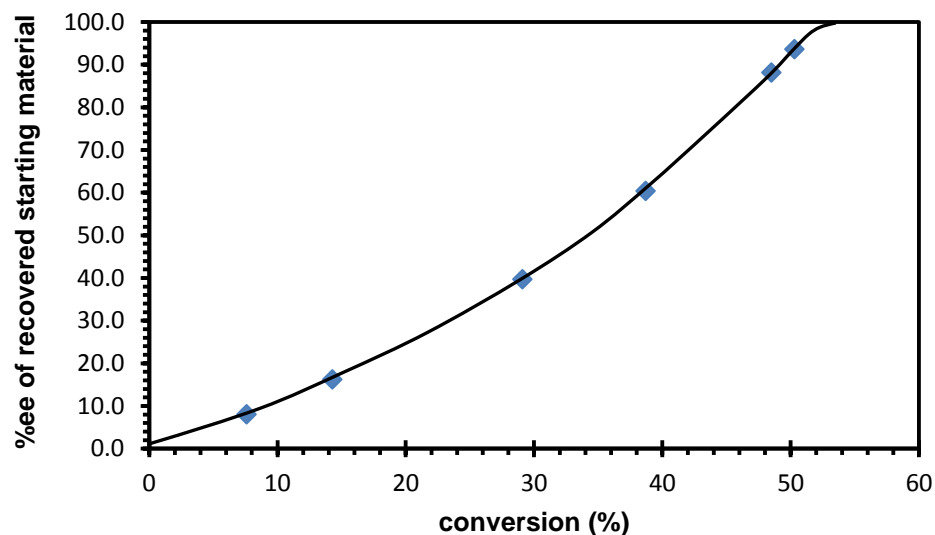
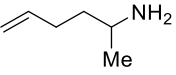
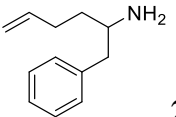
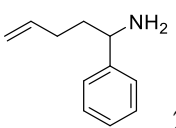
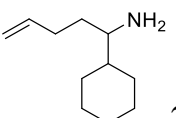


Figure 6-3. Dependence of enantiomeric excess of recovered starting material on conversion in the kinetic resolution of **25a** with (*R*)-**39c-Y** at 25 °C. The line was fitted to a resolution factor $f = 89.7$.

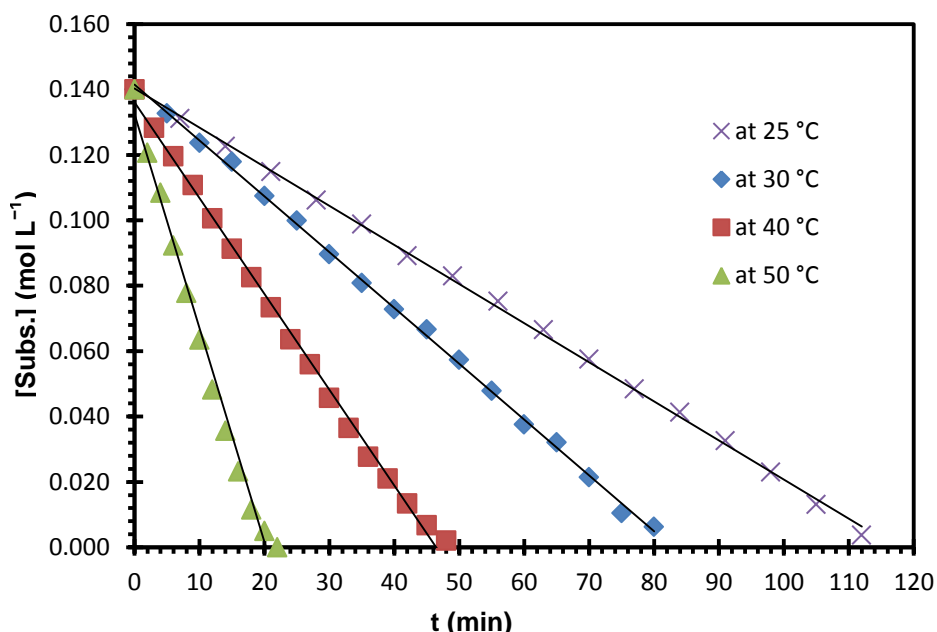
According to Eq. 6-9, the resolution factor f for **25a** using the binaphtholate catalyst (*R*)-**39c-Y** can be determined by plotting $\ln[(1-C)(1-ee)]$ versus $\ln[(1-C)(1+ee)]$ (Figure 6-2). The relationship between conversion and enantiomeric excess ee is expressed by Figure 6-3.

Inspired by the high resolution factor for the methyl-substituted aminopentene **25a** obtained with the cyclohexyldiphenylsilyl-substituted binaphtholate catalyst (*R*)-**39c-Y** at 25 °C, a large-scale kinetic resolution of **25a** was performed with (*S*)-**39c-Y**, giving (*S*)-**25a** (95% ee) in 38% yield re-isolated yield at 52% conversion. The yield of (*S*)-**25a** is lower than expected due to the compound's volatility (b.p. 114–116 °C at 760 Torr). The enantiopure α -substituted aminopentenenes **25b–25d** were also prepared using (*R*)-**39c-Y** and the resolution data are summarized in the Table 6-2.

Table 6-2. Large-scale preparation of enantiopure α -substituted aminopentenes *via* kinetic resolution using binaphtholate catalyst **39c-Y**.

Substrate	Cat.	T (°C)	t (h)	<i>f</i>	Conv. (%)	Re-isolated subs. (% yield) ^a	% ee
 25a	(<i>S</i>)- 39c-Y	25	9	90	52	(<i>S</i>)- 25a (38)	95
 25b	(<i>R</i>)- 39c-Y	25	22.5	43	57	(<i>S</i>)- 25b (40)	95
 25c	(<i>R</i>)- 39c-Y	40	31	47	54	(<i>S</i>)- 25c (40)	97
 25d	(<i>R</i>)- 39c-Y	25	9.5	6	77	(<i>S</i>)- 25d (18)	95

^a Note that the CIP priorities differ between substrate **25a** on the one side and substrate **25b–d** on the other side. Thus, (*R*)-**25a** is the matching substrate for the (*S*)-catalyst, while it is the (*R*) catalyst enantiomer for substrates (*R*)-**25b–d**. (CIP = Cahn-Ingold-Prelog).

**Figure 6-4.** Time dependence of the substrate concentration in the hydroamination of (*S*)-**25a** using (*R*)-**39c-Y** (matching pair; [(*S*)-**25a**]₀ = 0.140 mol L⁻¹, [(*R*)-**39c-Y**] = 2.73 mmol L⁻¹). The straight lines represent the least square linear regression.

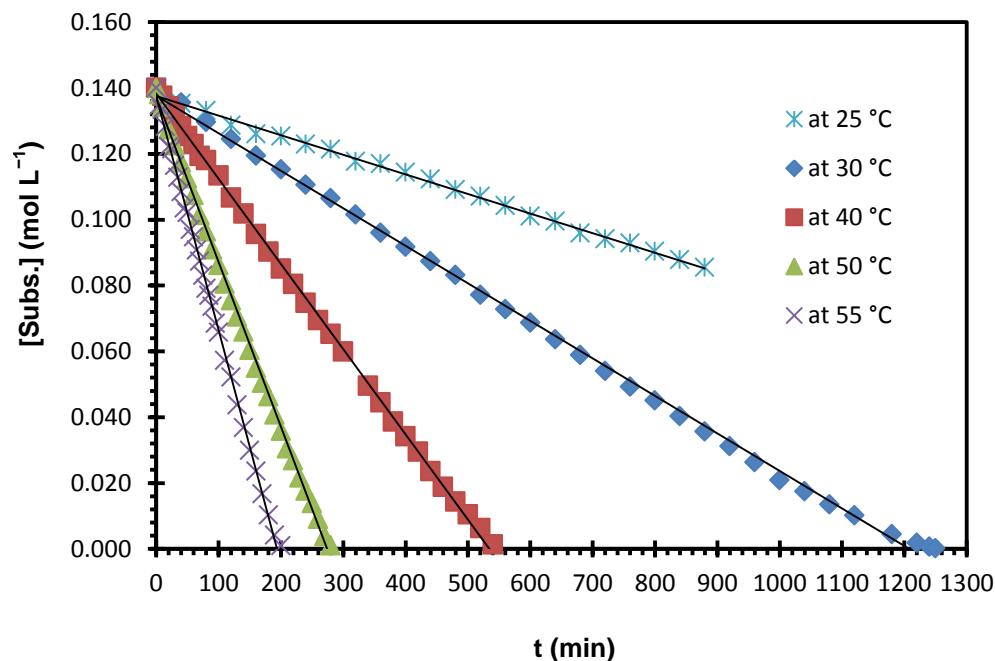


Figure 6-5. Time dependence of the substrate concentration in the hydroamination of (*S*)-**25a** using (*S*)-**39c-Y** (mismatching pair; $[(S)\text{-}25a]_0 = 0.140 \text{ mol L}^{-1}$, $[(S)\text{-}39c\text{-Y}] = 2.73 \text{ mmol L}^{-1}$). The straight lines represent the least square linear regression.

The rate constants k_{fast} and k_{slow} of the cyclization for the matching and mismatching substrate/catalyst combination, respectively, were obtained *via* kinetic measurements of the cyclization rates of the enantiopure (*S*)-**25a** using either (*R*)-**39c-Y** (Figure 6-4) or (*S*)-**39c-Y** (Figure 6-5).

The kinetic data and resolution parameters of α -substituted aminopentenes were determined with the alkylarylsilyl-substituted binaphtholate catalysts **39b-Y**, **39c-Y**, and **39e-Y** (Table 6-3). In agreement with the kinetic measurements reported previously for the methyl-substituted **25a** with the triphenylsilyl-substituted binaphtholate catalyst **19a-Y**,¹⁰⁴ the Curtin-Hammett pre-equilibrium favors the mismatching substrate/catalyst combination ($K^{dias} < 1$) for **25a** with **39b-Y** and **39e-Y** (Table 6-3, entries 2, 7). On the contrary, the equilibrium for the cyclohexyldiphenylsilyl-substituted binaphtholate catalyst **39c-Y** and substrate **25a** favors the matching substrate/catalyst complex ($K^{dias} >$

1); thus, effectively enhancing the efficiency of the kinetic resolution process. The relative rate k_{fast}/k_{slow} remains in the range of 9.0–17.6 for methyl-substituted **25a** with our novel binaphtholate catalysts **39b-Y**, **39c-Y**, and **39e-Y** at temperatures ranging from 25 to 50 °C, with the highest ratio being achieved with **39c-Y** at 25 °C. Dramatic differences in the *trans/cis* diastereoselectivities in the cyclization of (*S*)-**25a** using (*R*)-**39c-Y** (Figure 6-6, plot a, *trans/cis* = 39:1.0 for the matching pair) and (*S*)-**25a** using (*S*)-**39c-Y** (Figure 6-6, plot b, *trans/cis* = 1:1.2 for the mismatching pair) account for the low *trans/cis* selectivities observed in the kinetic resolution of racemic **25a** (*trans/cis* = 7–11:1, Table 6-1, entries 1, 2, 4, 5). Additionally, the *trans/cis* ratios decrease gradually as the resolution reaction proceeds (Figure 6-7). It is noteworthy that the reaction of (*S*)-**25a** using (*S*)-**39c-Y** (mismatching pair) preferentially produced the *cis*-product at all reaction temperatures in a range of 25–50 °C (Table 6-3, entries 3–6).

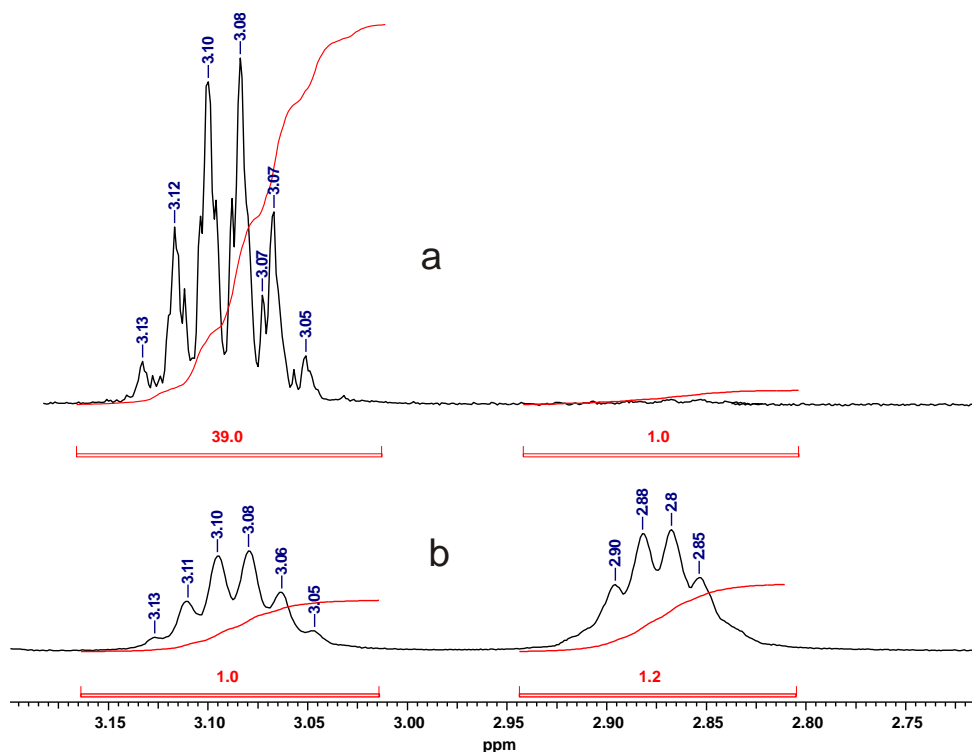


Figure 6-6. A stack plot of ¹H NMR spectra of hydroamination products obtained with matching pair of (*S*)-**25a** and (*R*)-**39c-Y** (plot a) and with mismatching pair of (*S*)-**25a** using (*S*)-**39c-Y** (plot b).

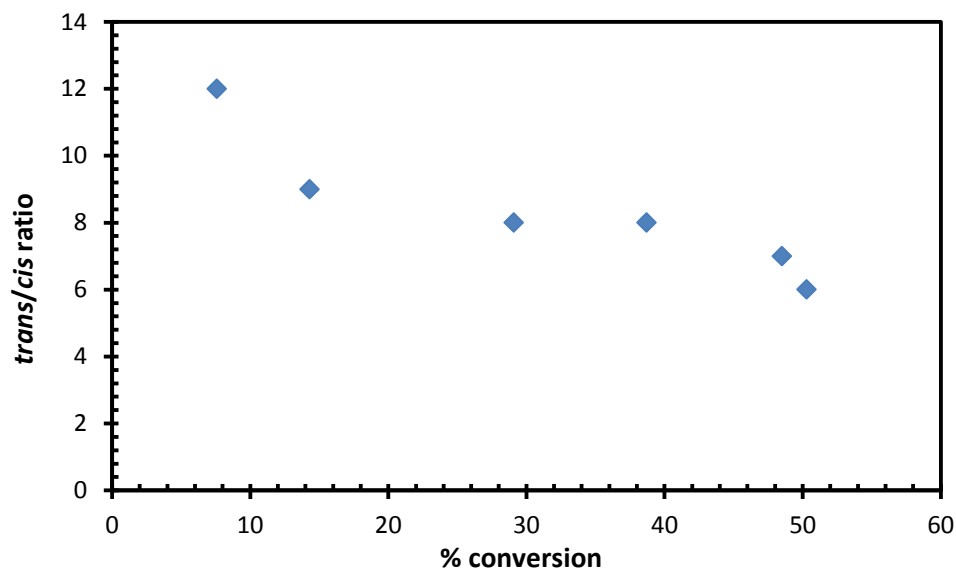
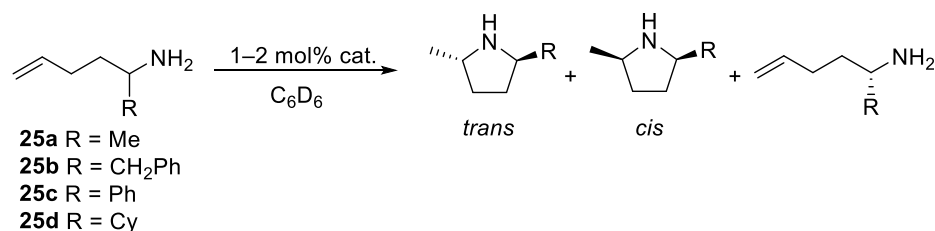


Figure 6-7. *Trans/cis* ratio of the cyclization product of *rac*-**25a** using 2 mol% of (*R*)-**39c-Y** as a function of conversion.

In agreement with the previous findings, the equilibrium in favor of the mismatching substrate/catalyst combination was observed for the benzyl-substituted aminopentene **25b** with catalyst **39b-Y** (Table 6-3, entry 9). Similar to that observed for **25a**, high efficiency in the kinetic resolution of **25b** was achieved with **39c-Y** as a combined effect of high relative rate, k_{fast}/k_{slow} , and the Curtin-Hammett pre-equilibrium in favor of the matching substrate/catalyst combination ($K^{dias} > 1$) (Table 6-3, entry 10). Although the formation of the matching substrate/catalyst pair was slightly more favorable in the pre-equilibrium, a low k_{fast}/k_{slow} ratio resulted in a low efficiency of the kinetic resolution of substrate **25b** with catalyst **39e-Y** (Table 6-3, entry 11). While the diastereoselectivities remained high for the matching pair of the substrate (*S*)-**25b** and the (*S*)-catalyst, significantly lower selectivities were observed for the mismatching pair (Table 6-3, entries 9-11), except the case where catalyst (*S*)-**19a-Y** was used.¹⁰⁴

Table 6-3. Kinetic resolution parameters of α -substituted aminopentenes

Entry	Subs.	Cat.	T (°C)	k_{fast} (10 ⁻³ s ⁻¹) ^a	$k_{\text{fast}}/k_{\text{slow}}$	f^b	K^{dias}	<i>trans/cis</i> fast [slow, conv. (%)]
1	25a	19a-Y	30	8.5	7.6	6.4	0.84	>30:1.0 [2.8:1.0] ^c
2		39b-Y	25	2.32	10.7	5.6	0.52	35:1.0 [2.2:1.0, 77]
3		39c-Y	25	7.35	17.6	90	5.11	39:1.0 [1:1.2, 100]
4		39c-Y	30	10.01	13.5	76.5	5.67	38:1.0 [1:1.2, 100]
5		39c-Y	40	19.60	11.6	45.9	3.96	38:1.0 [1:1.3, 100]
6		39c-Y	50	47.24	14.2	23.7	1.67	38:1.0 [1:1.2, 100]
7		39e-Y	25	3.09	9.0	2.8	0.31	35:1.0 [1.5:1.0, 60]
8	25b	19a-Y	30	2.5	9.6	2.6	0.27	>30:1.0 [>30.0:1.0] ^c
9		39b-Y	40	3.26	7.48	6.1	0.82	24:1.0 [4.0:1.0, 65]
10		39c-Y	40	5.38	10.5	32.3	3.08	25:1.0 [1.0:1.0, 70]
11		39e-Y	40	2.63	4.86	5.5	1.13	21:1.0 [1.7:1.0, 77]
12	25c	19a-Y	60	11.3	7.1	11.5	1.6	>50:1.0 [8.8:1.0] ^d
13		39b-Y	70	5.43	11.2	11.6	1.04	>50:1.0 [3.2:1.0, 45]
14		39c-Y	60	3.76	15.9	24.6	1.55	>50:1.0 [7.0:1.0, 30]
15		39c-Y	70	6.90	15.0	16.6	1.10	>50:1.0 [6.9:1.0, 30]
16		39e-Y	70	4.06	6.15	7.6	1.24	>50:1.0 [2.2:1.0, 100]
17	25d	19a-Y	30	8.5	8.5	2.7	0.32	9.0:1.0 [1.4:1.0] ^c
18		39b-Y	25	4.47	3.76	4.7	1.25	24:1.0 [1.0:2.4, 100]
19		39c-Y	25	3.12	3.9	5.6	1.43	23:1.0 [1.0:1.9, 100]
20		39e-Y	25	1.93	1.75	3.6	2.06	21:1.0 [1.2:1.0, 100]

^a $k_{\text{fast}} = k_{\text{R}}$ for the reaction of (*S*)-**25a** with (*R*)-catalyst; $k_{\text{fast}} = k_{\text{S}}$ for the reaction of (*S*)-**25b**, (*S*)-**25c**, (*S*)-**25d** with (*S*)-catalyst. ^b Determined from the slope of plot of $\ln(1-C)(1-ee)$ versus $\ln(1-C)(1+ee)$, with at least three data points. ^c From ref. 104. ^d From ref. 31.

High diastereoselectivities of up to 50:1 were observed for the phenyl-substituted substrate **25c** with all binaphtholate catalysts. Although the cyclization rate of the matching pair, involving substrate (*S*)-**25c** and catalyst (*S*)-**19a-Y**, was about three times faster than that of (*S*)-**25c** and (*S*)-**39c-Y** at 60 °C, a higher k_{fast}/k_{slow} ratio was observed for **25c** with **39c-Y** ($k_{fast}/k_{slow} = 15.9$ versus 7.1 with **19a-Y**) (Table 6-3, entries 12 and 14). As a result the cyclohexyldiphenylsilyl-substituted binaphtholate catalyst **39c-Y** exhibited higher efficiency in the kinetic resolution of **25c** in comparison to **19a-Y**.

The alkylarylsilyl-substituted binaphtholate catalysts **39b-Y**, **39c-Y**, and **39e-Y** behaved quite differently in the kinetic resolution of **25d** compared to the triphenylsilyl-substituted binaphtholate catalyst **19a-Y**. Lower k_{fast}/k_{slow} ratios were observed with **39b-Y**, **39c-Y**, and **39e-Y**; however, the Curtin-Hammett pre-equilibrium favors the matching substrate/catalyst combination for **25d** with these catalysts ($K^{dias} > 1$). These kinetic data are in agreement with the kinetic resolution of **25d** that we observed previously (see table 6-1 and ref. 104), indicating that **39b-Y**, **39c-Y**, and **39e-Y** are slightly more efficient catalysts for the kinetic resolution of **25d** in comparison to **19a-Y**.

The Eyring plot for k_{fast} and k_{slow} (Figure 6-8) provided an access to the activation parameters for the hydroamination/cyclization of (*S*)-**25a** using (*R*)-**39c-Y** (matching pair) ($\Delta H^\ddagger = 43(5) \text{ kJ mol}^{-1}$, $\Delta S^\ddagger = -136(17) \text{ J mol}^{-1} \text{ K}^{-1}$). Because the reaction of (*S*)-**25a** and (*S*)-**39c-Y** (mismatching pair) afforded the products with low *trans/cis* diastereoselectivities, the activation parameters for each diastereomer were obtained (*trans*: $\Delta H^\ddagger = 45(2) \text{ kJ mol}^{-1}$, $\Delta S^\ddagger = -160(7) \text{ J mol}^{-1} \text{ K}^{-1}$; *cis*: $\Delta H^\ddagger = 54(4) \text{ kJ mol}^{-1}$, $\Delta S^\ddagger = -130(14) \text{ J mol}^{-1} \text{ K}^{-1}$). The activation parameters for the matching and mismatching (*cis*) seem to be similar to those obtained previously for **25a** with catalyst **19a-Y**.

(matching pair: $\Delta H^\ddagger = 47.3(3.5) \text{ kJ mol}^{-1}$, $\Delta S^\ddagger = -128(11) \text{ J mol}^{-1} \text{ K}^{-1}$; mismatching pair: $\Delta H^\ddagger = 54.9(3.1) \text{ kJ mol}^{-1}$, $\Delta S^\ddagger = -121(9) \text{ J mol}^{-1} \text{ K}^{-1}$).¹⁰⁴ The negative activation entropy is indicative of a highly organized transition state.^{31,42}

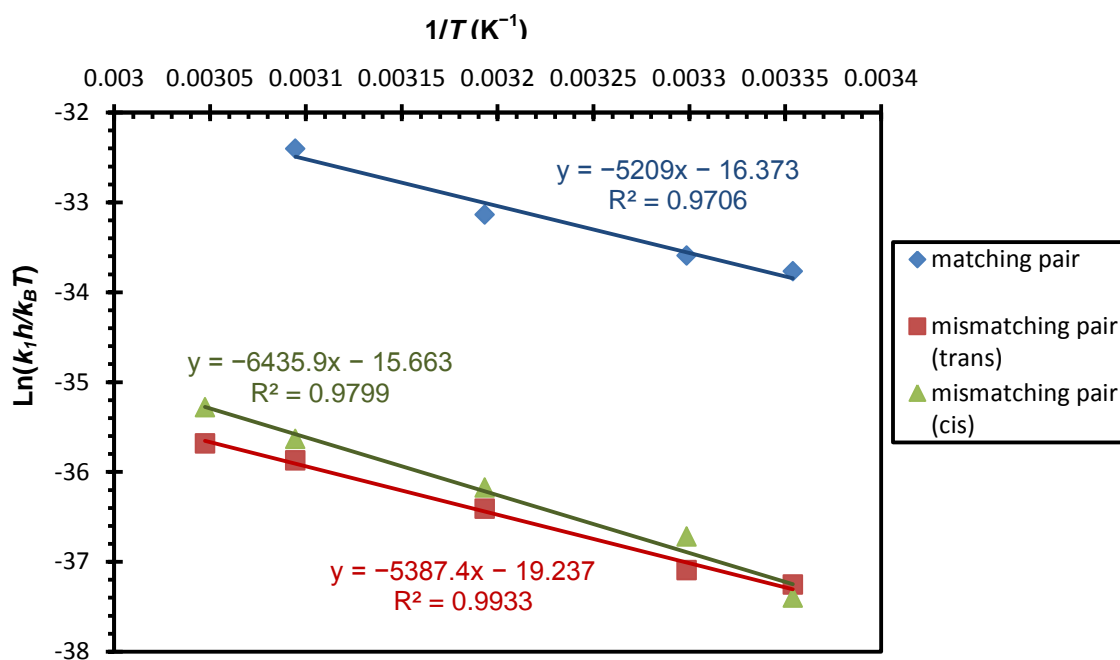
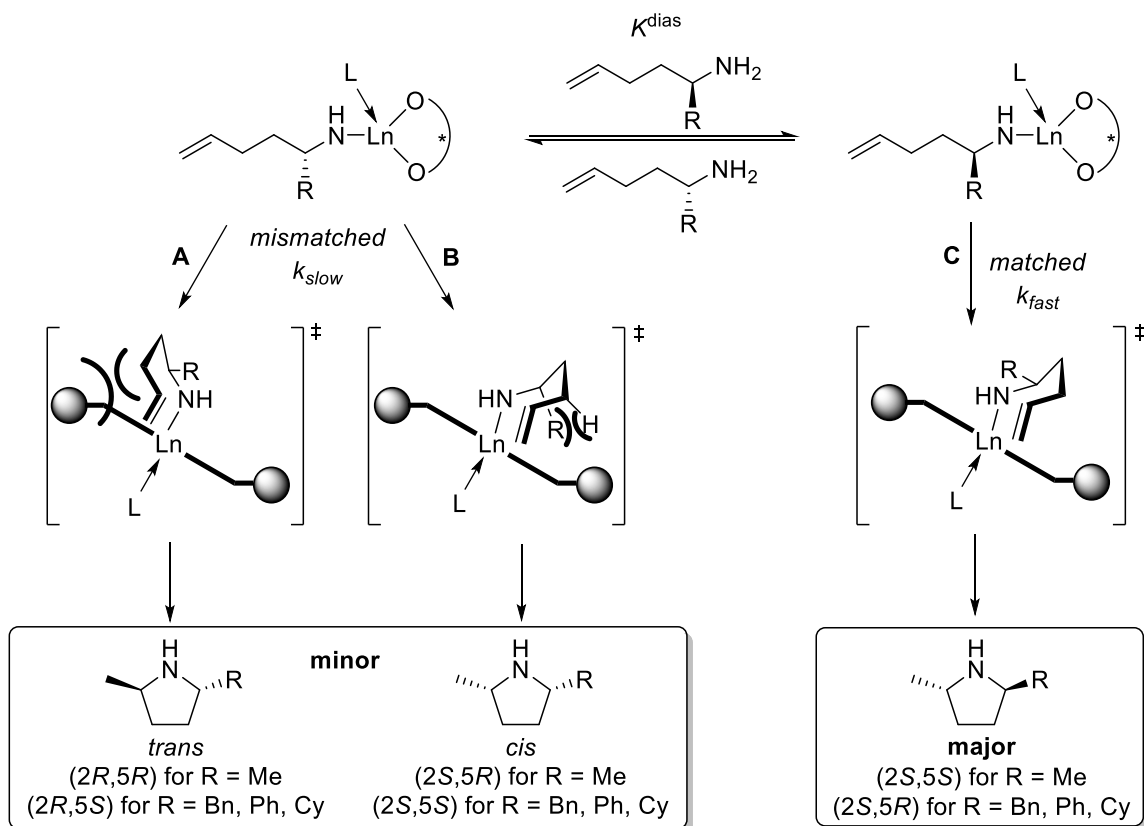


Figure 6-8. Eyring plot for the hydroamination/cyclization of (*S*)-**25a** using (*R*)-**39c-Y** (matching) and (*S*)-**39c-Y** (mismatching).

6.3 Stereomodel for the Kinetic Resolution of α -Substituted Aminopentenes

According to the proposed stereomodel for the kinetic resolution of α -substituted aminopentenes using rare-earth metal catalysts based on binaphtholate ligands, the diastereomers can be achieved *via* possible cyclization pathways as drawn in Scheme 6-3.^{31,104}



Scheme 6-3. Proposed stereomodel for the kinetic resolution of α -substituted aminopentenes.

In fact, the stereomodel for the kinetic resolution is in agreement with the general stereomodel for enantioselective hydroamination/cyclization of aminopentene **57** by (*R*)-binaphtholate rare-earth metal catalysts, in which the Ln–N bond preferentially approaches the *re* face of the olefin.³¹ In the case of the matching substrate/catalyst combination, the α -substituent of the aminoalkene rests in an equatorial position of the seven-membered chair-like transition state in the conformation that facilitates the approach of the Ln–N bond to the olefin from the *re* face (Scheme 6-3, pathway C). In the case of the mismatching substrate/catalyst combination, the sterically unfavorable interaction between the substrate and alkylarylsilyl-substituent of the binaphtholate

ligand restricts the approach of the Ln–N bond to the olefin from the *si* face (Scheme 6-3, pathway **A**). Pathway **B** provides an alternative to pathway **A**, allowing the mismatching substrate/catalyst combination to avoid the steric interaction between substrate and the bulky silyl group. However, it is hard to predict which pathway, **A** or **B**, is more favorable because pathway **B** requires the α -substituent of the aminopentene to rest in an axial position, which leads to unfavorable 1,3-diaxial interaction in the chair-like transition state and possibly steric interaction between the α -substituents R and the alkylarylsilyl-substituents of the binaphtholate ligand if R is sufficiently large.

Pathway **B** accounts for significantly reduced diastereoselectivities which were observed for the mismatching substrate/catalyst combinations except for **25b** using **19a-Y**. Moreover, the cyclization of the mismatching pair of (*S*)-**25a** with (*S*)-**39c-Y**, (*S*)-**25d** with (*S*)-**39b-Y**, and (*S*)-**25d** with (*S*)-**39c-Y** preferentially proceed through pathway **B**, generating predominantly *cis*-pyrrolidine products. The exceptionally high efficiency in the kinetic resolution of the methyl-substituted **25a** with **39c-Y** results from the Curtin-Hammett pre-equilibrium in favor of the matching substrate/catalyst combination and a high k_{fast}/k_{slow} ratio.

The large *trans/cis* selectivities exceeding 50:1, observed for phenyl-substituted aminopentene **25c** in comparison to the alkyl-substituted aminopentenenes **25a**, **25b**, and **25d**, may result from a coordinative interaction of the phenyl-substituent of **25c** with the metal center¹⁵⁸ or a π -interaction of the phenyl-substituent with a naphthyl ring of the binaphtholate ligand.

6.4 Conclusions

The kinetic resolution of α -substituted aminopentenes *via* asymmetric hydroamination/cyclization was studied using rare-earth metal catalysts based on 3,3'-bis(alkylarylsilyl)-substituted binaphtholate ligands. In general the cyclohexyldiphenylsilyl-substituted binaphtholate catalyst (*R*)-**39c-Y** displays high efficiency in the kinetic resolution of the methyl-, benzyl-, and phenyl-substituted substrates **25a**, **25b**, and **25c**, respectively. The highest resolution factor of up to 90 was observed for **25a** using (*R*)-**39c-Y**, which was determined by the plot of $\ln[(1-C)(1-ee)]$ versus $\ln[(1-C)(1+ee)]$. The cyclohexyl-substituted substrate **25d** exhibits low efficiency in the kinetic resolution with all binaphtholate catalysts screened in this study.

The kinetic data of (*S*)-**25a** with (*R*)-**39c-Y** (matching) and (*S*)-**25a** and (*S*)-**39c-Y** (mismatching) produced the activation parameters which are in agreement with the previously reported data obtained with **25a** and **19a-Y**. It is noteworthy that the mismatching substrate/catalyst combination of (*S*)-**25a** and (*S*)-**39c-Y** preferentially affords the *cis*-product. The kinetic resolution parameters show that high efficiency in the kinetic resolution of the methyl-substituted **25a** with **39c-Y** stems from the Curtin-Hammett pre-equilibrium in favor of the matching substrate/catalyst combination and a high k_{fast}/k_{slow} ratio. While high *trans/cis* selectivities were observed for the phenyl-substituted aminopentene **25c**, the alkyl-substituted substrates display diminished *trans/cis* selectivities. The high *trans/cis* selectivities observed for the phenyl-substituted aminopentene **25c** can be attributed to a coordinative interaction of the phenyl-substituent

of **25c** with the metal center or a π -interaction of the phenyl-substituent with a naphthyl ring of the binaphtholate ligand.

Chapter 7

Experimental Section

General Considerations

All reactions with air- or moisture sensitive materials were performed in oven (120 °C) and flame-dried glassware, under an inert atmosphere of dry nitrogen or argon, employing standard Schlenk and glovebox techniques. Pentane, hexanes, THF, Et₂O, and toluene were sparged with argon for 1 h and then pass through a column of activated alumina prior to use. Anhydrous CH₂Cl₂, CHCl₃, and DMF were distilled from finely powdered CaH₂. Benzene, toluene-d₈, and C₆D₆ were vacuum transferred from sodium/benzophenone ketyl. All other chemicals were commercially available and used as received unless otherwise stated. (*S*)-(+)- α -Methoxy- α -trifluoro-methylphenylacetic acid (Mosher acid) was transformed into the corresponding (*R*)-Mosher acid chloride according to the literature procedure.¹⁵⁹

¹H, ¹³C, and ¹⁹F NMR spectra were recorded on Varian (300, 400, 500 MHz) spectrometers at 25 °C unless otherwise stated. Silica gel (230–400 mesh, Sorbent Technologies) was used for column chromatography.

7.1 Synthesis of Chlorosilanes

Trichlorosilane and tetrachlorosilane were commercially available and distilled from finely powdered CaH_2 . Chloro(4-methoxyphenyl)(diphenyl)silane¹⁶⁰ was synthesized according to a literature procedure.

***Tert*-butyldiphenylchlorosilane.**¹⁶¹ To *t*BuLi (30.0 mL, 45.0 mmol, 1.5 M in pentane) in pentane (20 mL) was added dichloro(diphenyl)silane (9.79 g, 37.5 mmol) at room temperature. The resulting mixture was refluxed overnight. The precipitate lithium chloride salt was filtered off. Pentane was evaporated before the content was distilled in vacuo (0.5 torr, b.p. 107–109 °C), yielding a clear liquid (8.12 g, 79% yield). ¹H NMR (400 MHz, CDCl_3): δ = 7.80–7.75 (m, 4H, aryl-H), 7.50–7.38 (m, 6H, aryl-H), 1.17 (s, 9H, $\text{C}(\text{CH}_3)_3$); ¹³C{¹H} NMR (100 MHz, CDCl_3): δ = 135.4, 132.7, 130.5, 128.1 (aryl), 26.7 ($\text{C}(\text{CH}_3)_3$), 20.9 ($\text{C}(\text{CH}_3)_3$).

Cyclohexyldiphenylchlorosilane.^{162,163} To a suspension of finely cut lithium wire (1.60 g, 226.0 mmol) in pentane (150 mL) was added slowly chlorocyclohexane (15.42 g, 127.5 mmol) over a period of 1 hour while gently heating. The resulting mixture was heated to refluxing temperature for 5 hours. The violet mixture was chilled in an ice bath and a solution of diphenyldichlorosilane (13.31 g, 51.0 mmol) in pentane (10 mL) was added dropwise. The resulting mixture was allowed to warm to room temperature and was stirred overnight. Precipitate lithium chloride salt and excessive lithium were filtered off. The filtrate was treated with ice cold 2M HCl solution (30 mL) to quench the excess

cyclohexyllithium. The organic layer was separated, dried over anhydrous Na_2SO_4 , and concentrated to give a yellow oil. The product was purified by vacuum distillation, giving two main portions containing pure product, 100–148 °C (2.73 g) and 148–163 °C (6.03 g) at 0.5 torr. Both fractions were shown to be identical and pure cyclohexyldiphenylchlorosilane (8.76 g, 57% yield) by ^1H and ^{13}C NMR spectroscopy. ^1H NMR (300 MHz, CDCl_3): δ = 7.83–7.55 (m, 4H, aryl-H), 7.54–7.32 (m, 6H, aryl-H), 2.00–1.61 (m, 5H, Cy), 1.54–1.09 (m, 6H, Cy). $^{13}\text{C}\{^1\text{H}\}$ NMR (75 MHz, CDCl_3): δ = 134.9, 130.6, 128.2 (aryl), 27.9, 26.9, 26.8 (Cy).

Triisopropylchlorosilane.^{164,165} To a solution of tetrachlorosilane (17.63 g, 103.8 mmol) in toluene (150 mL) was added slowly the Grignard reagent $i\text{PrMgCl}$ which was prepared from $i\text{PrCl}$ (47.45 g, 580.0 mmol) and Mg shavings (14.27 g, 587.0 mmol) in THF (250 mL). To the resulting mixture was added methanol (3.32 g, 103.8 mmol) dropwise. The grey solution was stirred at refluxing temperature overnight. The reaction mixture was allowed to cool to room temperature and was treated with a saturated aqueous NH_4Cl solution (40 mL). The product was extracted with hexanes (3×50 mL). The organic layers were dried over anhydrous MgSO_4 , concentrated, and distilled at atmospheric pressure (b.p. 185–187 °C), yielding methoxy(triisopropyl)silane as a clear liquid (10.73 g, 55% yield). To methoxy(triisopropyl)silane (10.73 g, 56.96 mmol) in THF (20 mL) was added slowly concentrated HCl (37%, 16 mL, 192 mmol). The reaction mixture was stirred at room temperature overnight. The organic layer was separated. The product was extracted with CH_2Cl_2 (3×30 mL). The organic layers were combined, dried over anhydrous MgSO_4 , and distilled at atmospheric pressure, b.p. 193–197 °C, giving the

product as a clear liquid (8.49g, 78% yield). The product was shown to be contaminated with an unknown which showed peak as a multiplet at 1.03–1.07 ppm in ^1H NMR spectrum. The triisopropylchlorosilane was used for silylation reaction without further purification. ^1H NMR (500 MHz, CDCl_3): δ = 1.28–1.18 (m, 3H, $\text{CH}(\text{CH}_3)_2$), 1.15–1.07 (m, 18H, $\text{CH}(\text{CH}_3)_2$). $^{13}\text{C}\{^1\text{H}\}$ NMR (125 MHz, CDCl_3): δ = 19.4, 17.7.

2,2'-dibromobiphenyl.¹⁶⁶ To a solution of *o*-dibromobenzene (10.00 g, 41.54 mmol) in THF (50 mL) was added slowly *n*BuLi (8.8 mL, 20.8 mmol, 2.37 M in hexane) at -78°C . The acetone bath was removed to allow the reaction mixture to warm to room temperature. The reaction mixture was treated with HCl 10% solution (10 mL). The product was extracted with hexanes (3×30 mL). The organic layers were dried over anhydrous Na_2SO_4 , filtered, and concentrated in vacuo. The product was crystallized out of solution upon addition of absolute ethanol (10 mL). The solid was collected, washed with cold ethanol (2×2 mL) and dried in vacuo for 1 hour to give pure 2,2'-dibromobiphenyl as white solid (4.48 g, 70% yield). ^1H NMR (300 MHz, CDCl_3): δ = 7.67 (d, $^3J(\text{H,H}) = 7.3$ Hz, 2H), 7.38 (m, 2 H), 7.26 (m, 4H); $^{13}\text{C}\{^1\text{H}\}$ NMR (75 MHz, CDCl_3): δ = 142.3, 132.8, 131.2, 129.6, 127.4, 123.8.

5-chloro-5-phenyldibenzosilole.¹⁶⁷ To a stirred suspension of finely cut lithium wire (0.64 g, 92.7 mmol) in Et_2O (50 mL) was added a solution of 2,2'-dibromobiphenyl (4.13 g, 13.2 mmol) in Et_2O (25 mL) in several portions. The resulting reddish solution containing excessive lithium was heated to reflux for 14 hours. The content was added dropwise using a cannula to another flask containing phenyltrichlorosilane (4.62 g, 21.2

mmol) in Et₂O (20 mL) while it was gently refluxed. The resulting dark yellow mixture was refluxed for 4 hours. The precipitated lithium chloride was filtered off. The filtrate was distilled at atmospheric pressure, then under vacuum (0.5 Torr, bp 195–200 °C), giving the product as a light yellow, viscous liquid (2.30 g, 60% yield). ¹H NMR (300 MHz, CDCl₃): δ = 7.90–7.81 (m, 2H), 7.81–7.62 (m, 4H), 7.57–7.28 (m, 7H); ¹³C{¹H} NMR (75 MHz, CDCl₃): δ = 147.6, 147.3, 134.6, 134.4, 133.5, 133.4, 133.3, 133.2, 132.1, 131.2, 128.5, 128.3, 121.2.

Di-*tert*-butyl(phenyl)silane.¹²³ To an ice-cold solution of trichlorosilane (20.13 g, 148.6 mmol) in diethyl ether (25 mL) was slowly added the Grignard reagent PhMgBr, which was prepared from bromobenzene (23.57 g, 148.6 mmol) and Mg shavings (3.68 g, 153.3 mmol) in diethyl ether (100 mL). The reaction mixture was allowed to warm to room temperature before it was refluxed overnight. The white solid was filtered off. The filtrate was concentrated and distilled at atmospheric pressure (b.p. 180–185 °C), yielding dichloro(phenyl)silane (7.57 g) as a clear liquid. To dichloro(phenyl)silane (7.57 g, 42.74 mmol) in hexanes (25 mL) was added *t*BuLi (57 mL, 85.5 mmol, 1.5 M in pentane) at –30 °C. The resulting mixture was allowed to warm to room temperature and was stirred at this temperature overnight. The white precipitate of lithium chloride was filtered off. The hexane solvent was distilled off at atmospheric pressure before the remaining content was distilled at reduced pressure (5 torr, b.p. 115–118 °C), yielding di-*tert*-butyl(phenyl)silane (7.92 g, 24 % yield over 2 steps). ¹H NMR (500 MHz, CDCl₃): δ = 7.63–7.58 (m, 2H, aryl-H), 7.42–7.32 (m, 3H, aryl-H), 3.89 (s, 1H, SiH), 1.08 (s, 18H,

$C(CH_3)_3$; $^{13}C\{^1H\}$ NMR (125 MHz, $CDCl_3$): δ = 135.8, 135.6, 129.0, 127.5 (aryl), 29.0 ($C(CH_3)_3$), 19.1 ($C(CH_3)_3$).

Di-*tert*-butylphenylbromosilane.¹²² To a solution of di-*tert*-butyl(phenyl)silane (6.10 g, 27.7 mmol) in $CHCl_3$ (15 mL) was added slowly a solution of liquid Br_2 (1.5 mL, 28 mmol) in $CHCl_3$ (30 mL) at 0 °C. The reaction mixture was allowed to warm to room temperature and was stirred at this temperature overnight. The solvent was distilled off before the remaining content was distilled at reduced pressure (0.5 torr, 85–90 °C), yielding di-*tert*-butylphenylchlorosilane as a clear liquid 7.68 g (93% yield). 1H NMR (500 MHz, $CDCl_3$): δ = 7.86–7.82 (m, 2H, aryl-H), 7.45–7.36 (m, 3H, aryl-H), 1.17 (s, 18H, $C(CH_3)_3$); $^{13}C\{^1H\}$ NMR (125 MHz, $CDCl_3$): δ = 135.7, 132.5, 129.9, 127.8 (aryl), 28.6 ($C(CH_3)_3$), 22.7 ($C(CH_3)_3$).

Chloro(dicyclohexyl)phenylsilane. A procedure similar to that for cyclohexyldiphenylchlorosilane was used. To a suspension of finely cut lithium wire (1.60 g, 226.0 mmol) in pentane (100 mL) was added slowly chlorocyclohexane (19.2 g, 161.5 mmol) for 1 hour while gently heating. The resulting mixture was heated to refluxing temperature overnight. The violet mixture was chilled in an ice bath and a solution of trichlorophenylsilane (7.04 g, 32.2 mmol) in pentane (10 mL) was added dropwise. The resulting mixture was allowed to warm to room temperature and was stirred overnight. Precipitated lithium chloride salt and excessive lithium were filtered off. The filtrate was treated with ice cold HCl solution (4 M, 50 mL) to destroy the remaining cyclohexyl-lithium. The organic layer was separated, dried over anhydrous Na_2SO_4 , and concentrated

to give a yellow oil. The product was purified by vacuum distillation, giving two main fractions, 130–150 °C and above 150 °C at 0.5 torr, which solidified in the fridge. Both fractions were shown to be identical and impure by ^1H and ^{13}C NMR spectroscopy. An attempt to purify the desired product from dicyclohexylphenylsilane through recrystallization in pentane did not improve the purity (ca. 77% purity). ^1H NMR (400 MHz, CDCl_3): δ = 7.64–7.53 (m, 2H, phenyl-H), 7.45–7.28 (m, 3H, phenyl-H), 1.99–1.55 (m, 10H, Cy), 1.37–1.00 (m, 12H, Cy); $^{13}\text{C}\{^1\text{H}\}$ NMR (100 MHz, CDCl_3): δ = 135.5, 134.3, 132.5, 129.9, 127.8, 127.6 (aryl), 28.7, 28.4, 27.9, 27.7, 27.6, 26.8, 26.7, 26.6, 26.5, 25.2, 22.2 (Cy).

7.2 Synthesis of Binaphthol Ligands

(*R*)-3,3'-bis(5-phenyl-5H-dibenzo[*b,d*]silyl-5-yl)-1,1'-binaphthalene-2,2'-diol ((*R*)-30). To a solution of (*R*)-3,3'-dibromo-1,1'-binaphthalene-2,2'-diol (1.51 g, 3.40 mmol) in THF (65 mL) was added KH (409 mg, 10.2 mmol) in 3 portions. The resulting mixture was stirred for 30 minutes before a solution of 5-chloro-5-phenyldibenzosilole (2.17 g, 7.40 mmol) in THF (10 mL) was added at room temperature, to obtain a light orange reaction mixture which was then heated to 65 °C overnight. To the reaction mixture was added *t*BuLi (9.1 mL, 13.6 mmol, 1.5 M in pentane) dropwise at –50 °C. The bright yellow mixture was allowed to warm to room temperature slowly and was stirred for an additional hour. Solvent was evaporated *in vacuo*. The residue was dissolved in CH_2Cl_2 (50 mL) which was then treated with 1 M HCl (20 mL). The organic layer was separated, dried (Na_2SO_4), and concentrated. The product was purified using column

chromatography on silica (hexanes/CH₂Cl₂ 80:20) to afford a yellow solid (1.18 g, 43 %) which was crystallized from pentane, giving the pure product as a white powder (0.91 g, 33 % overall yield). ¹H NMR (500 MHz, C₆D₆): δ = 8.53 (s, 2H, aryl-H), 8.05 (m, 2H, aryl-H), 7.94 (d, ³J(H,H) = 6.9 Hz, 2H, aryl-H), 7.82 (m, 4H, aryl-H), 7.73 (dd, ³J(H,H) = 8.0 Hz, ⁴J(H,H) = 1.6 Hz, 4H, aryl-H), 7.48 (d, ³J(H,H) = 7.8 Hz, 2H, aryl-H), 7.40 (m, 4H, aryl-H), 7.35 (m, 2H, aryl-H), 7.25 (t, ³J(H,H) = 7.2 Hz, 2H, aryl-H), 7.16 (m, 6H, aryl-H overlapped with C₆D₅H), 7.09 (d, ³J(H,H) = 8.3 Hz, 2H, aryl-H), 7.04 (m, 2H, aryl-H), 6.97 (m, 2H, aryl-H), 4.78 (s, 2H, OH); ¹³C{¹H} NMR (125 MHz, C₆D₆): δ = 156.9 (CO), 149.3, 149.1, 140.0, 136.0, 135.5, 135.3, 135.1, 133.8, 131.0, 130.9, 129.8, 129.7, 129.0, 128.3, 128.0, 127.9, 127.8, 127.6, 124.2, 124.0, 122.9, 121.5, 121.4, 110.3. Anal. Calcd for C₅₆H₃₈O₂Si₂: C, 84.17; H, 4.79. Found: C, 83.87; H, 4.80.

(*R*)-3,3'-bis[*tert*-butyl(diphenyl)silyl]-1,1'-binaphthalene-2,2'-diol⁸⁹ (**(*R*)-31**). To a solution of 3,3'-dibromo-1,1'-binaphthalene-2,2'-diol (500 mg, 1.13 mmol) dissolved in DMF (5 mL) was added imidazole (0.46 g, 6.78 mmol) and *t*BuPh₂SiCl (1.0 g, 3.64 mmol). The reaction mixture was heated to 90 °C for 3 days. The reaction was quenched by addition of saturated solution of NaHCO₃ (3 mL). The product was extracted with CH₂Cl₂ (3 × 30 mL). The combined organic layers were washed with water (2 × 5 mL). The organic layer was dried over anhydrous Na₂SO₄, concentrated to give a yellow solid which was purified using column chromatography on silica (hexane, then hexanes/CH₂Cl₂, 9:1) to afford the crude bis(silylether) as a white powder (0.82g). The reaction was repeated once to obtain the desired amount of silyl ether used in the retro-Brook rearrangement. To a solution of the silyl ether (1.57 g, 1.70 mmol) in THF (40

mL) was added dropwise *t*-butyllithium (4.3 mL, 6.8 mmol, 1.6 M solution in pentane) at -60°C . The resulting mixture was allowed to slowly warm to room temperature and was stirred at that temperature for one hour. The reaction was quenched with saturated NH_4Cl solution (10 mL) and the resulting mixture was stirred vigorously to obtain a clear solution. The organic layer was separated and the product was extracted with CH_2Cl_2 (3×30 mL). The combined organic layers were dried over anhydrous Na_2SO_4 , concentrated, and the product was purified by column chromatography (hex/ CH_2Cl_2 , 8:2), giving a white solid (1.17 g). The product was contaminated, which showed peaks in the aliphatic region of the ^1H NMR spectrum. A suspension of the desired product in a mixture of pentane and diethyl ether (20 mL, 7:3) was stirred overnight. 3,3'-bis[*tert*-butyl(diphenyl)silyl]-1,1'-binaphthalene-2,2'-diol was then collected on a Hirsch funnel, washed with ice-cold pentane/diethyl ether solvent mixture, and was dried using a rotavap, giving a fine white powder (1.00 g, 77 %). ^1H NMR (500 MHz, C_6D_6): δ = 8.16 (s, 2H, aryl-H), 7.83–7.73 (m, 8H, aryl-H), 7.41 (d, $^3J(\text{H,H})$ = 7.8 Hz, 2H, aryl-H), 7.34–7.24 (m, 12H, aryl-H), 7.22 (d, $^3J(\text{H,H})$ = 8.3 Hz, 2H, aryl-H), 7.07 (t, $^3J(\text{H,H})$ = 7.0 Hz, 2H, aryl-H), 7.01 (t, $^3J(\text{H,H})$ = 7.3 Hz, 2H, aryl-H), 4.98 (s, 2H, OH), 1.34 (s, 18H, $\text{C}(\text{CH}_3)_3$). $^{13}\text{C}\{^1\text{H}\}$ NMR (125 MHz, C_6D_6): δ = 156.9, 143.0, 136.7, 135.7, 136.2, 129.9, 129.5, 128.5, 128.4, 128.29, 128.2, 128.1, 124.9, 124.1, 110.6 (aryl), 30.2 ($\text{C}(\text{CH}_3)_3$), 18.8 ($\text{C}(\text{CH}_3)_3$). The NMR data are in agreement with literature.⁸⁹

(*R*)-3,3'-Bis[cyclohexyl(diphenyl)silyl]-1,1'-binaphthalene-2,2'-diol ((*R*)-32). To a solution of (*R*)-3,3'-dibromo-1,1'-binaphthalene-2,2'-diol (1.50 g, 3.38 mmol) in DMF (11 mL) was added imidazole (1.39 g, 20.3 mmol) and chloro(cyclohexyl)diphenylsilane

(4.07 g, 13.5 mmol). The resulting mixture was stirred at 90 °C overnight. The reaction was quenched by addition of saturated aqueous NaHCO₃ (5 mL) and was diluted with CH₂Cl₂ (150 mL). The organic layer was separated. The product was extracted with CH₂Cl₂ (3 × 30 mL). The combined organic layers were washed with water (3 × 15 mL), dried (Na₂SO₄), and concentrated *in vacuo*. The product was purified using column chromatography on silica (hexanes, then hexanes/CH₂Cl₂, 9:1) to afford crude bis(silylether) as a white powder (2.78 g, 84 %) which was subjected to the next reaction without further purification. The crude bis(silylether) was dissolved in THF (50 mL), and a *t*-butyllithium solution (7.2 mL, 11.4 mmol, 1.6 M in pentane) was added dropwise at −60 °C. The yellow solution was stirred for 5 min at −60 °C and was then allowed to reach room temperature slowly, after which it was stirred for an additional hour. The reaction was quenched with saturated aqueous NH₄Cl (5 mL) and the product was extracted with CH₂Cl₂ (3 × 40 mL). The combined organic layers were dried (Na₂SO₄), concentrated and the product was purified using column chromatography on silica (hexanes/CH₂Cl₂, 8:2), to afford the pure product as a white powder (2.28 g, 82 % overall yield); mp 263–265 °C. ¹H NMR (500 MHz, C₆D₆): δ = 8.20 (s, 2H, aryl-H), 7.80–7.77 (m, 8H, aryl-H), 7.45–7.42 (m, 2H, aryl-H), 7.30–7.26 (m, 12H, aryl-H), 7.10–7.08 (m, 2H, aryl-H), 7.04–6.98 (m, 4H, aryl-H), 4.59 (s, 2H, OH), 2.09–2.02 (m, 4H, CH₂), 1.95–1.89 (m, 2H, CH₂), 1.78–1.71 (m, 6H, CH₂), 1.45–1.34 (m, 8H, CH₂), 1.23–1.16 (m, 2H, CH, Cy); ¹³C{¹H} NMR (125 MHz, C₆D₆): δ = 157.3 (CO), 141.4, 136.5, 135.2, 135.1, 135.0, 129.9, 124.2, 124.0, 110.3 (aryl), 29.2 (CH₂, Cy), 29.1 (CH₂, Cy), 28.84 (CH₂, Cy), 28.78 (CH₂, Cy), 27.4 (CH₂, Cy), 24.7 (CH, Cy). Anal. Calcd for C₅₆H₅₄O₂Si₂: C, 82.51; H, 6.68. Found: C, 82.31; H, 6.69.

(*R*)-3,3'-bis(triisopropylsilyl)-1,1'-binaphthalene-2,2'-diol ((*R*)-33). To a solution of (*R*)-3,3'-dibromo-1,1'-binaphthalene-2,2'-diol (1.50 g, 3.38 mmol) in DMF (20 mL) were added imidazole (0.70 g, 10.18 mmol) and chloro(triisopropyl)silane (1.63 g, 8.45 mmol). The resulting mixture was stirred at 90 °C overnight. The reaction was quenched by addition of saturated aqueous NaHCO₃ solution (10 mL) and the product was extracted with diethyl ether (3 × 30 mL). The combined ether layers were washed with water (3 × 10 mL), brine (10 mL), and dried (MgSO₄). The product was purified using column chromatography on silica (hexanes) to afford crude bis(silylether) as a white powder (1.72 g, 67 %) which was subjected to the next reaction without further purification. The crude bis(silylether) was dissolved in THF (25 mL) and *t*BuLi (6.0 mL, 9.0 mmol, 1.5 M in pentane) was added dropwise at −50 °C. The yellow solution was allowed to warm to room temperature slowly and was stirred for an additional hour. The reaction was quenched by addition of aqueous solution with saturated NH₄Cl (10 mL), and the product was extracted with CH₂Cl₂ (3 × 20 mL). The combined organic layers were dried (MgSO₄). The product was purified using column chromatography on silica to afford the pure product as a light yellow powder (1.25 g, 63% overall yield). ¹H NMR (400 MHz, CDCl₃): δ = 8.13 (s, 2H, aryl-H), 7.89 (d, ³*J*(H,H) = 8.2 Hz, 2H, aryl-H), 7.38–7.23 (m, 4H, aryl-H), 7.10 (d, ³*J*(H,H) = 8.2 Hz, 2H, aryl-H), 5.21 (s, 2H, OH), 1.64–1.51 (m, 6H, CH(CH₃)₂), 1.15–1.12 (m, 36H, CH(CH₃)₂); ¹³C{¹H} NMR (125 MHz, CDCl₃): δ = 157.2 (CO), 139.9, 134.1, 129.2, 128.6, 127.6, 124.5, 123.8, 123.6, 109.7 (aryl), 19.0 (CH(CH₃)₂), 11.7 (CH(CH₃)₂). Anal. Calcd for C₃₈H₅₄O₂Si₂: C, 76.19; H, 9.08. Found: C, 75.97; H, 9.14.

(*R*)-3,3'-bis(dicyclohexylphenylsilyl)-1,1'-binaphtholene-2,2'-diol ((*R*)-34). To a solution of 3,3'-dibromo-1,1'-binaphthalene-2,2'-diol (500 mg, 1.13 mmol) in DMF (5 mL) were added imidazole (466 mg, 6.78 mmol) and dicyclohexylphenylchlorosilane (1.50 g, ca. 77% purity, 3.67 mmol) at room temperature. The resulting mixture was stirred at 90 °C overnight. The reaction was quenched with a saturated aqueous NaHCO₃ solution (5 mL) and the product was extracted with CH₂Cl₂ (3 × 30 mL). The combined organic layers were dried (NaSO₄) and concentrated. The product was purified using column chromatography on silica (hexanes, then hexanes/CH₂Cl₂, 9:1) to afford crude bis(silylether) as a white powder (1.04 g, 94%) which was subjected to the next reaction without further purification. The bis(silylether) was dissolved in THF (30 mL) and *t*BuLi (2.7 mL, 4.1 mmol, 1.6 M in pentane) was added dropwise at –60 °C. The bright yellow reaction mixture was allowed to warm slowly to room temperature and was stirred for two additional hours. The reaction was quenched with a saturated aqueous NH₄Cl solution (5 mL) to obtain a clear solution. The organic layer was separated and the product was extracted with CH₂Cl₂ (3 × 30 mL). The combined organic layers were dried (NaSO₄) and concentrated. The product was purified using column chromatography on silica (hexanes/ethyl acetate 95:5) to afford the pure product as a white powder (0.72 g, 80% overall yield). ¹H NMR (500 MHz, 25 °C, C₆D₆): δ = 8.21 (s, 2H, aryl-H), 7.81 (d, ³*J*(H,H) = 6.4 Hz, 4H, aryl-H), 7.54–7.46 (m, 2H, aryl-H), 7.46–7.29 (m, 6H, aryl-H), 7.22 (d, ³*J*(H,H) = 7.8 Hz, 2H, aryl-H), 7.13–7.02 (m, 4H, aryl-H), 4.83 (s, 2H, OH), 2.16–1.90 (m, 8H, CH₂), 1.89–1.58 (m, 16H, CH₂), 1.55–1.27 (m, 12H, CH₂), 1.26–1.04 (m, 8H, CH₂ and CH); ¹³C{¹H} NMR (125 MHz, 25 °C, C₆D₆): δ = 157.5 (CO), 141.7, 136.2, 134.7, 134.5, 129.6, 129.2, 129.0, 128.3, 128.1, 127.9, 127.8, 127.7, 123.9, 123.8,

123.6, 110.2 (aryl), 28.7 (CH₂), 28.6 (CH₂), 28.53 (CH₂), 28.50 (CH₂), 28.39 (CH₂), 28.33 (CH₂), 27.2(CH₂), 22.9 (CH, Cy), 22.6 (CH, Cy). Anal. Calcd for C₅₆H₆₆O₂Si₂: C, 81.30; H, 8.04. Found: C, 82.58; H, 8.29.

(*R*)-3,3'-bis[4-methoxyphenyl(diphenyl)silyl]-1,1'-binaphtholene-2,2'-diol.[‡] To a solution of (*R*)-3,3'-dibromo-1,1'-binaphthalene-2,2'-diol (400 mg, 0.90 mmol) in THF (20 mL) was added KH (80 mg, 2.0 mmol) under stirring. The mixture was stirred at room temperature for 30 minutes and then chloro(4-methoxyphenyl)(diphenyl)silane¹⁶⁰ (601 mg, 1.85 mmol) was added. The mixture was heated to 70 °C overnight. The reaction mixture was cooled down to −78 °C and to that was added dropwise *t*-BuLi (2.5 mL, 3.7 mmol, 1.5 M in pentane). The yellow solution was stirred for 5 min at −78 °C and was then allowed to reach room temperature slowly, after which it was stirred for an additional hour. The reaction was quenched with saturated aqueous NH₄Cl (50 mL) and the product was extracted with diethyl ether (3 × 20 mL). The combined organic layers were dried (Na₂SO₄) and concentrated. The product was purified using column chromatography on silica (hexanes/CH₂Cl₂, 70:30), to afford the pure diol proligand as a white powder (535 mg, 69% overall yield). ¹H NMR (400 MHz, CDCl₃): δ = 7.97 (s, 2H), 7.76 (d, ³*J*(H,H) = 7.8 Hz, 2H), 7.69 (d, ³*J*(H,H) = 7.1 Hz, 8H), 7.63 (d, ³*J*(H,H) = 8.6 Hz, 4H), 7.48–7.29 (m, 18H), 6.96 (d, ³*J*(H,H) = 8.2 Hz, 4H), 5.36 (s, 2H, OH), 3.87 (s, 6H, OCH₃); ¹³C{¹H} NMR (100 MHz, CDCl₃): δ = 160.8, 156.5 (CO), 142.0, 137.9, 136.2, 134.7, 134.6, 129.4, 129.2, 129.0, 128.1, 127.8, 124.8, 123.93, 123.91, 123.8, 113.6, 110.7 (aryl), 55.0 (CH₃O).

[‡] This ligand was prepared by Dr. Alexander L. Reznichenko, a former PhD candidate in the Hultsch research group.

7.3 Synthesis of Octahydrobinaphthol Ligands

(*R*)-5,5',6,6',7,7',8,8'-octahydro-2,2'-dihydroxy-1,1-binaphthylene.¹³⁹ To a suspension of (*R*)-BINOL (4.00 g, 13.97 mmol) in ethanol (25 mL) was added Pd/C (2.09 g, 55% wet, 10% on Carbon). The autoclave was heated to 70 °C using an oil bath and hydrogen gas was introduced to a pressure of 60 bar. The reaction mixture was stirred for 16 hours. The solid was filtered off through a Hirsch funnel containing a 2 cm layer of celite, and was then washed with ethanol (60 mL). The filtrate was concentrated to yield a grey solid which was passed through a short column of silica gel (hexane/ethyl acetate, 7:3), giving a white solid (3.92 g, 95 % yield). ¹H NMR (400 MHz, 25 °C, CDCl₃): δ = 7.08–7.03 (m, 2H, aryl-H), 6.84–6.79 (m, 2H, aryl-H), 4.57 (s, 2H, OH), 2.78–2.71 (m, 4H, CH₂), 2.34–2.10 (m, 4H, CH₂), 1.78–1.61 (m, 8H, CH₂). ¹³C{¹H} NMR (100 MHz, 25 °C, CDCl₃): δ = 151.4, 137.1, 131.1, 130.1, 118.8, 113.0 (aryl), 29.2, 27.1, 22.9 (CH₂). The NMR data were in agreement with literature.¹³⁹

(*R*)-3,3'-dibromo-5,5',6,6',7,7',8,8'-octahydro-2,2'-dihydroxy-1,1-binaphthylene

((*R*)-40).¹⁴² To a solution of (*R*)-5,5',6,6',7,7',8,8'-octahydro-2,2'-dihydroxy-1,1-binaphthylene (3.92 g, 13.30 mmol) in dichloromethane (75 mL) was added dropwise liquid bromine (1.6 mL, 29.96 mmol) at –30 °C. The resulting mixture was stirred at that temperature for 30 minutes before it was allowed to warm to room temperature and was stirred overnight. The reaction was quenched by addition of a saturated aqueous sodium thiosulfate solution (30 mL). The organic layer was separated and the product was extracted with CH₂Cl₂ (2 × 30 mL). The combined organic layers were dried over

anhydrous Na_2SO_4 and evaporated. The product was purified using column chromatography on silica gel (hexane, then hexane/ethyl acetate, 9:1), giving a white foamy solid (5.18 g, 86 % yield). ^1H NMR (400 MHz, 25 °C, CDCl_3): δ = 7.27 (s, 2H, aryl-H), 5.10 (s, 2H, OH), 2.77–2.70 (m, 4H, CH_2), 2.34–2.02 (m, 4H, CH_2), 1.79–1.58 (m, 8H, CH_2). $^{13}\text{C}\{^1\text{H}\}$ NMR (100 MHz, 25 °C, CDCl_3): δ = 147.1, 136.7, 132.6, 132.4, 131.5, 122.2, 107.2, 104.7 (aryl), 29.0, 26.9, 22.8, 22.7 (CH_2). The NMR data are in agreement with literature.¹⁴²

(*R*)-3,3'-bis(triphenylsilyl)-5,5',6,6',7,7',8,8'-octahydro-2,2'-dihydroxy-1,1-binaphthylene ((*R*)-44). To a solution of (*R*)-3,3'-dibromo-5,5',6,6',7,7',8,8'-octahydro-2,2'-dihydroxy-1,1-binaphthylene (400 mg, 0.89 mmol) in THF (30 mL) was added KH (110 mg, 2.75 mmol). The yellow mixture was stirred at room temperature for 30 minutes before Ph_3SiCl (548 mg, 1.86 mmol) was added. The resulting reaction mixture was heated to 65 °C overnight. The content was cooled to –60 °C and to that *t*BuLi (2.2 mL, 3.54 mmol, 1.5 M in pentane) was added dropwise. The green solution was stirred at that temperature for 15 minutes before it was allowed to warm to room temperature and was stirred for 2 hours. The reaction was quenched by addition of diluted HCl solution (10 mL, 1 M) at 0 °C and a saturated aqueous NH_4Cl solution (10 mL). The organic layer was separated and the product was extracted with dichloromethane (3×40 mL). The combined organic layers were dried over anhydrous Na_2SO_4 and were concentrated. The product was purified using column chromatography on silica gel (hexanes/ethyl acetate, 9:1), giving a white foamy solid (412 mg, 57% yield). ^1H NMR (500 MHz, 25 °C, C_6D_6): δ = 7.89–7.67 (m, 12H, aryl-H), 7.30–7.16 (m, 18H, aryl-H), 7.12 (s, 2H, aryl-H), 4.49

(s, 2H; OH), 2.48–2.17 (m, 8H, CH₂), 1.53–1.31 (m, 8H, CH₂); ¹³C{¹H} NMR (125 MHz, 25 °C, C₆D₆): δ = 156.8, 140.2, 140.0, 136.8, 135.4, 130.2, 129.6, 128.5, 128.1, 119.0, 118.1 (aryl), 29.3, 27.8, 23.2 (CH₂). The NMR spectra are in agreement with literature.¹⁴³

(*R*)-3,3'-bis(*tert*-butyldiphenylsilyl)-5,5',6,6',7,7',8,8'-octahydro-2,2'-dihydroxy-1,1-binaphthylene ((*R*)-45). To a suspension of imidazole (0.948 g, 13.9 mmol, 6.0 eq.), and *tert*-butyldiphenylchlorosilane (2.55 g, 9.28 mmol, 4.0 eq.) in DMF (7 mL) was added (*R*)-3,3'-dibromo-5,5',6,6',7,7',8,8'-octahydro-2,2'-dihydroxy-1,1-binaphthylene (1.05 g, 2.32 mmol). The resulting mixture was heated to 90 °C overnight. The reaction which was quenched by addition of a saturated aqueous NaHCO₃ solution (10 mL), followed by dilution with CH₂Cl₂ (150 mL). The organic layer was separated, and was then washed with water (3 × 10 mL) and a saturated NaHCO₃ solution (10 mL). The organic layer was dried over anhydrous Na₂SO₄ and was concentrated. The product was purified using column chromatography on silica gel (hexane/ CH₂Cl₂, 9:1), giving the silyl ether product as a white solid (410 mg, 19% yield) which was used without further purification. The main component obtained was the monosilylation product (1.10 g, 69% yield). To a solution of the bis-silyl ether (0.40 g, 0.43 mmol) in THF (15 mL) was added *t*BuLi (1.0 mL, 1.7 mmol, 1.7 M in pentane) dropwise at –60 °C. The resulting yellow mixture was allowed to slowly warm to room temperature and was stirred for 2 hours. The reaction was quenched with a saturated aqueous NH₄Cl solution (5 mL). The organic layer was separated and the product was extracted with dichloromethane (3 × 30 mL). The combined organic layers were dried over anhydrous Na₂SO₄ and were concentrated.

The product was purified using column chromatography on silica gel (hexane/CH₂Cl₂, 90:10, then 85:15), giving the product as a white foamy solid (285 mg, 16% yield after 2 steps). ¹H NMR (400 MHz, 25 °C, C₆D₆): δ = 7.85–7.73 (m, 6H, aryl-H), 7.29 (s, 2H, aryl-H), 7.28–7.21 (m, 8H, aryl-H), 7.19–7.14 (m, 6H, aryl-H, overlapped with C₆D₆ peak), 4.84 (s, 2H, OH), 2.49–2.25 (m, 8H, CH₂), 1.53–1.39 (m, 8H, CH₂), 1.37 (s, 18H, C(CH₃)₃); ¹³C{¹H} NMR (100 MHz, 25 °C, C₆D₆): δ = 156.6 (CO), 140.9, 139.5, 136.7, 136.0, 135.9, 130.1, 129.3, 127.9, 118.9, 118.7 (aryl), 30.1 (C(CH₃)₃), 29.4 (CH₂), 27.7 (CH₂), 23.2 (CH₂), 18.9 (C(CH₃)₃).

(*R*)-3,3'-bis(cyclohexyldiphenylsilyl)-5,5',6,6',7,7',8,8'-octahydro-2,2'-dihydroxy-1,1-binaphthylene ((*R*)-46). To a suspension of imidazole (0.903 mg, 13.3 mmol), and cyclohexyldiphenylchlorosilane (2.66 g, 8.84 mmol) in DMF (7 mL) was added (*R*)-3,3'-dibromo-5,5',6,6',7,7',8,8'-octahydro-2,2'-dihydroxy-1,1-binaphthylene (1.00 g, 2.21 mmol). The resulting mixture was heated to 90 °C overnight. The reaction which was quenched by addition of a saturated aqueous NaHCO₃ solution (10 mL), was diluted with dichloromethane (150 mL). The organic layer was separated, and was then washed with water (3 × 10 mL) and saturated NaHCO₃ solution (10 mL). The organic layer was dried over anhydrous Na₂SO₄ and was concentrated. The product was purified using column chromatography on silica gel (hexane), giving silyl ether product as waxy solid, which turned to white solid overnight (1.71 g, 79% yield), which was used without further purification. To a solution of the silyl ether (1.40 g, 1.43 mmol) in THF (40 mL) was added *t*BuLi (3.6 mL, 5.7 mmol, 1.6 M in pentane) dropwise at –60 °C. The resulting yellow mixture was allowed to slowly warm to room temperature and was stirred for 2

hours. The reaction was quenched with a saturated aqueous NH_4Cl solution (10 mL). The organic layer was separated and the product was extracted with dichloromethane (3×30 mL). The combined organic layers were dried over anhydrous Na_2SO_4 and were concentrated. The product was purified using column chromatography on silica gel (hexane/ CH_2Cl_2 , 9:1, then 8:2), giving the product as a white foamy solid (1.05 g, 70% yield after 2 steps). ^1H NMR (400 MHz, 25 °C, C_6D_6): δ = 7.85–7.74 (m, 6H, aryl-H), 7.36 (s, 2H, aryl-H), 7.29–7.24 (m, 8H, aryl-H); 7.18–7.14 (m, 6H, aryl-H, overlapped with C_6D_6 peak), 4.48 (s, 2H, OH), 2.57–2.41 (m, 4H, CH_2), 2.35–2.03 (m, 8H, CH_2), 2.00–1.86 (m, 2H, CH_2), 1.85–1.67 (m, 6H, CH_2), 1.52–1.32 (m, 16H, CH_2), 1.27–1.10 (m, 2H, CH_2). $^{13}\text{C}\{^1\text{H}\}$ NMR (100 MHz, 25 °C, C_6D_6): δ = 156.9 (CO), 139.4, 136.5, 135.5, 129.9, 129.3, 118.59, 118.55 (aryl), 29.4, 29.1, 29.0, 28.9, 28.8, 27.6, 27.4 (CH_2 of Cy and H_8BINOL), 24.6 (CH, Cy), 23.3, 23.2 (CH_2 , H_8BINOL).

7.4 Synthesis of Rare Earth Metal Complexes

$[\text{Y}(\text{o}-\text{C}_6\text{H}_4\text{CH}_2\text{NMe}_2)_3]^{124}$ and $[\text{Lu}(\text{o}-\text{C}_6\text{H}_4\text{CH}_2\text{NMe}_2)_3]^{125}$ were synthesized according to literature procedure.

General procedure for isolation of yttrium complexes

In a glove box, to a screw cap NMR tube containing a mixture of binaphthol ligand (0.06 mmol) and $[\text{Y}(\text{o}-\text{C}_6\text{H}_4\text{CH}_2\text{NMe}_2)_3]$ (29.6 mg, 0.06 mmol) was added C_6D_6 (1.0 mL). The mixture was kept at room temperature for 1 h. ^1H NMR spectrum was acquired to confirm clean formation of binaphtholate complex. In the glove box, the content was

transferred to a HPLC vial (2 mL), which was loosely capped and was then placed in a Schlenk tube. Volatile solvent was removed in vacuum using freeze-drying technique, giving a white or pale yellow solid in quantitative yield. Elemental analyses were performed by Robertson Microlit Laboratories, Inc., Ledgewood, NJ.

7.4.1 Binaphtholate Rare Earth Metal Complexes

(*R*)-[Y{PDBS₂BINO}(*o*-C₆H₄CH₂NMe₂)(Me₂NCH₂Ph)] ((*R*)-39a-Y**).** To a mixture of (*R*)-**30** (24.0 mg, 0.03 mmol) and [Y(*o*-C₆H₄CH₂NMe₂)₃] (14.8 mg, 0.03 mmol) was added C₆D₆ (0.70 mL). The mixture was kept at room temperature for 1 h. ¹H and ¹³C NMR spectra showed clean formation of (*R*)-**39a-Y**, which was used directly for catalytic experiments. ¹H NMR (500 MHz, 25 °C, C₆D₆): δ = 8.56 (s, 2H, aryl-H), 8.37–8.24 (m, 2H, aryl-H), 7.98 (m, 2H, aryl-H), 7.92 (m, 2H, aryl-H), 7.82 (d, ³J(H,H) = 7.83 Hz, 2H, aryl-H), 7.76 (d, ³J(H,H) = 7.58 Hz, 1H, aryl-H), 7.71 (d, ³J(H,H) = 7.83 Hz, 1H, aryl-H), 7.63 (d, ³J(H,H) = 7.58 Hz, 1H, aryl-H), 7.57 (m, 1H, aryl-H), 7.48 (t, ³J(H,H) = 7.58 Hz, 2H, aryl-H), 7.43–6.81 (m, 28H, aryl-H including free PhCH₂NMe₂), 6.76 (q, ³J(H,H) = 7.42 Hz, 3H, aryl H), 6.50 (t, ³J(H,H) = 7.21 Hz, 1H, aryl-H), 6.41 (d, ³J(H,H) = 7.58 Hz, 2H, aryl-H), 3.80 (d, ²J(H,H) = 14.43 Hz, 1H, *o*-C₆H₄CH₂Me₂), 3.23 (m, 4H, free and coordinated PhCH₂NMe₂), 2.05 (s, 6H, free PhCH₂NMe₂), 2.67 (d, ²J(H,H) = 14.43 Hz, 1H, *o*-C₆H₄CH₂NMe₂), 1.48 (s, 3H, N(CH₃)₂), 1.42 (s, 3H, N(CH₃)₂), 1.23 (s, 3H, N(CH₃)₂), 1.15 (s, 3H, N(CH₃)₂); ¹³C{¹H} NMR (125 MHz, 25 °C, C₆D₆): δ = 182.2 (d, ¹J(Y,C) = 53.5 Hz), 162.3 (CO), 161.8 (CO), 149.30, 149.25, 149.1, 148.4, 140.6, 140.4, 140.0, 139.5, 139.4, 138.3, 138.0, 137.64, 137.61, 137.4, 135.8, 135.7, 135.6, 135.4,

135.2, 135.0, 134.3, 131.7, 131.0, 130.9, 130.0, 129.9, 129.5, 129.3, 129.10, 129.08, 129.0, 128.8, 128.7, 128.6, 128.53, 128.45, 128.4, 128.3, 127.7, 127.2, 126.4, 126.3, 125.7, 125.2, 122.93, 122.89, 122.7, 121.7, 121.3, 117.6, 116.3 (aryl), 67.9 (*o*-C₆H₄CH₂NMe₂), 64.5 (s, free PhCH₂NMe₂), 58.2 (PhCH₂NMe₂), 47.2 (N(CH₃)₂), 45.4 (s, free PhCH₂NMe₂), 44.1 (N(CH₃)₂), 40.51 (PhCH₂NMe₂), 40.45 (PhCH₂NMe₂). Anal. Calcd. for C₇₄H₆₁N₂O₂Si₂Y: C, 76.93; H, 5.32; N, 2.42. Found: C, 70.76; H, 4.66; N, 1.92.

(*R*)-[Lu{PDBS₂BINO}(*o*-C₆H₄CH₂NMe₂)(Me₂NCH₂Ph)] ((*R*)-39a-Lu**).** To a mixture of (*R*)-**30** (25.5 mg, 0.032 mmol) and [Lu(*o*-C₆H₄CH₂NMe₂)₃] (18.4 mg, 0.032 mmol) was added C₆D₆ (0.80 mL). The mixture was kept at room temperature for 1 h. ¹H and ¹³C NMR spectra showed clean formation of (*R*)-**39a-Lu**, which was used directly for catalytic experiments. ¹H NMR (400 MHz, 25 °C, C₆D₆): δ = 8.63 (s, 1H, aryl-H), 8.61 (s, 1H, aryl-H), 8.33 (d, ³*J*(H,H) = 7.04 Hz, 1H), 8.26 (d, ³*J*(H,H) = 7.04 Hz, 1H), 8.05 (m, 2H, aryl-H), 7.99 (d, ³*J*(H,H) = 6.65 Hz, 1H, aryl-H), 7.91 (m, 2H, aryl-H), 7.80 (m, 5H, aryl-H), 7.69 (d, ³*J*(H,H) = 7.43 Hz, 1H, aryl-H), 7.63 (m, 1H, aryl-H), 7.54 (m, 2H, aryl-H), 7.48 (t, ³*J*(H,H) = 7.04 Hz, 1H, aryl-H), 7.44–6.84 (m, 24H, aryl-H including free PhCH₂NMe₂), 6.80 (m, 4H), 6.54 (t, ³*J*(H,H) = 7.24 Hz, 1H, aryl-H), 6.44 (d, ³*J*(H,H) = 7.04 Hz, 2H, aryl-H), 3.81 (d, ²*J*(H,H) = 14.48 Hz, 1H, *o*-C₆H₄CH₂NMe₂), 3.36 (s, 2H, PhCH₂NMe₂), 3.27 (s, 2H, free PhCH₂NMe₂), 2.67 (d, ²*J*(H,H) = 14.48 Hz, 1H, *o*-C₆H₄CH₂NMe₂), 2.09 (s, 6H, CH₃ of free PhCH₂NMe₂), 1.49 (s, 3H, N(CH₃)₂), 1.43 (s, 3H, N(CH₃)₂), 1.30 (s, 3H, N(CH₃)₂), 1.24 (s, 3H, N(CH₃)₂); ¹³C{¹H} NMR (100 MHz, 25 °C, C₆D₆): δ = 191.3 (C-Lu), 162.7 (CO), 162.2 (CO), 149.4, 149.3, 149.2,

148.8, 140.2, 139.9, 139.6, 139.4, 137.7, 137.3, 135.9, 135.7, 135.5, 135.2, 135.1, 131.8, 130.9, 129.9, 129.5, 129.1, 128.9, 128.7, 128.5, 127.6, 127.5, 127.2, 126.62, 126.59, 126.0, 125.7, 125.0, 122.8, 122.7, 121.7, 121.5, 121.3, 117.3, 116.3 (aryl), 67.3 (*o*-C₆H₄CH₂NMe₂), 64.5 (s, free PhCH₂NMe₂), 58.4 (PhCH₂NMe₂), 47.8 (N(CH₃)₂), 46.2 (N(CH₃)₂), 45.4 (s, free PhCH₂NMe₂), 44.5 (N(CH₃)₂), 40.84 (PhCH₂NMe₂), 40.78 (PhCH₂NMe₂).

(*R*)-[Y{TBDPs₂BINO}(*o*-C₆H₄CH₂NMe₂)(Me₂NCH₂Ph)] ((*R*)-39b-Y**).** To a mixture of (*R*)-**31** (45.6 mg, 0.06 mmol) and [Y(*o*-C₆H₄CH₂NMe₂)₃] (29.3 mg, 0.06 mmol) was added toluene-*d*₈ (0.55 mL). The mixture was kept at room temperature for 1 h. ¹H and ¹³C NMR showed clean formation of (*R*)-**39b-Y**, which was used directly for catalytic experiments. ¹H NMR (125 MHz, toluene-*d*₈, 0 °C): δ = 8.55 (s, 1H, aryl-H), 8.52 (s, 1H, aryl-H), 8.07 (d, ³*J*(H,H) = 8.1 Hz, 2H, aryl-H), 7.95 (m, 1H, aryl-H), 7.93 (m, 1H, aryl-H), 7.89–7.84 (m, 4H, aryl-H), 7.57 (d, ³*J*(H,H) = 6.9 Hz, 1H, aryl-H), 7.55 (d, ³*J*(H,H) = 8.1 Hz, 1H, aryl-H), 7.48–7.46 (m, 1H, aryl-H), 7.34–6.94 (m, 28H, aryl-H, including 5H from free PhCH₂NMe₂), 6.77 (d, ³*J*(H,H) = 7.6 Hz, 1H, aryl-H), 6.62 (d, ³*J*(H,H) = 6.9 Hz, 2H, aryl-H), 3.44 (d, ²*J*(H,H) = 13.9 Hz, 1H, *o*-C₆H₄CH₂NMe₂), 3.20 (s, 2H, free PhCH₂NMe₂), 3.09 (br s, 2H, PhCH₂NMe₂), 2.52 (d, ²*J*(H,H) = 13.2 Hz, 1H, *o*-C₆H₄CH₂NMe₂), 2.05 (s, 6H, free PhCH₂NMe₂), 1.44 (s, 9H, *t*-Bu), 1.41 (s, 3H, *o*-C₆H₄CH₂NMe₂), 1.39 (s, 9H, *t*-Bu), 1.29 (s, 3H, PhCH₂NMe₂), 1.24 (s, 3H, PhCH₂NMe₂), 1.19 (s, 3H, *o*-C₆H₄CH₂NMe₂); ¹³C{¹H} NMR (125 MHz, toluene-*d*₈, 0 °C): δ = 181.9 (d, ¹*J*(Y,C) = 52.6 Hz), 163.4 (CO), 162.8 (CO), 148.3, 141.4, 141.2, 139.3, 138.9, 138.3, 137.18, 137.15, 136.83, 136.75, 136.71, 136.68, 136.5, 131.9, 130.0,

129.7, 129.3, 129.24, 129.23, 128.82, 128.76, 128.6, 128.4, 128.3, 128.2, 128.1, 127.7, 127.5, 127.4, 127.2, 126.0, 125.8, 125.6, 125.5, 122.6, 122.4, 117.18, 117.15 (aryl), 68.0 (*o*-C₆H₄CH₂NMe₂), 64.5 (s, free PhCH₂NMe₂), 58.0 (PhCH₂NMe₂), 46.8 (N(CH₃)₂), 45.4 (s, free PhCH₂NMe₂), 44.2 (N(CH₃)₂), 40.4 (PhCH₂NMe₂), 40.3 (PhCH₂NMe₂), 29.7 (C(CH₃)₃), 29.4 (C(CH₃)₃), 19.7 (C(CH₃)₃), 19.6 (C(CH₃)₃). Anal. Calcd. for C₇₀H₇₃N₂O₂Si₂Y: C, 75.11; H, 6.57; N, 2.50. Found: C, 72.09; H, 6.60; N, 2.23.

(*R*)-[Lu{TBdPS₂BINO}(*o*-C₆H₄CH₂NMe₂)(Me₂NCH₂Ph)] ((*R*)-39b-Lu**).** To a mixture of (*R*)-**31** (22.9 mg, 0.030 mmol) and [Lu(*o*-C₆H₄CH₂NMe₂)₃] (17.3 mg, 0.030 mmol) was added C₆D₆ (0.50 mL). The mixture was kept at room temperature for 1.5 h. ¹H and ¹³C NMR spectra showed clean formation of (*R*)-**39b-Lu**, which was used directly for catalytic experiments. ¹H NMR (400 MHz, 25 °C, C₆D₆): δ = 8.63 (s, 2H, aryl-H), 8.12 (d, ³*J*(H,H) = 6.65 Hz, 2H, aryl-H), 8.04 (d, ³*J*(H,H) = 6.26 Hz, 2H, aryl-H), 7.98–7.89 (m, 4H, aryl-H), 7.76–7.62 (m, 2H, aryl-H), 7.56 (d, ³*J*(H,H) = 7.04 Hz, 1H, aryl-H), 7.41–7.28 (m, 3H, aryl-H), 7.06 (m, 25H, aryl-H including free PhCH₂NMe₂), 6.86 (d, ³*J*(H,H) = 7.43 Hz, 1H, aryl-H), 6.68 (d, ³*J*(H,H) = 6.65 Hz, 2H, aryl-H), 3.36 (d, ²*J*(H,H) = 14.09 Hz, 1H, *o*-C₆H₄CH₂NMe₂), 3.27 (s, 2H, free PhCH₂NMe₂), 3.20 (d, ²*J*(H,H) = 13.7 Hz, 1H, PhCH₂NMe₂), 3.13 (d, ²*J*(H,H) = 13.3 Hz, 1H, PhCH₂NMe₂), 2.50 (d, ²*J*(H,H) = 14.09 Hz, 1H, *o*-C₆H₄CH₂NMe₂), 2.09 (s, 6H, free PhCH₂NMe₂), 1.47 (s, 9H, *t*-Bu), 1.44 (s, 3H, *o*-C₆H₄CH₂NMe₂), 1.42 (s, 9H, *t*-Bu), 1.35 (s, 3H, PhCH₂NMe₂), 1.28 (s, 3H, PhCH₂NMe₂), 1.21 (s, 3H, *o*-C₆H₄CH₂NMe₂); ¹³C{¹H} NMR (100 MHz, 25 °C, C₆D₆): δ = 191.4 (C-Lu), 163.7 (CO), 163.5 (CO), 148.8, 140.79, 140.76, 140.65, 140.62, 140.0, 139.67, 139.63, 139.4, 139.2, 137.3, 137.2, 136.9, 136.8, 136.64, 136.55, 132.0,

129.9, 129.1, 128.9, 128.8, 128.7, 128.5, 128.37, 128.32, 127.5, 127.4, 127.3, 127.2, 126.1, 125.9, 125.2, 122.3, 117.4, 116.9 (aryl), 67.3 (*o*-C₆H₄CH₂Me₂), 64.5 (s, free PhCH₂NMe₂), 58.0 (PhCH₂Me₂), 46.9 (N(CH₃)₂), 45.4 (s, free PhCH₂NMe₂), 44.3 (N(CH₃)₂), 40.7 (PhCH₂NMe₂), 29.5 (C(CH₃)₃), 29.4 (C(CH₃)₃), 19.6 (C(CH₃)₃), 19.5 (C(CH₃)₃).

(*R*)-[Y{CDPS₂BINO}(*o*-C₆H₄CH₂NMe₂)(Me₂NCH₂Ph)] ((*R*)-39c-Y**).** To a mixture of (*R*)-**32** (48.9 mg, 0.06 mmol) and [Y(*o*-C₆H₄CH₂NMe₂)₃] (29.3 mg, 0.06 mmol) was added C₆D₆ (0.55 mL). The mixture was kept at room temperature for 1 h. ¹H and ¹³C NMR showed clean formation of (*R*)-**39c-Y**, which was used directly for catalytic experiments. ¹H NMR (500 MHz, 25 °C, C₆D₆): δ = 8.48 (s, 1H, aryl-H), 8.47 (s, 1H, aryl-H), 7.94–7.91 (m, 2H, aryl-H), 7.29–7.87 (m, 4H, aryl-H), 7.87–7.82 (m, 2H, aryl-H), 7.70–7.68 (m, 1H, aryl-H), 7.65 (d, ³J(H,H) = 6.9 Hz, 1H, aryl-H), 7.60 (d, ³J(H,H) = 8.0 Hz, 1H, aryl-H), 7.55 (m, 2H, aryl-H), 7.34–6.94 (m, 26H, aryl-H including free PhCH₂NMe₂), 6.80 (d, ³J(H,H) = 7.3 Hz, 1H, aryl-H), 6.67 (m, 2H, aryl-H), 3.25 (s, 2H, free PhCH₂NMe₂), 3.13 (d, ²J(H,H) = 13.9 Hz, 1H, *o*-C₆H₄CH₂NMe₂), 2.99 (d, ²J(H,H) = 13.2 Hz, 1H, PhCH₂NMe₂), 2.93 (d, ²J(H,H) = 13.2 Hz, 1H, PhCH₂NMe₂), 2.33 (d, ²J(H,H) = 13.9 Hz, 1H, *o*-C₆H₄CH₂NMe₂), 2.28–2.12 (m, 6H), 2.09 (s, 6H, free PhCH₂NMe₂), 1.76–1.60 (m, 10H), 1.44–1.26 (m, 12H), 1.06–0.97 (m, 6H); ¹³C{¹H} NMR (125 MHz, 25 °C, C₆D₆): δ = 181.5 (d, ¹J(Y,C) = 53.5 Hz), 163.5 (CO), 162.5 (CO), 148.8, 140.1, 140.0, 139.2, 139.1, 138.3, 136.9, 136.7, 136.2, 135.72, 135.67, 135.57, 135.46, 131.8, 130.3, 129.3, 129.2, 129.1, 128.8, 128.7, 128.51, 128.45, 128.38, 128.29, 127.9, 127.2, 126.0, 125.8, 125.6, 125.5, 124.8, 122.54, 122.48, 116.93, 116.85

(aryl), 67.6 (CH₂), 64.5 (s, free PhCH₂NMe₂), 57.9 (PhCH₂NMe₂), 46.1 (N(CH₃)₂), 45.4 (s, free PhCH₂NMe₂), 43.6 (N(CH₃)₂), 40.5 (PhCH₂NMe₂), 40.2 (PhCH₂NMe₂), 29.0 (CH₂, Cy), 28.9 (CH₂, Cy), 28.8 (CH₂, Cy), 28.6 (2 C, CH₂, Cy), 28.5 (CH₂, Cy), 27.9 (CH₂, Cy), 27.8 (CH₂, Cy), 27.21 (CH₂, Cy), 27.20 (CH₂, Cy), 23.7 (CH, Cy), 23.4 (CH, Cy). Anal. Calcd. for C₇₄H₇₇N₂O₂Si₂Y: C, 75.87; H, 6.62; N, 2.39. Found: C, 72.50; H, 7.02; N, 2.11.

(*R*)-[Lu{CDPS₂BINO}(*o*-C₆H₄CH₂NMe₂)(Me₂NCH₂Ph)] ((*R*)-39c-Lu**).** To a mixture of (*R*)-**32** (24.9 mg, 0.031 mmol) and [Lu(*o*-C₆H₄CH₂NMe₂)₃] (17.6 mg, 0.031 mmol) was added C₆D₆ (0.50 mL). The mixture was kept at room temperature for 1.5 h. ¹H and ¹³C NMR spectra showed clean formation of (*R*)-**39c-Lu**, which was used directly for catalytic experiments. ¹H NMR (500 MHz, 25 °C, C₆D₆): δ = 8.51 (s, 1H, aryl-H), 8.50 (s, 1H, aryl-H), 8.06–7.80 (m, 8H, aryl-H), 7.66 (dd, ³*J*(H,H) = 6.11 Hz, ⁴*J*(H,H) = 3.18 Hz, 1H, aryl-H), 7.47–7.30 (m, 3H, aryl-H), 7.30–6.90 (m, 27H, aryl-H including free PhCH₂NMe₂), 6.85 (d, ³*J*(H,H) = 7.34 Hz, 1H, aryl-H), 6.68 (dd, ³*J*(H,H) = 7.34 Hz, ⁴*J*(H,H) = 1.96 Hz, 2H, aryl-H), 3.27 (s, 2H, free PhCH₂NMe₂), 3.08 (d, ²*J*(H,H) = 14.2 Hz, 1H, *o*-C₆H₄CH₂Me₂), 2.99 (d, ²*J*(H,H) = 13.2 Hz, 1H, PhCH₂NMe₂), 2.94 (d, ²*J*(H,H) = 13.2 Hz, 1H, PhCH₂NMe₂), 2.21 (d, ²*J*(H,H) = 13.9 Hz, 1H, *o*-C₆H₄CH₂NMe₂), 2.20–2.08 (m, 6H), 2.09 (s, 6H, free PhCH₂NMe₂), 1.80–1.55 (m, 10H), 1.52–1.25 (m, 12H), 1.11–0.85 (m, 6H); ¹³C{¹H} NMR (125 MHz, 25 °C, C₆D₆): δ = 191.0 (C-Lu), 164.0 (CO), 163.0 (CO), 149.3, 140.0, 139.6, 139.5, 139.37, 139.33, 139.2, 136.9, 136.7, 136.2, 135.6, 135.5, 131.9, 130.1, 129.3, 129.2, 129.1, 128.9, 128.7, 128.6, 128.53, 128.48, 128.4, 128.3, 128.2, 127.2, 127.1, 127.0, 126.2, 125.9, 125.8, 125.2, 122.4, 122.3,

116.8, 115.9 (aryl), 66.9 (CH₂), 64.5 (s, free PhCH₂NMe₂), 57.7 (PhCH₂NMe₂), 46.4 (N(CH₃)₂), 45.4 (s, free PhCH₂NMe₂), 43.8 (N(CH₃)₂), 40.9 (PhCH₂NMe₂), 40.3 (PhCH₂NMe₂), 29.0 (CH₂, Cy), 28.9 (CH₂, Cy), 28.8 (CH₂, Cy), 28.6 (3C, CH₂, Cy), 27.9 (CH₂, Cy), 27.8 (CH₂, Cy), 27.2 (2 C, CH₂, Cy), 23.6 (CH, Cy), 23.4 (CH, Cy).

(R)-[Y{TiPS₂BINO}(o-C₆H₄CH₂NMe₂)(Me₂NCH₂Ph)] ((R)-39d-Y). To a mixture of (R)-33 (16.2 mg, 0.027 mmol) and [Y(o-C₆H₄CH₂NMe₂)₃] (13.3 mg, 0.027 mmol) was added C₆D₆ (0.50 mL). The mixture was kept at room temperature for 1 h. ¹H and ¹³C NMR spectra showed clean formation of (R)-39d-Y, which was used directly for catalytic experiments. ¹H NMR (400 MHz, 25 °C, C₆D₆): δ = 8.42 (s, 1H, aryl-H), 8.39 (s, 1H, aryl-H), 8.10 (d, ³J(H,H) = 6.60 Hz, 1H, aryl-H), 8.02–7.78 (m, 3H, aryl-H), 7.66–6.94 (m, 18H, aryl-H including free PhCH₂NMe₃), 4.28–4.01 (br m, 3H), 3.69–3.36 (br m, 3H), 2.48–2.14 (m, 9H), 2.14–2.07 (s, 4H), 2.07–1.90 (m, 6H, CH(CH₃)₂), 1.89–1.80 (m, 2H), 1.77 (s, 3 H, N(CH₃)₂), 1.71–0.90 (m, 36H, CH(CH₃)₂); ¹³C{¹H} NMR (100 MHz, 25 °C, C₆D₆): δ = 181.5 (d, ¹J(Y,C) = 53.1 Hz), 163.9 (CO), 163.3 (CO), 148.2, 140.8, 140.5, 138.9, 138.5, 138.2, 131.7, 130.5, 129.5, 129.1, 128.7, 128.6, 127.24, 127.19, 126.3, 125.7, 125.6, 125.4, 125.2, 122.8, 122.6, 117.0, 116.6 (aryl), 68.5 (o-C₆H₄CH₂NMe₂), 64.5 (s, free PhCH₂NMe₂), 59.7 (PhCH₂NMe₂), 47.0 (N(CH₃)₂), 45.4 (s, free PhCH₂NMe₂), 44.7 (N(CH₃)₂), 41.9 (PhCH₂NMe₂), 19.9 (3 C, CH(CH₃)₂), 19.8 (3 C, CH(CH₃)₂), 19.7 (6 C, CH(CH₃)₂), 12.8 (3 C, CH(CH₃)₂), 12.7 (3 C, CH(CH₃)₂). Anal. Calcd. for C₅₆H₇₇N₂O₂Si₂Y: C, 70.41; H, 8.12; N, 2.93. Found: C, 63.81; H, 7.95; N, 1.47.

(*R*)-[Lu{TIPS₂BINO}(*o*-C₆H₄CH₂NMe₂)(Me₂NCH₂Ph)] ((*R*)-39d-Lu). To a mixture of (*R*)-33 (15.0 mg, 0.025 mmol) and [Lu(*o*-C₆H₄CH₂NMe₂)₃] (14.4 mg, 0.025 mmol) was added C₆D₆ (0.50 mL). The mixture was kept at room temperature for 1 h. ¹H and ¹³C NMR spectra showed clean formation of (*R*)-39d-Lu, which was used directly for catalytic experiments. ¹H NMR (400 MHz, 25 °C, C₆D₆): δ = 8.45 (s, 1H, aryl-H), 8.43 (s, 1H, aryl-H), 8.21 (d, ³*J*(H,H) = 6.26 Hz, 1H, aryl-H), 8.13–7.83 (m, 2H, aryl-H), 7.82–6.78 (m, 19H, aryl-H including free PhCH₂NMe₂), 4.24 (br s, 2H), 4.08 (d, ²*J*(H,H) = 13.7 Hz, 1H, *o*-C₆H₄CH₂NMe₂), 3.51 (br m, 3H including free PhCH₂NMe₂), 2.32 (s, 6H), 2.20 (s, 3H), 2.10 (s, 6H, free PhCH₂NMe₂), 2.07–1.94 (m, 6H, CH(CH₃)₂), 1.85 (s, 3H, N(CH₃)₂), 1.80–1.02 (m, 36H, CH(CH₃)₂); ¹³C{¹H} NMR (100 MHz, 25 °C, C₆D₆): δ = 190.2 (C-Lu), 163.9 (CO), 163.3 (CO), 148.3, 139.8, 139.7, 139.4, 138.8, 138.5, 131.6, 129.6, 128.9, 128.4, 128.2, 126.9, 126.84, 126.80, 126.2, 125.8, 125.6, 125.5, 125.3, 122.3, 122.1, 116.5, 116.4 (aryl), 67.5 (*o*-C₆H₄CH₂NMe₂), 64.3 (s, free PhCH₂NMe₂), 59.4 (PhCH₂NMe₂), 47.0 (N(CH₃)₂), 45.1 (s, free PhCH₂NMe₂), 44.7 (N(CH₃)₂), 41.8 (PhCH₂NMe₂), 19.6 (CH(CH₃)₂), 19.51 (CH(CH₃)₂), 19.46 (CH(CH₃)₂), 19.45 (CH(CH₃)₂), 12.7 (CH(CH₃)₂), 12.6 (CH(CH₃)₂).

(*R*)-[Y{DCPS₂BINO}(*o*-C₆H₄CH₂NMe₂)(Me₂NCH₂Ph)] ((*R*)-39e-Y). To a mixture of (*R*)-34 (51.0 mg, 0.061 mmol) and [Y(*o*-C₆H₄CH₂NMe₂)₃] (29.9 mg, 0.061 mmol) was added C₆D₆ (0.60 mL). The mixture was kept at room temperature for 1 h. ¹H and ¹³C NMR spectra showed clean formation of (*R*)-39e-Y, which was used directly for catalytic experiments. ¹H NMR (500 MHz, 6 °C, C₆D₆): δ = 8.29 (s, 2H, aryl-H), 7.83 (d, ³*J*(H,H) = 6.85 Hz, 2H, aryl-H), 7.75 (d, ³*J*(H,H) = 6.85 Hz, 2H, aryl-H), 7.58 (d, ³*J*(H,H) = 7.34

Hz, 2H, aryl-H), 7.38–7.27 (m, 4H, aryl-H), 7.26–6.89 (m, 20H, aryl-H including free PhCH₂NMe₂), 6.87–6.76 (m, 2H, aryl-H), 3.86 (d, ²*J*(H,H) = 13.94 Hz, 1H, *o*-C₆H₄CH₂NMe₂), 3.49 (d, ²*J*(H,H) = 13.45 Hz, 1H, PhCH₂NMe₂), 3.32 (d, ²*J*(H,H) = 13.45 Hz, 1H, PhCH₂NMe₂), 3.23 (s, 2H, free PhCH₂NMe₂), 3.08 (d, ²*J*(H,H) = 13.94 Hz, 1H, *o*-C₆H₄CH₂NMe₂), 2.42–2.25 (m, 4H, Cy), 2.22–2.08 (m, 6H, Cy), 2.05 (s, 6H, free PhCH₂NMe₂), 2.01–1.08 (m, 50H, Cy and N(CH₃)₂); ¹³C{¹H} NMR (125 MHz, 6 °C, C₆D₆): δ = 181.5 (d, ¹*J*(Y,C) = 53.5 Hz), 163.1 (CO), 162.8 (CO), 148.3, 141.2, 140.00, 139.97, 139.0, 138.6, 138.4, 137.7, 136.3, 135.7, 131.8, 130.3, 129.4, 129.3, 129.1, 128.8, 128.6, 128.5, 128.3, 127.9, 127.8, 127.3, 126.2, 125.8, 125.5, 125.3, 125.2, 122.8, 122.6, 116.6, 116.4 (aryl), 68.2 (*o*-C₆H₄CH₂NMe₂), 64.5 (s, free PhCH₂NMe₂), 58.2 (PhCH₂NMe₂), 47.0 (N(CH₃)₂), 45.4 (s, free PhCH₂NMe₂), 44.7 (N(CH₃)₂), 40.9, 40.7 (PhCH₂NMe₂), 29.6, 29.29, 29.25, 29.22, 29.14, 29.05, 28.95, 28.88, 28.84, 28.72, 28.65, 28.62, 28.3, 27.7, 27.5, 27.4, 27.3 (CH₂, Cy), 24.4, 24.1, 23.9, 23.0 (CH, Cy). Anal. Calcd. for C₇₄H₈₉N₂O₂Si₂Y: C, 75.09; H, 7.58; N, 2.37. Found: C, 71.52; H, 8.03; N, 2.01.

(*R*)-[Lu{DCPS₂BINO}(*o*-C₆H₄CH₂NMe₂)(Me₂NCH₂Ph)] ((*R*)-39e-Lu). To a mixture of (*R*)-**34** (25.9 mg, 0.031 mmol) and [Lu(*o*-C₆H₄CH₂NMe₂)₃] (18.1 mg, 0.031 mmol) was added C₆D₆ (0.50 mL). The mixture was kept at room temperature for 1 h. ¹H and ¹³C NMR spectra showed clean formation of (*R*)-**39e-Lu**, which was used directly for catalytic experiments. ¹H NMR (500 MHz, 7 °C, C₆D₆): δ = 8.34 (s, 1H, aryl-H), 8.32 (s, 1H, aryl-H), 7.93 (d, ³*J*(H,H) = 6.60 Hz, 2H, aryl-H), 7.85 (d, ³*J*(H,H) = 7.09 Hz, 2H, aryl-H), 7.79 (d, ³*J*(H,H) = 7.09 Hz, 2H, aryl-H), 7.68–7.60 (m, 6H, aryl-H), 7.46–6.92

(m, 18H, aryl-H including free PhCH₂NMe₂), 6.91–6.81 (m, 2H, aryl-H), 3.79 (d, ²*J*(H,H) = 13.94 Hz, 1H, *o*-C₆H₄CH₂NMe₂), 3.52 (d, ²*J*(H,H) = 13.21 Hz, 1H, PhCH₂NMe₂), 3.33 (d, ²*J*(H,H) = 13.45 Hz, 1H, PhCH₂NMe₂), 3.25 (s, 2H, free PhCH₂NMe₂), 3.01 (d, ²*J*(H,H) = 13.94 Hz, 1H, *o*-C₆H₄CH₂NMe₂), 2.45–2.29 (m, 2H), 2.29–2.09 (m, 10H), 2.07 (s, 6H, free PhCH₂NMe₂), 2.04–1.03 (m, 43H, Cy and N(CH₃)₂); ¹³C{¹H} NMR (125 MHz, 7 °C, C₆D₆): δ = 190.6 (C-Lu), 163.5 (CO), 163.3 (CO), 148.7, 140.3, 139.9, 139.1, 138.8, 136.8, 136.4, 135.8, 132.0, 130.1, 129.1, 128.8, 128.7, 128.5, 127.2, 127.1, 126.4, 126.1, 125.8, 125.7, 116.5, 116.3 (aryl), 67.4 (*o*-C₆H₄CH₂NMe₂), 64.5 (s, free PhCH₂NMe₂), 58.1 (PhCH₂NMe₂), 47.3, 46.1 (N(CH₃)₂), 45.4 (s, free PhCH₂NMe₂), 44.8, 41.2, 40.9 (N(CH₃)₂), 29.7, 29.5, 29.3, 29.1, 29.0, 28.9, 28.81, 28.76, 28.6, 28.4, 27.7, 27.51, 27.45, 27.3 (CH₂, Cy), 24.4, 24.3, 24.1, 23.3 (CH, Cy).

(*R*)-[Y{MPDP₂BINO}(*o*-C₆H₄CH₂NMe₂)(Me₂NCH₂Ph)] ((*R*)-39f-Y**).** To a mixture of (*R*)-3,3'-bis[4-methoxyphenyl(diphenyl)silyl]-1,1'-binaphtholene-2,2'-diol (24.9 mg, 0.03 mmol) and [Y(*o*-C₆H₄CH₂NMe₂)₃] (14.7 mg, 0.03 mmol) was added C₆D₆ (0.50 mL). The mixture was kept at room temperature for 1 h. ¹H and ¹³C NMR spectra showed clean formation of (*R*)-**39f-Y**, which was used directly for catalytic experiments. ¹H NMR (400 MHz, 25 °C, C₆D₆): δ = 8.41 (br s, 2H, aryl-H), 8.10–7.91 (br m, 6H, aryl-H), 7.60–6.57 (br m, 44H, aryl-H including free PhCH₂NMe₂), 3.27, (br s, 4H, free and coordinate PhCH₂NMe₂), 3.21 (d, partially overlapped by other signal, 1H, *o*-C₆H₄CH₂NMe₂), 2.59 (d, ²*J*(H,H) = 14.1 Hz, 1H, *o*-C₆H₄CH₂NMe₂), 2.34 (br s 6H, aryl-CH₃), 2.07 (s, 6H, free PhCH₂NMe₂), 1.59 (s, 3H, N(CH₃)₂), 1.40 (br s, 6H,

PhCH₂NMe₂), 1.29 (br s, 3H, N(CH₃)₂); ¹³C{¹H} NMR (100 MHz, 25 °C, C₆D₆): δ = 181.6 (d, ¹J(Y,C) = 52.3 Hz), 163.3 (CO), 160.0 (CO), 148.5, 145.0, 144.8, 141.6, 140.0 (br s), 139.6, 139.5, 138.4, 138.3, 137.0, 136.8, 136.6, 136.3, 136.1, 135.8, 134.3, 134.1, 131.9 (br s), 130.7, 130.0, 129.5, 129.3, 128.9, 128.8, 127.4, 127.5, 127.3, 126.0, 125.73, 125.65, 124.8, 122.5, 117.3, 116.8 (aryl), 67.9, 64.6 (br s, free PhCH₂NMe₂), 58.4 (br s, PhCH₂NMe₂), 46.5 (N(CH₃)₂), 45.4 (br s, free PhCH₂NMe₂), 44.5 (N(CH₃)₂), 40.6 (br s, PhCH₂NMe₂), 24.6 (aryl-CH₃), 24.4 (aryl-CH₃).

(*R*)-[Lu{MPDPS₂BINO}(*o*-C₆H₄CH₂NMe₂)(Me₂NCH₂Ph)] ((*R*)-39f-Lu**).** To a mixture of (*R*)-3,3'-bis[4-methoxyphenyl(diphenyl)silyl]-1,1'-binaphtholene-2,2'-diol (24.9 mg, 0.03 mmol) and [Lu(*o*-C₆H₄CH₂NMe₂)₃] (17.3 mg, 0.03 mmol) was added C₆D₆ (0.50 mL). The mixture was kept at room temperature for 1 h. ¹H and ¹³C NMR spectra showed clean formation of (*R*)-**39f-Lu**, which was used directly for catalytic experiments. ¹H NMR (300 MHz, 25 °C, C₆D₆): δ = 8.42 (br s, partially overlapped by other signal, 1H, aryl-H), 8.38 (br s, partially overlapped by other signal, 1H, aryl-H), 8.20–7.82 (br m, 6H, aryl-H), 7.75–7.65 (br d, ³J(H,H) = 7.70 Hz, 2H, aryl-H), 7.57–7.50 (br d, ³J(H,H) = 7.53 Hz, 2H, aryl-H), 7.50–7.40 (br d, ³J(H,H) = 7.45 Hz, 2H, aryl-H), 7.50–6.85 (m, 34H, aryl-H including free PhCH₂NMe₂), 6.85–6.72 (br d, ³J(H,H) = 6.79 Hz, 2H, aryl-H), 6.72–6.52 (br d, ³J(H,H) = 6.63 Hz, 2H, aryl-H), 3.26 (br s, 2H, free PhCH₂NMe₂), 3.12 (d, ²J(H,H) = 14.0 Hz, 1H, *o*-C₆H₄CH₂NMe₂), 2.46 (d, ²J(H,H) = 14.7 Hz, 1H, *o*-C₆H₄CH₂NMe₂), 2.35 (s, 2H, PhCH₂NMe₂), 2.08 (s, 12H, aryl-CH₃ and free PhCH₂NMe₂), 1.55 (br s, 3H, N(CH₃)₂), 1.38 (br s, partially overlapped by other signal, 3H, N(CH₃)₂), 1.38 (br s, partially overlapped by other signal, 3H, NCH₃), 1.25 (br s, 3H,

NCH₃); ¹³C{¹H} NMR (100 MHz, 25 °C, C₆D₆): δ = 191.1 (C-Lu), 163.8, 163.4 (CO), 148.9, 147.3, 144.9, 144.8, 141.2, 141.0, 139.9, 139.68, 139.63, 139.57, 138.4, 138.3, 137.3, 137.1, 136.8, 136.6, 136.5, 136.2, 135.8, 134.3, 134.1, 132.0, 130.6, 130.0, 129.93, 129.87, 129.4, 129.3, 129.2, 129.1, 128.9, 128.8, 128.76, 128.72, 128.71, 128.6, 128.53, 128.45, 128.1, 127.3, 127.2, 126.1, 126.0, 125.9, 125.7, 125.5, 125.4, 125.1, 125.0, 122.3, 117.1, 116.6 (aryl), 67.2 (*o*-C₆H₄CH₂NMe₂), 64.5 (free PhCH₂NMe₂), 58.2 (PhCH₂NMe₂), 46.7 (N(CH₃)₂), 46.2 (N(CH₃)₂), 45.3 (free PhCH₂NMe₂), 44.5 (N(CH₃)₂), 40.7 (N(CH₃)₂), 24.5 (aryl-CH₃), 24.3 (aryl-CH₃).

7.4.2 Octahydrobinaphtholate Rare Earth Metal Complexes

(*R*)-[Y{H8-TPS₂BINO}(*o*-C₆H₄CH₂NMe₂)(Me₂NCH₂Ph)] ((*R*)-50a-Y). To a mixture of (*R*)-**44** (48.7 mg, 0.060 mmol) and [Y(*o*-C₆H₄CH₂NMe₂)₃] (29.5 mg, 0.060 mmol) was added C₆D₆ (0.60 mL). The mixture was kept at room temperature for 10 minutes. ¹H and ¹³C NMR spectra showed clean formation of (*R*)-**50a-Y**, which was used directly for catalytic experiments. ¹H NMR (500 MHz, 6 °C, C₆D₆): δ = 8.02–7.84 (m, 12H, aryl-H), 7.67–7.59 (m, 3H, aryl-H), 7.33 (d, ³*J*(H,H) = 6.9 Hz, 2H, aryl-H), 7.29–6.98 (m, 27H, including 5H from free PhCH₂NMe₂), 6.84–6.73 (m, 2H, aryl-H), 3.36 (m, 2H, 1H from *o*-C₆H₄CH₂NMe₂ and 1H from C₆H₅CH₂NMe₂), 2.84 (d, ²*J*(H,H) = 13.21 Hz, 1H, C₆H₅CH₂NMe₂), 2.70–2.16 (m, 9H; 8H from CH₂ of H8-BINOL-TPS and 1H from *o*-C₆H₄CH₂NMe₂), 1.81–1.34 (m, 20H, 8H from CH₂ of H8-BINOL-TPS and 12H from N(CH₃)₂); ¹³C{¹H} NMR (125 MHz, 6 °C, C₆D₆): δ = 182.1 (d, ¹*J*(Y,C) = 52.6 Hz), 163.7, 162.9, 148.6, 142.2, 141.7, 139.9, 138.1, 137.0, 136.9, 136.6, 136.5, 131.9, 130.6,

129.6, 129.3, 129.0, 128.9, 128.7, 128.5, 128.3, 127.9, 127.0, 126.7, 125.9, 125.5, 124.8, 122.0, 121.9 (aryl), 67.7 (*o*-C₆H₄CH₂NMe₂), 58.4 (C₆H₅CH₂NMe₂), 46.21 (*o*-C₆H₄CH₂NMe₂), 44.2 (*o*-C₆H₄CH₂NMe₂), 40.3 (C₆H₅CH₂NMe₂), 39.9 (C₆H₅CH₂NMe₂), 29.9, 29.8, 29.6, 28.9, 28.8, 28.7, 24.0, 23.9, 23.7 (CH₂, H8-BINOL).

(*R*)-[Lu{H8-TPS₂BINOL-TPS}(*o*-C₆H₄CH₂NMe₂)(Me₂NCH₂Ph)] ((*R*)-50a-Lu). To a mixture of (*R*)-**44** (29.2 mg, 0.036 mmol) and [Lu(*o*-C₆H₄CH₂NMe₂)₃] (20.8 mg, 0.036 mmol) was added C₆D₆ (0.6 mL). The mixture was kept at room temperature for 30 minutes. ¹H and ¹³C NMR spectra showed clean formation of (*R*)-**50a-Lu**, which was used directly for catalytic experiments. ¹H NMR (400 MHz, 9 °C, C₆D₆): δ = 8.06–7.88 (m, 12H, aryl-H), 7.71–7.66 (m, 2H, aryl-H), 7.64 (s, 1H, aryl-H), 7.42–7.29 (m, 4H, aryl-H), 7.29–6.99 (m, 24H, aryl-H, including 5H from free PhCH₂NMe₂), 6.86 (d, ³J(H,H) = 7.4 Hz, 1H, aryl-H), 6.83–6.75 (m, 2H, aryl-H), 3.44–3.28 (m, 2H, 1H from *o*-C₆H₄CH₂NMe₂ and 1H from C₆H₅CH₂NMe₂), 2.85 (d, ²J(H,H) = 13.3 Hz, 1H, C₆H₅CH₂NMe₂), 2.75–2.28 (m, 9H, 8H from CH₂ of H8-BINOL-TPS and 1H from *o*-C₆H₄CH₂NMe₂), 1.87–1.19 (m, 20H, 8H from CH₂ of H8-BINOL-TPS and 12H from N(CH₃)₂); ¹³C{¹H} NMR (100 MHz, 9 °C, C₆D₆): δ = 191.7, 164.5, 163.8, 148.9, 142.1, 141.6, 139.9, 139.5, 139.4, 139.3, 136.9, 136.8, 136.5, 132.0, 129.2, 129.1, 128.7, 128.5, 127.9, 127.8, 127.2, 126.9, 126.0, 125.2, 125.1, 121.2, 120.9 (aryl), 67.5 (*o*-C₆H₄CH₂NMe₂), 58.4 (C₆H₅CH₂NMe₂), 46.6 (*o*-C₆H₄CH₂NMe₂), 44.1 (*o*-C₆H₄CH₂NMe₂), 40.4 (C₆H₅CH₂NMe₂), 39.8 (C₆H₅CH₂NMe₂), 29.9, 29.8, 29.6, 28.9, 24.2, 23.9, 23.8 (CH₂, H8-BINOL).

(R)-[Y{H8-TBDPS₂BINO}(*o*-C₆H₄CH₂NMe₂)(Me₂NCH₂Ph)] ((R)-50b-Y). To a mixture of (*R*)-**45** (30.0 mg, 0.039 mmol) and [Y(*o*-C₆H₄CH₂NMe₂)₃] (19.1 mg, 0.039 mmol) was added C₆D₆ (0.6 mL). The mixture was kept at room temperature for 10 minutes. ¹H and ¹³C NMR spectra showed clean formation of (*R*)-**50b-Y**, which was used directly for catalytic experiments. ¹H NMR (500 MHz, 6 °C, C₆D₆): δ = 8.09 (d, ³J(H,H) = 7.6 Hz, 2H, aryl-H), 7.99 (d, ³J(H,H) = 6.6 Hz, 2H, aryl-H), 7.93 (d, ³J(H,H) = 7.8 Hz, 4H, aryl-H), 7.69 (d, ³J(H,H) = 4.9 Hz, 2H, aryl-H), 7.65 (d, ³J(H,H) = 6.4 Hz, 2H, aryl-H), 7.43–6.98 (m, 22H, aryl-H, including 5H from free PhCH₂NMe₂), 6.91 (d, ³J(H,H) = 7.3 Hz, 1H, aryl-H), 6.88–6.80 (m, 2H, aryl-H), 3.63 (d, ²J(H,H) = 14.2 Hz, 1H, *o*-C₆H₄CH₂NMe₂), 3.40 (d, ²J(H,H) = 13.2 Hz, 1H, C₆H₅CH₂NMe₂), 2.92 (d, ²J(H,H) = 13.0 Hz, 1H, C₆H₅CH₂NMe₂), 2.80–2.13 (m, 9H, 8H from CH₂ of H8-BINOL-TBDPS and 1H from *o*-C₆H₄CH₂NMe₂), 1.83 (s, 3H, *o*-C₆H₄CH₂NMe₂), 1.78–1.27 (m, 35H, 8H from CH₂ of H8-BINOL-TBDPS, 3H from *o*-C₆H₄CH₂NMe₂, 6H from C₆H₅CH₂NMe₂, and 18H of *t*Bu); ¹³C{¹H} NMR (125 MHz, 6 °C, C₆D₆): δ = 182.2 (d, ¹J(Y,C) = 52.6 Hz), 163.2, 163.0, 148.5, 141.6, 141.5, 140.1, 139.9, 138.3, 137.7, 137.5, 137.4, 137.2, 137.1, 136.9, 136.8, 135.7, 131.9, 129.1, 128.9, 128.7, 128.6, 128.4, 128.3, 127.8, 127.3, 127.1, 126.8, 126.6, 125.9, 125.6, 124.9, 122.7, 122.5 (aryl), 67.5 (*o*-C₆H₄CH₂NMe₂), 58.4 (C₆H₅CH₂NMe₂), 46.4 (*o*-C₆H₄CH₂NMe₂), 44.3 (*o*-C₆H₄CH₂NMe₂), 40.5 (C₆H₅CH₂NMe₂), 40.2 (C₆H₅CH₂NMe₂), 31.1, 30.1, 30.0, 29.9, 29.5, 29.4, 28.7, 28.6, 26.4, 23.9, 23.8, 23.7, 23.1, 19.6, 19.5 (CH₂ of H8-BINOL, and *t*Bu).

(R)-[Lu{H8-TBDPS₂BINO}(*o*-C₆H₄CH₂NMe₂)(Me₂NCH₂Ph)] ((R)-50b-Lu). To a mixture of (*R*)-**45** (30.0 mg, 0.039 mmol) and [Lu(*o*-C₆H₄CH₂NMe₂)₃] (22.5 mg, 0.039

mmol) was added C₆D₆ (0.6 mL). The mixture was kept at room temperature for 2 hours. ¹H and ¹³C NMR spectra showed clean formation of (*R*)-**50b-Lu**, which was used directly for catalytic experiments. ¹H NMR (500 MHz, 6 °C, C₆D₆): δ = 8.09 (d, ³*J*(H,H) = 7.6 Hz, 2H, aryl-H), 8.02 (d, ³*J*(H,H) = 6.4 Hz, 2H, aryl-H), 7.99–7.90 (m, 4H, aryl-H), 7.76–7.66 (m, 3H, aryl-H), 7.44–7.30 (m, 4H, aryl-H), 7.30–6.95 (m, 18H, aryl-H, including 5H from free PhCH₂NMe₂), 6.95 (d, ³*J*(H,H) = 7.3 Hz, aryl-H), 6.88–6.79 (m, 2H, aryl-H), 3.49 (d, ²*J*(H,H) = 13.9 Hz, 1H, *o*-C₆H₄CH₂NMe₂), 3.36 (d, ²*J*(H,H) = 13.5 Hz, 1H, C₆H₅CH₂NMe₂), 2.85 (d, ²*J*(H,H) = 13.5 Hz, 1H, C₆H₅CH₂NMe₂), 2.81–2.11 (m, 9H, 8H from CH₂ of H8-BINOL-TBDPS and 1H from *o*-C₆H₄CH₂NMe₂), 1.85–1.14 (m, 35H, 8H of CH₂ of H8-BINOL-TBDPS, 3H from *o*-C₆H₄CH₂NMe₂, 6H from C₆H₅CH₂NMe₂, and 18H from C(CH₃)₃); ¹³C{¹H} NMR (125 MHz, 6 °C, C₆D₆): δ = 191.6, 164.2, 163.6, 148.9, 141.6, 141.2, 139.9, 139.6, 139.4, 139.3, 137.7, 137.4, 137.3, 137.2, 137.1, 136.9, 132.1, 130.1, 129.1, 128.9, 128.6, 128.5, 128.3, 128.2, 127.2, 127.1, 126.8, 126.6, 125.9, 125.2, 121.7, 121.5 (aryl), 67.2 (*o*-C₆H₄CH₂NMe₂), 58.4 (C₆H₅CH₂NMe₂), 46.7 (*o*-C₆H₄CH₂NMe₂), 44.2 (*o*-C₆H₄CH₂NMe₂), 40.5 (C₆H₅CH₂NMe₂), 40.0 (C₆H₅CH₂NMe₂), 31.3, 30.1, 29.9, 29.4, 29.3, 28.9, 28.8, 24.1, 23.9, 23.8, 19.6, 19.5 (CH₂ of H8-BINOL, and *t*Bu).

(*R*)-[Y{H8-CDPS₂BINO}(*o*-C₆H₄CH₂NMe₂)(Me₂NCH₂Ph)] ((*R*)-**50c-Y**). To a mixture of (*R*)-**46** (34.8 mg, 0.0423 mmol) and [Y(*o*-C₆H₄CH₂NMe₂)₃] (20.8 mg, 0.0423 mmol) was added C₆D₆ (0.6 mL). The mixture was kept at room temperature for 10 minutes. ¹H and ¹³C NMR spectra showed clean formation of (*R*)-**50c-Y**, which was used directly for catalytic experiments. ¹H NMR (500 MHz, 6 °C, C₆D₆): δ = 7.95–7.77 (m, 8H, aryl-H),

7.69–7.59 (m, 2H, aryl-H), 7.43–7.24 (m, 4H, aryl-H), 7.24–7.02 (m, 20H, aryl-H, including 5H from free PhCH₂NMe₂), 6.92–6.80 (m, 2H, aryl-H), 3.18 (d, ²J(H,H) = 13.9 Hz, 1H, *o*-C₆H₄CH₂NMe₂), 3.07 (d, ²J(H,H) = 13.5 Hz, 1H, C₆H₅CH₂NMe₂), 2.93–2.12 (m, 16H, 1H from *o*-C₆H₄CH₂NMe₂, 1H from C₆H₅CH₂NMe₂, and 14H from CH₂), 1.97 (s, 3H, *o*-C₆H₄CH₂NMe₂), 1.84–1.19 (m, 31H, 22H from CH₂, 3H from *o*-C₆H₄CH₂NMe₂, and 6H from C₆H₅CH₂NMe₂), 1.06–0.81 (m, 4H, CH and CH₂); ¹³C{¹H} NMR (125 MHz, 6 °C, C₆D₆): δ = 181.7 (d, ¹J(Y,C) = 52.5 Hz), 164.1 (CO), 162.4 (CO), 141.5, 140.8, 139.9, 138.3, 138.2, 136.7, 136.6, 136.2, 136.1, 131.9, 129.1, 128.8, 128.7, 128.6, 128.5, 128.3, 128.11, 127.8, 126.6, 126.5, 125.8, 125.7, 125.1, 124.7, 122.5, 121.1 (aryl), 67.5 (*o*-C₆H₄CH₂NMe₂), 58.2 (C₆H₅CH₂NMe₂), 45.8 (*o*-C₆H₄CH₂NMe₂), 43.7 (*o*-C₆H₄CH₂NMe₂), 40.4 (C₆H₅CH₂NMe₂), 39.3 (C₆H₅CH₂NMe₂), 30.1, 29.9, 29.0, 28.9, 28.7, 28.6, 28.2, 27.8, 27.7, 27.2, 24.0, 23.8, 23.3, 22.9 (CH₂ of H8-BINOL, CH and CH₂ of Cy).

(*R*)-[Lu{H8-CDPS₂BINO}(*o*-C₆H₄CH₂NMe₂)(Me₂NCH₂Ph)] ((*R*)-50c-Lu). To a mixture of (*R*)-**46** (34.0 mg, 0.0413 mmol) and [Lu(*o*-C₆H₄CH₂NMe₂)₃] (23.9 mg, 0.0413 mmol) was added C₆D₆ (0.6 mL). The mixture was kept at room temperature for 2 hours. ¹H and ¹³C NMR spectra showed clean formation of (*R*)-**50c-Lu**, which was used directly for catalytic experiments. ¹H NMR (500 MHz, 6 °C, C₆D₆): δ = 7.95–7.77 (m, 8H, aryl-H), 7.71 (d, ³J(H,H) = 6.6 Hz, 1H, aryl-H), 7.64 (d, ³J(H,H) = 5.4 Hz, 2H, aryl-H), 7.42–7.33 (m, 3H, aryl-H), 7.32–7.01 (m, 19H, aryl-H, including 5H from free PhCH₂NMe₂), 6.90 (d, ³J(H,H) = 7.6 Hz, 1H, aryl-H), 6.84 (d, ³J(H,H) = 6.6 Hz, 2H, aryl-H), 3.14 (d, ²J(H,H) = 13.5 Hz, 1H, C₆H₅CH₂NMe₂), 3.03 (d, ²J(H,H) = 14.2 Hz,

1H, *o*-C₆H₄CH₂NMe₂), 2.95–2.00 (m, 18H, 1H from *o*-C₆H₄CH₂NMe₂, 1H from C₆H₅CH₂NMe₂, and 16H from CH₂ of Cy and H8-BINOL), 1.88 (s, 3H, *o*-C₆H₄CH₂NMe₂), 1.84–1.27 (m, 24H, 6H from C₆H₅CH₂NMe₂, 18H from CH₂ of Cy and H8-BINOL), 1.23 (s, 3H, *o*-C₆H₄CH₂NMe₂), 1.04–0.87 (m, 4H, CH and CH₂); ¹³C{¹H} NMR (125 MHz, 6 °C, C₆D₆): δ = 191.2, 164.8, 163.3, 149.6, 141.3, 140.7, 139.9, 139.7, 137.8, 137.7, 136.8, 136.7, 136.3, 136.2, 132.0, 130.8, 129.1, 129.0, 128.8, 128.7, 128.5, 128.4, 128.3, 128.2, 128.1, 127.9, 127.7, 127.2, 126.7, 126.4, 126.2, 126.0, 125.9, 125.0, 121.4, 120.4 (aryl), 66.9 (*o*-C₆H₄CH₂NMe₂), 58.3 (C₆H₅CH₂NMe₂), 46.1 (*o*-C₆H₄CH₂NMe₂), 43.8 (*o*-C₆H₄CH₂NMe₂), 40.5 (C₆H₅CH₂NMe₂), 39.3 (C₆H₅CH₂NMe₂), 30.1, 29.9, 29.0, 28.9, 28.7, 28.6, 28.3, 27.7, 27.2, 24.1, 23.8, 23.2, 22.8 (CH₂ of H8-BINOL, CH and CH₂ of Cy).

7.5 Synthesis and Characterization of Aminoalkene Substrates

Substrates pent-4-enylamine (**57**),⁴² 2,2-diphenylhex-5-enylamine (**59**),¹⁶⁸ 2,2-diphenylhept-6-enylamine (**61**),⁸² (4*E*)-2,2,5-triphenylpent-4-enylamine (**63**),¹⁶⁹ 1-methylpent-4-enylamine (**25a**),¹⁷⁰ 1-benzylpent-4-enylamine (**25b**),³¹ 1-phenylpent-4-enylamine (**25c**)³¹, 1-cyclohexylpent-4-enylamine (**25d**)¹⁰⁴ were synthesized as described in the literature. The substrates were distilled from finely powder CaH₂, stored over molecular sieves, and kept in the fridge of a glovebox.

2,2-Diphenylpent-4-enylamine (51).⁵⁶ To a suspension of NaH (1.38g, 55.7 mmol) in DMF (50 mL) was added a solution of diphenylacetonitrile (10.56 g, 53.0 mmol) in DMF

(20 mL). The reaction mixture was stirred at room temperature for 1 hr before it was allowed to cool to 0 °C in an ice bath. To that allylbromide (7.05 g, 58.3 mmol) was added dropwise. The resulting bright yellow mixture was allowed to warm to room temperature and stirred overnight. The reaction was quenched by pouring the content to an ice/water mixture (150 mL). The product was extracted with hexanes (3 × 50 mL). The combined organic layers were washed with water (2 × 25 mL) and then were dried over anhydrous MgSO₄. The volatile solvent was removed by rotary evaporation, giving 12.28 g, 99.0%. The nitrile was used for further reaction without purification. To a suspension of LAH (7.72g, 197.2 mmol) in dry Et₂O (100 mL) was added 2,2-diphenyl-4-pentenitrile (10.99 g, 47.10 mmol) dropwise at room temperature. The resulting mixture was heated to reflux and stirred overnight. The reaction mixture was allowed to cool to 0 °C before it was quenched by cautiously adding of water (8 mL), NaOH solution (25%, 8 mL), and water (40 mL). The content was diluted with *tert*-butyl methyl ether (150 mL) before it was heated to reflux for 2 hrs. The solid was filtered off and the residue was washed with Et₂O (4 × 15 mL). The combined organic layers were dried over anhydrous MgSO₄. The volatile solvents were removed by rotary evaporation. The residue was distilled under reduced pressure (0.5 Torr, b.p. 130–132 °C), giving 2,2-diphenylpent-4-enylamine as pale yellow, viscous oil 7.88g (70.0%). ¹H NMR (500 MHz, CDCl₃): δ = 7.35–7.30 (m, 4H, aryl), 7.24–7.18 (m, 6H, aryl), 5.48–5.38 (m, 1H, CH), 5.07 (d, ²J(H,H) = 17.0 Hz, 1H, CH=CH₂), 5.01 (d, ³J(H,H) = 12.0 Hz, 1H, CH=CH₂), 3.36 (s, 2H, CH₂–NH₂), 2.94 (d, ³J(H,H) = 6 Hz, 2H, CH₂–CH), 0.85 (br s, 2H, NH₂); ¹³C{¹H} NMR (125 MHz, CDCl₃): δ = 147.3, 135.6, 128.7, 129.0, 126.5, 118.3, 51.8, 48.9, 41.6.

(1-Allylcyclohexyl)-methanamine (53).¹⁰⁰ To a solution of diisopropyl amine (15.71 g, 155.3 mmol) in THF (80 mL) was added *n*BuLi (62 mL, 155.3 mmol) slowly at -78°C . The resulting mixture was stirred at 0°C for 1 hr. The reaction mixture was allowed to cool to -78°C before cyclohexanecarbonitrile was added slowly (17.12 g, 155.3 mmol). The resulting mixture was allowed to warm to -40°C and was stirred at that temperature for 1 hr. The temperature was brought down to -78°C before allyl bromide was added dropwise (38.73 g, 310.5 mmol). The resulting mixture was allowed to warm to room temperature and was stirred overnight. The reaction was quenched by adding a saturated aqueous NH_4Cl solution (5 mL), then was diluted with CH_2Cl_2 (50 mL). The organic layers were washed with water (3×50 mL), dried over anhydrous MgSO_4 , and was concentrated by using rotary evaporation. The residue was distilled under reduced pressure (5 Torr, b.p. $88-90^{\circ}\text{C}$), giving 1-allylcyclohexanecarbonitrile as a clear liquid (19.46 g, 84%). To a suspension of LAH (7.86 g, 201.0 mmol) in Et_2O (120 mL) was added dropwise 1-allylcyclohexanecarbonitrile (15.00 g, 100.5 mmol) at 0°C in a period of 20 minutes. The reaction mixture was allowed to warm to room temperature and was heated to reflux overnight. The reaction mixture was allowed to cool to 0°C before it was quenched by cautiously adding of water (8 mL), NaOH solution (25%, 8 mL), and water (40 mL). To the content was added Et_2O (50 mL) and the mixture was stirred at room temperature for 2 hrs. The solid was filtered off. The product was extracted with Et_2O ($2 \times 20\text{mL}$), which was then dried over anhydrous MgSO_4 . The volatile solvent was evaporated by rotary evaporation before the content was distilled under reduced pressure (5.0 torr, $82-84^{\circ}\text{C}$), giving (1-allylcyclohexyl)-methanamine as clear liquid (13.52 g,

88%). ^1H NMR (400 MHz, CDCl_3): δ = 5.79 (m, 1H, $\text{CH}=\text{CH}_2$), 5.08–5.02 (m, 2H, $\text{CH}=\text{CH}_2$), 2.52 (s, 2H), 2.06 (m, 2H), 1.45–1.23 (m, 10H), 0.97 (br s, 2H, NH_2); $^{13}\text{C}\{^1\text{H}\}$ NMR (100 MHz, CDCl_3): δ = 135.4, 116.8, 49.2, 40.2, 37.3, 33.4, 26.7, 21.8.

2,2-Dimethyl-pent-4-enylamine (55).¹⁰⁰ In a procedure similar to that for (1-allylcyclohexyl)-methylamine (**53**), 2,2-dimethyl-pent-4-enylamine (**55**) was obtained as a clear liquid (5.32 g, 45% after 2 steps, b.p. 143–145 °C under atm pressure). ^1H NMR (400 MHz, CDCl_3): δ = 5.85–5.74 (m, 1H, $\text{CH}=\text{CH}_2$), 5.04–4.97 (m, 2H, $\text{CH}=\text{CH}_2$), 2.45 (s, 2H), 1.97 (m, 2H), 1.18 (s, 6H, $\text{C}(\text{CH}_3)_2$); $^{13}\text{C}\{^1\text{H}\}$ NMR (100 MHz, CDCl_3): δ = 135.5, 117.5, 52.6, 44.1, 34.9, 24.8.

***N*-benzyl-*N*-(2,2-dimethylpent-4-enyl)amine (65).**¹⁰⁰ A solution of benzaldehyde (3.92 g, 36.2 mmol) in methanol (50 mL) was added 2,2-dimethyl-pent-4-enylamine (**55**) (3.92 g, 34.5 mmol) at room temperature. The reaction mixture was stirred for 3.5 hrs before it was treated with NaBH_4 (2.00 g, 51.7 mmol) in three portions and was stirred overnight. The reaction was quenched with water (10 mL) and a solution of 1M NaOH (5 mL). The product was extracted with CH_2Cl_2 (3×25 mL). The organic layers were dried over anhydrous MgSO_4 and were evaporated by rotary evaporation. The residue was distilled under reduced pressure (0.5 torr, 175–180 °C), giving *N*-benzyl-*N*-(2,2-dimethylpent-4-enyl)amine as a clear liquid (3.50 g, 50%). ^1H NMR (500 MHz, CDCl_3): δ = 7.39–7.25 (m, 5H, Ph), 5.84–5.75 (m, 1H, $\text{CH}=\text{CH}_2$), 5.04–4.99 (m, 2H, $\text{CH}=\text{CH}_2$), 2.41 (s, 2H), 2.10–2.03 (m, 2H), 0.92 (s, 6H, $\text{C}(\text{CH}_3)_2$); $^{13}\text{C}\{\text{H}\}$ NMR (125 MHz, CDCl_3): δ = 135.8, 128.5, 127.2, 117.0, 59.7, 54.8, 44.9, 34.4, 25.7.

***N*-benzyl-*N*-(2,2-diphenylpent-4-enyl)amine (67).**¹⁰⁰ In a procedure similar to that for *N*-benzyl-*N*-(2,2-dimethylpent-4-enyl)amine (65), *N*-benzyl-*N*-(2,2-diphenylpent-4-enyl)amine (67) was obtained as a viscous oil, but turning into a waxy solid upon standing at $-30\text{ }^{\circ}\text{C}$ in the fridge of the glovebox (6.85 g, 70%, b.p $175\text{--}180\text{ }^{\circ}\text{C}$ at 0.5 torr). ^1H NMR (500 MHz, CDCl_3): δ = 7.31–7.12 (m, 15H, Ph), 5.37–5.30 (m, 1H, $\text{CH}=\text{CH}_2$), 5.02–4.92 (m, 2H, $\text{CH}=\text{CH}_2$), 3.73 (s, 2H), 3.22–3.19 (m, 2H), 3.12–3.02 (m, 2H), 0.95 (br s, 1H, NHBn). $^{13}\text{C}\{^1\text{H}\}$ NMR (125 MHz, CDCl_3): δ = 147.9, 140.8, 135.3, 129.1, 128.5, 126.9, 126.1, 117.8, 55.4, 54.3, 50.3, 41.7.

7.6 Procedures for Catalytic Hydroamination/Cyclization of Aminoalkenes

General procedure for catalytic asymmetric hydroamination/cyclization of aminoalkenes. In a glovebox, a screw cap NMR tube was charged with aminoalkene (0.03–0.10 mmol), ferrocene (3.0 mg, 16.1 μmol), C_6D_6 (to give a total volume of 0.5 mL), and catalysts (0.60–3.0 μmol , 0.060 M in C_6D_6). The NMR tube was capped, immediately removed from the glovebox, and shaken well to dissolve ferrocene. The progress of cyclization was monitored by ^1H NMR spectroscopy by following the disappearance of the olefinic signals of the substrate relative to the internal standard ferrocene. The NMR tube was heated in a thermostatic oil bath, if required. The time was recorded after a conversion of at least 95% was achieved.

General procedure for preparing Mosher amides. The amine (0.01–0.03 mmol) was dissolved in CDCl_3 , C_6D_6 , or toluene- d_8 (0.5 mL) in an NMR tube. Hünig's base (2.5 equiv. with respect to amine and (*R*)-Mosher chloride (1.5 equiv. with respect to amine) were added. Enantiomeric excess was determined by ^{19}F NMR at 60–110 °C.

General procedure for determining enantiomeric excess of *N*-benzyl hydroamination product via debenzylation/Mosher amide formation sequence. This procedure is similar to that for determining enantiomeric excess of *N*-benzyl hydroamination product of intermolecular hydroamination reaction, *via* debenzylation/Mosher amide formation sequence. A completed reaction mixture containing *N*-benzyl hydroamination product (0.07 mmol) was transferred to a 25 mL round bottom flask and the volatiles were evaporated. The residue was dissolved in absolute ethanol (2 mL) and to that were added ammonium formate (40 mg, 0.62 mmol) and 10% Palladium on charcoal (20 mg, 0.019 mmol). The content was stirred at reflux for 30 minutes. The solid was filtered off and the filtrate was treated with 4M HCl (1 mL). The volatiles were removed in *vacuo* and the residue was dissolved in distilled water (5 mL) which was then evaporated under reduced pressure. The residue was dissolved in CDCl_3 or C_6D_6 (0.6 mL) which was allowed to pass through a short pad of celite. The Mosher amide was prepared by the procedure, described above, and enantiomeric excess was determined by ^{19}F NMR at 60–80 °C.

General procedure for kinetic catalytic hydroamination/cyclization reactions. In a glovebox, a screw cap NMR tube were charged with enantiopure α -substituted

aminopentene solution (2.0% in C₆D₆, 200–375 μ L, 58.0–74.0 μ mol), ferrocene (3.0 mg), C₆D₆ (to give a total volume of 500 μ L), and catalyst (2.0 mol%, 1.16–1.48 μ mol, 21–24 μ L stock solution in C₆D₆). The tube was placed in either 400 or 500 MHz NMR thermostatic probe with temperature of 25–70 °C and an arrayed experiment was set up to record ¹H NMR spectra automatically in time intervals (30 sec., 1 min., 3 min., 5 min., or 10 min.). The conversion was determined based on the disappearance of the olefinic signals of the substrate relative to the internal standard ferrocene. The linear part of the data was fit by least square analysis and $k_{obs.}$ was determined from the slope α of a plot of concentration of amine (M) versus time (min.).

$$k_{obs.} = -(\alpha \times 60)/[\text{cat.}] \text{ (s}^{-1}\text{M}^{-1}\text{)}$$

Hydroamination/cyclization products. Hydroamination products 2-methyl-4,4-diphenylpyrrolidine (**52**),⁵⁶ 3-methyl-2-azaspiro[4,5]decane (**54**),⁵² 2,4,4-trimethylpyrrolidine (**56**),⁴² 2-methylpyrrolidine (**58**),⁴² 2-methyl-5,5-diphenylpiperidine (**60**),¹⁷¹ 2-methyl-6,6-diphenylazepane (**62**),¹⁷² 2-benzyl-4,4-diphenylpyrrolidine (**64**),⁸² 1-benzyl-2,4,4-trimethylpyrrolidine (**66**),¹⁰⁰ 1-benzyl-2-methyl-4,4-diphenylpyrrolidine (**68**),¹⁰⁰ 2,5-dimethyl pyrrolidine,¹⁷³ 2-benzyl-5-methylpyrrolidine,³¹ 2-methyl-5-phenylpyrrolidine,³¹ and 2-cyclohexyl-5-methylpyrrolidine¹⁰⁴ are known compounds and were identified by comparison to the literature NMR spectroscopic data.

7.7 Procedures for Kinetic Resolution of α -Substituted Aminopentenes via Asymmetric Hydroamination

General procedure for NMR-scale kinetic resolution of chiral α -substituted aminopentenes. In a glove box, a screw cap NMR tube was charged with racemic aminoalkene (20.0 mg, 0.10–0.20 mmol), ferrocene (3.0 mg, 16.1 μ mol), C₆D₆ (to give a total volume of 0.5 mL), and catalysts (2.0 mol% with respect to racemic aminoalkene, 2.0–4.0 μ mol, 0.060 M in C₆D₆). The NMR tube was capped, immediately removed from the glovebox, and shaken well to dissolve ferrocene. The reaction mixture was heated in a thermostatic oil bath, if required. The conversion was monitored by ¹H NMR spectroscopy by following the disappearance of the olefinic signals of the substrate relative to the internal standard ferrocene. And the reaction was stopped after ca. 50% conversion was achieved. Aminoalkene starting material was isolated in form of hydrochloride salt and enantiomeric excess was determined, using the previously reported procedure.⁵⁸

General procedure for preparation of chiral α -substituted aminopentenes by kinetic resolution.

In a glovebox, a 20 mL vial was charged with *rac*-1-phenylpent-4-enylamine (0.80 g, 5.0 mmol) or *rac*-1-alkylpent-4-enylamine (1.50 g, 8.0–9.0 mmol), benzene (5.0 mL), and (*R*)-**39c-Y** (0.8–0.9 mL of solution, 0.20 M in benzene, 0.16–0.18 mmol, 2.0 mol%). The vial was kept at 25 °C or heated to 40 °C in the case of resolving *rac*-1-phenylpent-4-enylamine. Small aliquots (20 μ L) were syringed to NMR tubes, which was then diluted with CDCl₃ (0.55 mL), and ¹H NMR was recorded to monitor the conversion. The reaction was stopped after enantiomeric excess of the starting material

reached at least 95 %ee, determined by ^{19}F NMR of its corresponding Mosher amide at 40–65°C. The chiral α -substituted aminopentenes were purified by extraction method as reported previously.³¹

(S)-1-Methylpent-4-enylamine (S-25a). This compound was prepared by kinetic resolution using (S)-**39c-Y** at 25 °C, c. a. 52% conversion after 9.0 hours. The enantioenriched starting material was recovered as colorless oil (38% yield, b.p. 114–116 °C at 760 Torr, 95% ee). ^1H and ^{13}C NMR spectra are in agreement with those of *rac*-1-methylpent-4-enylamine.¹⁷⁰

(S)-1-Benzylpent-4-enylamine (S-25b). This compound was prepared by kinetic resolution using (R)-**39c-Y** at 25 °C, c. a. 57% conversion after 22.5 hours. The enantioenriched starting material was recovered as colorless oil (40% yield, 95% ee). ^1H and ^{13}C NMR spectra are in agreement with those of *rac*-1-benzylpent-4-enylamine.³¹

(S)-1-Phenylpent-4-enylamine (S-25c). This compound was prepared by kinetic resolution using (R)-**39c-Y** at 40 °C, c. a. 54% conversion after 31.0 hours. The enantioenriched starting material was recovered as colorless oil (40% yield, 97% ee). ^1H and ^{13}C NMR spectra are in agreement with those of *rac*-1-phenylpent-4-enylamine.³¹

(S)-1-Cyclohexylpent-4-enylamine (S-25d). This compound was prepared by kinetic resolution using (R)-**39c-Y** at 25 °C, c. a. 77% conversion after 9.5 hours. The enantioenriched starting material was recovered as colorless oil (18% yield, 95% ee). ^1H

and ^{13}C NMR spectra are in agreement with those of *rac*-1-cyclohexylpent-4-enylamine.¹⁰⁴

7.8 Procedures for Asymmetric Intermolecular Hydroamination

General procedure for NMR-scale intermolecular hydroamination reactions. In the glovebox, a screw cap NMR tube was charged with an appropriate amine (0.2 mmol), alkene (3 mmol) and a solution of catalyst (0.1 M in C_6D_6 or toluene- d_8 , 0.1 mL, 10.0 μmol , 5 mol%). The tube was then sealed, removed from the glovebox and placed into the thermostated oil bath. The progress of the reaction was monitored by ^1H NMR spectroscopy. After completion of the reaction, the mixture was concentrated in vacuo and purified by column chromatography on a 3 cm height pad of silica or alumina (hexanes/EtOAc, 100:06; pentane/EtOAc, 100:0.6; or CH_2Cl_2 /7 M NH_3 in MeOH 100:1).

Determination of enantiomeric excess through diastereomeric salt formation (Method A). The isolated hydroamination product (25 μmol) and (*R*)-*O*-acetylmandelic acid (5.8 mg, 30 μmol) were dissolved in CDCl_3 (0.6 mL). The solution was allowed to stay 30 minutes at room temperature, and then the ^1H NMR spectra was recorded. Integration of CH_3CHNH signals of diastereomeric salts afforded the enantiomeric excess value for the hydroamination product.

Determination of enantiomeric excess via debenzylation/Mosher amide formation sequence (Method B). The isolated *N*-benzyl hydroamination product (0.03 mmol) was

dissolved in absolute ethanol (2 mL). Ammonium formate (32 mg, 0.5 mmol) and 10% Palladium on charcoal (11 mg, 0.01 mmol) were added, and the mixture was stirred at reflux for 30 min. The precipitate was filtered off, and the filtrate was treated with 1M HCl (2 mL). The volatiles were removed *in vacuo*, the residue was dissolved in water (5 mL) and then water was removed under reduced pressure. The residue was then dissolved in CDCl₃ or C₆D₆ (0.6 mL) and filtered through a short pad of celite into the NMR tube containing (*R*)-Mosher chloride (10 mg, 0.04 mmol) and Hünig's base (26 mg, 0.2 mmol). A ¹⁹F NMR spectrum was then taken to determine the enantiomeric excess.

Intermolecular hydroamination products.

(*R*)-*N*-Benzylheptan-2-amine¹⁷⁴ (**69**) was prepared from 1-heptene and benzylamine according to Table 5-2, entry 1. The product was purified by column chromatography on alumina (hexanes/EtOAc 100:0.6), giving a colorless oil, 62% yield, 57% ee. ¹H NMR (400 MHz, CDCl₃): δ = 7.32–7.30 (m, 4H, aryl-H) 7.25–7.21 (m, 1H, aryl-H), 3.82 (d, ²*J*(H,H) = 13.0 Hz, 1H, PhCH₂NH), 3.73 (d, ²*J*(H,H) = 13.0 Hz, 1H, PhCH₂NH), 2.68 (sext, ³*J*(H,H) = 6.2 Hz, 1H, CHNH), 1.50–1.41 (m, 1H, CH₂) 1.34–1.23 (m, 8H, CH₂ and NH), 1.07 (d, ³*J*(H,H) = 6.2 Hz, 3H, CH₃CHNH), 0.89 (t, ³*J*(H,H) = 6.9 Hz, 3H, CH₃CH₂); ¹³C{¹H} NMR (100 MHz, CDCl₃): δ = 140.9 (C_{ipso}), 128.4, 128.1, 126.8 (aryl), 52.5 (CH(CH₃)NH), 51.4 (CH₂NH), 37.1 (CH₂), 32.1 (CH₂), 25.7 (CH₂), 22.7 (CH₂), 20.3 (CH₃CHNH), 14.1 (CH₃CH₂). ¹⁹F NMR of Mosher amide of heptan-2-amine (470 MHz, C₆D₆, 60 °C): δ = –69.35 (*S*-isomer, minor), –69.42 (*R*-isomer, major).

(*R*)-*N*-Benzyloctan-2-amine¹⁷⁵ (**70**) was prepared from 1-octene and benzylamine according to Table 5-1, entry 11. The product was purified by column chromatography on alumina (hexanes/EtOAc 100:0.4), giving a colorless oil, 56% yield, 40% ee. ¹H NMR (500 MHz, CDCl₃): δ = 7.33–7.30 (m, 4H, aryl-H), 7.25–7.21 (m, 1H, aryl-H), 3.82 (d, ²*J*(H,H) = 13.0 Hz, 1H, PhCH₂NH), 3.73 (d, ²*J*(H,H) = 13.0 Hz, 1H, PhCH₂NH), 2.68 (sext, ³*J*(H,H) = 6.3 Hz, 1H, CHNH), 1.50–1.46 (m, 2H, CH₂ and NH), 1.33–1.25 (m, 9H; CH₂), 1.07 (d, ³*J*(H,H) = 6.4 Hz, 3H, CH₃CHNH), 0.87 (t, ³*J*(H,H) = 6.8 Hz, 3H, CH₃CH₂); ¹³C{¹H} NMR (125 MHz, CDCl₃): δ = 140.9 (C_{ipso}), 128.4, 128.1, 126.8 (aryl), 52.5 (CH(CH₃)NH), 51.4 (CH₂NH), 37.1 (CH₂), 31.9 (CH₂), 29.5 (CH₂), 26.0 (CH₂), 22.6 (CH₂), 20.3 (CH₃CHNH), 14.1 (CH₃CH₂). ¹⁹F NMR of Mosher amide of octan-2-amine (470 MHz, C₆D₆, 60 °C): δ = –69.25 (*S*-isomer, minor), –69.32 (*R*-isomer, major).

(*R*)-*N*-Benzyl-4-phenylbutan-2-amine¹⁷⁴ (**71**) was prepared from 4-phenyl-1-butene and benzylamine according to Table 5-2, entry 6. The product was purified by column chromatography on silica (CH₂Cl₂/7 M NH₃ in MeOH 100:1), giving a colorless oil, 68% yield, 67% ee. ¹H NMR (500 MHz, CDCl₃): δ = 7.34–7.22 (m, 7H, aryl-H), 7.19–7.16 (m, 3H, aryl-H), 3.82 (d, ²*J*(H,H) = 13.0 Hz, 1H, PhCH₂NH), 3.73 (d, ²*J*(H,H) = 12.9 Hz, 1H, PhCH₂NH), 2.69 (sext, ³*J*(H,H) = 6.3 Hz, 1H, CHNH), 2.70–2.61 (m, 2H), 1.85–1.78 (m, 1H), 1.71–1.64 (m, 1H), 1.49 (br s, 1H, NH), 1.14 (d, ³*J*(H,H) = 6.4 Hz, 3H, CH₃CHNH); ¹³C{¹H} NMR (125 MHz, CDCl₃): δ = 142.5 (C_{quart}), 140.8 (C_{quart}), 128.35, 128.32, 128.30, 128.1, 126.8, 125.7 (aryl), 52.0 (CH(CH₃)NH), 51.3 (CH₂NH),

38.7 (CH₂), 32.3 (CH₂), 20.4 (CH₃). ¹⁹F NMR of Mosher amide of octan-2-amine (470 MHz, C₆D₆, 60 °C): δ = -69.22 (*S*-isomer, minor), -69.35 (*R*-isomer, major).

(*R*)-*N*-(4-Phenylbutan-2-yl)cyclopentanamine¹⁵⁶ (**72**) was prepared from 4-phenyl-1-butene and cyclopentanamine according to Table 5-2, entry 11. The product was purified by column chromatography on silica (CH₂Cl₂/7 M NH₃ in MeOH 100:1), giving a colorless oil, 37% yield, 51% ee. ¹H NMR (400 MHz, CDCl₃): δ = 7.29–7.25 (m, 3H, aryl-H), 7.19–7.15 (m, 2H, aryl-H), 3.15 (quint, ³*J*(H,H) = 7.0 Hz, 1H, (CH₂)₄CHNH), 2.71 (sext, ³*J*(H,H) = 6.3 Hz, 1H, CHNH), 2.67–2.58 (m, 2H), 1.88–1.72 (m, 3H), 1.70–1.61 (m, 3H), 1.56–1.45 (m, 2H), 1.28–1.18 (m, 3H), 1.09 (d, ³*J*(H,H) = 6.3 Hz, 3H, CH₃CHNH); ¹³C{¹H} NMR (100 MHz, CDCl₃): δ = 142.5 (C_{ipso}), 129.31, 129.29, 128.31, 125.7 (aryl), 56.9 ((CH₂)₄CHNH), 51.0 (CH(CH₃)NH), 39.0 (CH₂), 33.9 (CH₂), 33.4 (CH₂), 32.4 (CH₂), 23.86 (CH₂), 23.84 (CH₂), 20.8 (CH₃).

(*R*)-*N*-(*p*-Methoxybenzyl)-4-phenylbutan-2-amine¹⁷⁶ (**73**) was prepared from 4-phenyl-1-butene and *p*-methoxy benzylamine according to Table 5-2, entry 12. The product was purified by column chromatography on silica (CH₂Cl₂/7 M NH₃ in MeOH 100:1), giving a colorless oil, 31% yield, 61% ee. ¹H NMR (400 MHz, CDCl₃): δ = 7.29–7.15 (m, 7H, aryl-H), 6.85 (d, ³*J*(H,H) = 8.6 Hz, 2H, aryl-H), 3.79 (s, 3H, CH₃O), 3.76 (d, ²*J*(H,H) = 12.5 Hz, 1H, ArCH₂NH), 3.66 (d, ²*J*(H,H) = 12.5 Hz, 1H, ArCH₂NH), 2.72 (sext, ³*J*(H,H) = 6.3 Hz, 1H, CHNH), 2.68–2.59 (m, 2H), 1.84–1.76 (m, 1H), 1.70–1.61 (m, 1H), 1.43 (br s, 1H, NH), 1.13 (d, ³*J*(H,H) = 6.3 Hz, 3H, CH₃CHNH); ¹³C{¹H} NMR

(100 MHz, CDCl_3): δ = 158.5 (CH_3OC), 142.5 (C_{quart}), 132.9 (C_{quart}), 129.3, 128.33, 128.31, 125.7, 113.8 (aryl), 55.3 (CH_3O), 51.9 ($\text{CH}(\text{CH}_3)\text{NH}$), 50.7 (CH_2NH), 38.7 (CH_2), 32.3 (CH_2), 20.4 (CH_3). ^{19}F NMR of Mosher amide of 4-phenylbutan-2-amine (470 MHz, C_6D_6 , 60 °C): δ = -69.22 (*S*-isomer, major), -69.35 (*R*-isomer, minor).

Chapter 8

References

- (1) Ricci, A. *Modern Amination Methods*; Wiley-VCH: Weinheim, Germany, 2000.
- (2) Ricci, A. *Amino Group Chemistry: From Synthesis to the Life Sciences*; Wiley-VCH: Weinheim, Germany, 2008.
- (3) *Chiral Amine Synthesis: Methods, Developments and Applications*; Nugent, T, Ed.; Wiley-VCH: Weinheim, Germany, 2010.
- (4) King, A. G.; Meinwald, J. *Chem. Rev.* **1996**, 96, 1105.
- (5) Calayden, J.; Greeves, N.; Warren, S.; Wothers, P. *Organic Chemistry*; Oxford University Press Inc, 2001.
- (6) Smith, M. B.; March, J. *March's Advanced Organic Chemistry (6th Ed)*; Wiley: New York, 2007.
- (7) Seayad, J.; Tillack, A.; Hartung, C. G.; Beller, M. *Adv. Synth. Catal.* **2002**, 344, 795.
- (8) Müller, T. E.; Beller, M. *Chem. Rev.* **1998**, 98, 675.
- (9) Müller, T. E.; Hultzs, K. C.; Yus, M.; Foubelo, F.; Tada, M. *Chem. Rev.* **2008**, 108, 3795.
- (10) Reznichenko, A. L.; Hultzs, K. C. *Top. Organomet. Chem.* **2012**, 43, 51.
- (11) Pohlki, F.; Doye, S. *Chem. Soc. Rev.* **2003**, 32, 104.
- (12) Hong, S.; Marks, T. J. *Acc. Chem. Res.* **2004**, 37, 673.
- (13) Hartwig, J. F. *Pure Appl. Chem.* **2004**, 76, 507.
- (14) Severin, R.; Doye, S. *Chem. Soc. Rev.* **2007**, 36, 1407.
- (15) Reznichenko, A. L.; Hultzs, K. C. In *Organic Reactions*; Denmark, S. E., Charette, A., Eds.; John Wiley & Son, Inc.: Hoboken, NJ, 2016; Vol. 88, p 1.
- (16) Zhang, X.; Tobisch, S.; Hultzs, K. C. *Chem. Eur. J.* **2015**, 21, 7841.
- (17) Straub, T.; Haskel, A.; Neyroud, T. G.; Kapon, M.; Botoshansky, M.; Eisen, M. S. *Organometallics* **2001**, 20, 5017.
- (18) Haggins, J. *Chem. Eng. News.* **1993**, 71 (20), 23.
- (19) Brunet, J. J.; Neibecker, D.; Niedercorn, F. *J. Mol. Catal.* **1989**, 49, 235.
- (20) Johns, A. M.; Sakai, N.; Ridder, A.; Hartwig, J. F. *J. Am. Chem. Soc.* **2006**, 128, 9306.
- (21) Steinborn, D.; Taube, R. *Z. Chem.* **1986**, 26, 349.
- (22) Taube, R. *Reaction with Nitrogen Compounds: Hydroamination*; 2 ed.; Wiley-VCH: Weinheim, 2002; Vol. 1.
- (23) Bozel, J. J.; Hegedus, L. S.; Louis, S. *J. Org. Chem.* **1981**, 46, 2561.
- (24) Kawatsura, M.; Hartwig, J. F. *Organometallics* **2001**, 20, 1960.
- (25) Hultzs, K. C. *Adv. Synth. Catal.* **2005**, 347, 367.
- (26) Hultzs, K. C. *Org. Biomol. Chem.* **2005**, 3, 1819.
- (27) Reznichenko, A. L.; Hultzs, K. C. *Struct. Bond.* **2010**, 137, 1.

- (28) Reznichenko, A. L.; Hultzs, K. C. In *Chiral Amine Synthesis: Methods, Developments and Applications*; 1st ed.; Nugent, T., Ed.; Wiley-VCH: 2010, p 341.
- (29) Roesky, P. W.; Müller, T. E. *Angew. Chem. Int. Ed.* **2003**, 42, 2708.
- (30) Gribkov, D. V.; Hultzs, K. C.; Hampel, F. *Chem. Eur. J.* **2003**, 9, 4796.
- (31) Gribkov, D. V.; Hultzs, K. C.; Hampel, F. *J. Am. Chem. Soc.* **2006**, 128, 3748.
- (32) O'Shaughnessy, P. N.; Gillespie, K. M.; Knight, P. D.; Munslow, I.; Scott, P. *Dalton Trans.* **2004**, 2251.
- (33) O'Shaughnessy, P. N.; Scott, P. *Tetrahedron: Asymmetry* **2003**, 14, 1979.
- (34) Kim, H.; Kim, Y. K.; Shim, J. H.; Kim, M.; Han, M.; Livinghouse, T.; Lee, P. H. *Adv. Synth. Catal.* **2006**, 348, 2609.
- (35) Heck, R.; Schulz, E.; Collin, J.; Carpentier, J. F. *J. Mol. Catal. A* **2007**, 268, 163.
- (36) O'Shaughnessy, P. N.; Knight, P. D.; Morton, C.; Gillespie, K. M.; Scott, P. *Chem. Commun.* **2003**, 1770.
- (37) Kim, J. Y.; Livinghouse, T. *Org. Lett.* **2005**, 7, 1737.
- (38) Gribkov, D. V.; Hampel, F.; Hultzs, K. C. *Eur. J. Inorg. Chem.* **2004**, 4091.
- (39) Hannedouche, J.; Schulz, E. *Chem. Eur. J.* **2013**, 19, 4972.
- (40) Gagné, M. R.; Marks, T. J. *J. Am. Chem. Soc.* **1989**, 111, 4108.
- (41) Li, Y.; Marks, T. J. *J. Am. Chem. Soc.* **1996**, 118, 9295.
- (42) Gagné, M. R.; Stern, C. L.; Marks, T. J. *J. Am. Chem. Soc.* **1992**, 114, 275.
- (43) Gagné, M. R.; Brard, L.; Conticello, V. P.; Giardello, M. A.; Stern, C. L.; Marks, T. J. *Organometallics* **1992**, 11, 2003.
- (44) Giardello, M. A.; Conticello, V. P.; Brard, L.; Gagné, M. R.; Marks, T. J. *J. Am. Chem. Soc.* **1994**, 116, 10241.
- (45) Giardello, M. A.; Conticello, V. P.; Brard, L.; Sabat, M.; Rheingold, A. L.; Stern, C. L.; Marks, T. J. *J. Am. Chem. Soc.* **1994**, 116, 10212.
- (46) Ryu, J.-S.; Marks, T. J.; McDonald, F. E. *J. Org. Chem.* **2004**, 69, 1038.
- (47) Douglass, M. R.; Ogasawara, M.; Hong, S.; Metz, M. V.; Marks, T. J. *Organometallics* **2002**, 21, 283.
- (48) Vitanova, D. V.; Hampel, F.; Hultzs, K. C. *J. Organomet. Chem.* **2007**, 692, 4690.
- (49) Hong, S.; Marks, T. J. *J. Am. Chem. Soc.* **2002**, 124, 7886.
- (50) Riegert, D.; Collin, J.; Daran, J.-D.; Fillebeen, T.; Schulz, E.; Lyubov, D.; Fukin, G.; Trifonov, A. *Eur. J. Inorg. Chem.* **2007**, 1159.
- (51) Riegert, D.; Collin, J.; Meddour, A.; Schulz, E.; Trifonov, A. *J. Org. Chem.* **2006**, 71, 2514.
- (52) Collin, J.; Daran, J.-D.; Jacquet, O.; Schulz, E.; Trifonov, A. *Chem. Eur. J.* **2005**, 11, 3455.
- (53) Collin, J.; Daran, J.-D.; Schulz, E.; Trifonov, A. *Chem. Commun.* **2003**, 3048.
- (54) Aillaud, I.; Wright, K.; Collin, J.; Schulz, E.; Mazaleyrat, J.-P. *Tetrahedron: Asymmetry* **2008**, 19, 82.
- (55) Aillaud, I.; Collin, J.; Duhayon, C.; Guillot, R.; Lyubov, D.; Schulz, E.; Trifonov, A. *Chem. Eur. J.* **2008**, 14, 2189.
- (56) Hong, S.; Tian, S.; Metz, M. V.; Marks, T. J. *J. Am. Chem. Soc.* **2003**, 125, 14768.
- (57) Yu, X.; Marks, T. J. *Organometallics* **2007**, 26, 365.

- (58) Gribkov, D. V.; Hultsch, K. C. *Chem. Commun.* **2004**, 730.
- (59) Reznichenko, A. L.; Hultsch, K. C. *Organometallics* **2013**, 32, 1394.
- (60) Johnson, J. S.; Evans, D. A. *Acc. Chem. Res.* **2000**, 33, 325.
- (61) Manna, K.; Kruse, M. L.; Sadow, A. D. *ACS Catal.* **2011**, 1, 1637.
- (62) McKnight, A. L.; Waymouth, R. M. *Chem. Rev.* **1998**, 98, 2587.
- (63) Alt, H. G.; Köppl, A. *Chem. Rev.* **2000**, 100, 1205.
- (64) Doye, S. *Synlett* **2004**, 1653.
- (65) Bytschkov, I.; Doye, S. *Eur. J. Org. Chem.* **2003**, 935.
- (66) Odom, A. L. *Dalton Trans.* **2005**, 225.
- (67) Gribkov, D. V.; Hultsch, K. C. *Angew. Chem. Int. Ed.* **2004**, 44, 5542.
- (68) Wood, M. C.; Leitch, D. C.; Yeung, C. S.; Kozak, J. A.; Schafer, L. L. *Angew. Chem. Int. Ed.* **2007**, 46, 354.
- (69) Kim, H.; Lee, P. H.; Livinghouse, T. *Chem. Commun.* **2005**, 5205.
- (70) Knight, P. D.; Munslow, I.; O'Shaughnessy, P. N.; Scott, P. *Chem. Commun.* **2004**, 894.
- (71) Gott, A. L.; Clarke, A. J.; Clarkson, G. J.; Scott, P. *Organometallics* **2007**, 26, 1729.
- (72) Reznichenko, A. L.; Hultsch, K. C. *Organometallics* **2010**, 29, 24.
- (73) Kissounko, D. A.; Epshteyn, A.; Fettingner, J. C.; Sita, L. R. *Organometallics* **2006**, 25, 1076.
- (74) Wood, M. C.; Leitch, D. C.; Yeung, C. S.; Kozak, J. A.; Schafer, L. L. *Angew. Chem., Int. Ed.* **2009**, 48, 6938.
- (75) Walsh, P. J.; Baranger, A. M.; Bergman, R. G. *J. Am. Chem. Soc.* **1992**, 114, 1708.
- (76) Baranger, A. M.; Walsh, P. J.; Bergman, R. G. *J. Am. Chem. Soc.* **1993**, 115, 2753.
- (77) Walsh, P. J.; Hollander, F. J.; Bergman, R. G. *Organometallics* **1993**, 12, 3705.
- (78) Straub, B. F.; Bergman, R. G. *Angew. Chem. Int. Ed.* **2001**, 40, 4632.
- (79) Polse, J. L.; Andersen, R. A.; Bergman, R. G. *J. Am. Chem. Soc.* **1998**, 120, 13405.
- (80) Lee, S. Y.; Bergman, R. G. *Tetrahedron* **1995**, 51, 4255.
- (81) Tobisch, S. *Chem. Eur. J.* **2007**, 13, 4884.
- (82) Bexrud, J. A.; Beard, J. D.; Leitch, D. C.; Schafer, L. L. *Org. Lett.* **2005**, 7, 1959.
- (83) Watson, D. A.; Chiu, M.; Bergman, R. G. *Organometallics* **2006**, 25, 4731.
- (84) Manna, K.; Everett, W. C.; Schoendorff, G.; Ellern, A.; Windus, T. L.; Sadow, A. *J. Am. Chem. Soc.* **2013**, 135, 7235.
- (85) Manna, K.; Ellern, A.; Sadow, A. D. *Chem. Commun.* **2010**, 339.
- (86) Motta, A.; Lanza, G.; Fragalà, I. L.; Marks, T. J. *Organometallics* **2004**, 23, 4097.
- (87) Motta, A.; Fragalà, I. L.; Marks, T. J. *Organometallics* **2006**, 25, 5533.
- (88) Pohlki, F.; Doye, S. *Angew. Chem. Int. Ed.* **2001**, 40, 2305.
- (89) Maruoka, K.; Itoh, T.; Araki, Y.; Shirasaka, T.; Yamamoto, H. *Bull. Chem. Soc. Jpn.* **1988**, 61, 2975.
- (90) Ambühl, J.; Pregosin, P. S.; Venanzi, L. M.; Consiglio, G.; Bachechi, F.; Zambonelli, L. J. *J. Organomet. Chem.* **1979**, 181, 255.
- (91) Seligson, A. L.; Trogler, W. C. *Organometallics* **1993**, 12, 744.

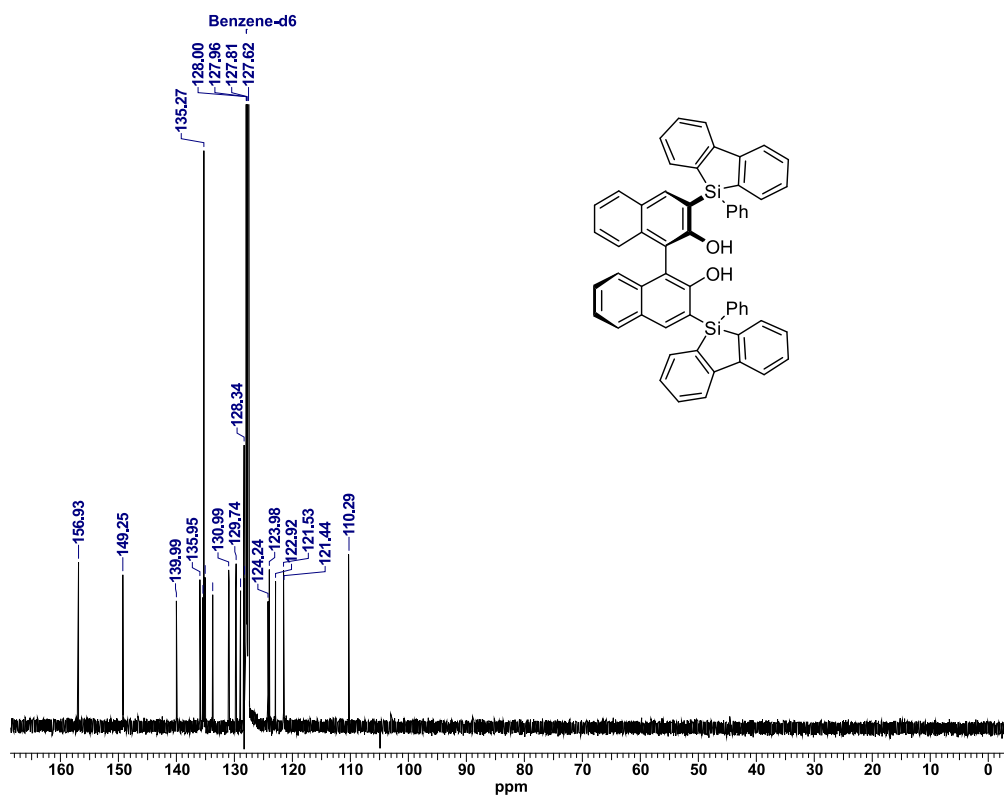
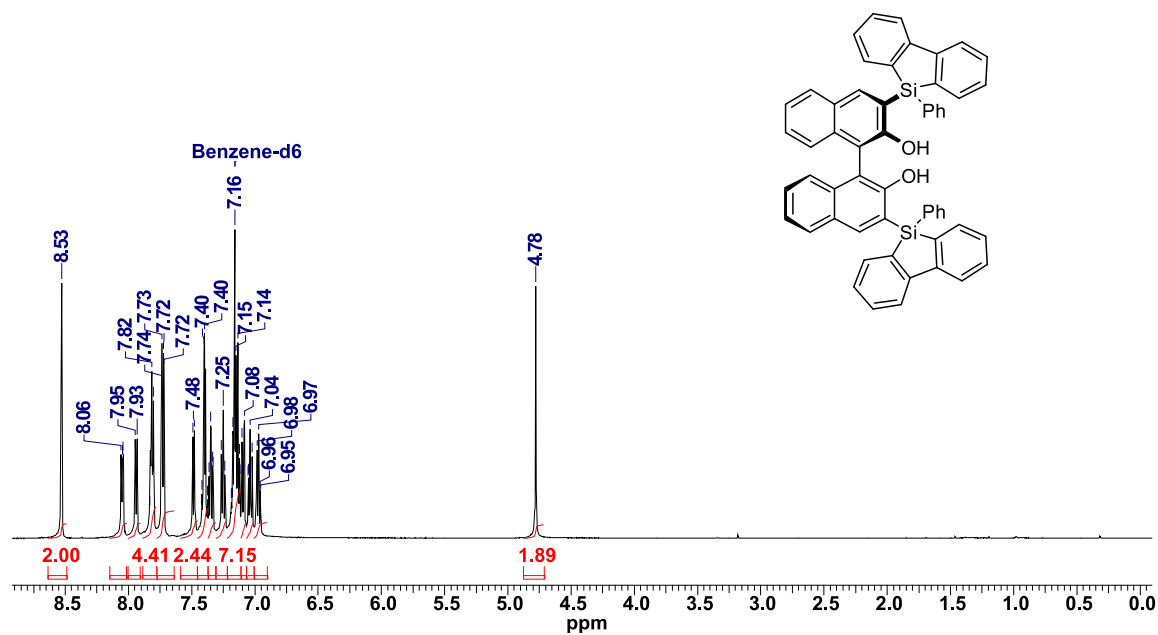
- (92) Beller, M.; Trauthwein, H.; Eichberger, M.; Breindl, C.; Herwig, J.; Müller, T. E.; Thiel, O. R. *Chem.-Eur. J.* **1999**, *5*, 1306.
- (93) Beller, M.; Trauthwein, H.; Eichberger, M.; Breindl, C.; Müller, T. E. *J. Inorg. Chem.* **1999**, 1121.
- (94) Kawatsura, M.; Hartwig, J. F. *J. Am. Chem. Soc.* **2000**, *122*, 9546.
- (95) Beller, M.; Eichberger, M.; Trauthwein, H. *Angew. Chem., Int. Ed.* **1997**, *36*, 2225.
- (96) Sappa, E.; Milone, L. *J. Organomet. Chem.* **1973**, *61*, 383.
- (97) Zhao, J.; Goldman, A. S.; Hartwig, J. F. *Science* **2005**, *307*, 1080.
- (98) Cowan, R. L.; Trogler, W. C. *Organometallics* **1987**, *6*, 2451.
- (99) Cowan, R. L.; Trogler, W. C. *J. Am. Chem. Soc.* **1989**, *111*, 4750.
- (100) Bender, C. F.; Widenhoefer, R. A. *J. Am. Chem. Soc.* **2005**, *127*, 1070.
- (101) Liu, C.; Hartwig, J. F. *J. Am. Chem. Soc.* **2008**, *130*, 1570.
- (102) Gaertzen, O.; Buchwald, S. L. *J. Org. Chem.* **2002**, *67*, 465.
- (103) Shen, X.; Buchwald, S. L. *Angew. Chem. Int. Ed.* **2010**, *49*, 564.
- (104) Reznichenko, A. L.; Hampel, F.; Hultzs, K. C. *Chem. Eur. J.* **2009**, *15*, 12819.
- (105) Li, Y.; Marks, T. J. *Organometallics* **1996**, *15*, 3770.
- (106) Nettekoven, U.; Hartwig, J. F. *J. Am. Chem. Soc.* **2002**, *124*, 1166.
- (107) Takaya, J.; Hartwig, J. F. *J. Am. Chem. Soc.* **2005**, *127*, 5756.
- (108) Dorta, R.; Egli, P.; Zürcher, F.; Togni, A. *J. Am. Chem. Soc.* **1997**, *119*, 10857.
- (109) Zhou, J.; Hartwig, J. F. *J. Am. Chem. Soc.* **2008**, *130*, 12220.
- (110) Sevov, C. S.; Zhou, J.; Hartwig, J. F. *J. Am. Chem. Soc.* **2012**, *134*, 11960.
- (111) Sevov, C. S.; Zhou, J.; Hartwig, J. F. *J. Am. Chem. Soc.* **2014**, *136*, 3200.
- (112) Wang, X.; Widenhoefer, R. A. *Organometallics* **2004**, *23*, 1649.
- (113) Qian, H.; Widenhoefer, R. A. *Org. Lett.* **2005**, *7*, 2635.
- (114) Zhang, J.; Yang, C.-G.; He, C. *J. Am. Chem. Soc.* **2006**, *128*, 1798.
- (115) Zhang, Z.; Lee, S. D.; Widenhoefer, R. A. *J. Am. Chem. Soc.* **2009**, *131*, 5372.
- (116) Taylor, J. G.; Whittall, N.; Hii, K. K. *Org. Lett.* **2006**, *8*, 3561.
- (117) Michaux, J.; Tarrasson, V.; Marque, S.; Wehbe, J.; Prim, D.; Campagne, J.-M. *Eur. J. Org. Chem.* **2007**, 2601.
- (118) Casalnuovo, A. L.; Calabrese, J. C.; Milstein, D. *J. Am. Chem. Soc.* **1988**, *110*, 6738.
- (119) Gribkov, D. V. PhD, Universität Erlangen-Nürnberg, 2005.
- (120) Gong, L.-Z.; Pu, L. *Tetrahedron Lett.* **2000**, *41*, 2327.
- (121) Cox, P. J.; Wang, W.; Sniechus, V. *Tetrahedron Lett.* **1992**, *33*, 2253.
- (122) Lerner, H.-W.; Scholz, S.; Bolte, M. *Z. Anorg. Allg. Chem.* **2001**, *627*, 1638.
- (123) Kusakawa, T.; Ando, W. *J. Organomet. Chem.* **1998**, *559*, 11.
- (124) Booi, M.; Kiers, N. H.; Teuben, J. H. *J. Organomet. Chem.* **1989**, *364*, 79.
- (125) Wayda, A. L. *Organometallics* **1985**, *4*, 1440.
- (126) Manzer, L. E. *J. Am. Chem. Soc.* **1978**, *100*, 8068.
- (127) Au-Yeung, T. L.-L.; Chan, S.-S.; Chan, A. S. C. *Adv. Synth. Catal.* **2003**, *345*, 537.
- (128) Matsunaga, S.; Kinoshita, T.; Okada, S.; Harada, S.; Shibasaki, M. *J. Am. Chem. Soc.* **2004**, *126*, 7559.
- (129) Kumaraswamy, G.; Jena, N.; Sastry, M. N. V.; Padmaja, M.; Markondaiah, B. *Adv. Synth. Catal.* **2005**, *347*, 867.

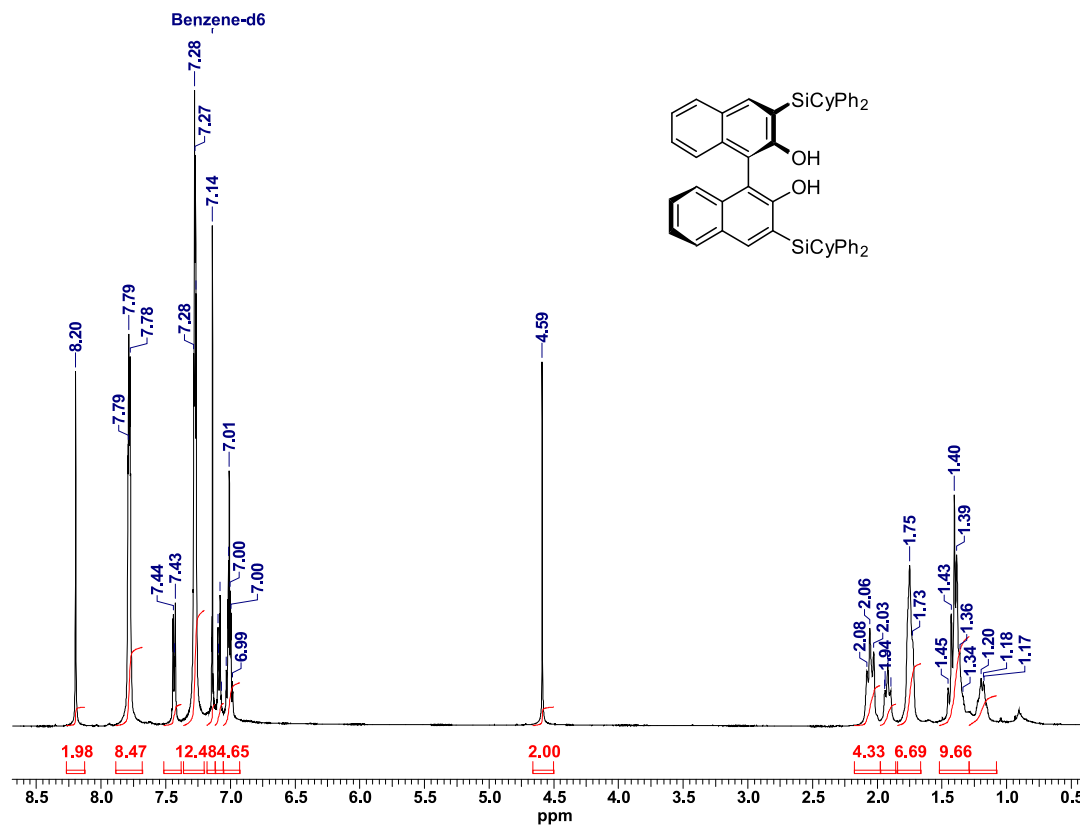
- (130) Huang, H.; Liu, X.; Chen, H.; Zheng, Z. *Tetrahedron: Asymmetry* **2005**, *16*, 693.
- (131) Kim, J. G.; Camp, E. H.; Walsh, P. J. *Org. Lett.* **2006**, *8*, 3.
- (132) Wu, K.-H.; Gau, H.-M. *J. Am. Chem. Soc.* **2006**, *128*, 14808.
- (133) Muramatsu, Y.; Harada, T. *Chem. Eur. J.* **2008**, *14*, 10560.
- (134) Jiang, J.; Yu, J.; Sun, X.-X.; Rao, Q.-Q.; Gong, L.-Z. *Angew. Chem., Int. Ed.* **2008**, *47*, 2458.
- (135) Zhou, S.; Wu, K.-H.; Chen, C.-A.; Gau, H.-M. *J. Org. Chem.* **2009**, *74*, 3500.
- (136) Aeilts, S. L.; Cefalo, D. R.; Bonitatebus, P. J.; Houser, J. H.; Hoveyda, A. H.; Schrock, R. R. *Angew. Chem., Int. Ed.* **2001**, *40*, 1452.
- (137) Chan, A. S. C.; Zhang, F.-Y.; Yip, C.-W. *J. Am. Chem. Soc.* **1997**, *119*, 4080.
- (138) Zhang, F.-Y.; Chan, A. S. C. *Tetrahedron: Asymmetry* **1997**, *8*, 3651.
- (139) Korostylev, A.; Tararov, V. I.; Fischer, C.; Monsees, A.; Börner, A. *J. Org. Chem.* **2004**, *69*, 3220.
- (140) Hu, Q.-S.; Pugh, V.; Sabat, M.; Pu, L. *J. Org. Chem.* **1999**, *64*, 7528.
- (141) O'Dell, R.; McConville, D. H.; Hofmeister, G. E.; Schrock, R. R. *J. Am. Chem. Soc.* **1994**, *116*, 3414.
- (142) Cram, D. J.; Helgeson, R. C.; Peacock, S. C.; Kaplan, L. J.; Domeier, L. A.; Moreau, P.; Koga, K.; Mayer, J. M.; Chao, Y.; Seigel, M. G.; Hoffman, D. H.; Sogah, G. D. *J. Org. Chem.* **1978**, *43*, 1030.
- (143) Rueping, M.; Nachtsheim, B. J.; Koenigs, R. M.; Ieawsuwan, W. *Chem. Eur. J.* **2010**, *16*, 13116.
- (144) Aillaud, I.; Collin, J.; Hannedouche, J.; Schulz, E. *Dalton Trans.* **2007**, 5105.
- (145) Hii, K. K. *Pure Appl. Chem.* **2006**, *78*, 341.
- (146) Jung, M. E.; Pizzi, G. *Chem. Rev.* **2005**, *105*, 1735.
- (147) Doye, S. *Science of Synthesis* **2009**, *40a*, 241.
- (148) Müller, T. E.; Beller, M. *Transition Metals for Organic Synthesis*; VCH-Wiley: Weinheim, 1998; Vol. 2.
- (149) Beller, M.; Breindl, C.; Eichberger, M.; Hartung, C. G.; Seayad, J.; Thiel, O. R.; Tillack, A.; Trauthwein, H. *Synlett* **2002**, 1579.
- (150) Ryu, J.-S.; Li, G. Y.; Marks, T. J. *J. Am. Chem. Soc.* **2003**, *125*, 12584.
- (151) Brunet, J. J.; Chu, N. C.; Diallo, O. *Organometallics* **2005**, *24*, 3104.
- (152) Khedkar, V.; Tillack, A.; Benisch, C.; Melder, J.-P.; Beller, M. *J. Mol. Catal.* **2005**, *241*, 175.
- (153) Yuen, H. F.; Marks, T. J. *Organometallics* **2009**, *28*, 2423.
- (154) Li, Y.; Marks, T. J. *J. Am. Chem. Soc.* **1998**, *120*, 1757.
- (155) Shannon, R. D. *Acta Crystallogr.* **1976**, 751.
- (156) Reznichenko, A. L. PhD, Rutgers University-New Brunswick, 2012.
- (157) Hultsch, K. C.; Gribkov, D. V.; Hampel, F. *J. Organomet. Chem.* **2005**, *690*, 4441.
- (158) Bochkarev, M. N. *Chem. Rev.* **2002**, *102*, 2089.
- (159) Smith, P. M.; Thomas, E. J. *J. Chem. Perkin Trans. 1* **1998**, 3541.
- (160) Gilman, H.; Dunn, G. E. *J. Am. Chem. Soc.* **1951**, *73*, 3404.
- (161) Sommer, L. H.; Tyler, L. J. *J. Am. Chem. Soc.* **1954**, *76*, 1030.
- (162) Nadvornik, M.; Handlir, K.; Holecek, J.; Klikorka, J.; Lycka, A. *Z. Chem.* **1980**, *20*, 343.
- (163) Nebergall, W. H.; Johnson, O. H. *J. Am. Chem. Soc.* **1949**, *71*, 4022.

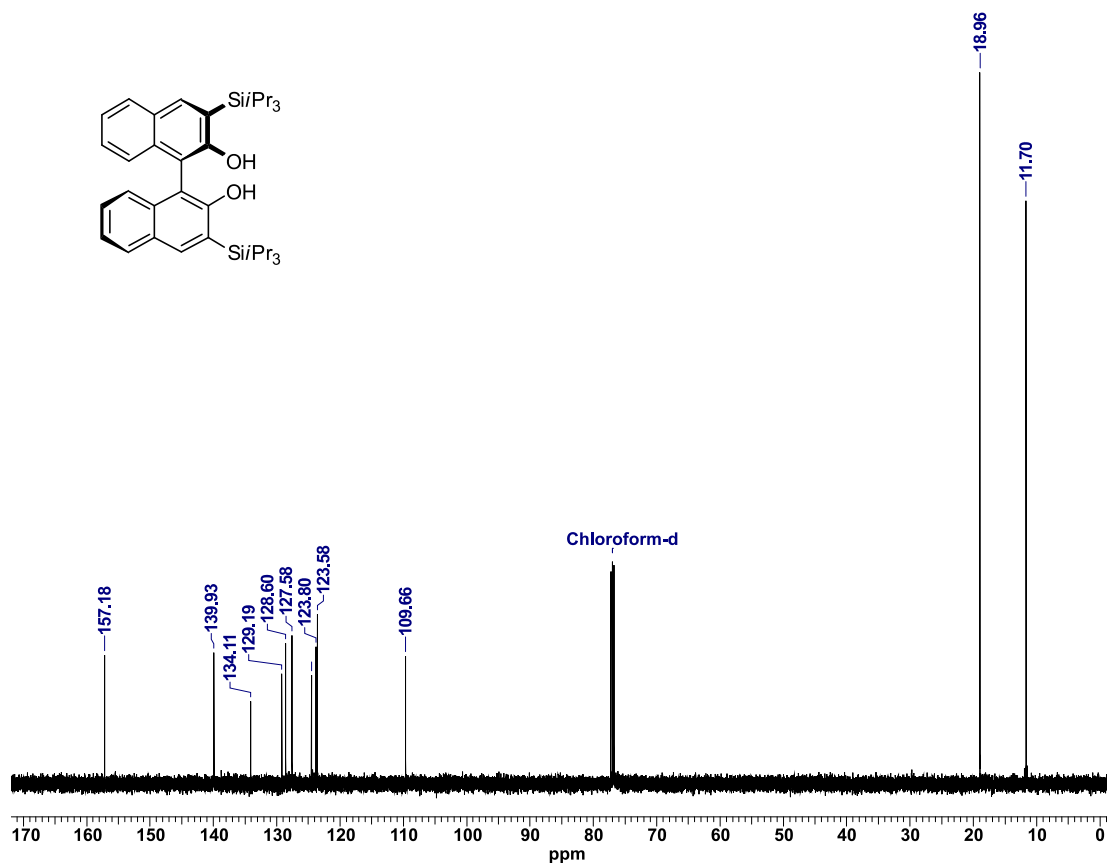
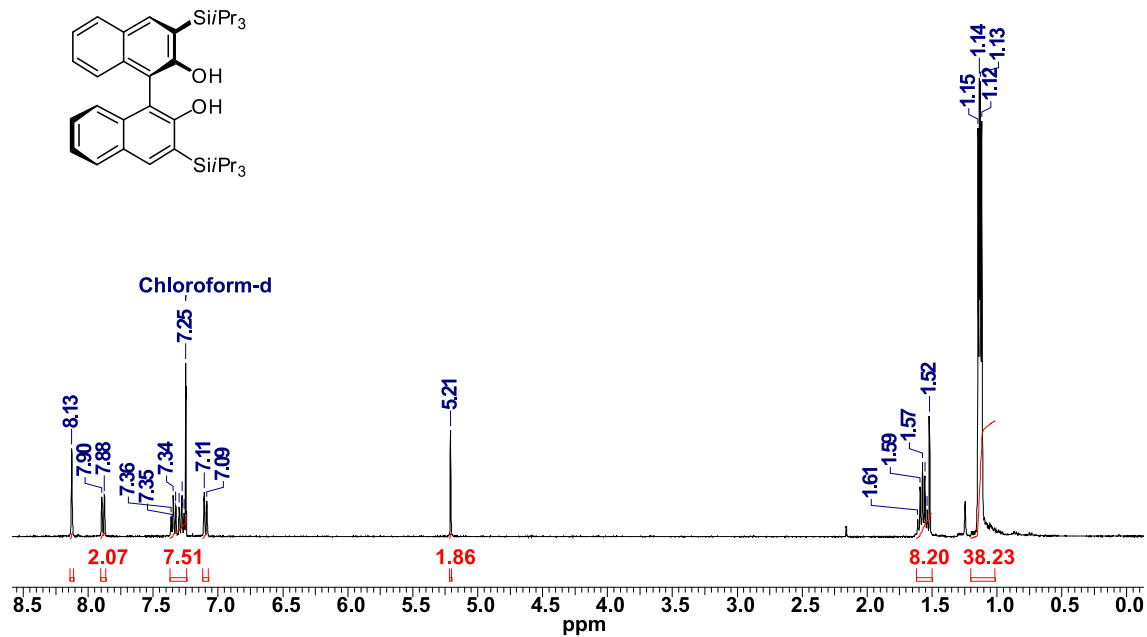
- (164) Masaoka, S.; Banno, T.; Ishikawa, M. *J. Organomet. Chem.* **2006**, 691, 182.
- (165) Masaoka, S.; Banno, T.; Ishikawa, M. *J. Organomet. Chem.* **2006**, 691, 174.
- (166) Gilman, H.; Gaj, B. J. *J. Org. Chem.* **1957**, 22, 447.
- (167) Gilman, H.; Gorsich, R. *J. Am. Chem. Soc.* **1958**, 80, 1883.
- (168) Kondo, T.; Okada, T.; Mitsudo, T.-a. *J Am. Chem. Soc.* **2002**, 124, 186.
- (169) Black, D. S. C.; Doyle, J. *Austr. J. Chem.* **1978**, 31, 2247.
- (170) Kim, J. Y.; Livinghouse, T. *Org. Lett.* **2005**, 7, 2575.
- (171) Lauterwasser, F.; Hayes, P. G.; Braese, S.; Piers, W. E.; Schafer, L. L. *Organometallics* **2004**, 23, 2234.
- (172) Bexrud, J. A.; Eisenberger, P.; Leitch, D. C.; Payne, P. R.; Schafer, L. L. *J. Am. Chem. Soc.* **2009**, 131, 2116.
- (173) Katritzky, A. R.; Cui, X.-L.; Yang, B.; Steel, P. J. *J. Org. Chem.* **1999**, 64, 1979.
- (174) Peterson, M.; Bowman, A.; Morgan, S. *Synth. Commun.* **2002**, 32, 443.
- (175) Lopez, R. M.; Fu, G. C. *Tetrahedron* **1997**, 53, 16349.
- (176) Sugiura, M.; Kumahara, M.; Nakajima, M. *Chem. Commun.* **2009**, 3585.

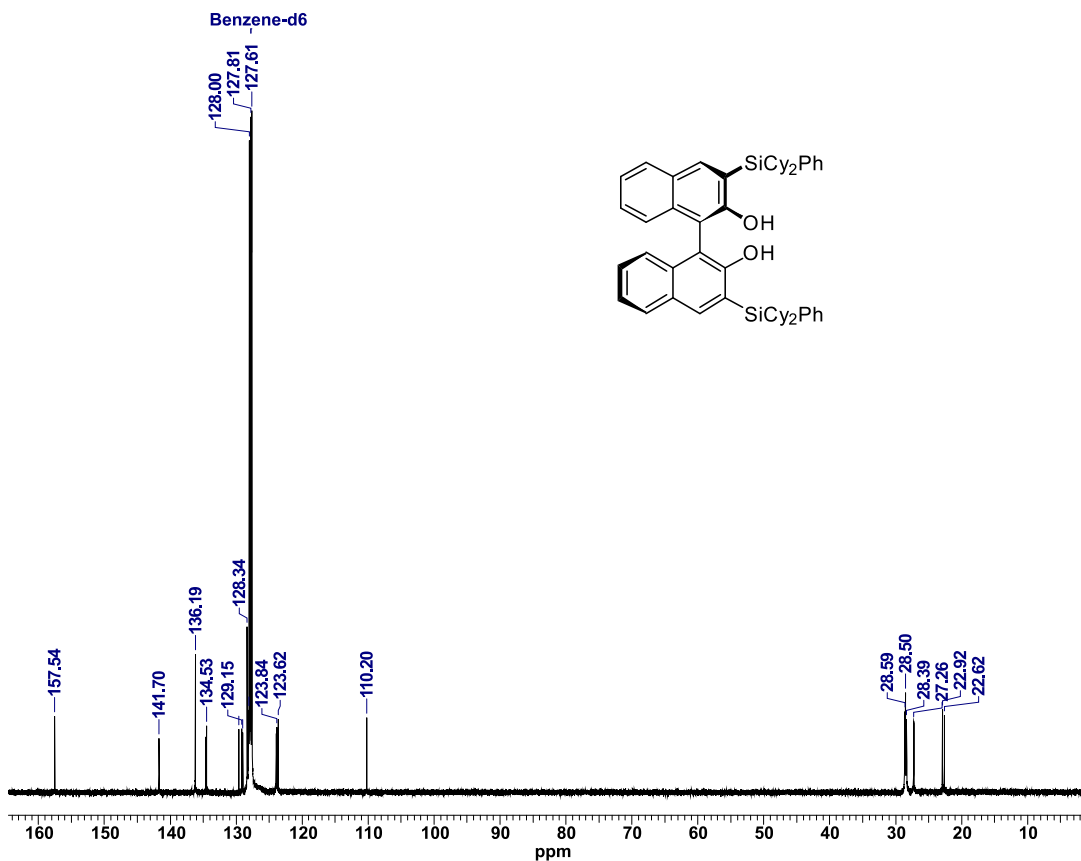
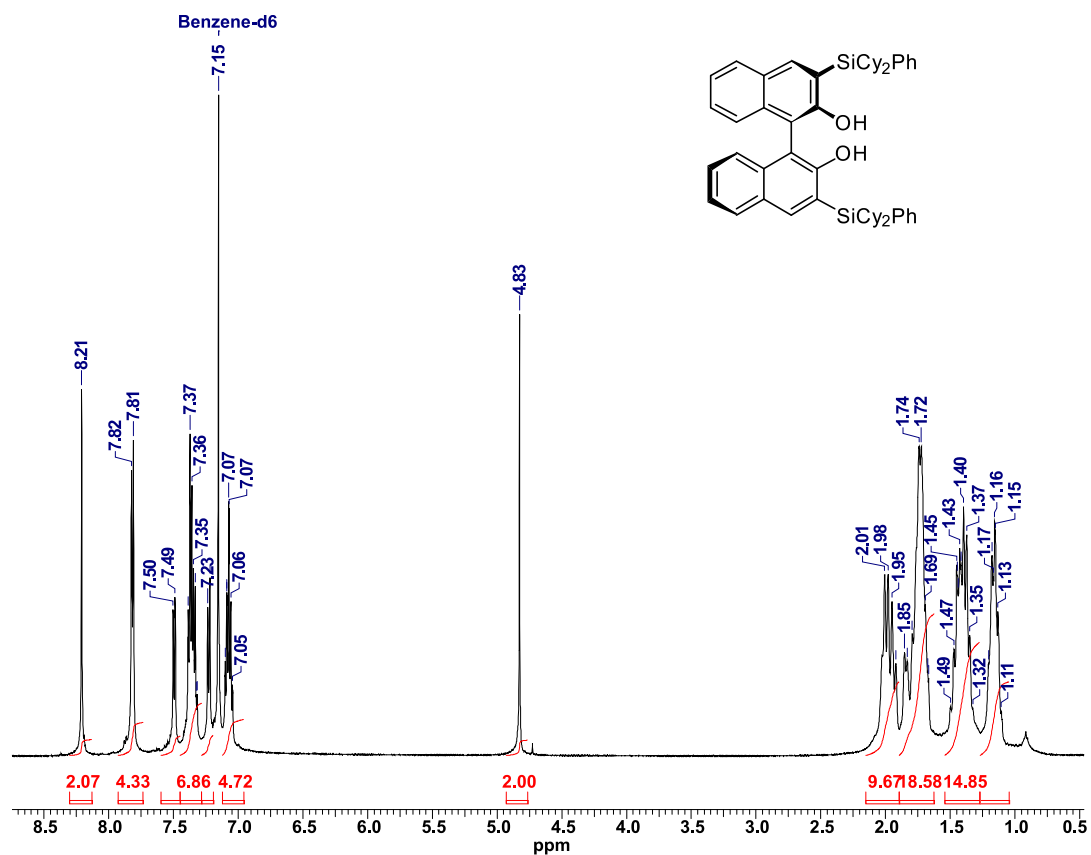
Appendix

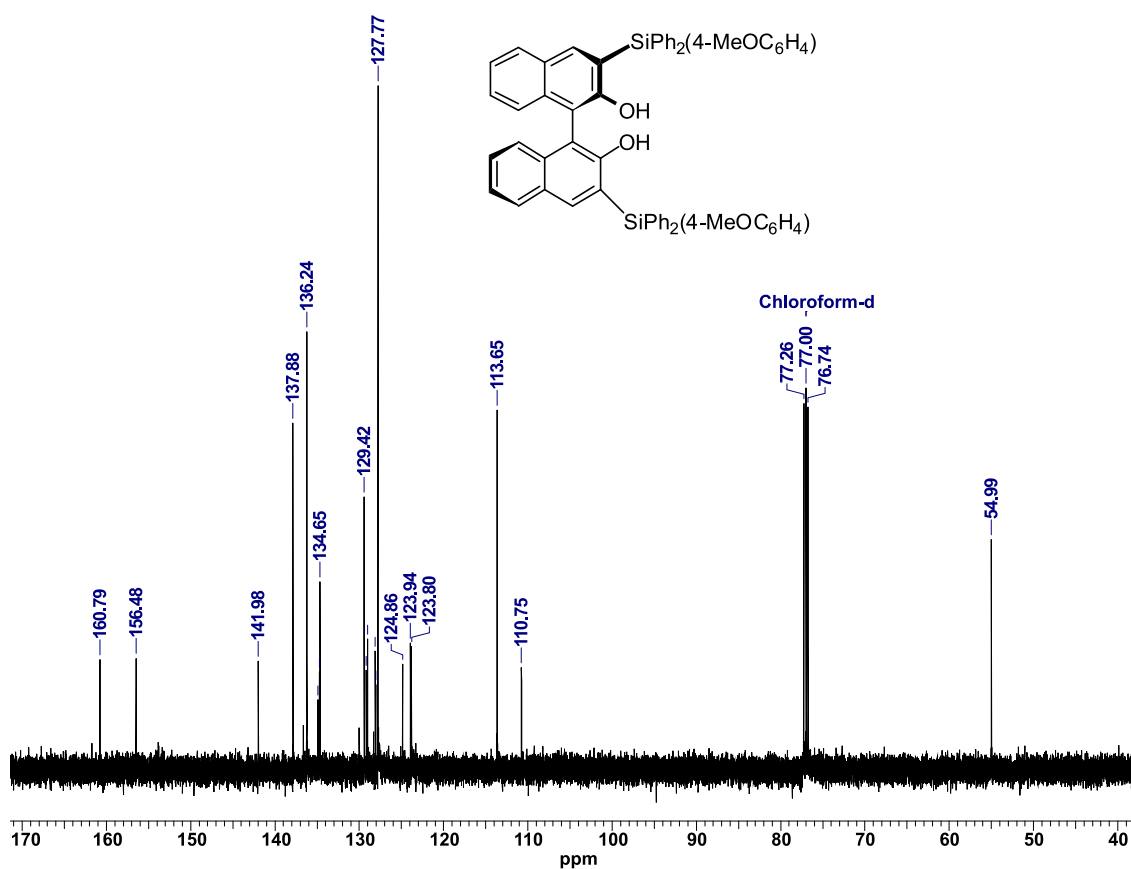
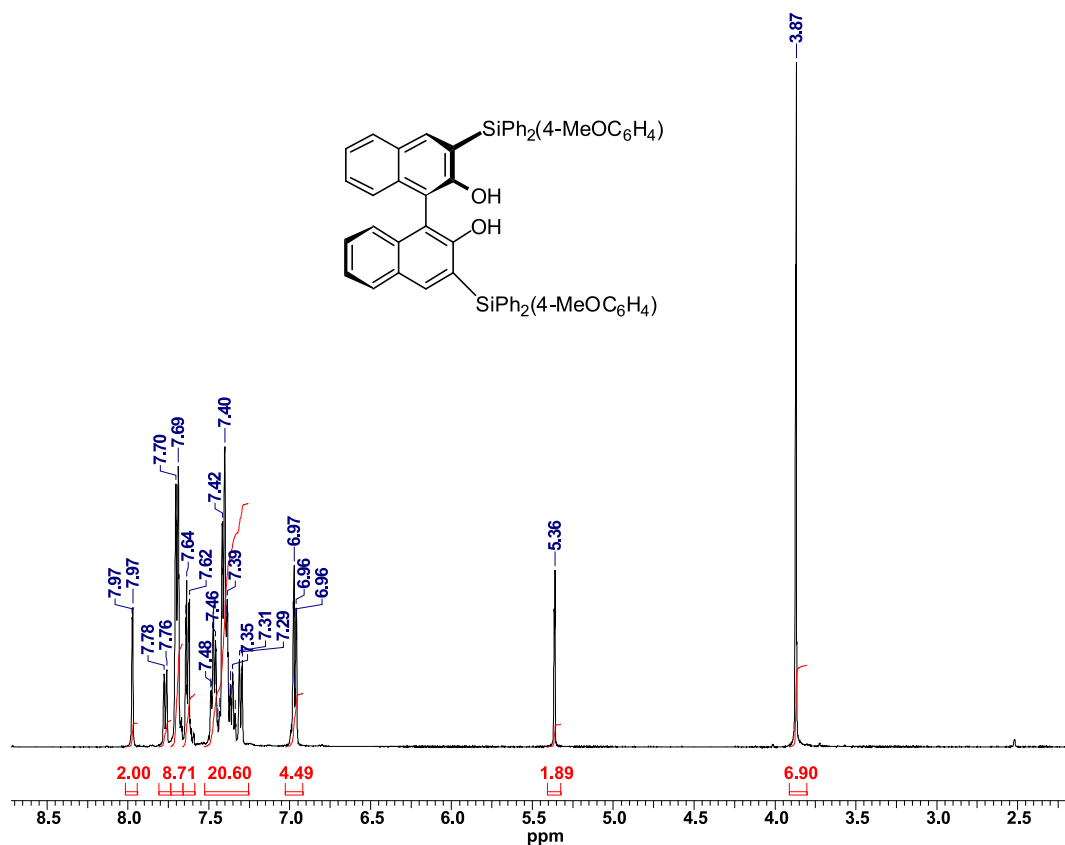
Appendix A: ^1H , ^{13}C , and ^{19}F NMR Spectra

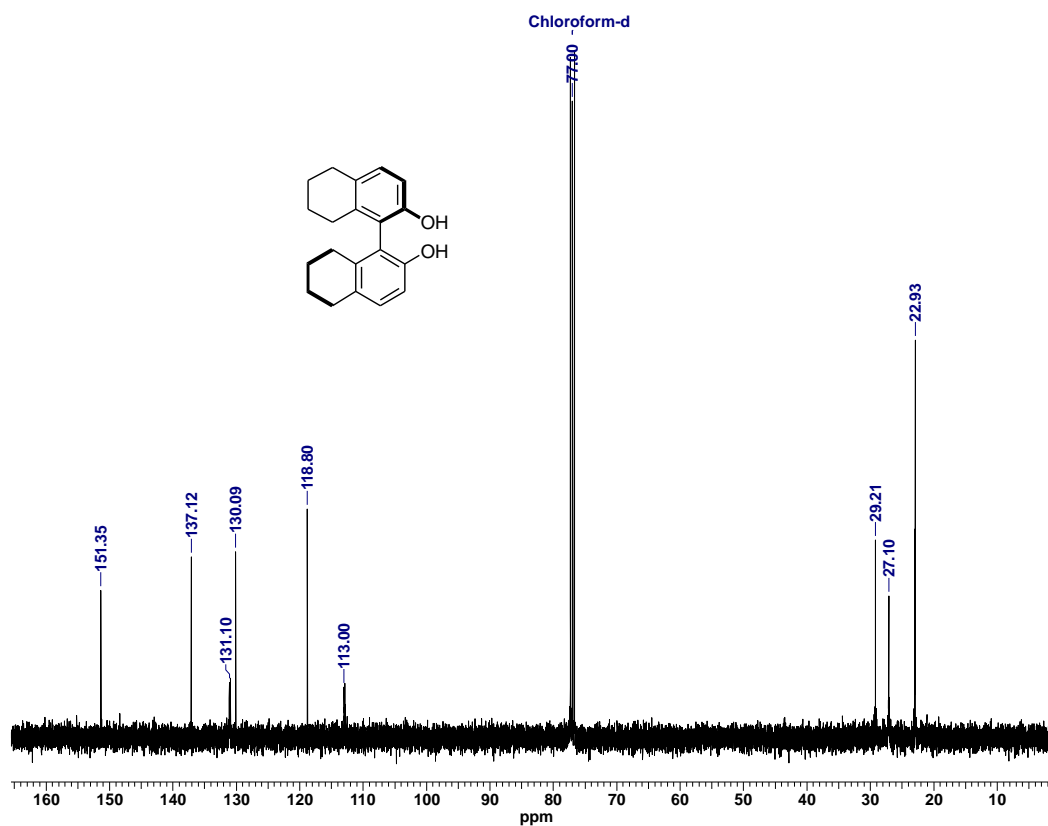
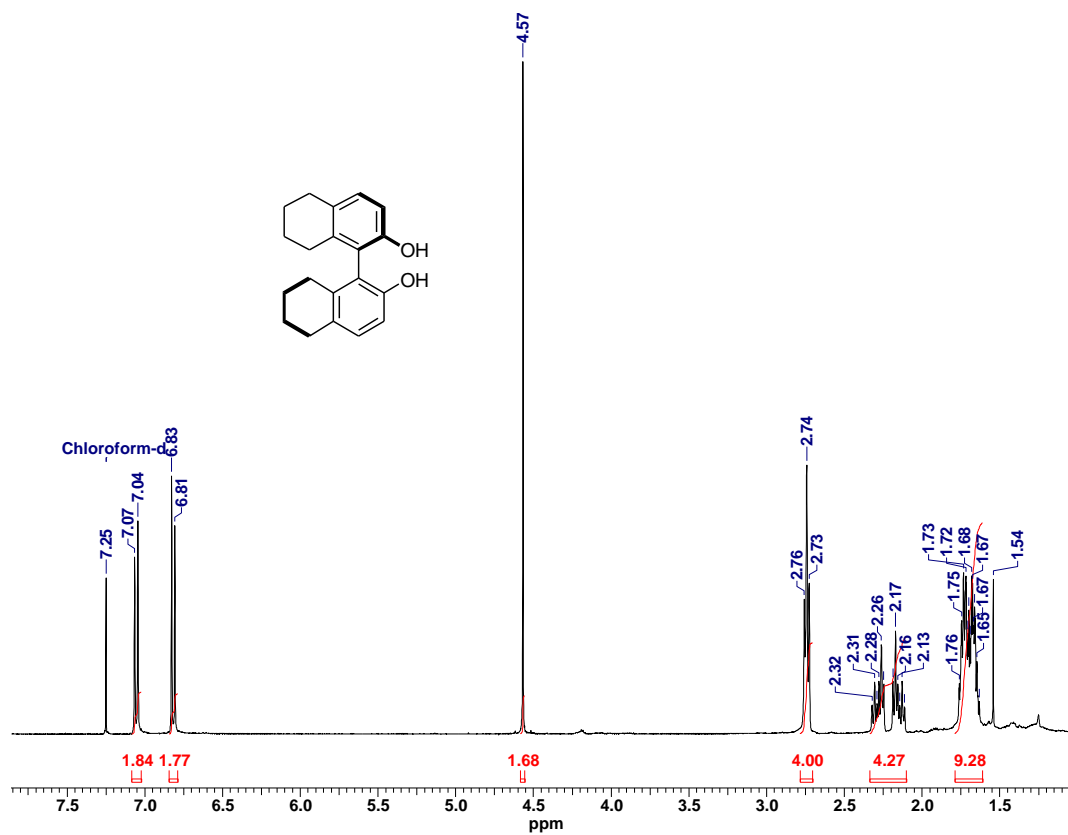


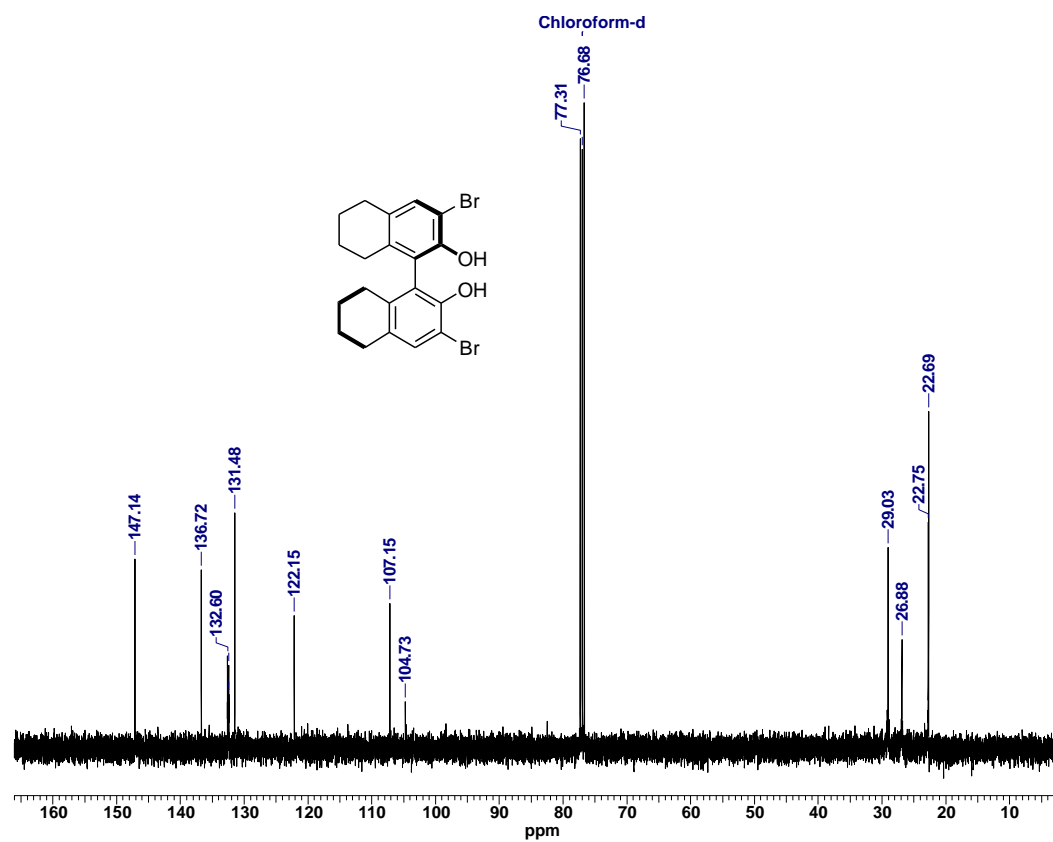
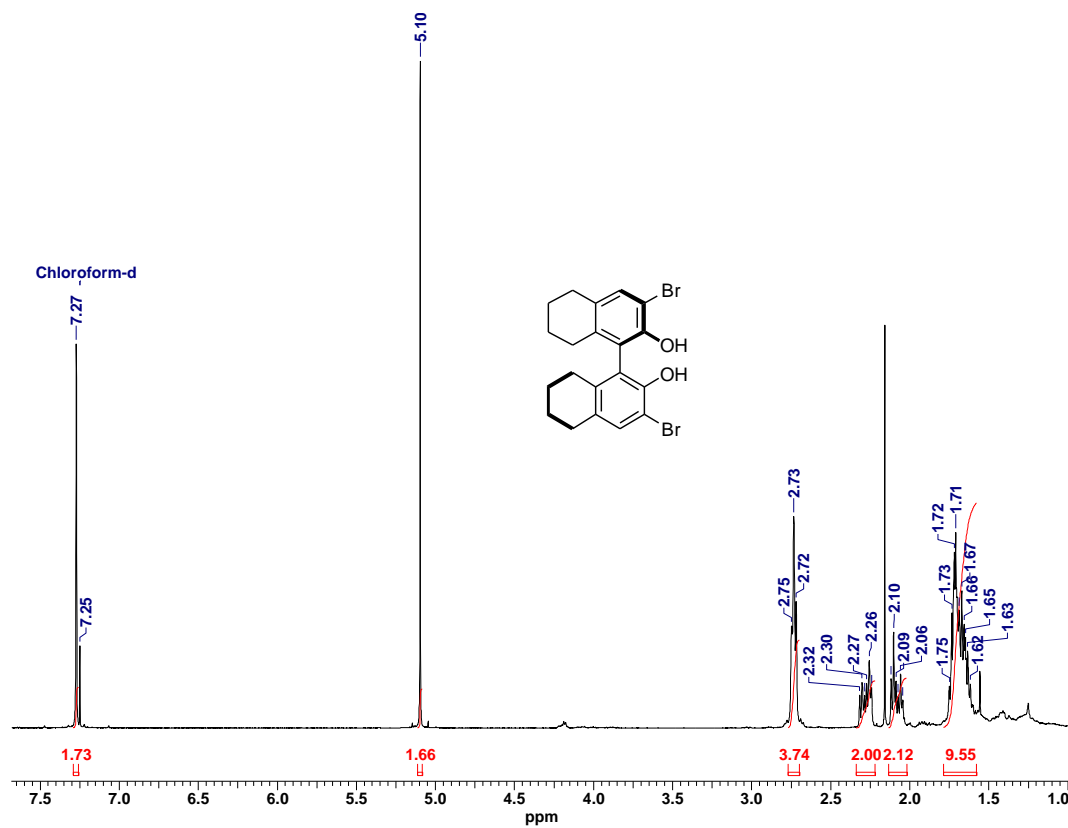


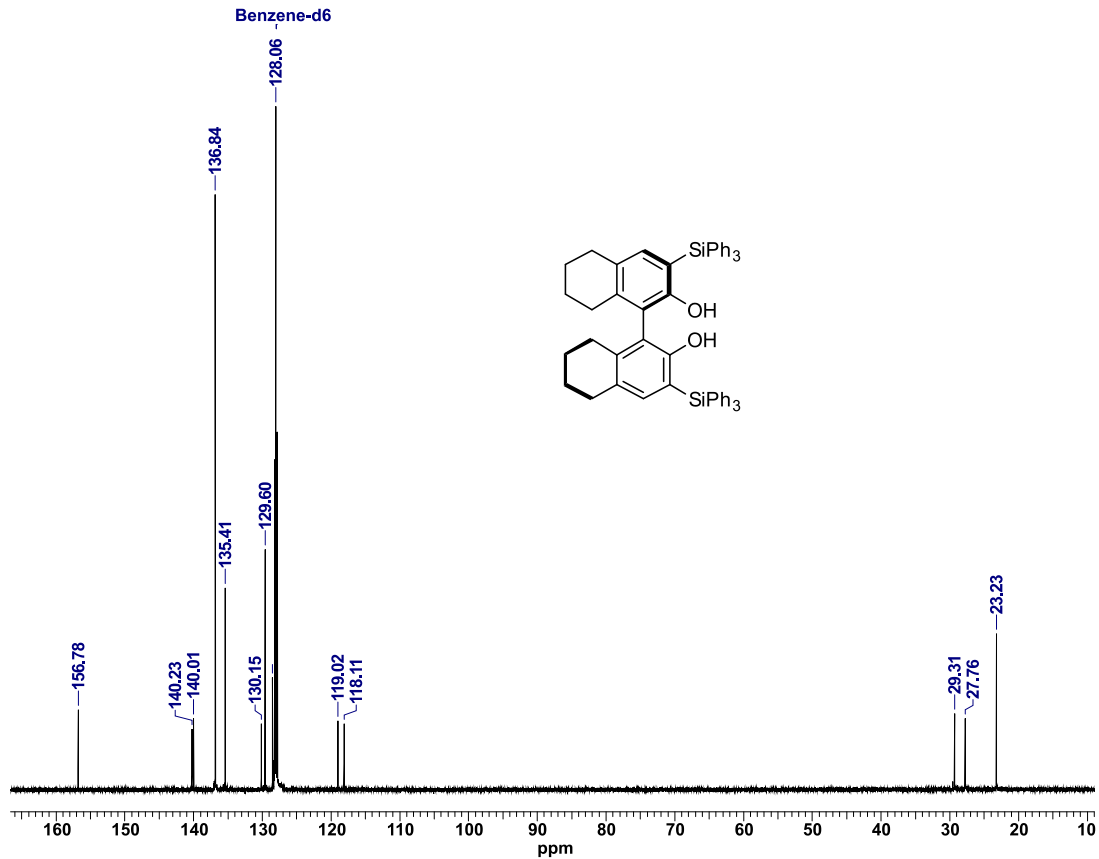
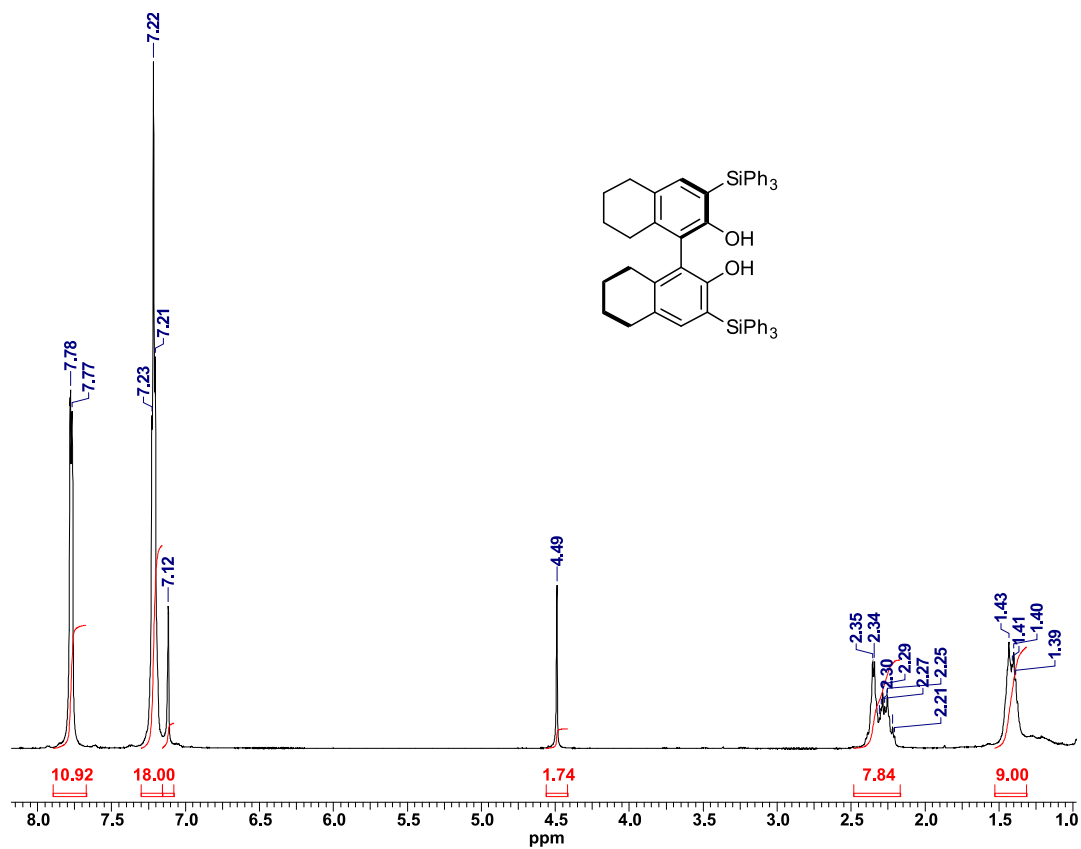


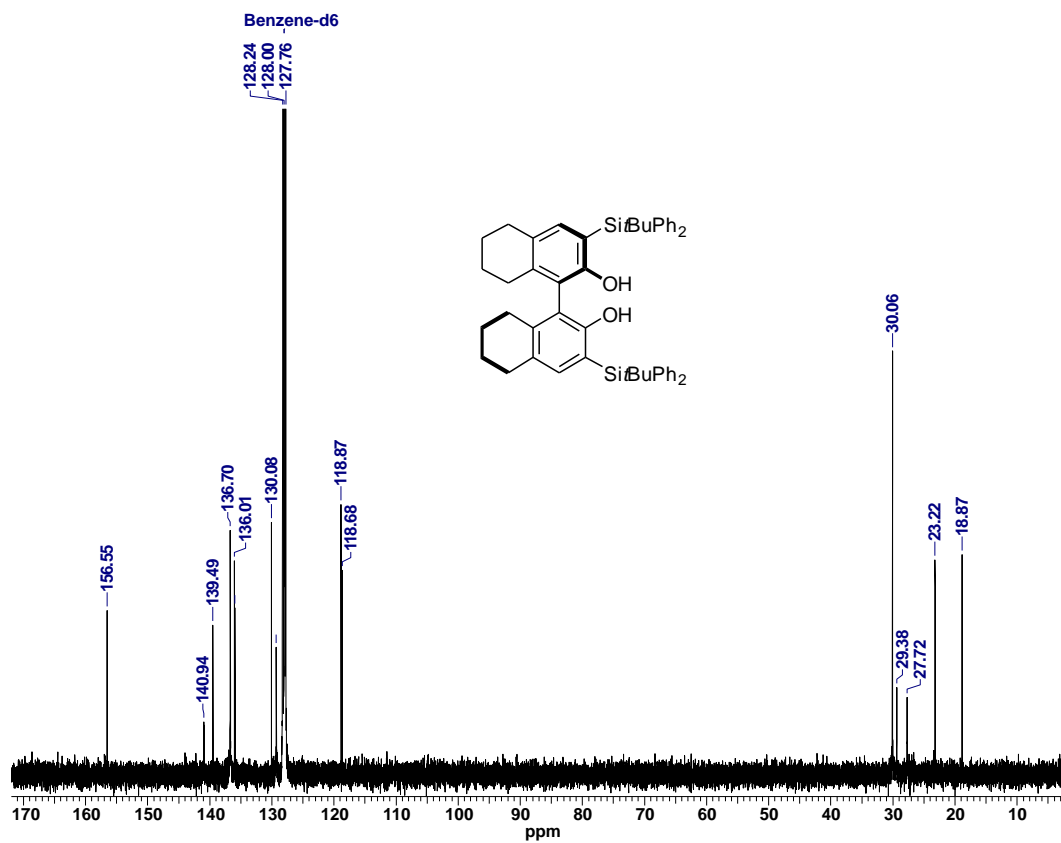
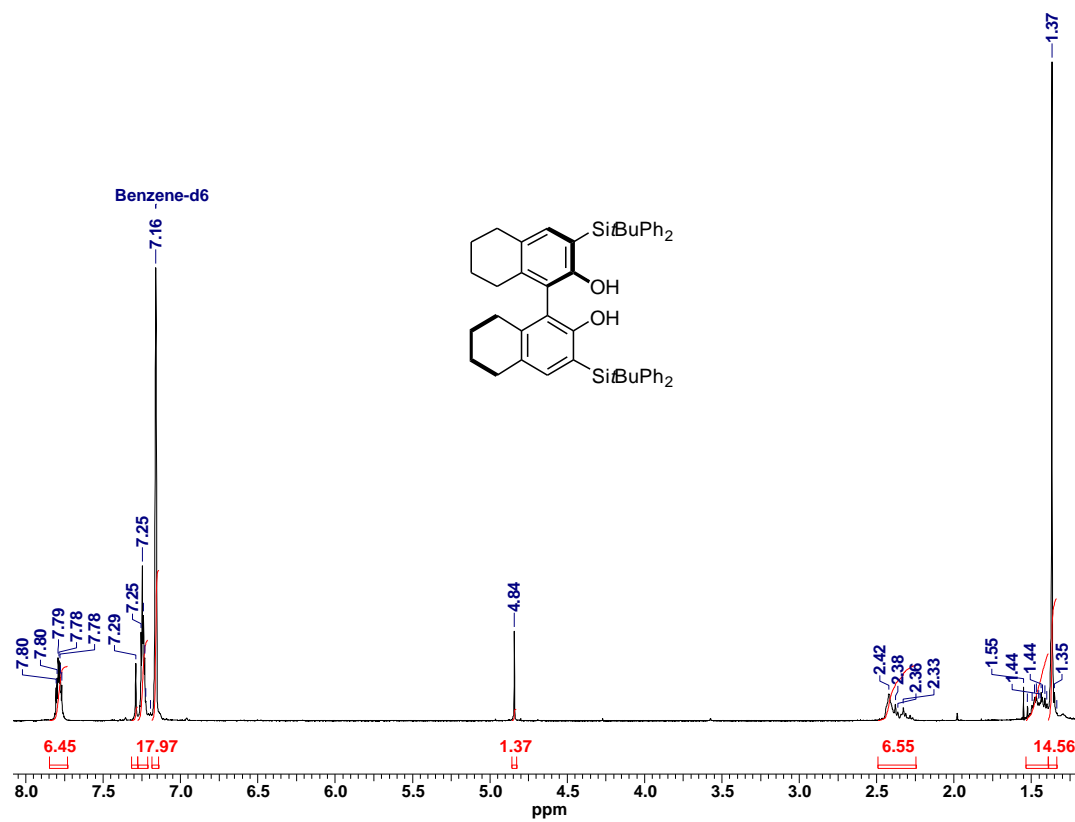


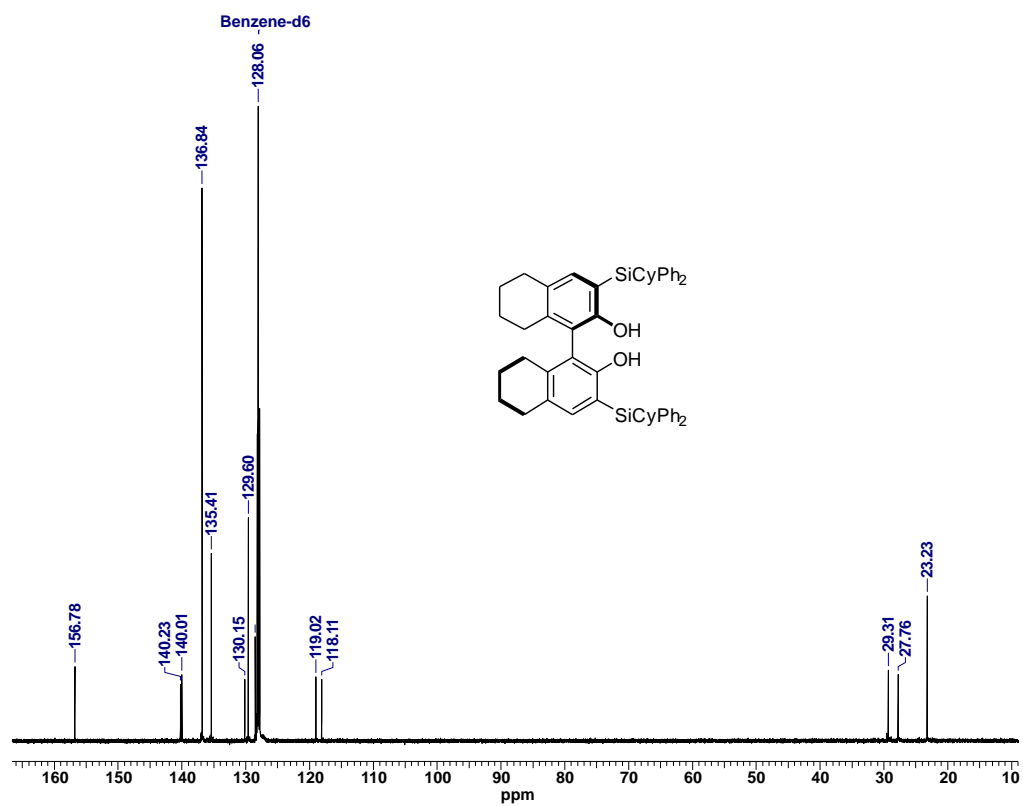
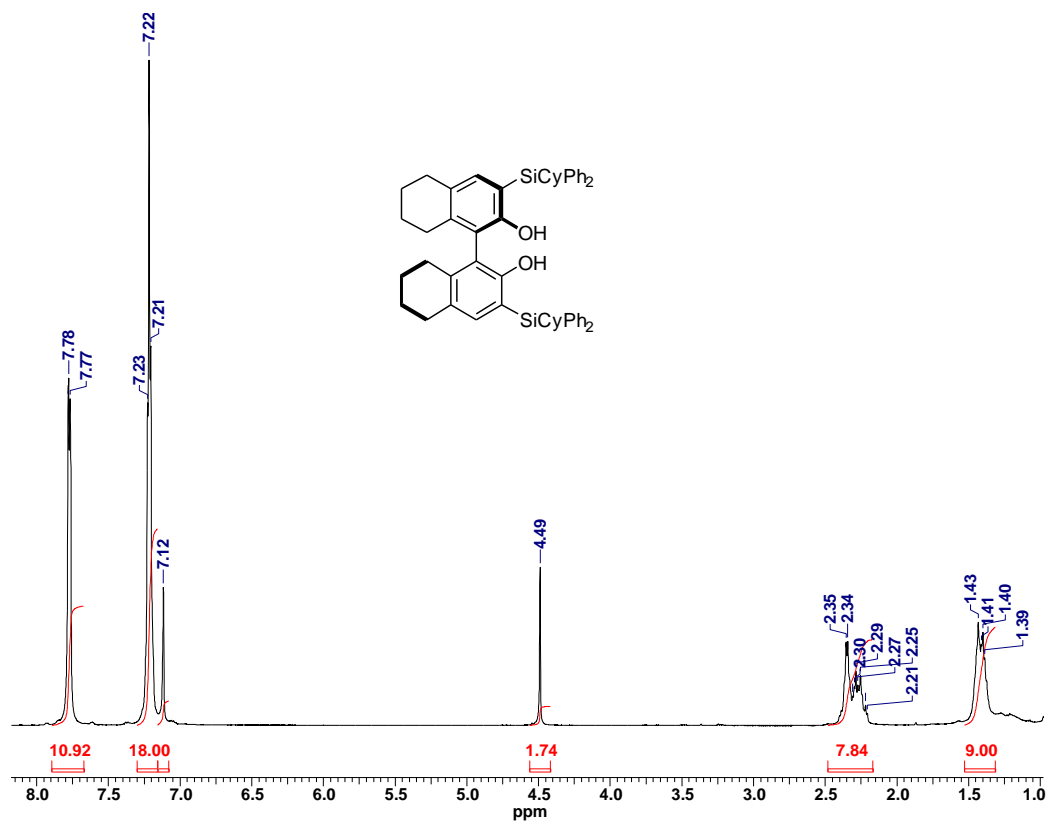


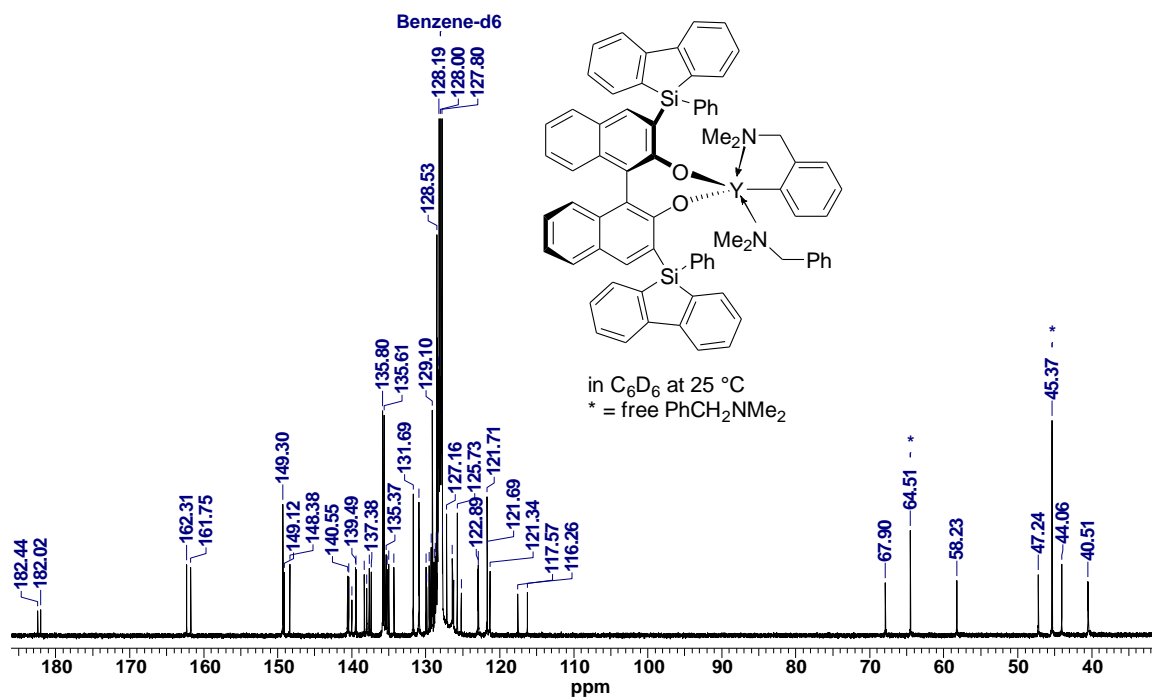
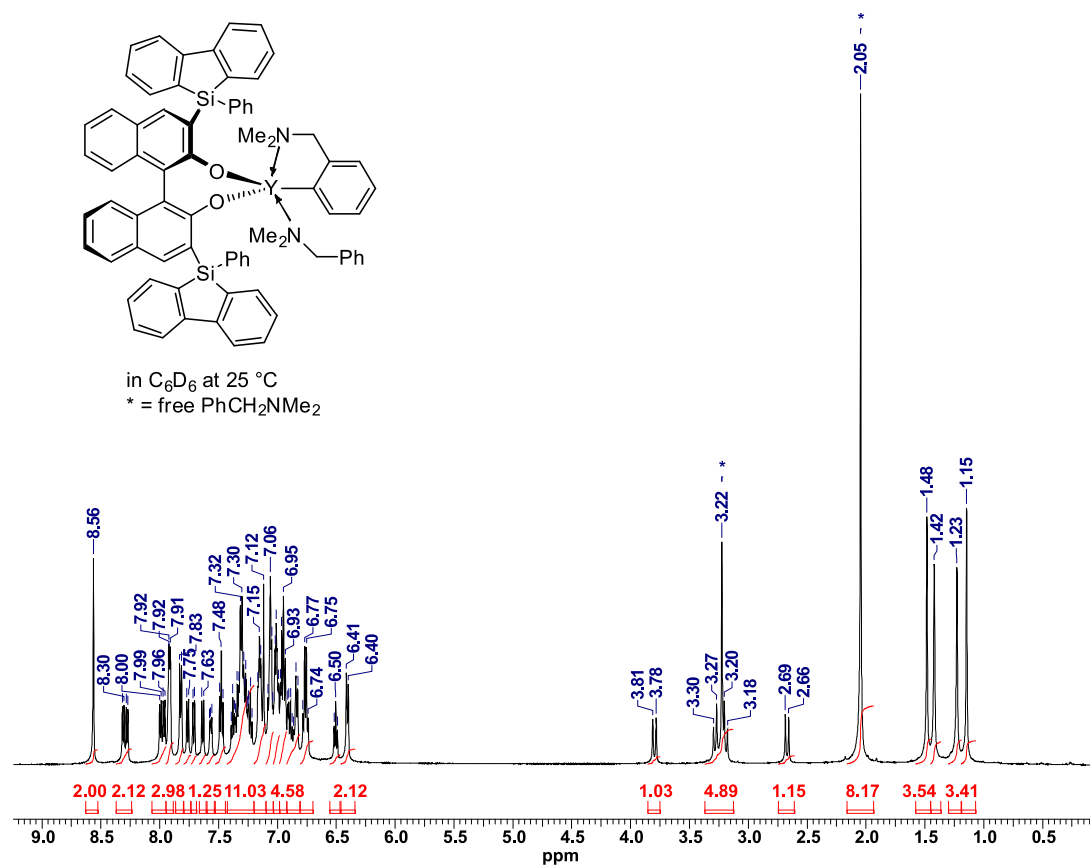


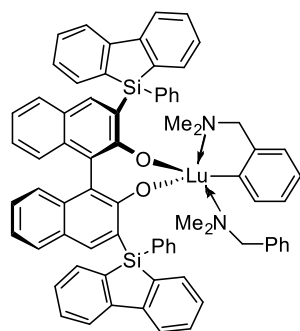




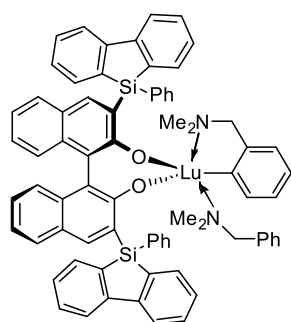
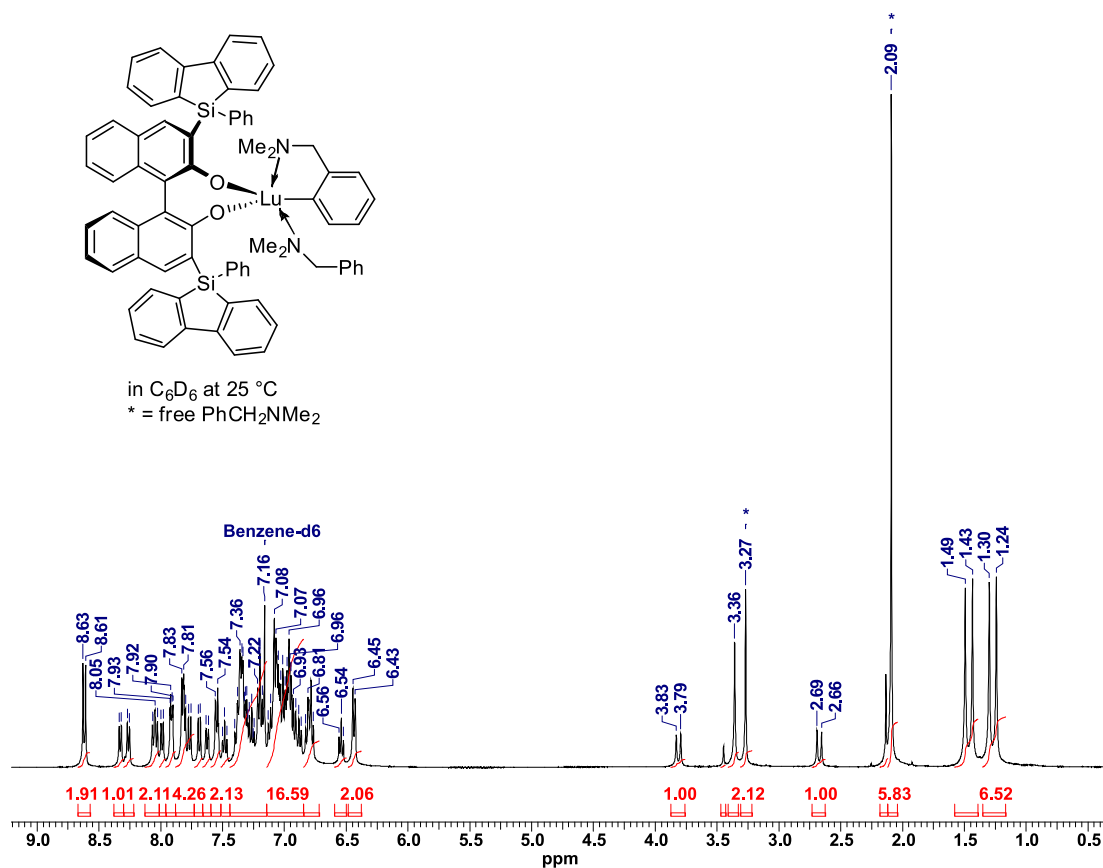




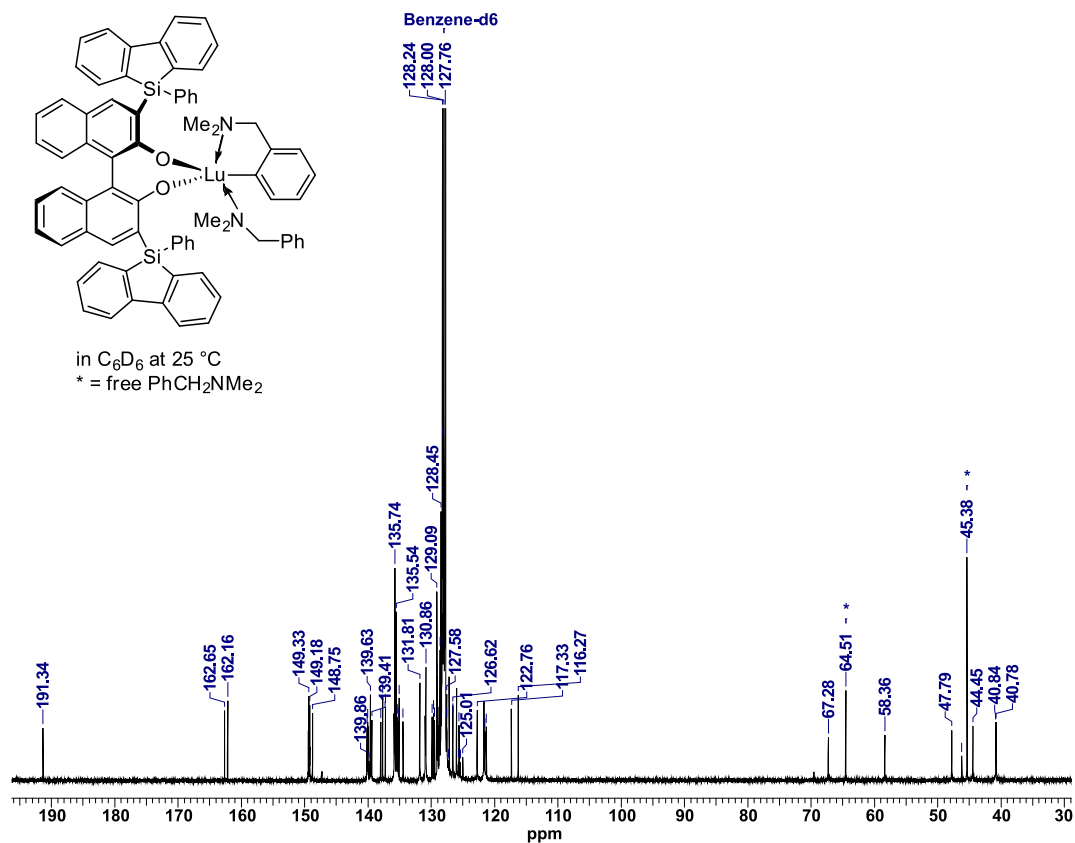


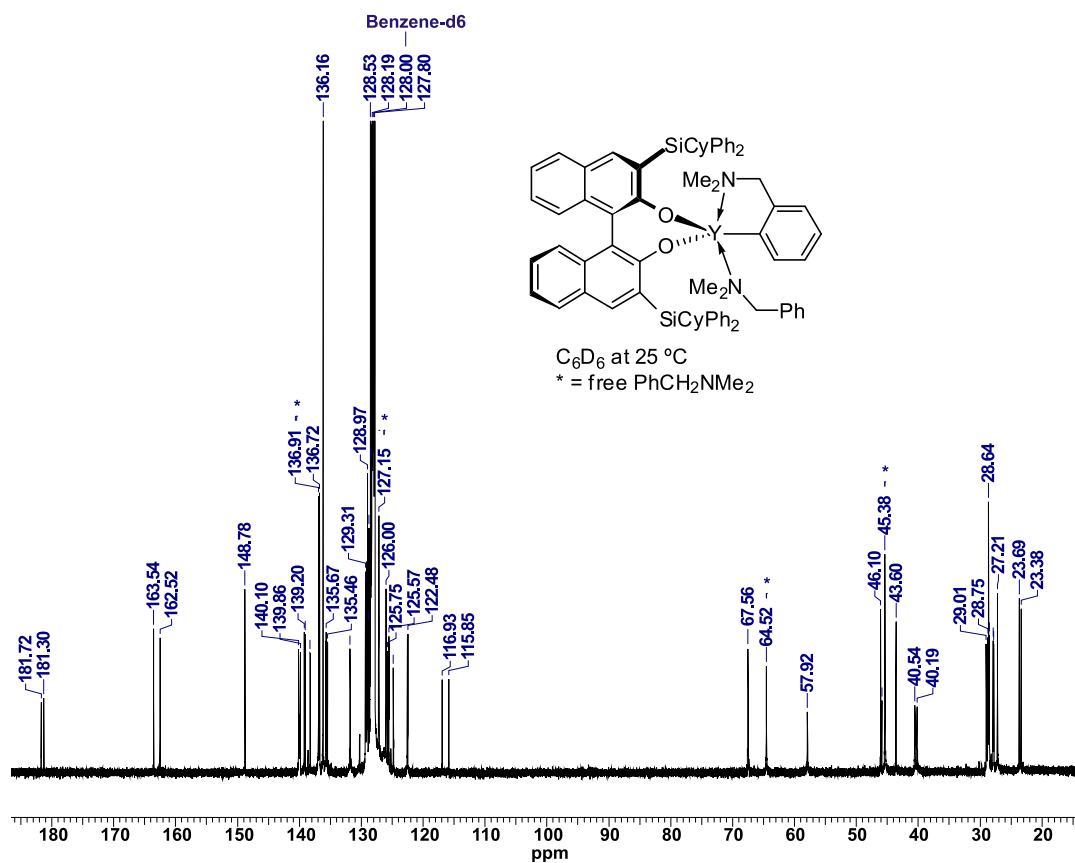
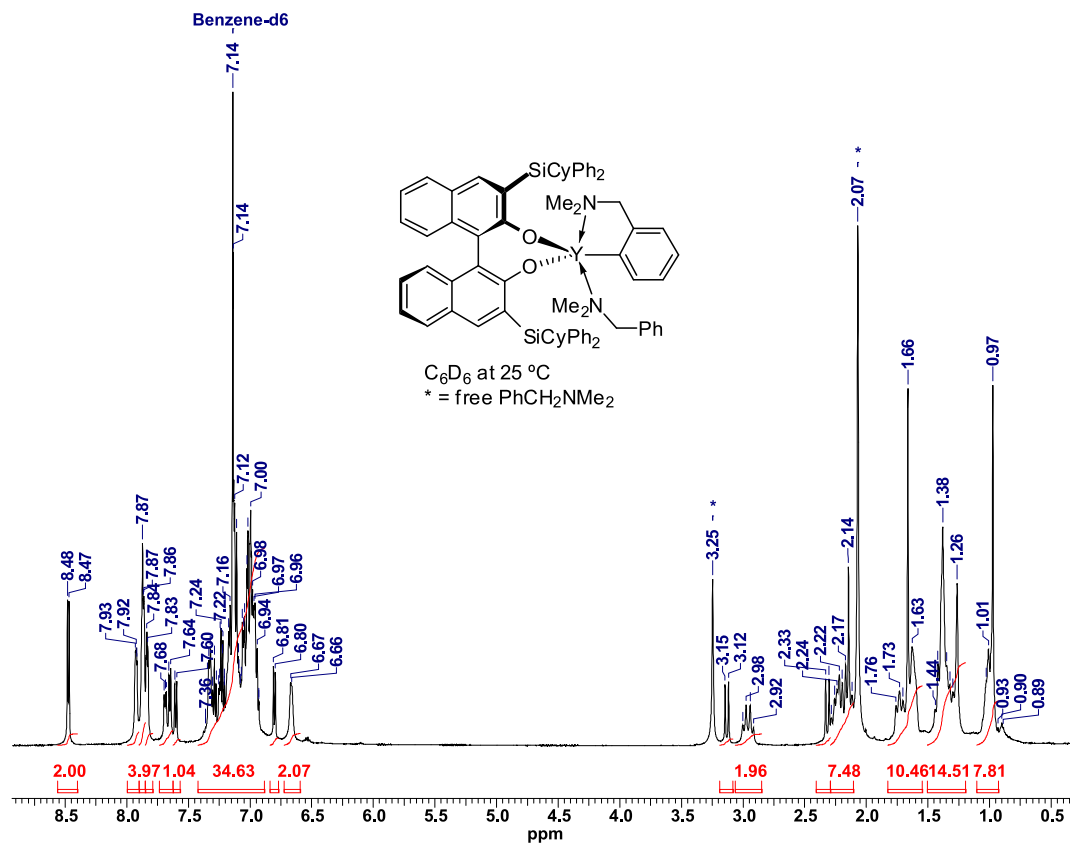


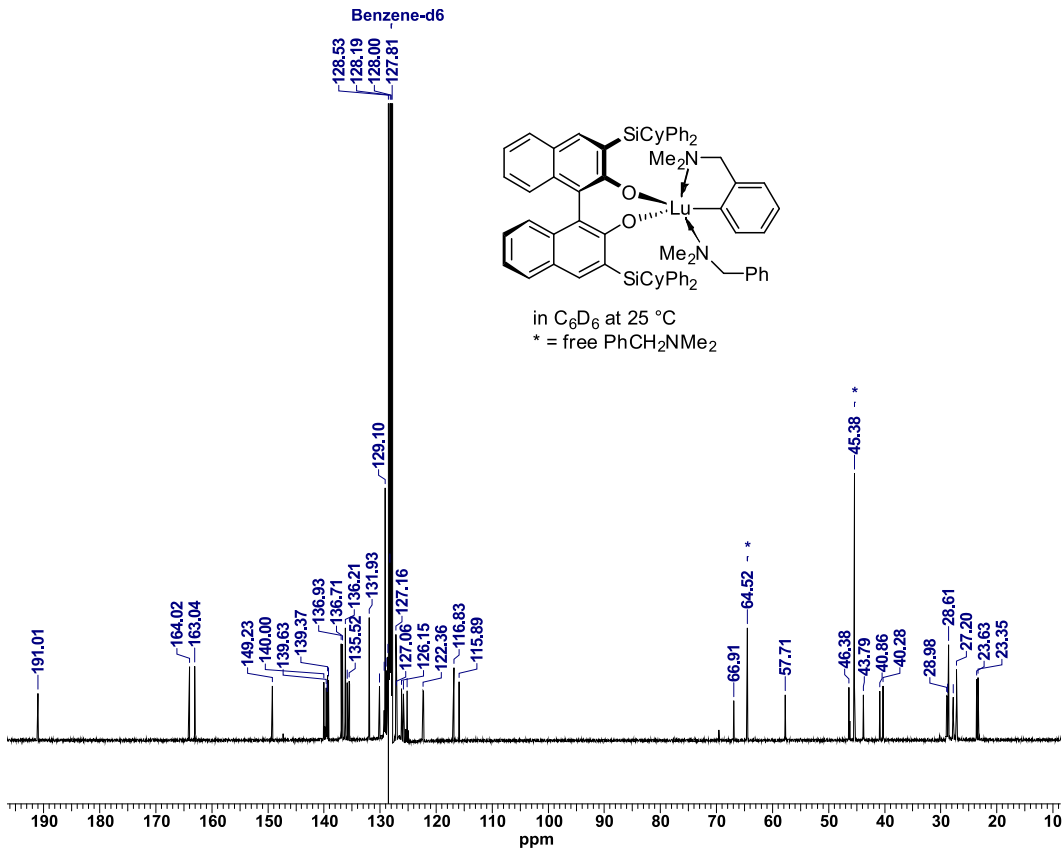
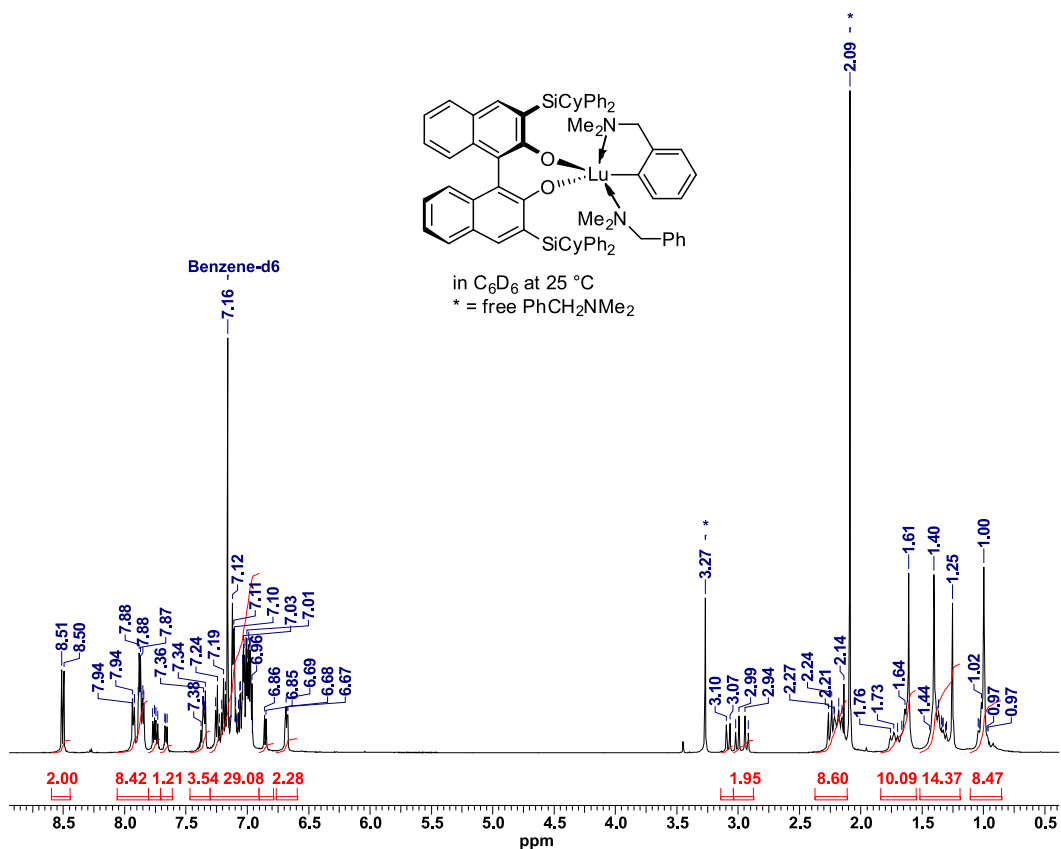
in C₆D₆ at 25 °C
 * = free PhCH₂NMe₂

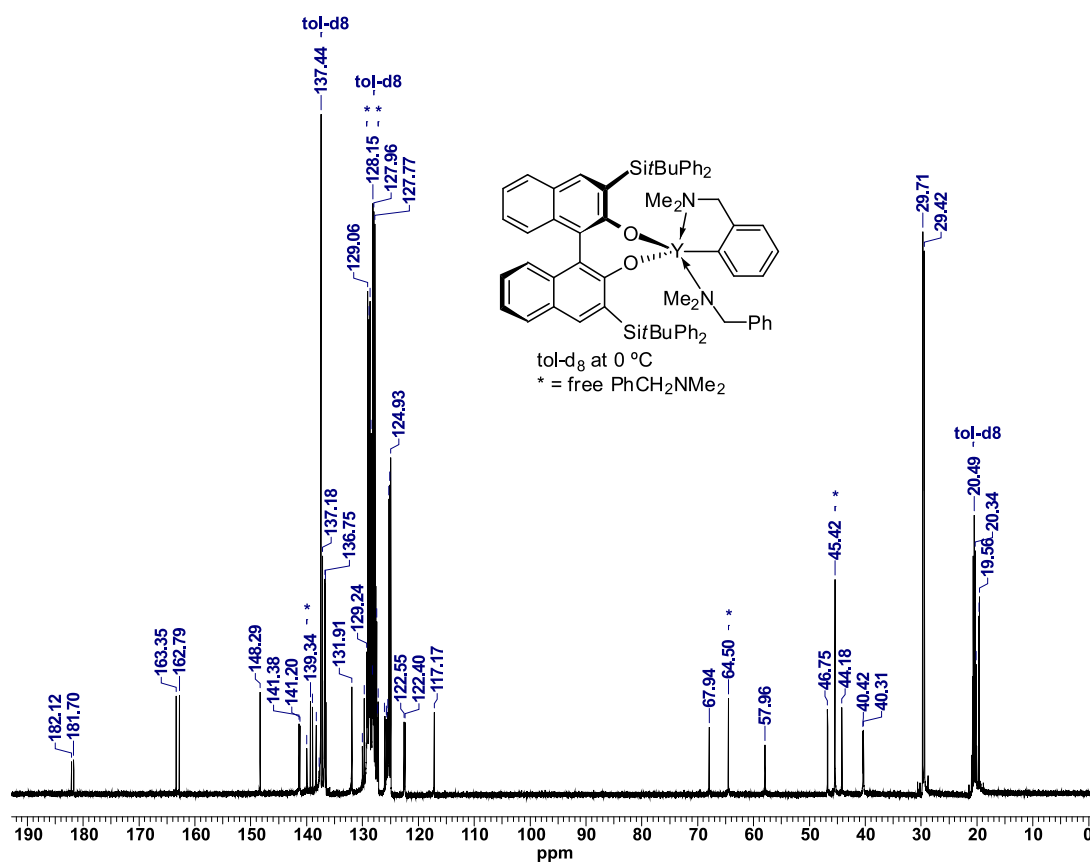
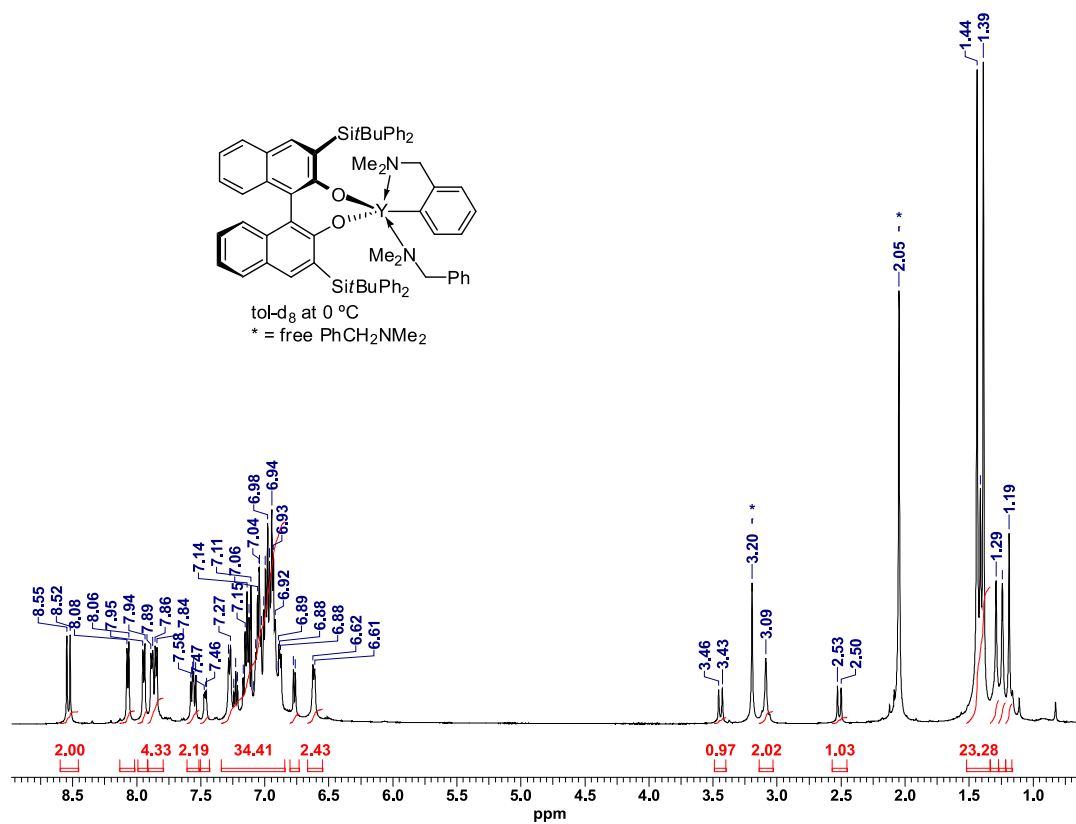


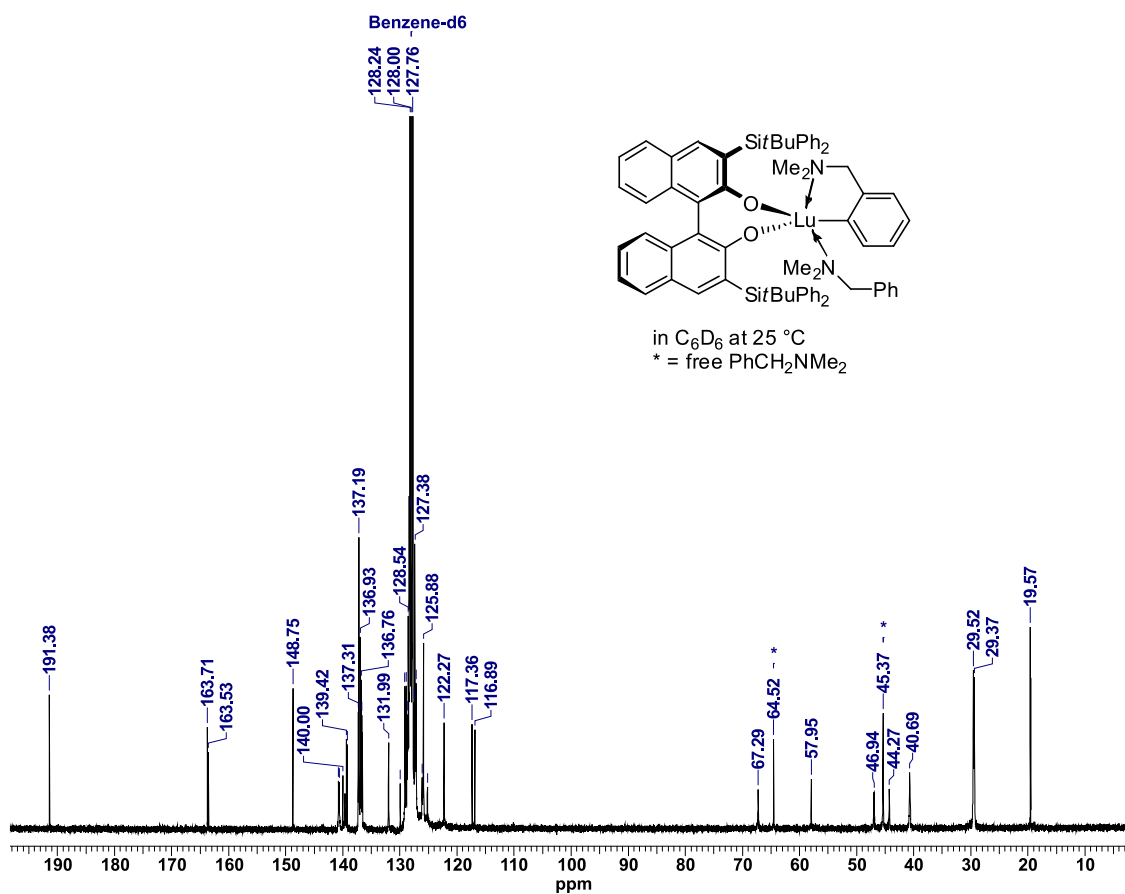
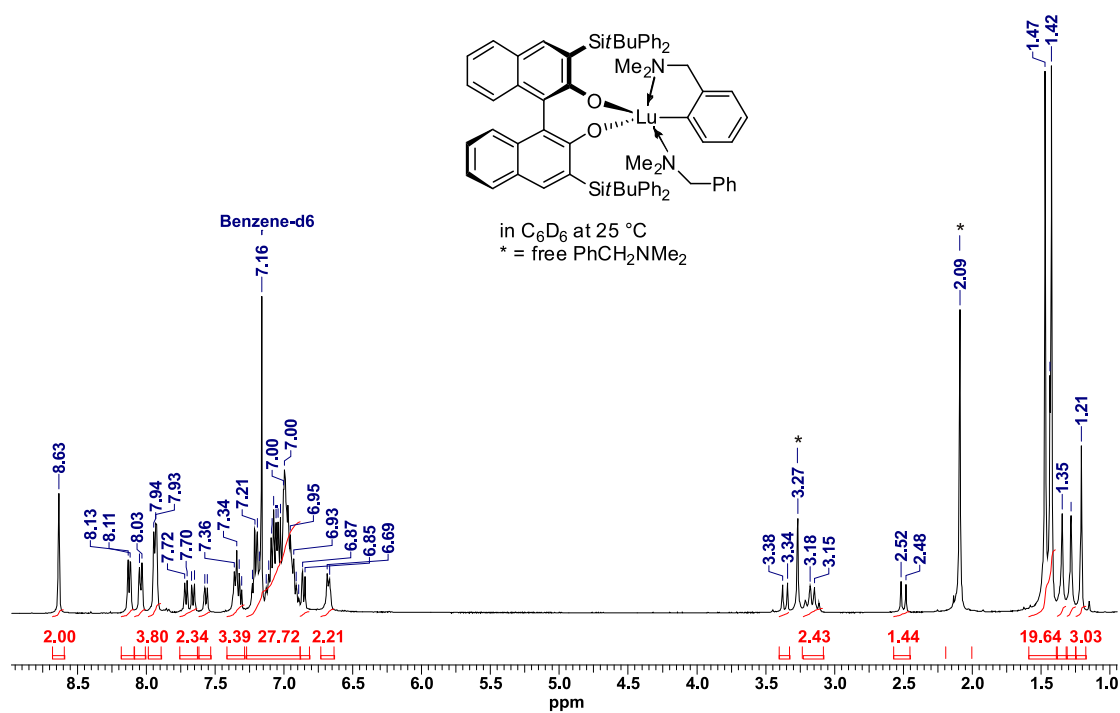
in C₆D₆ at 25 °C
 * = free PhCH₂NMe₂

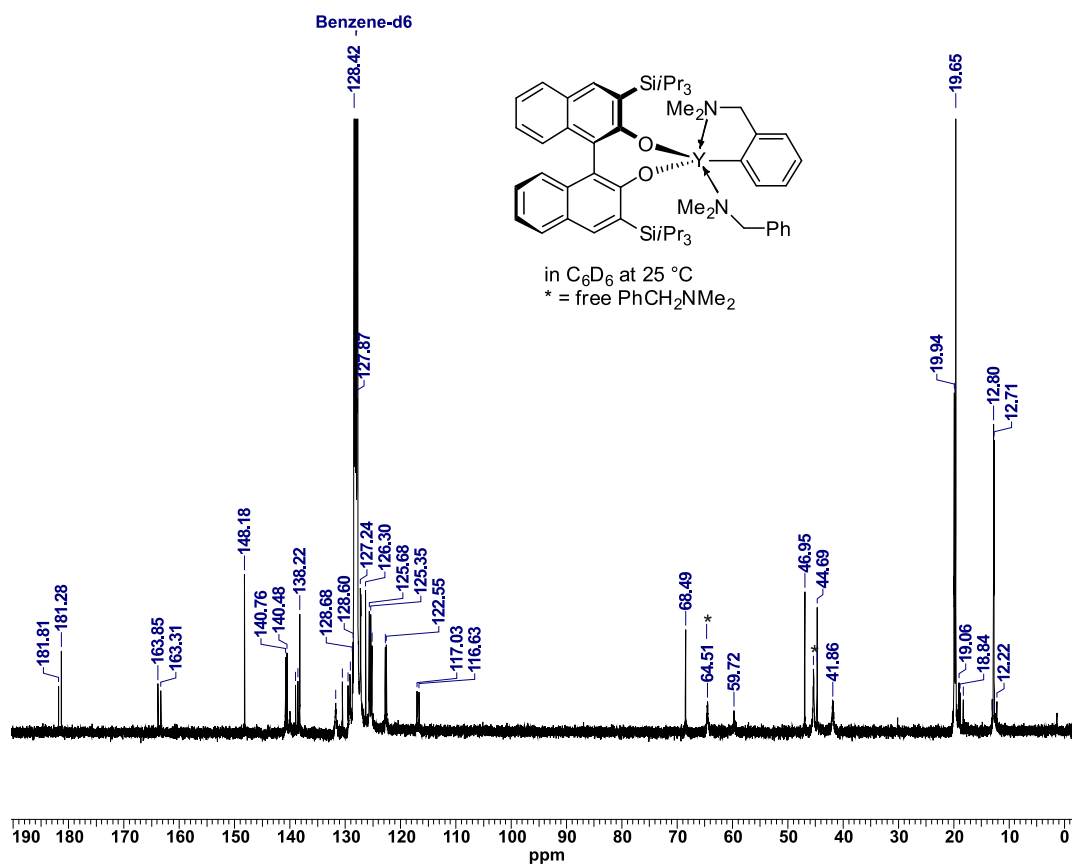
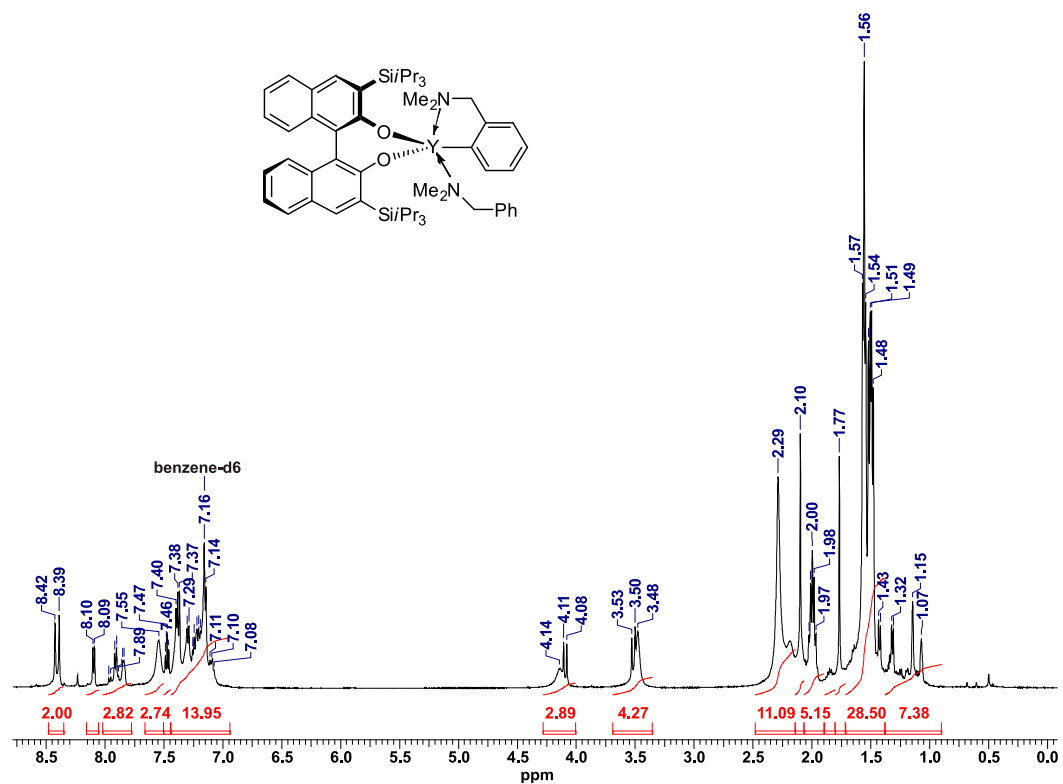


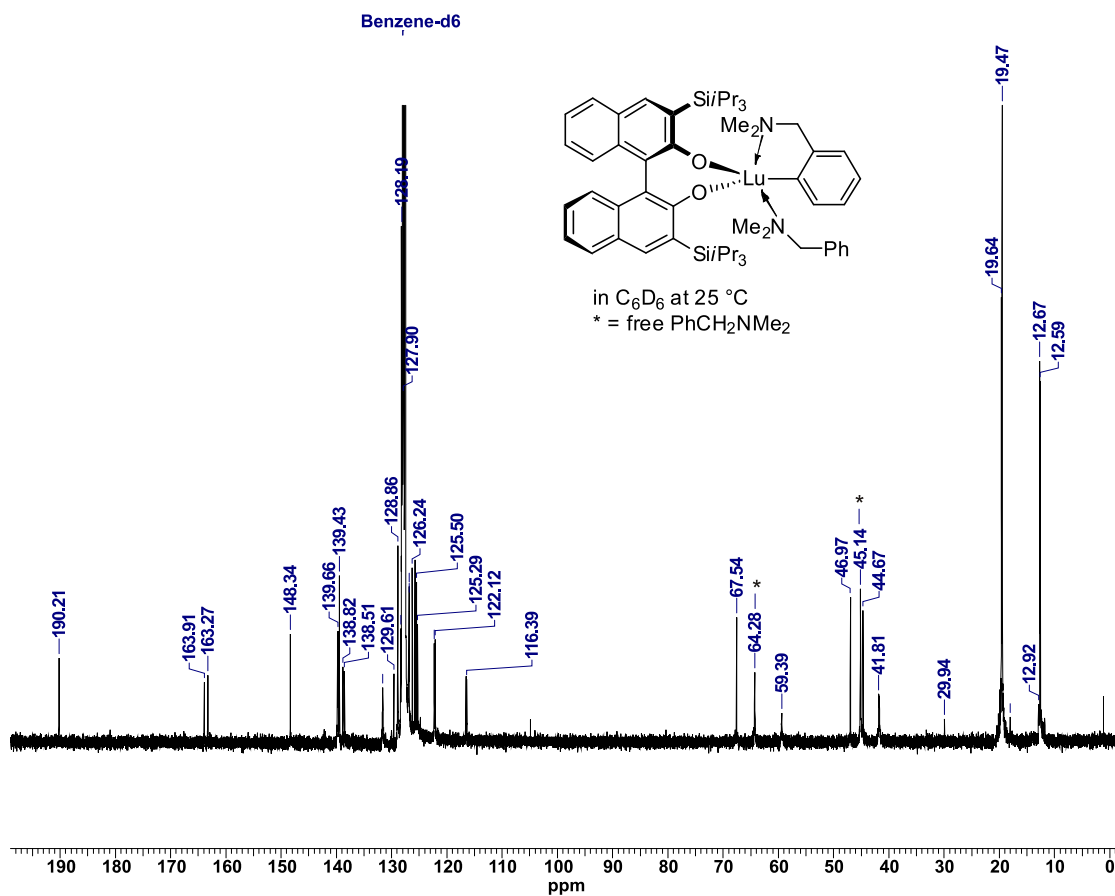
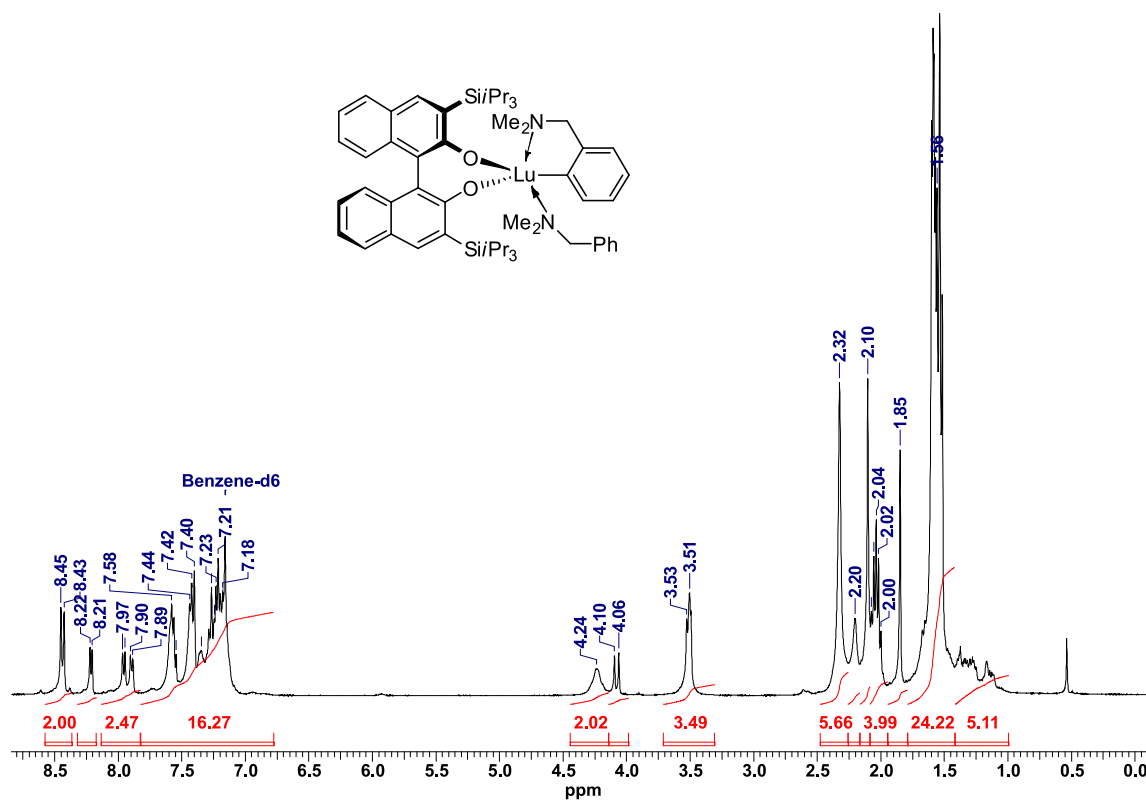


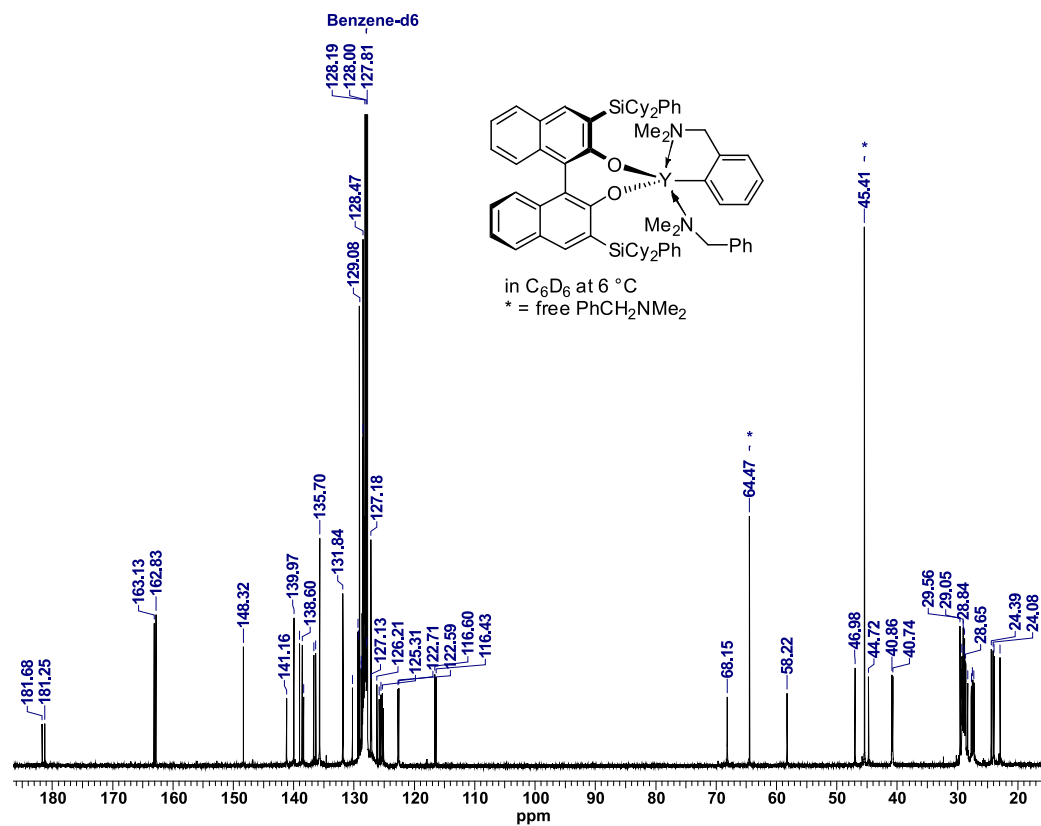
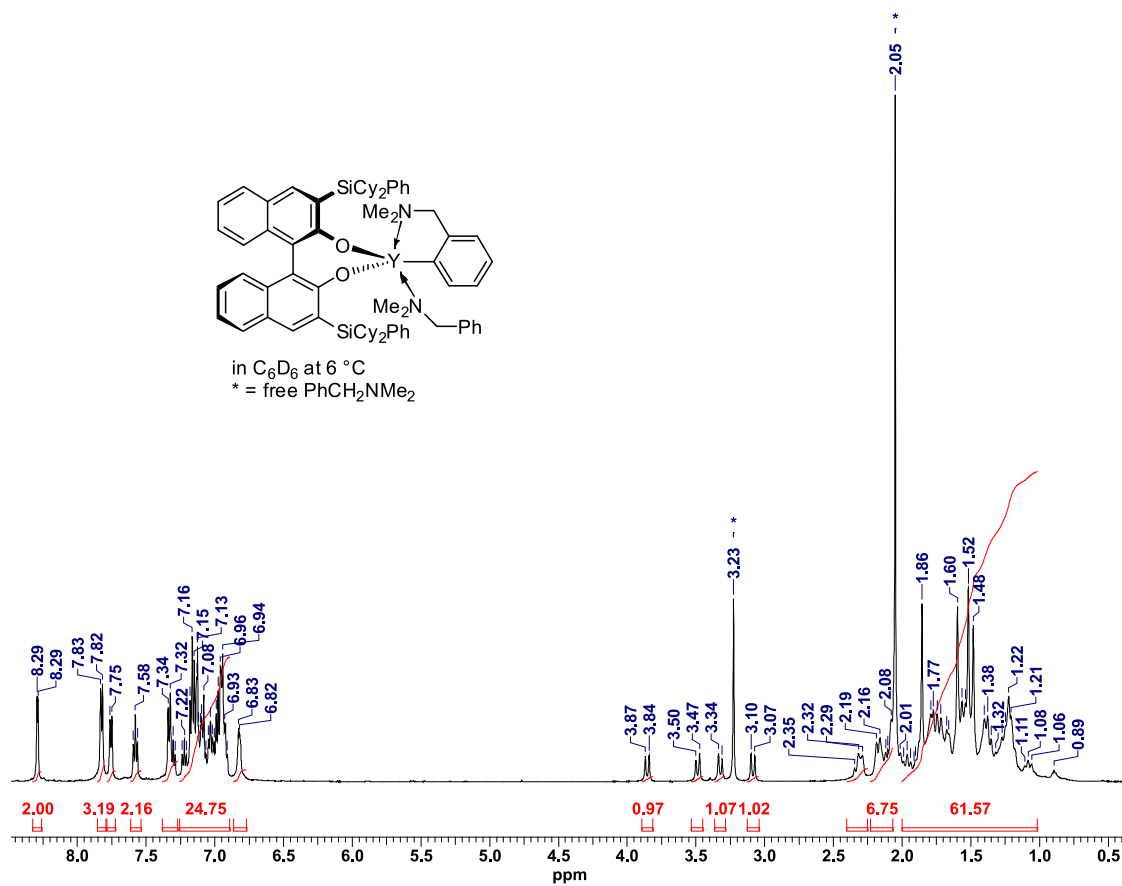


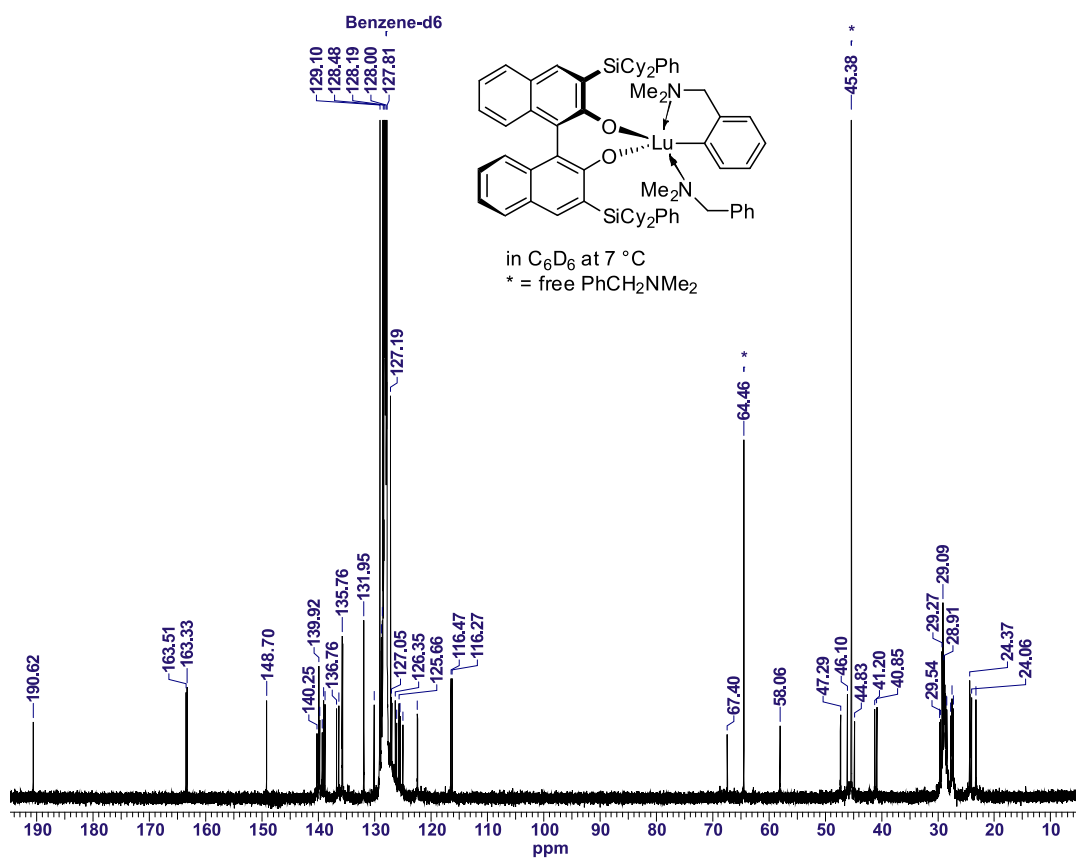
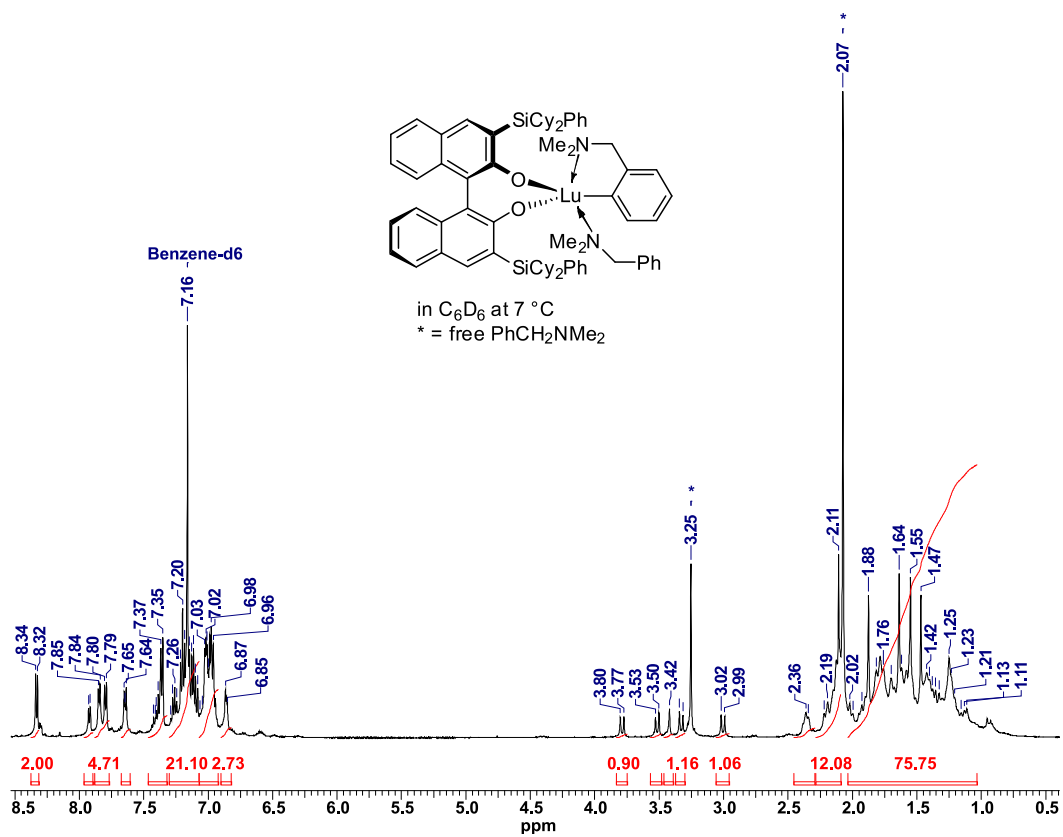


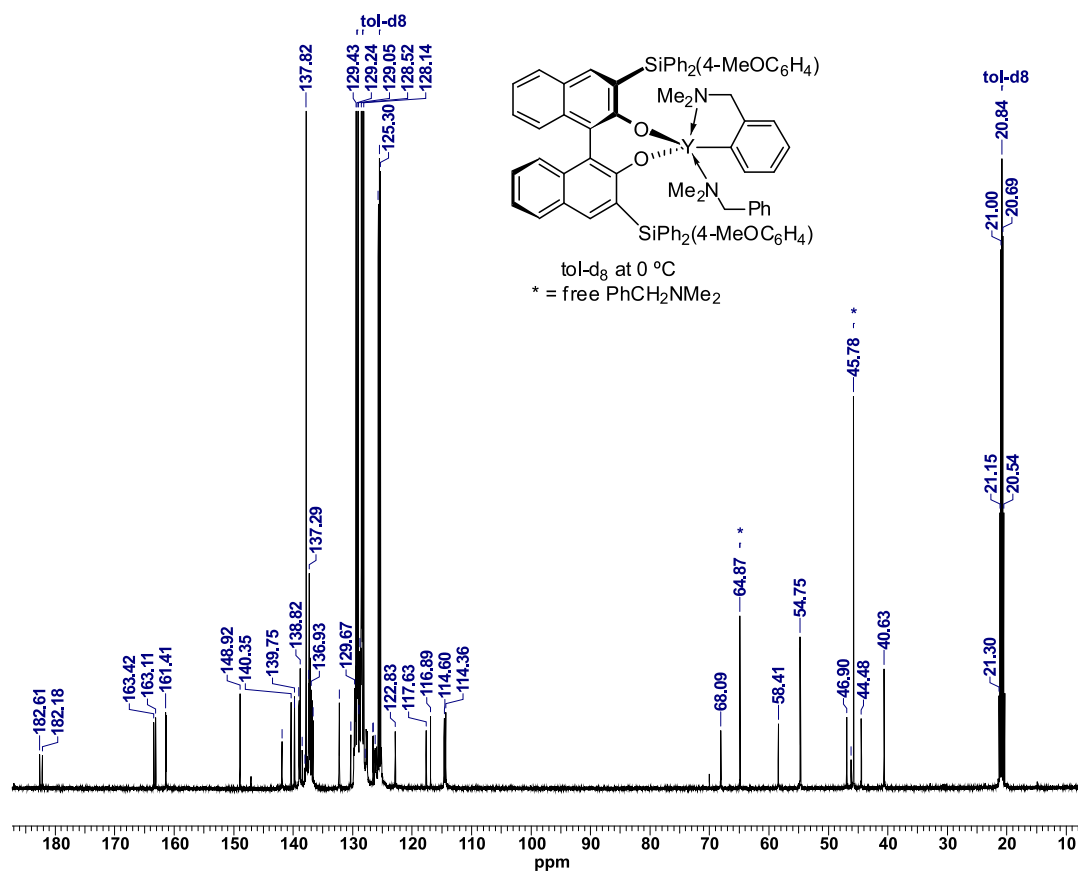
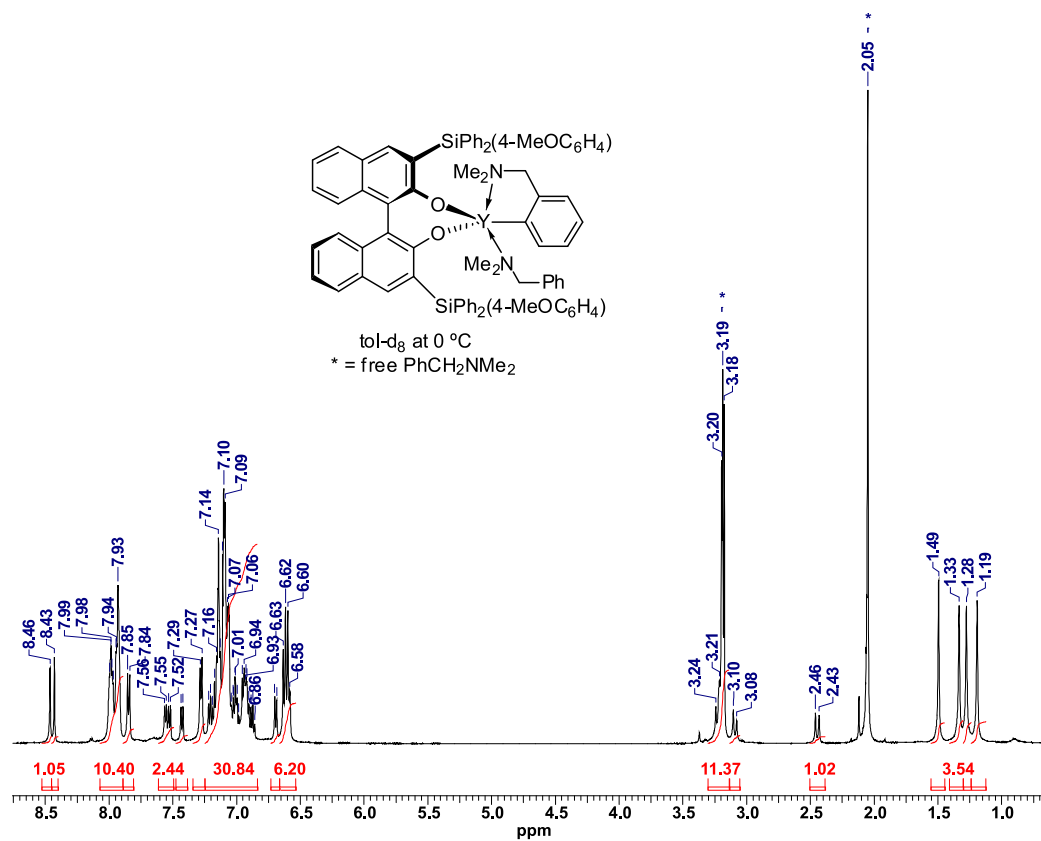


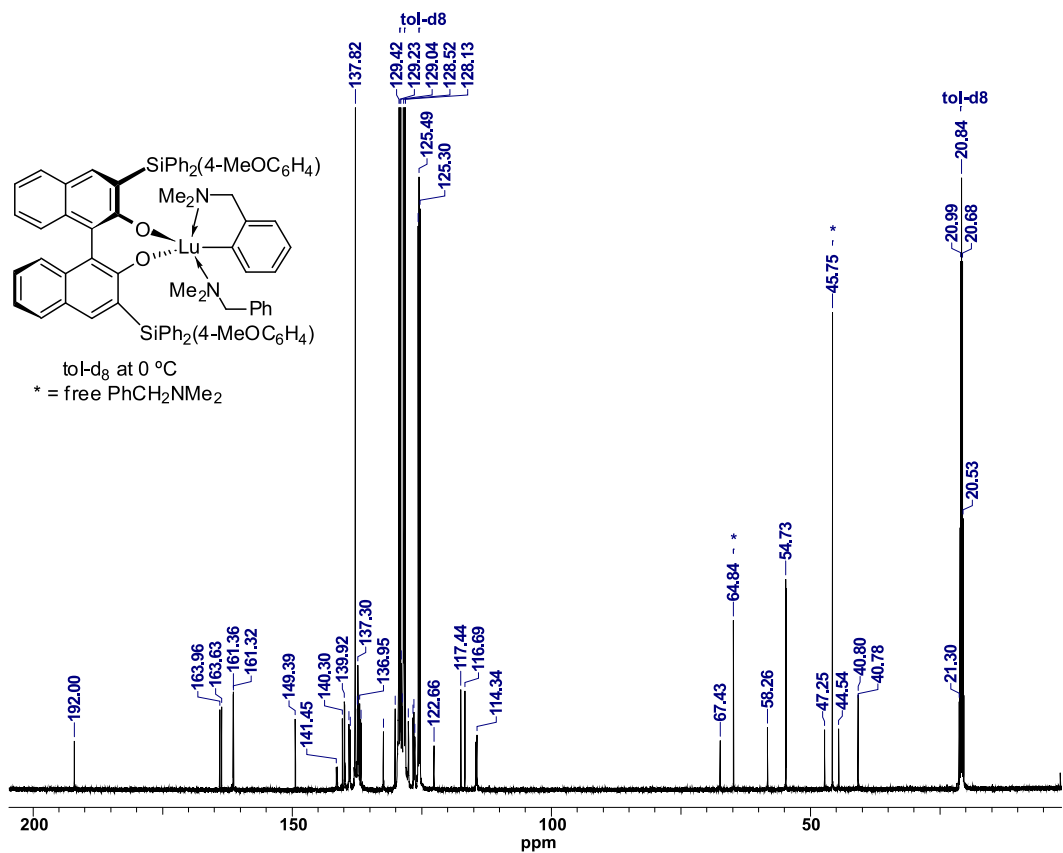
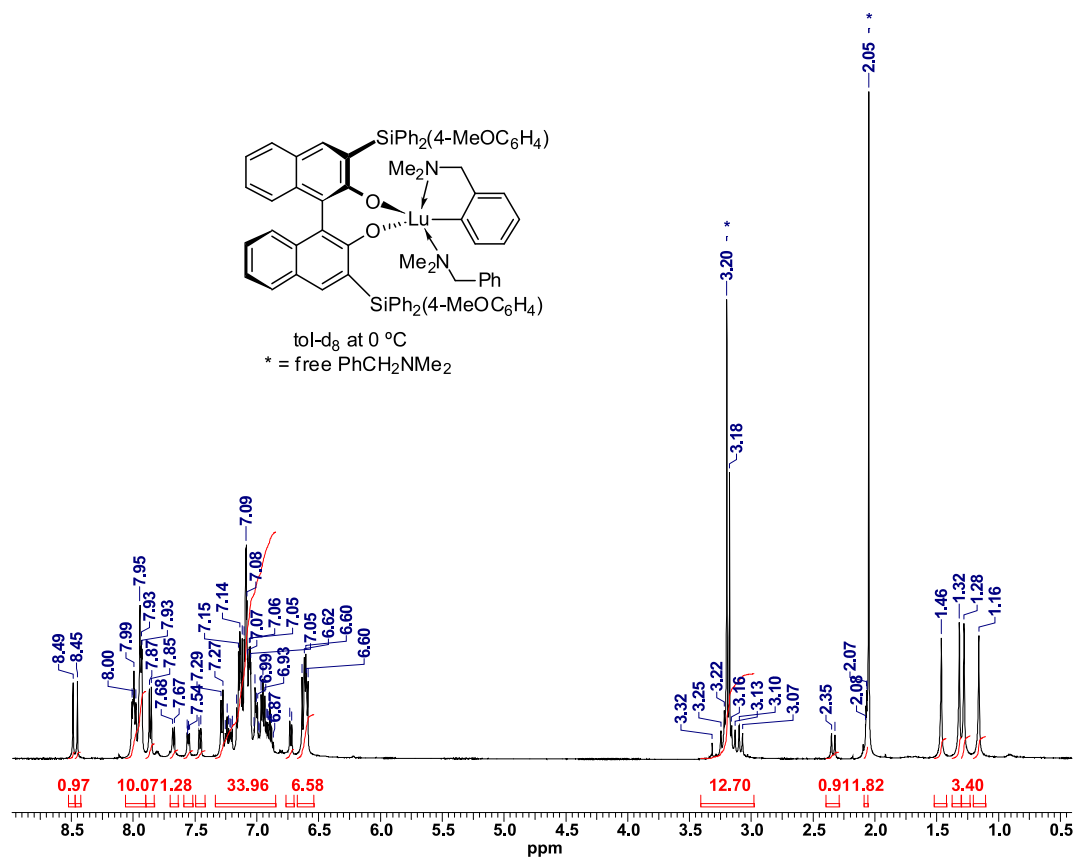


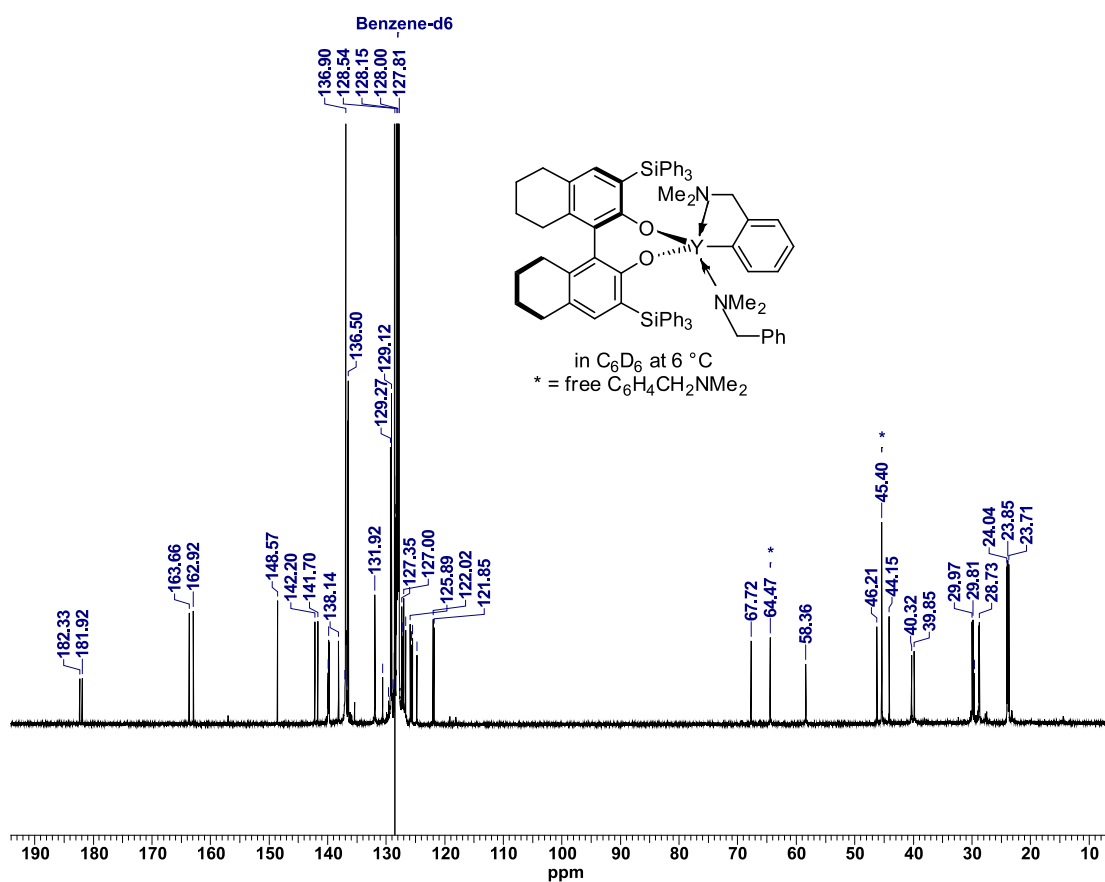
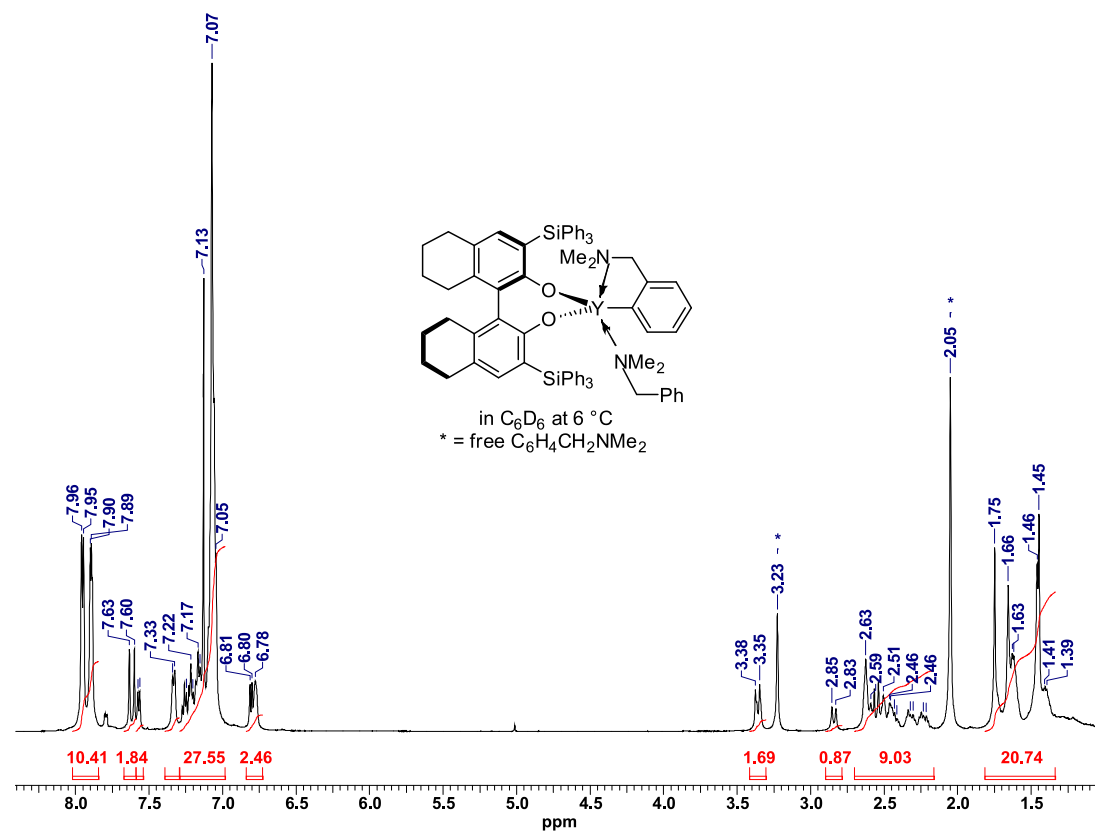


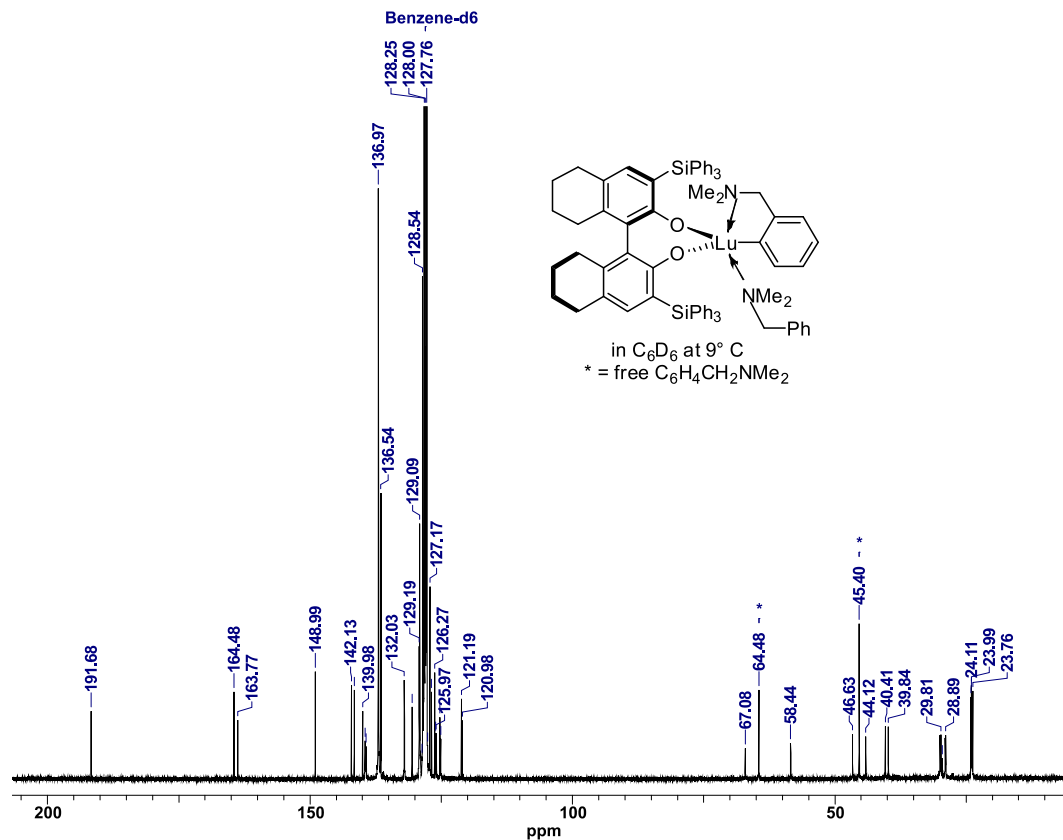
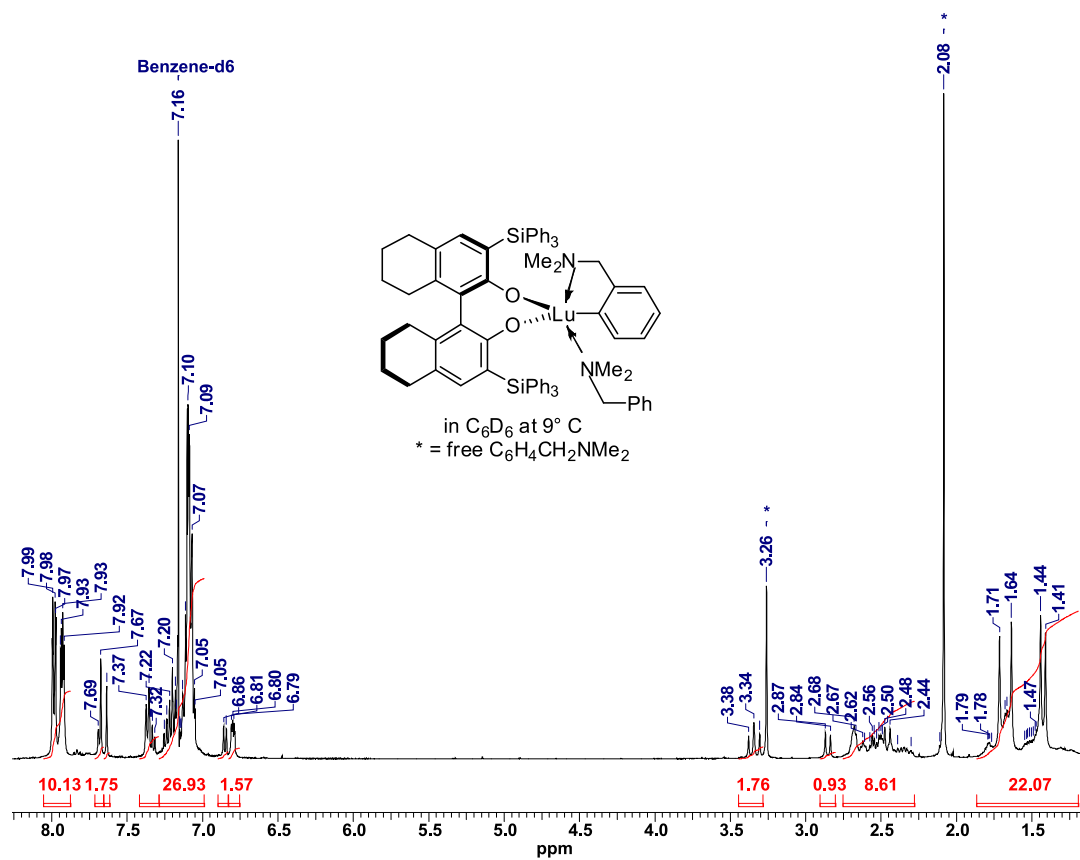


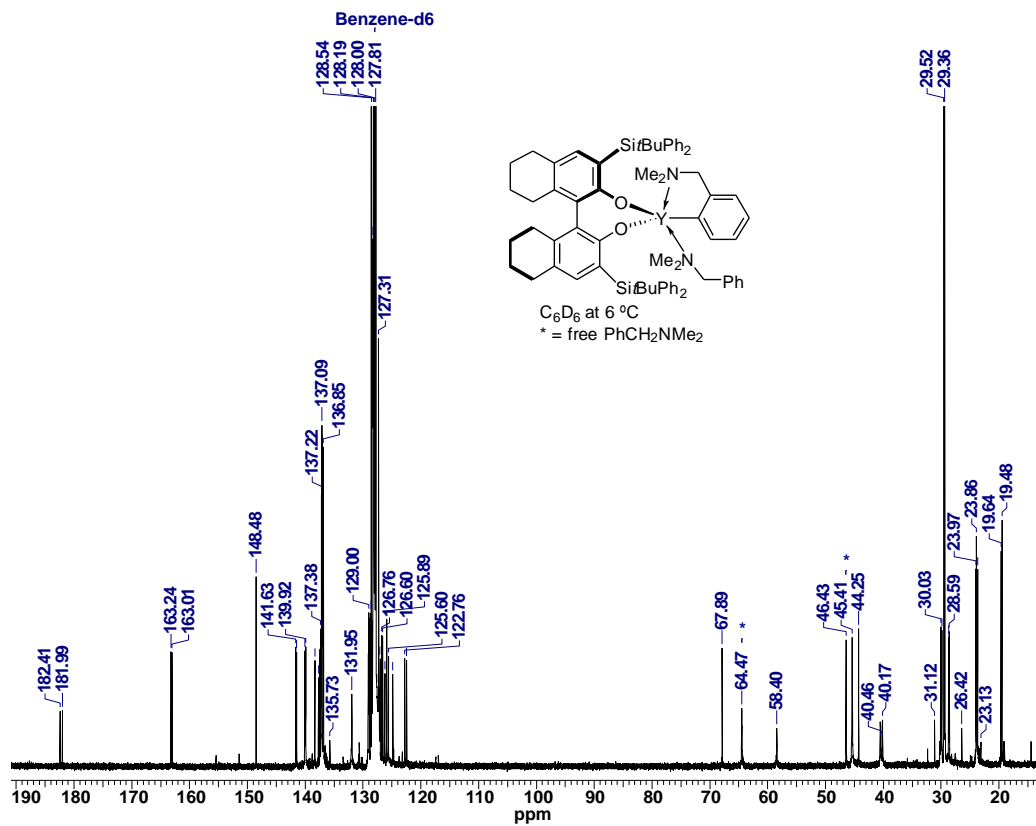
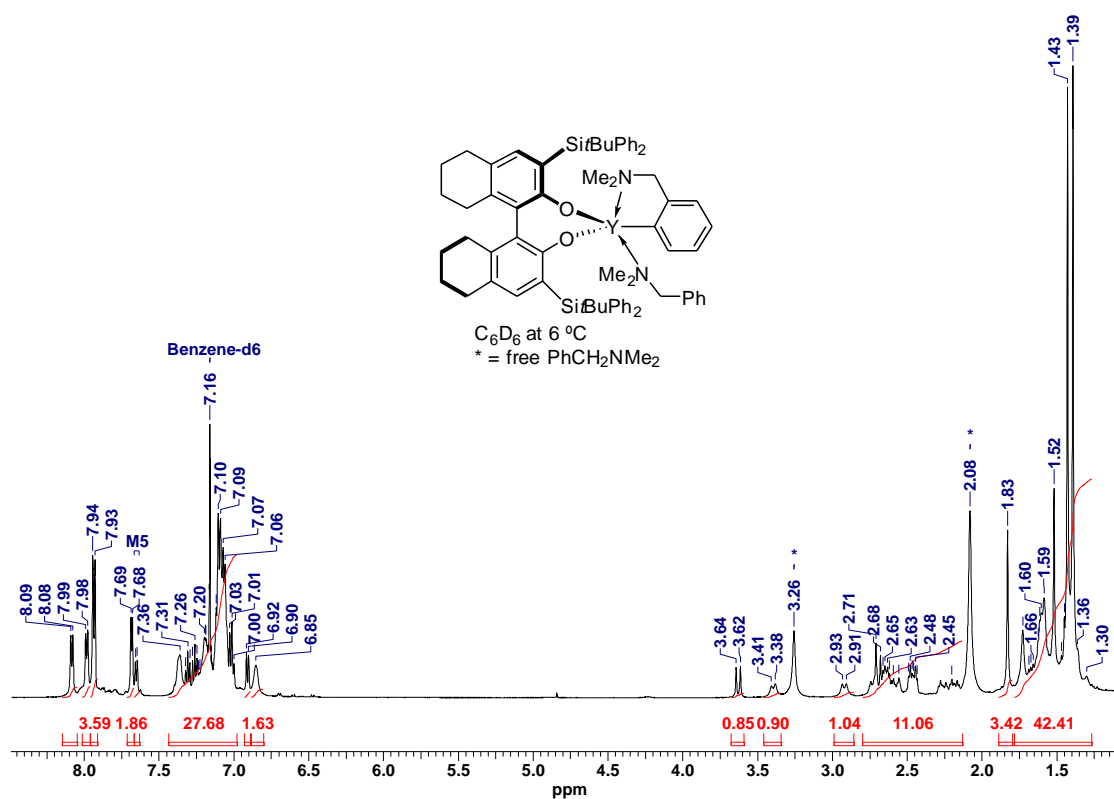


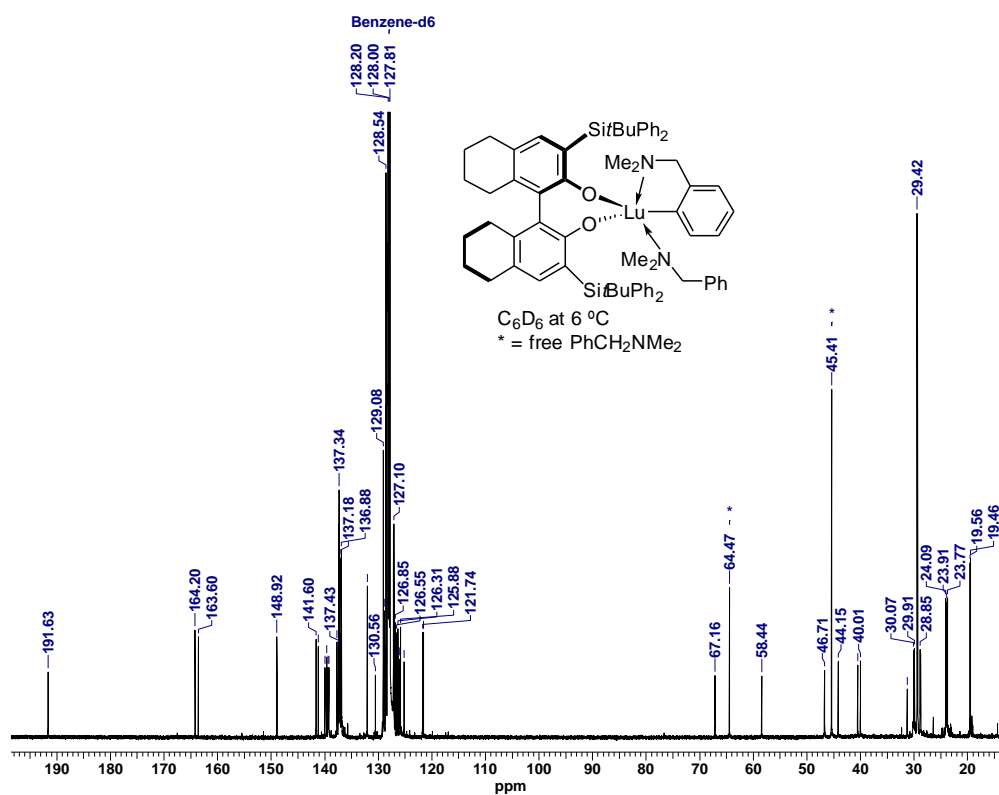
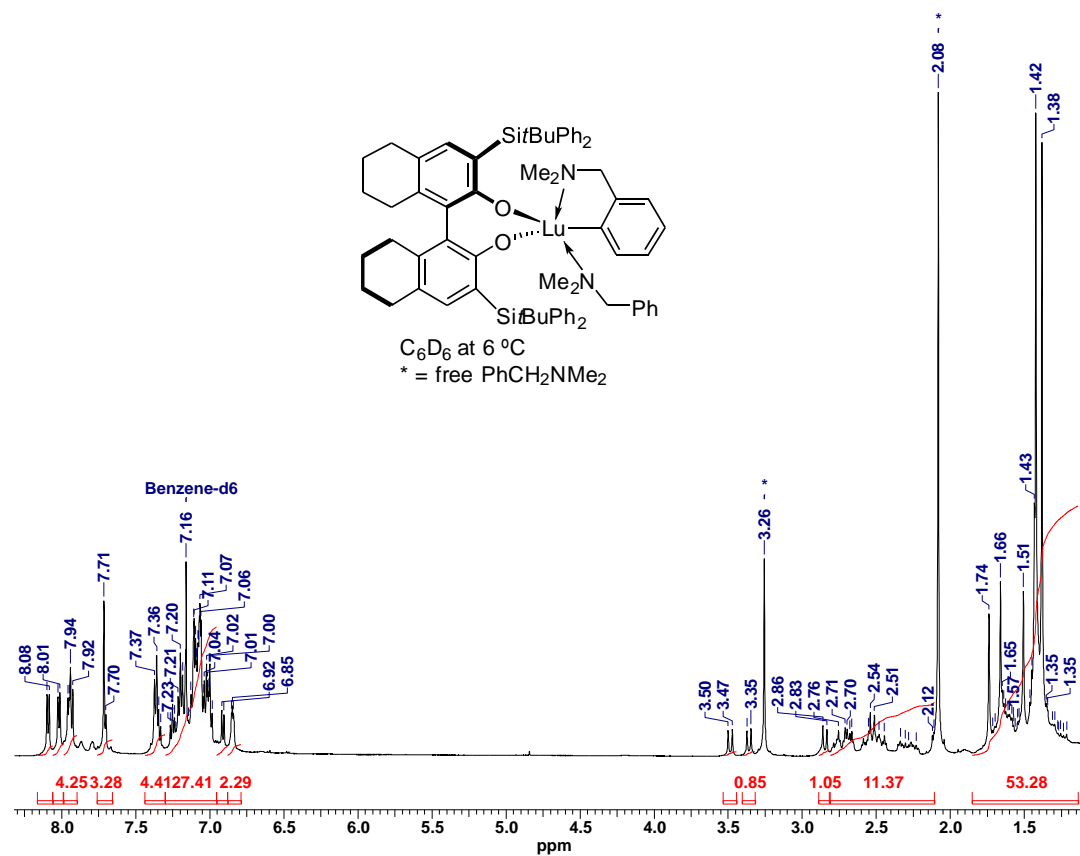


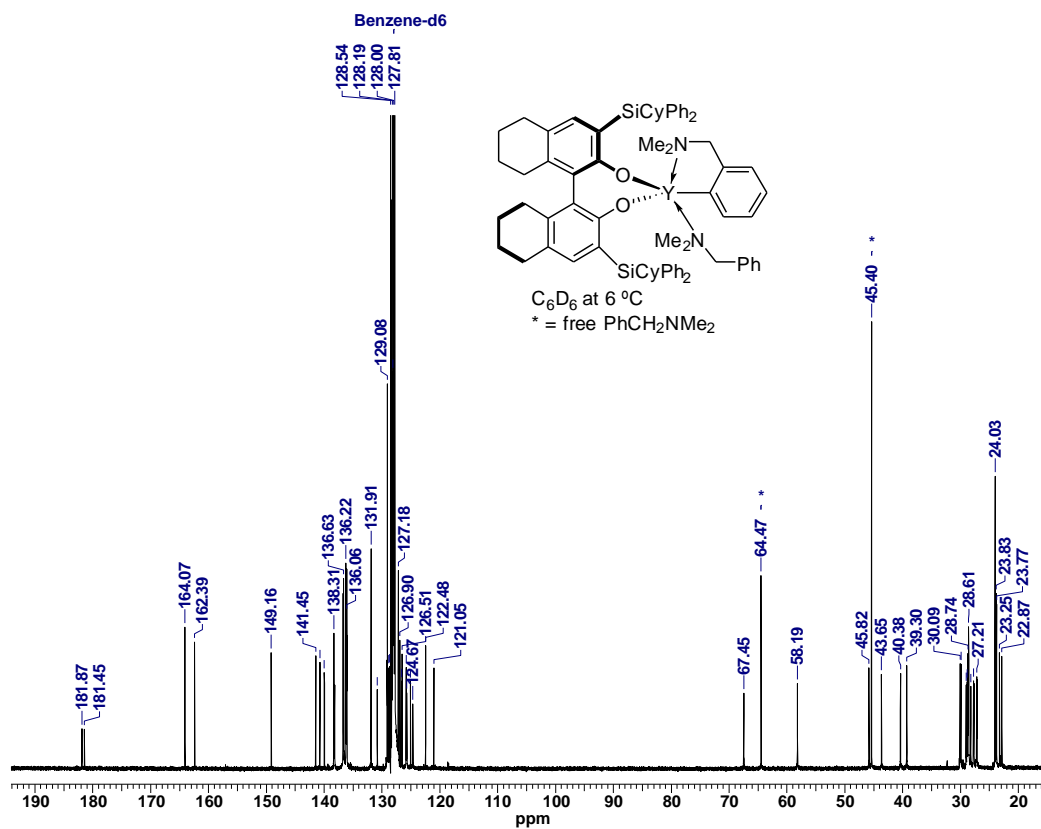
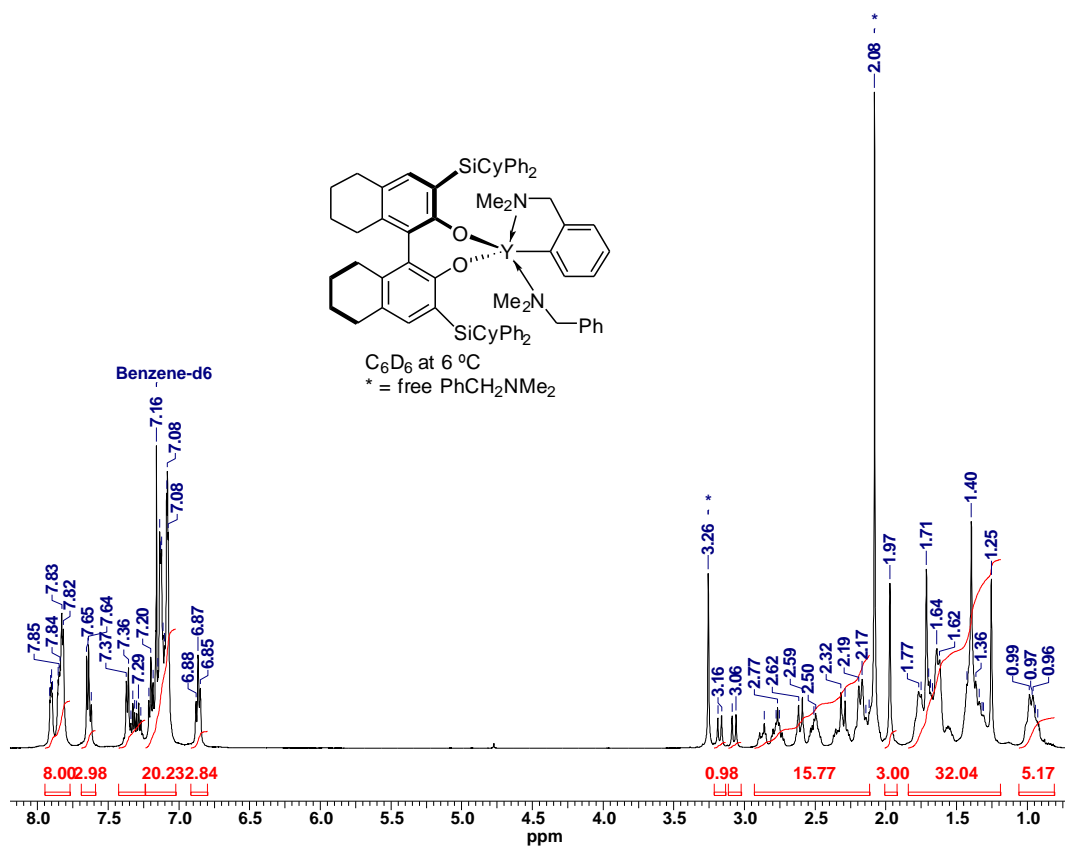


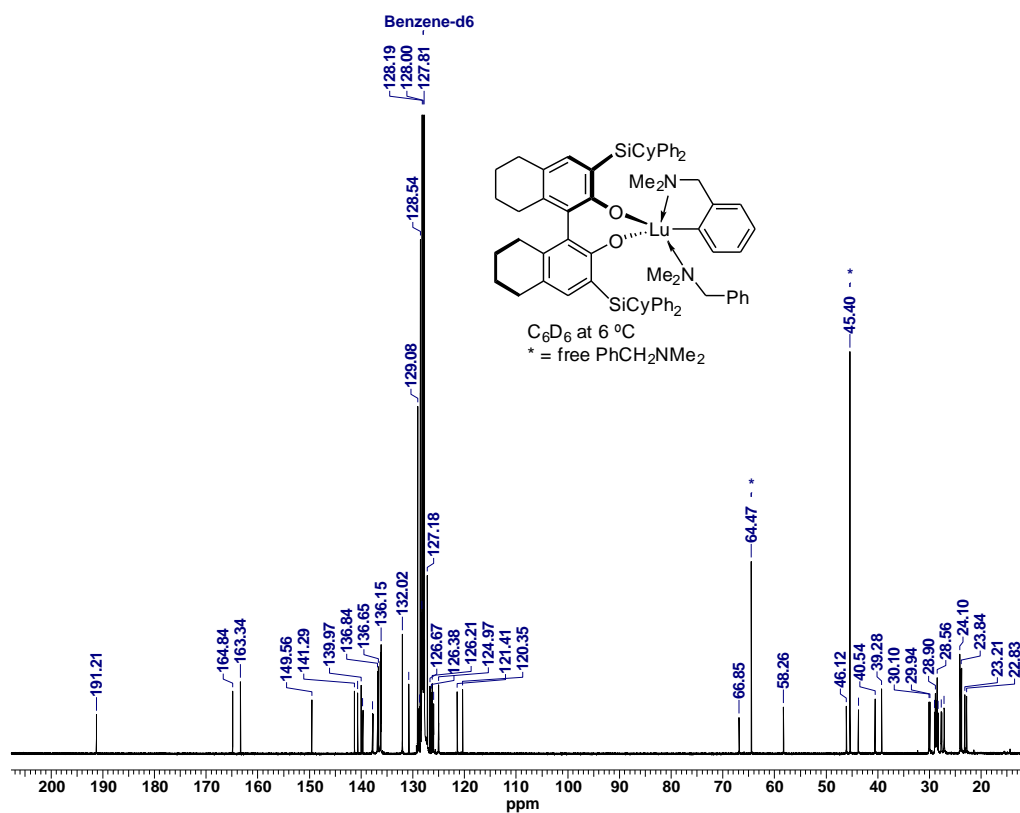
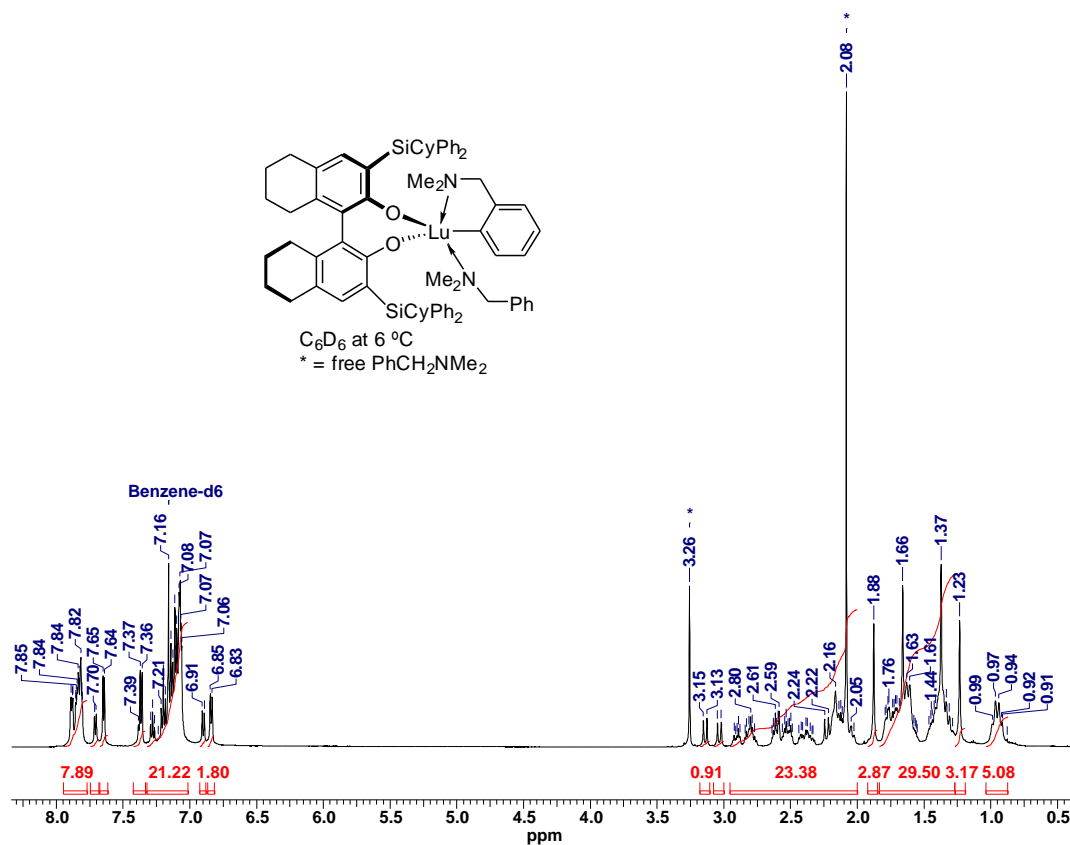


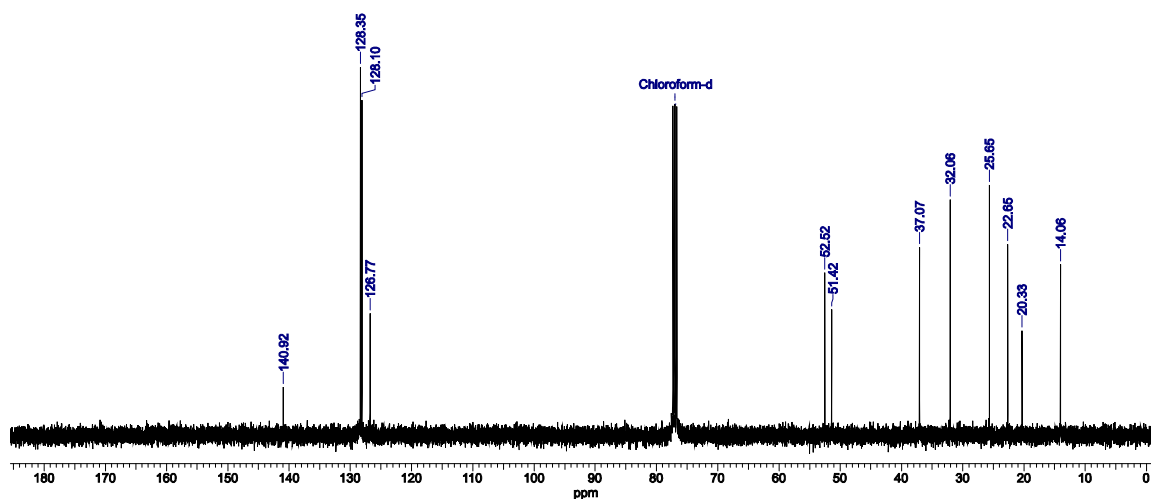
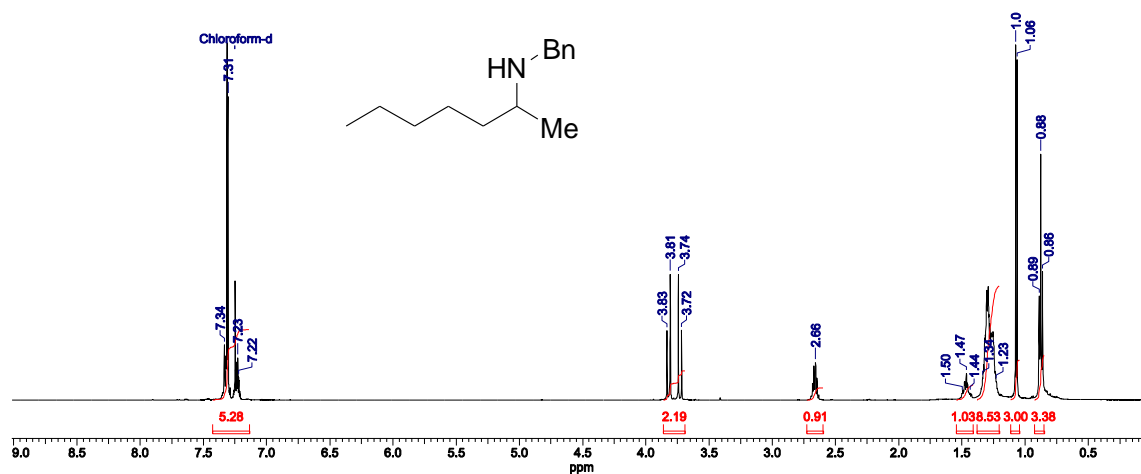


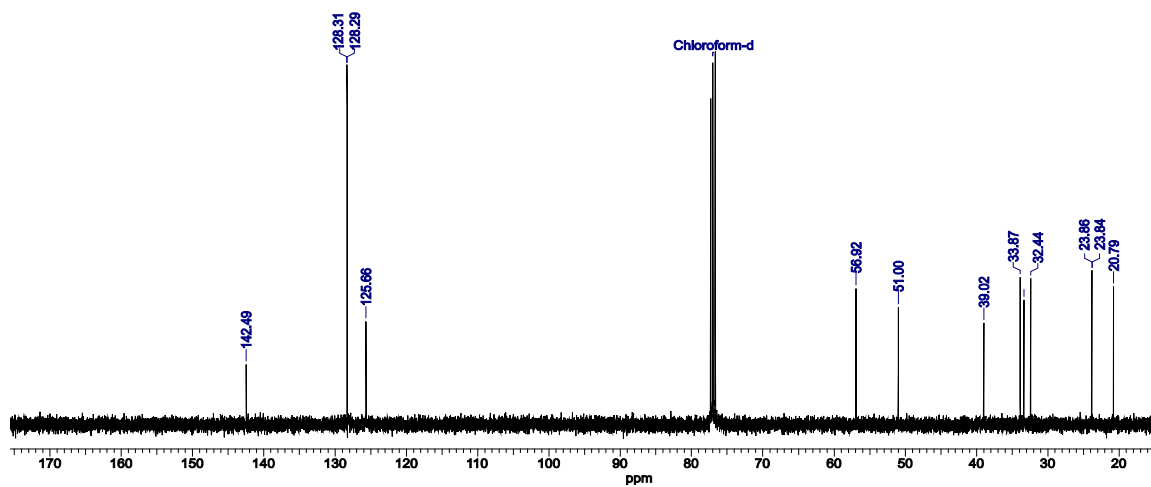
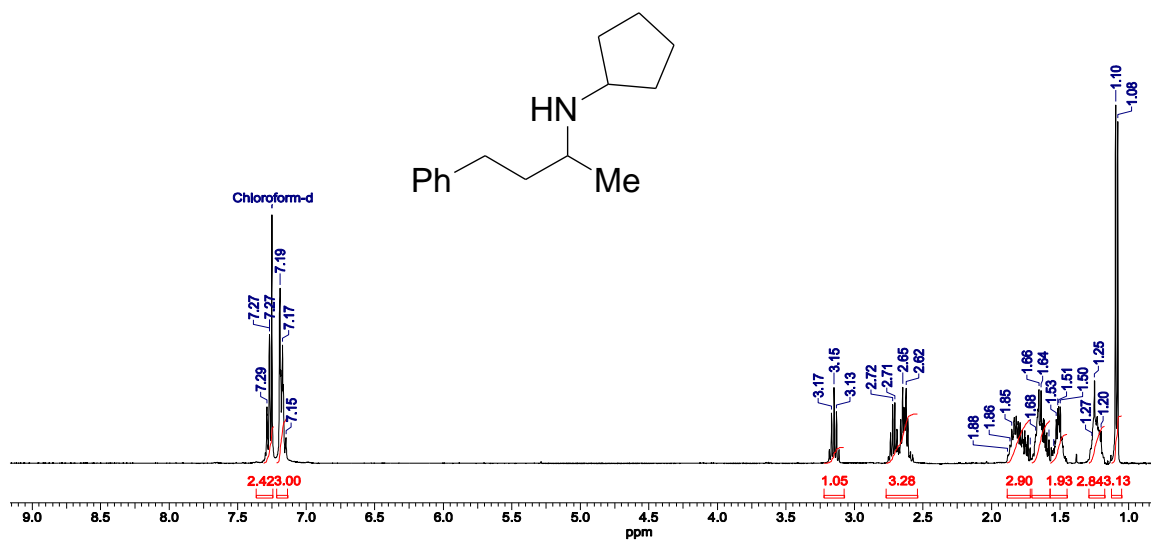


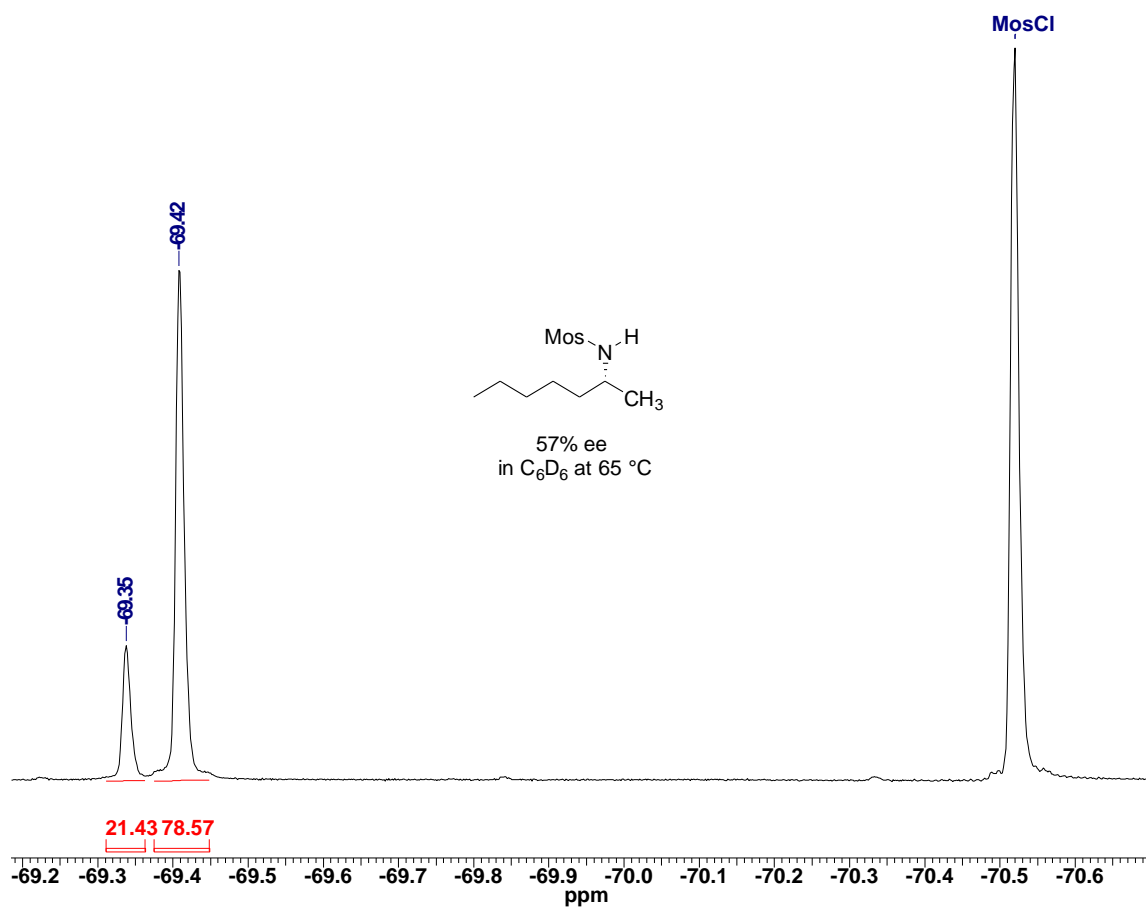
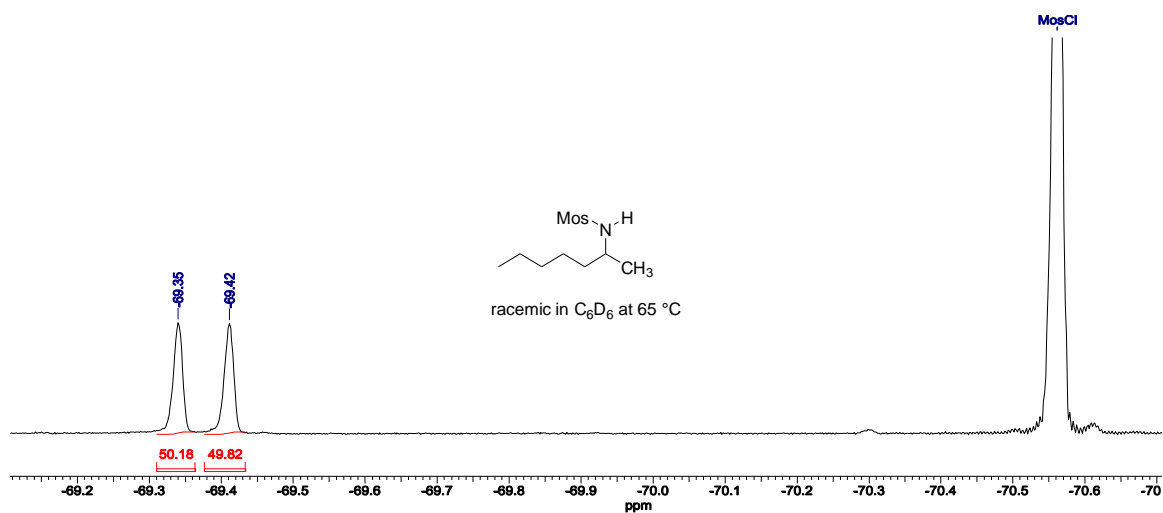


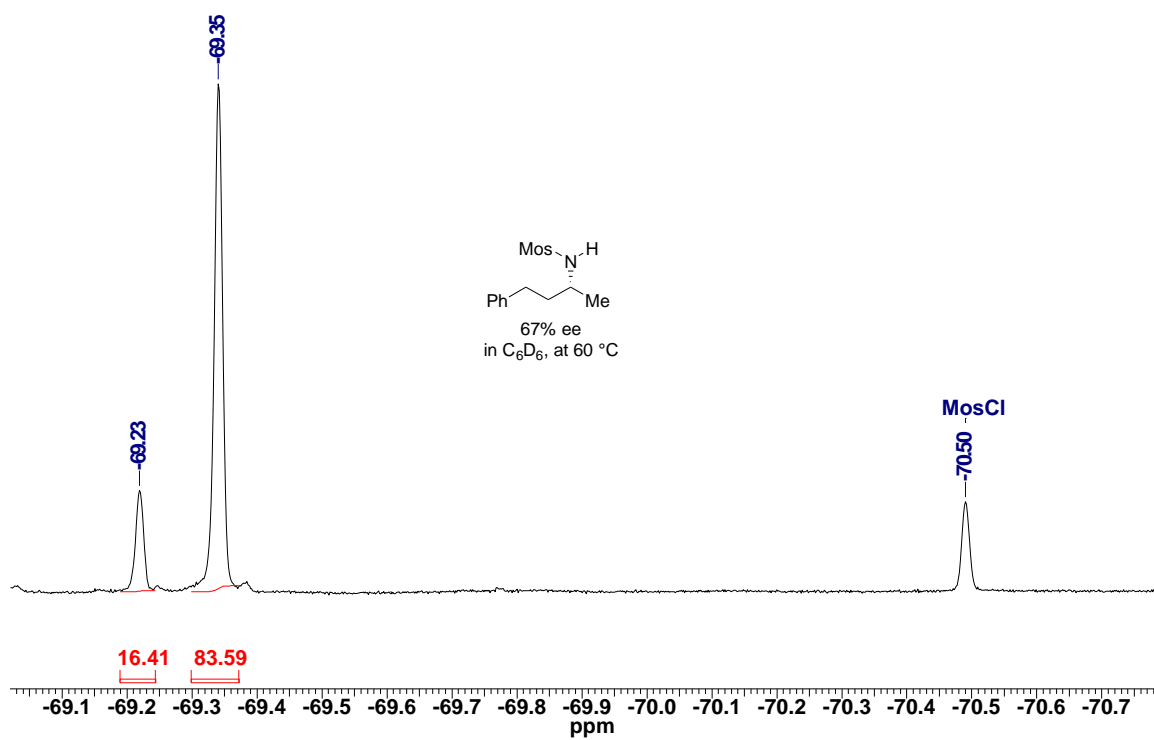
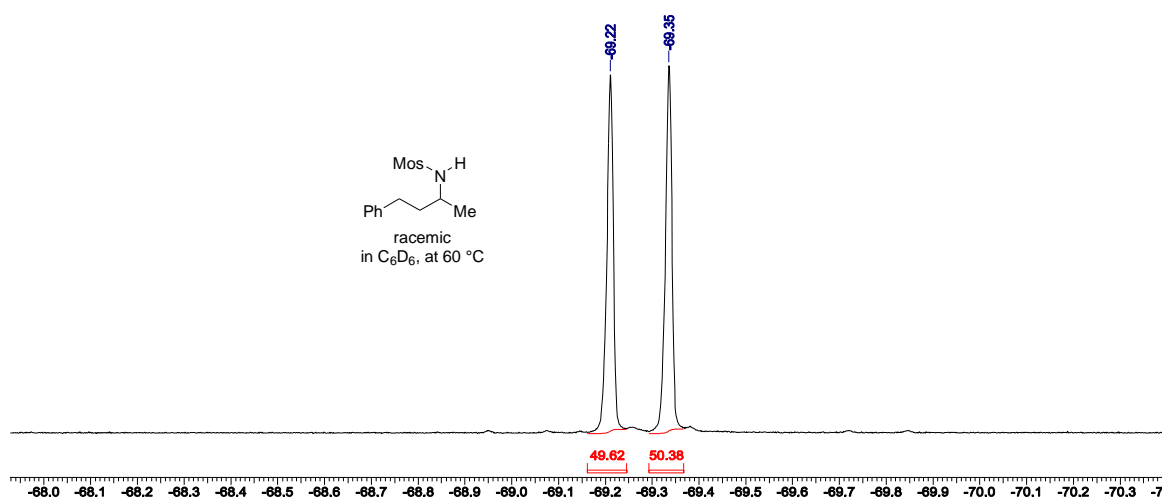


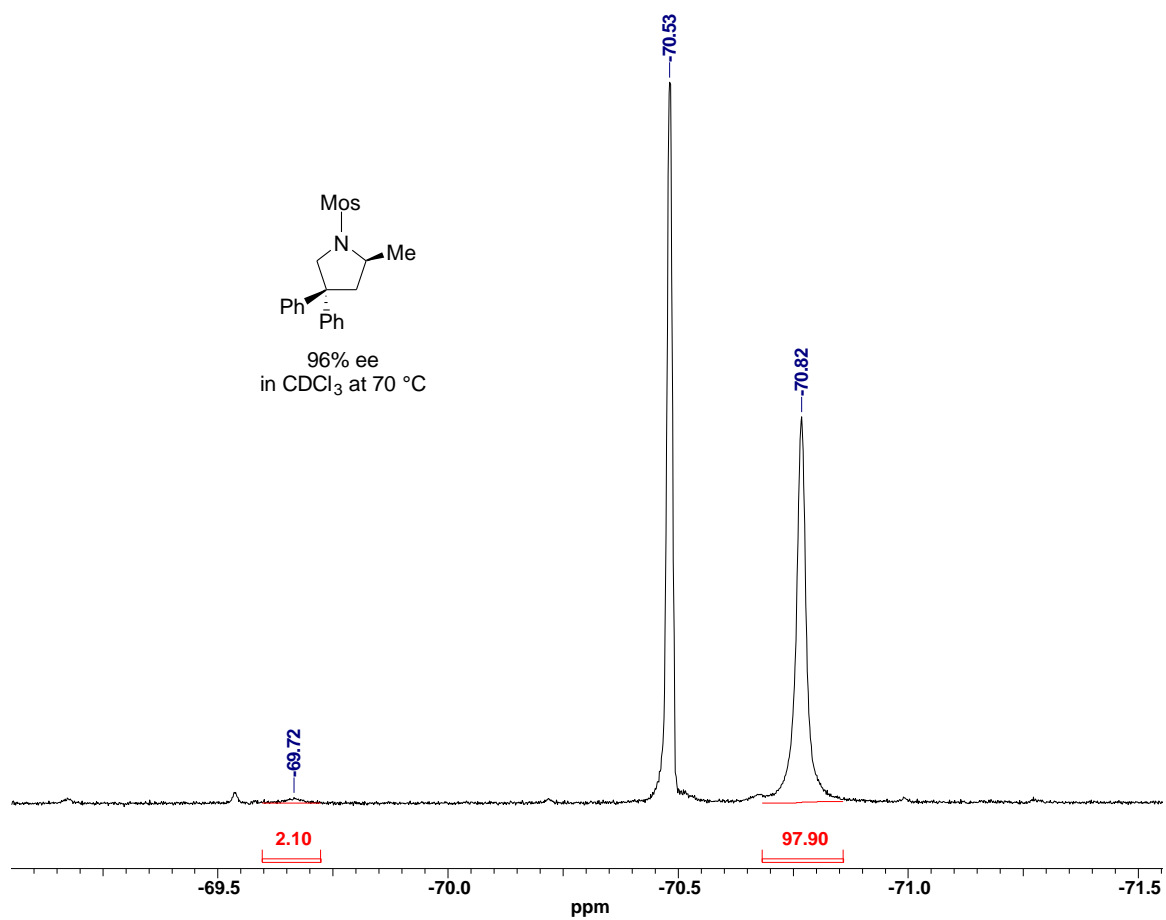
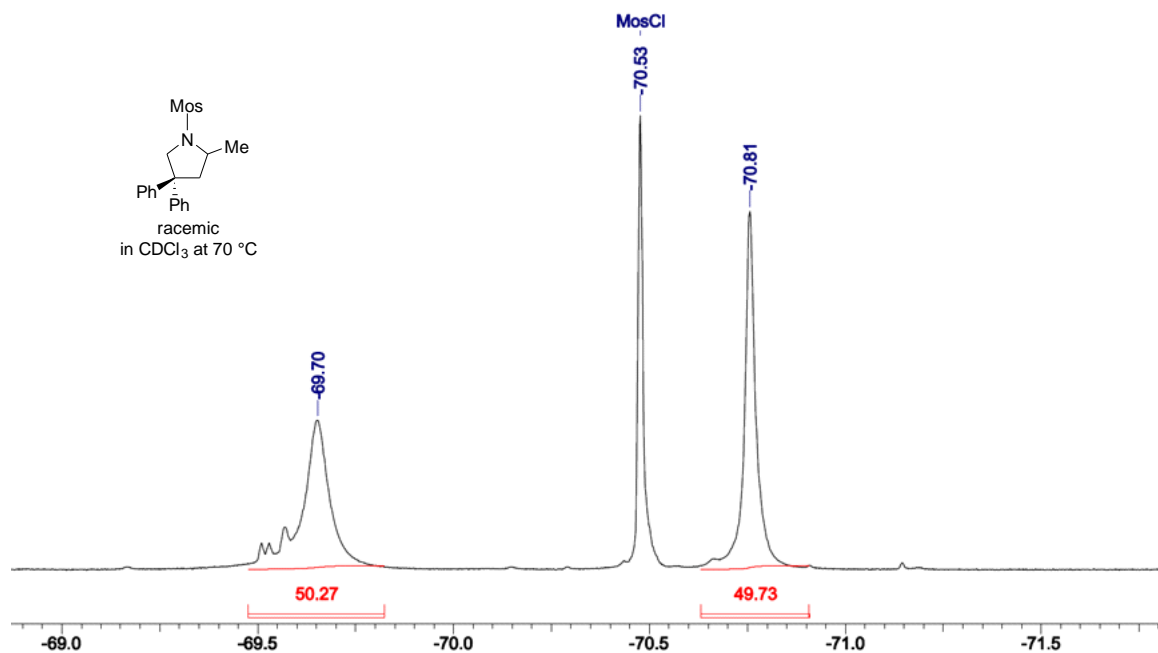


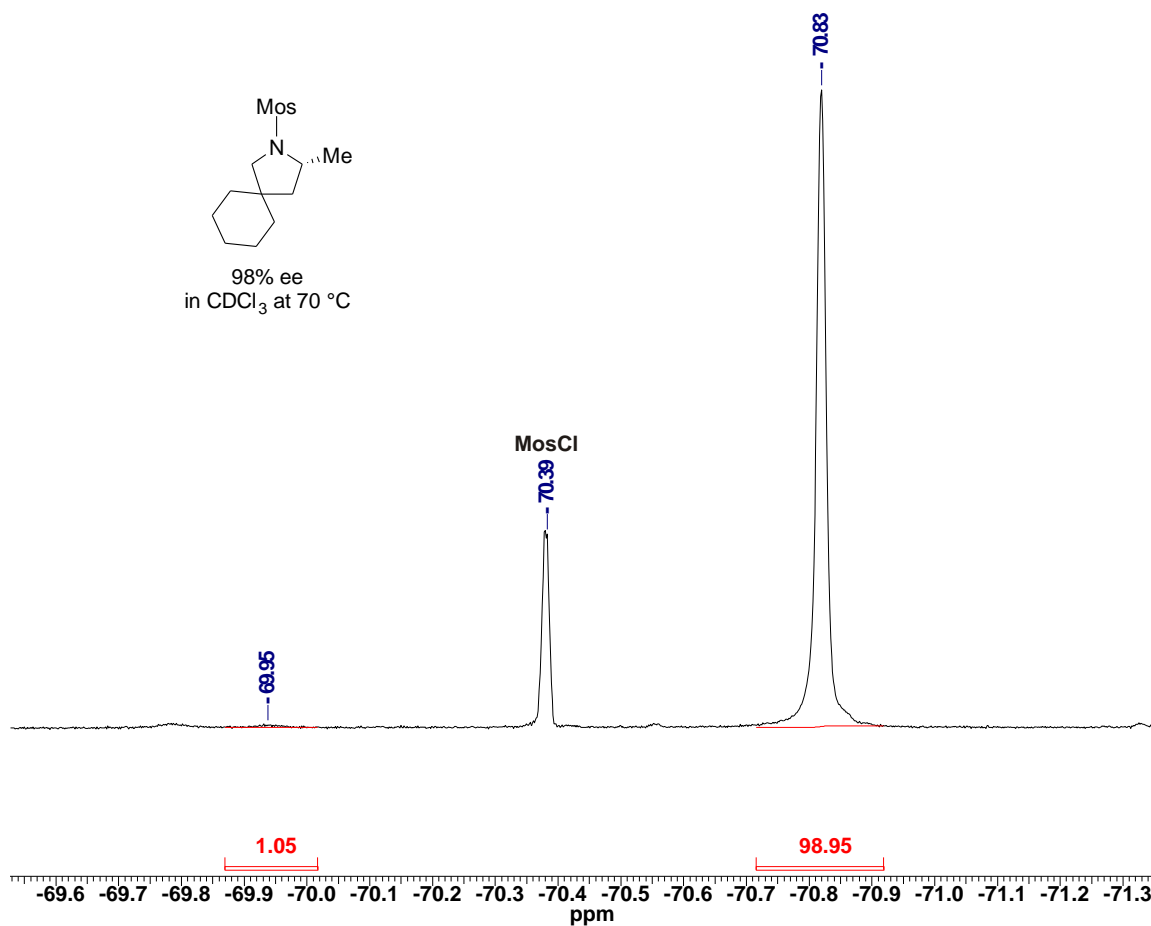
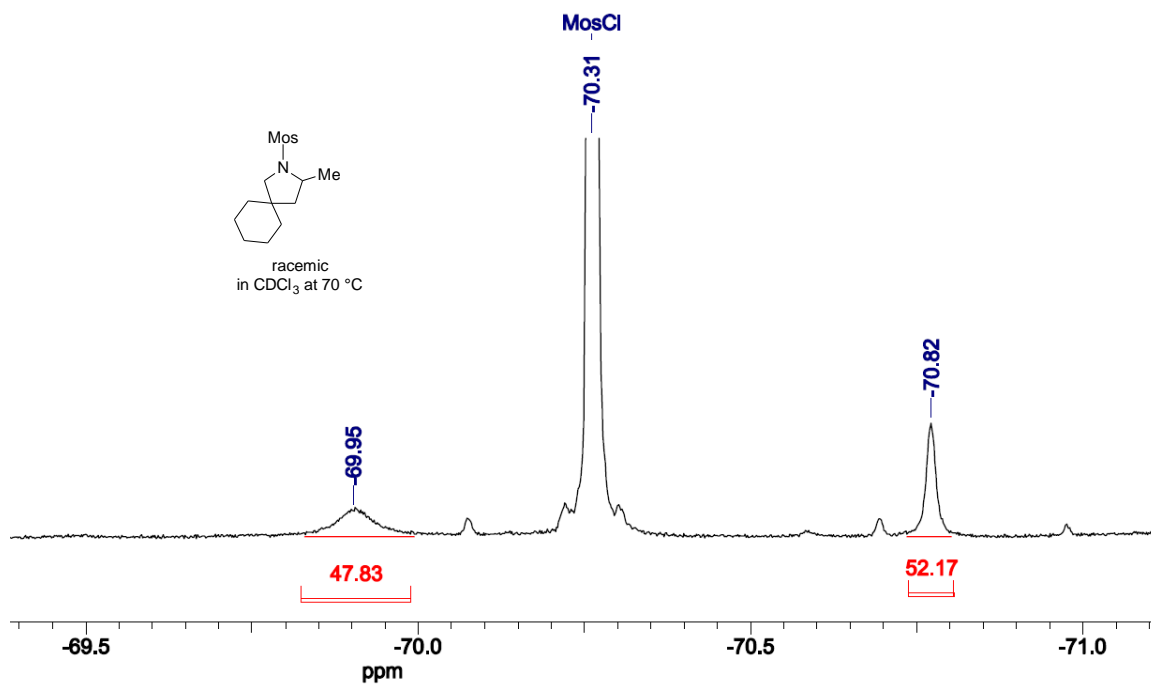


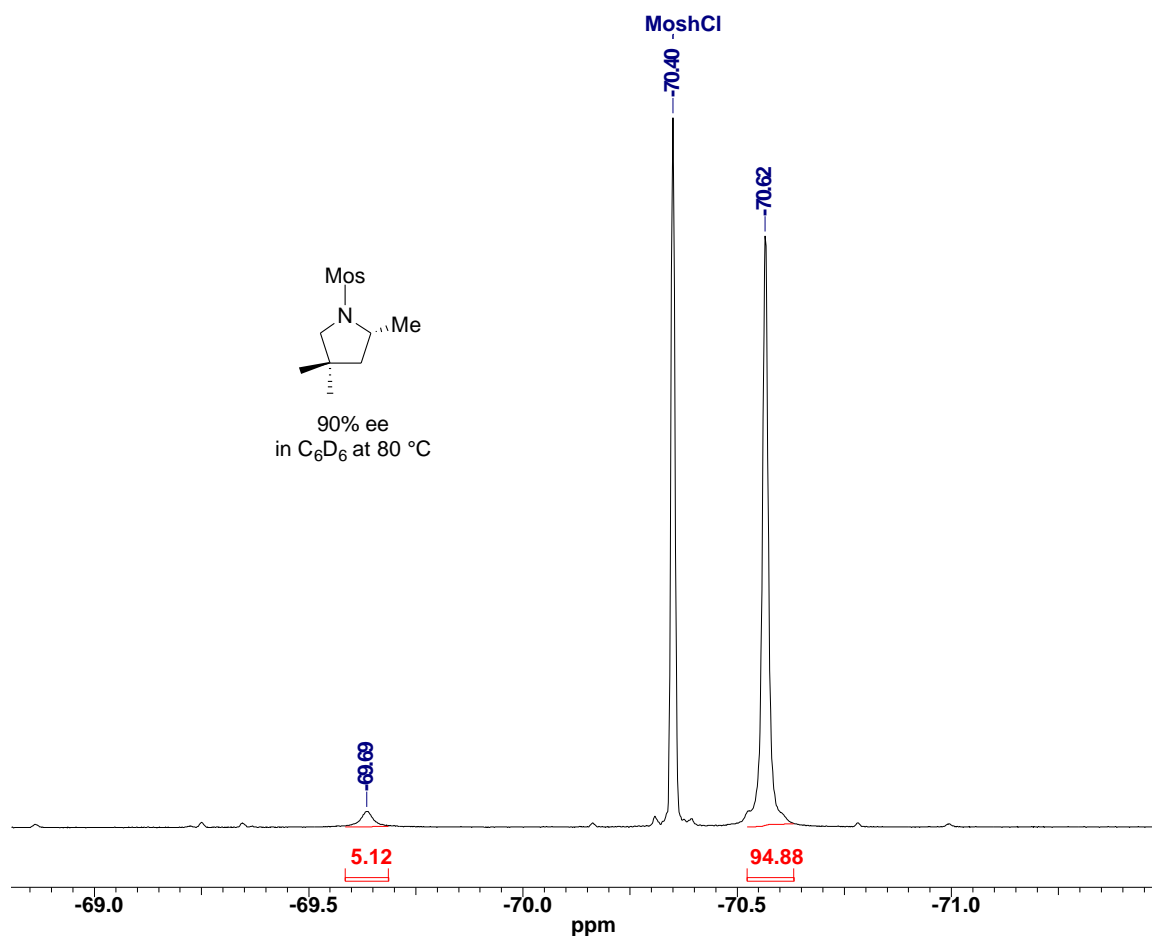


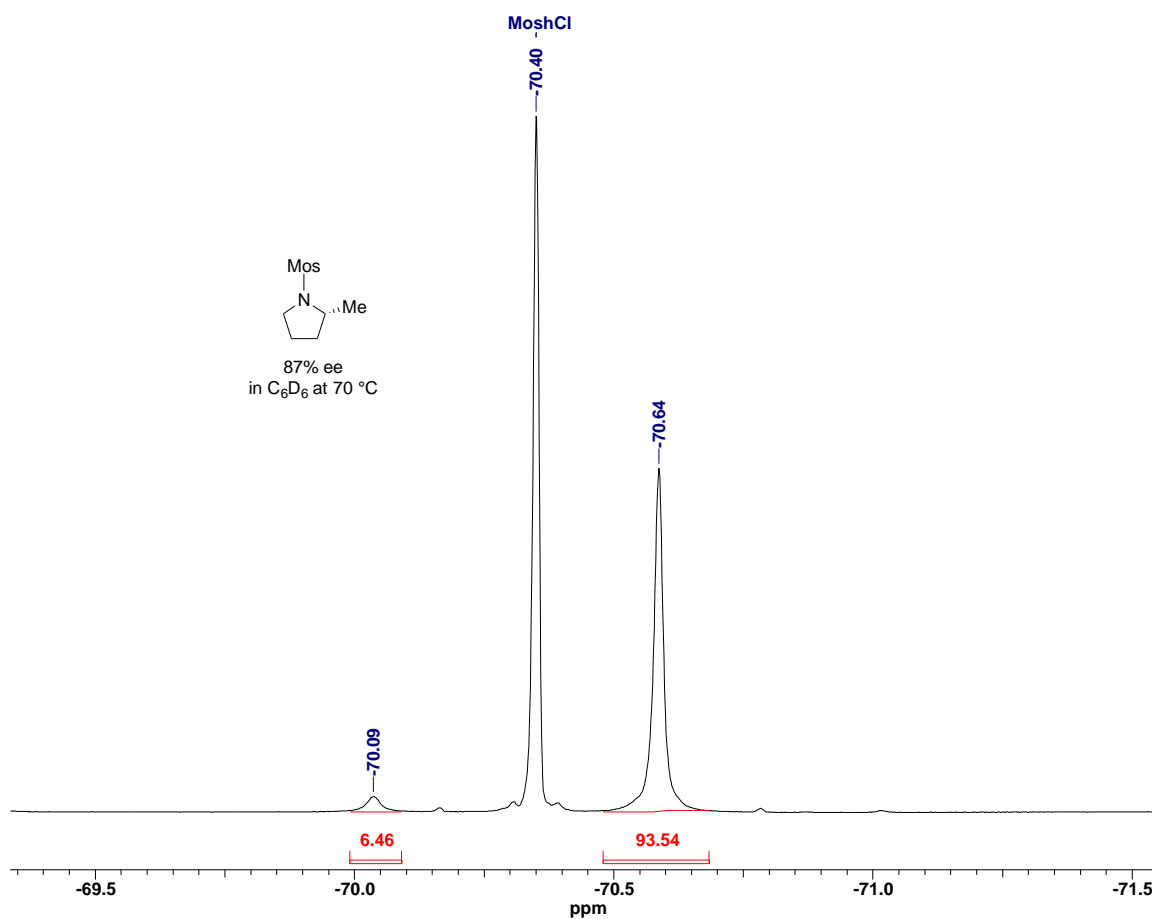
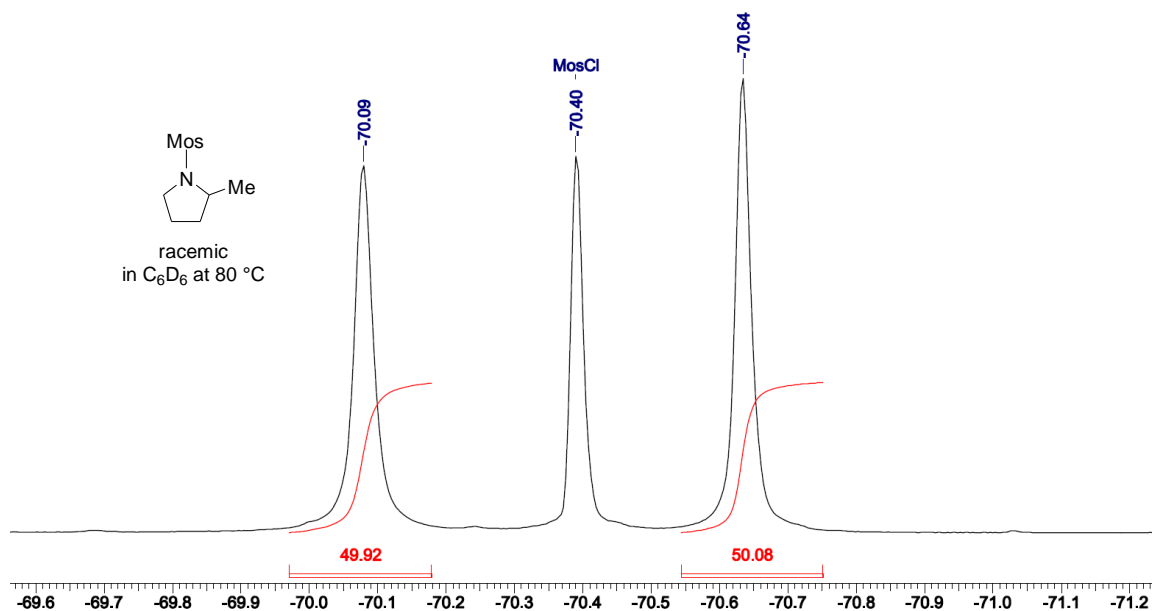


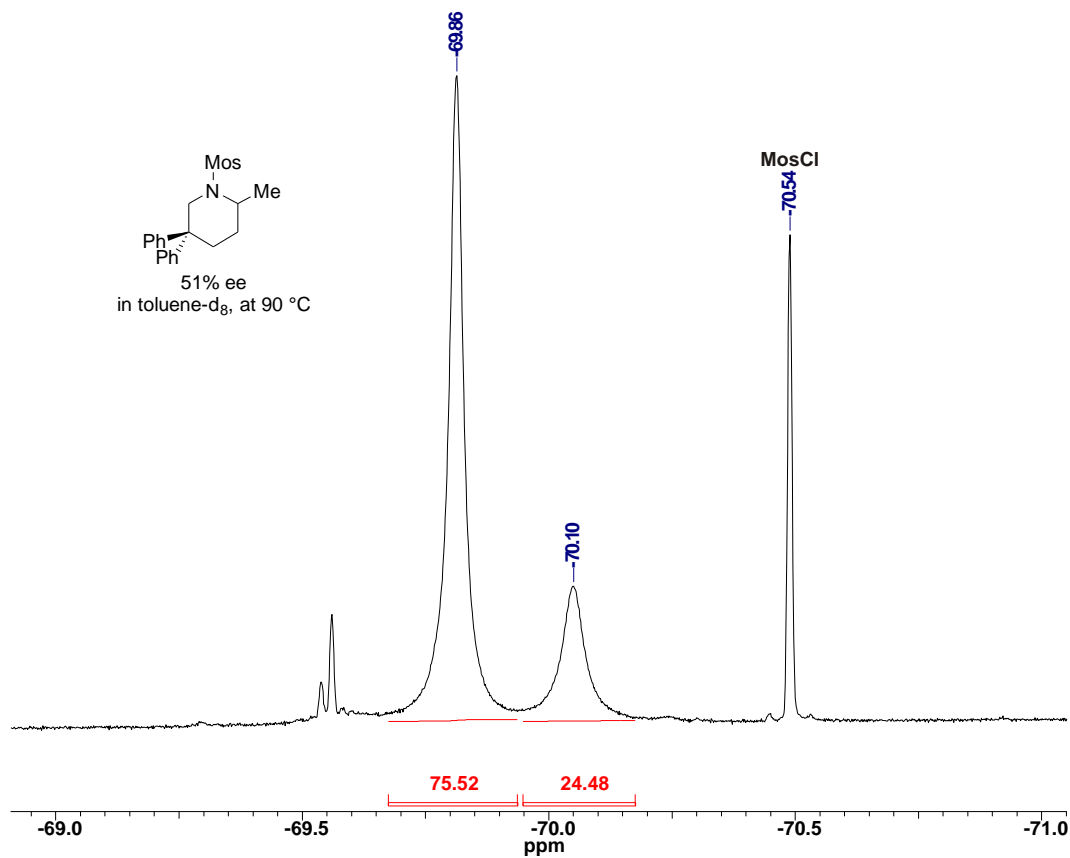
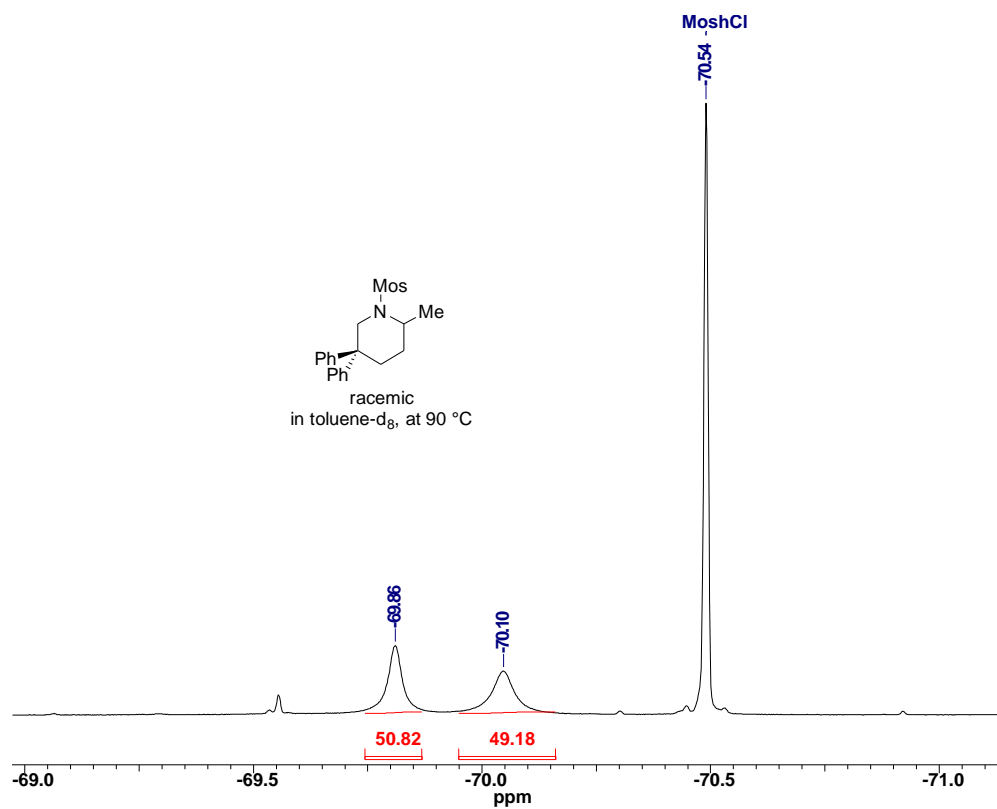


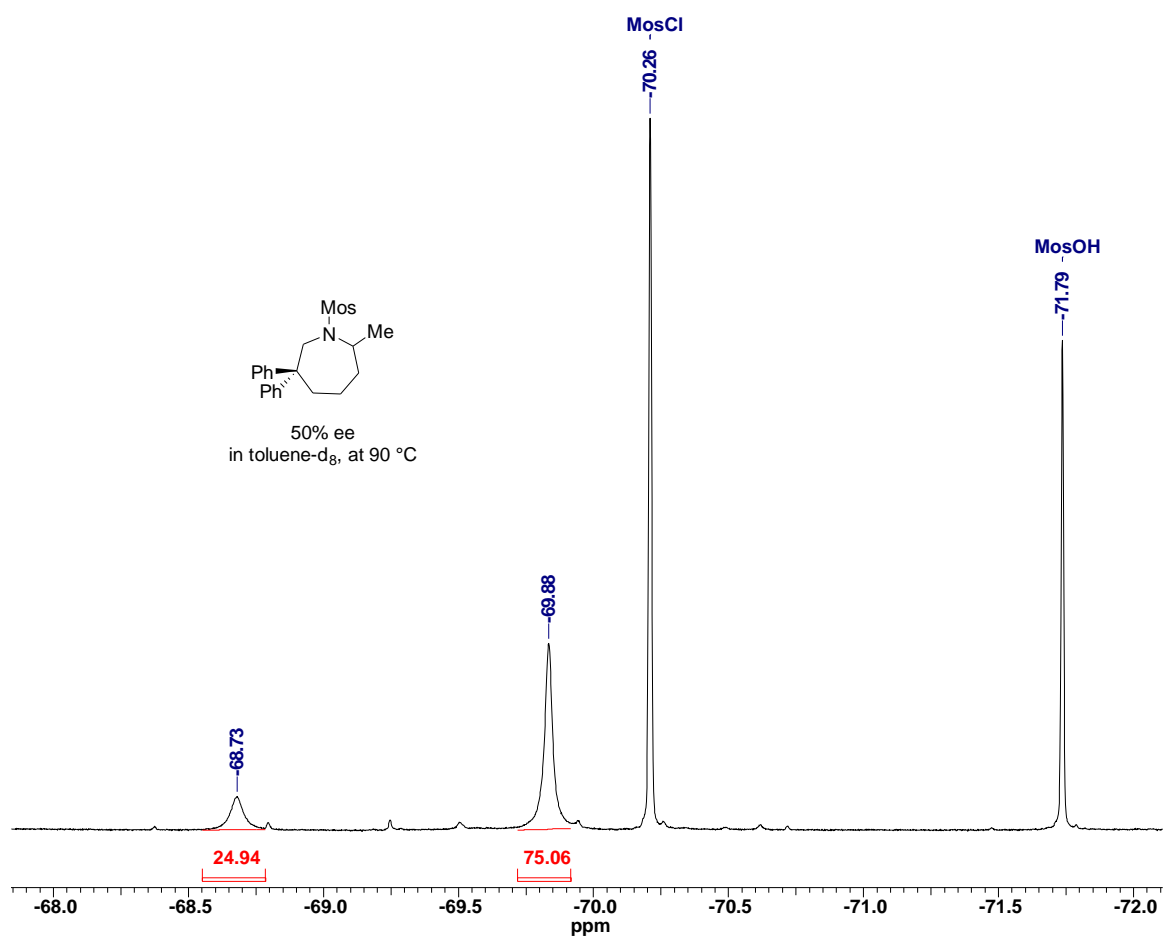
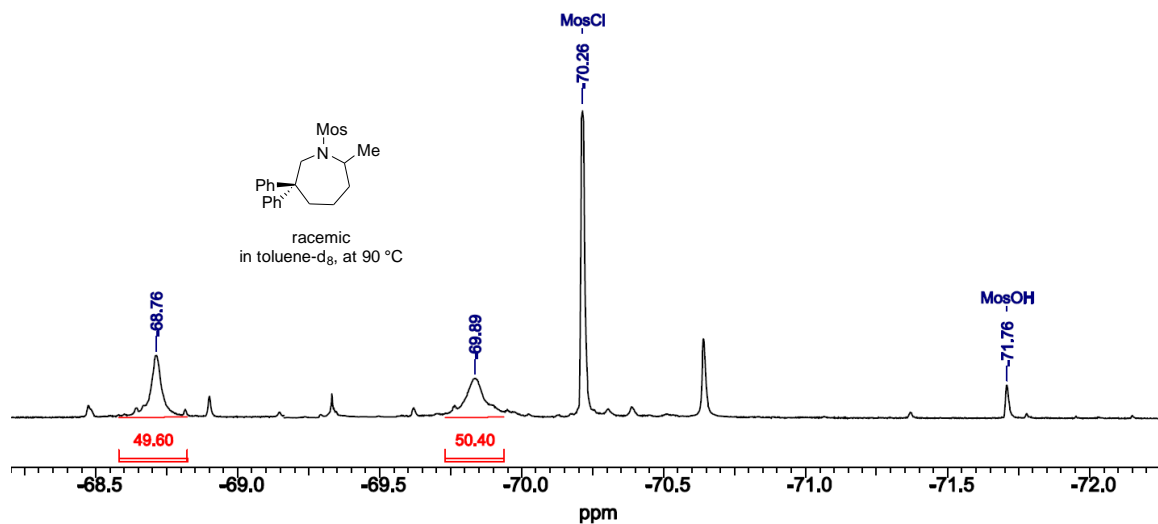


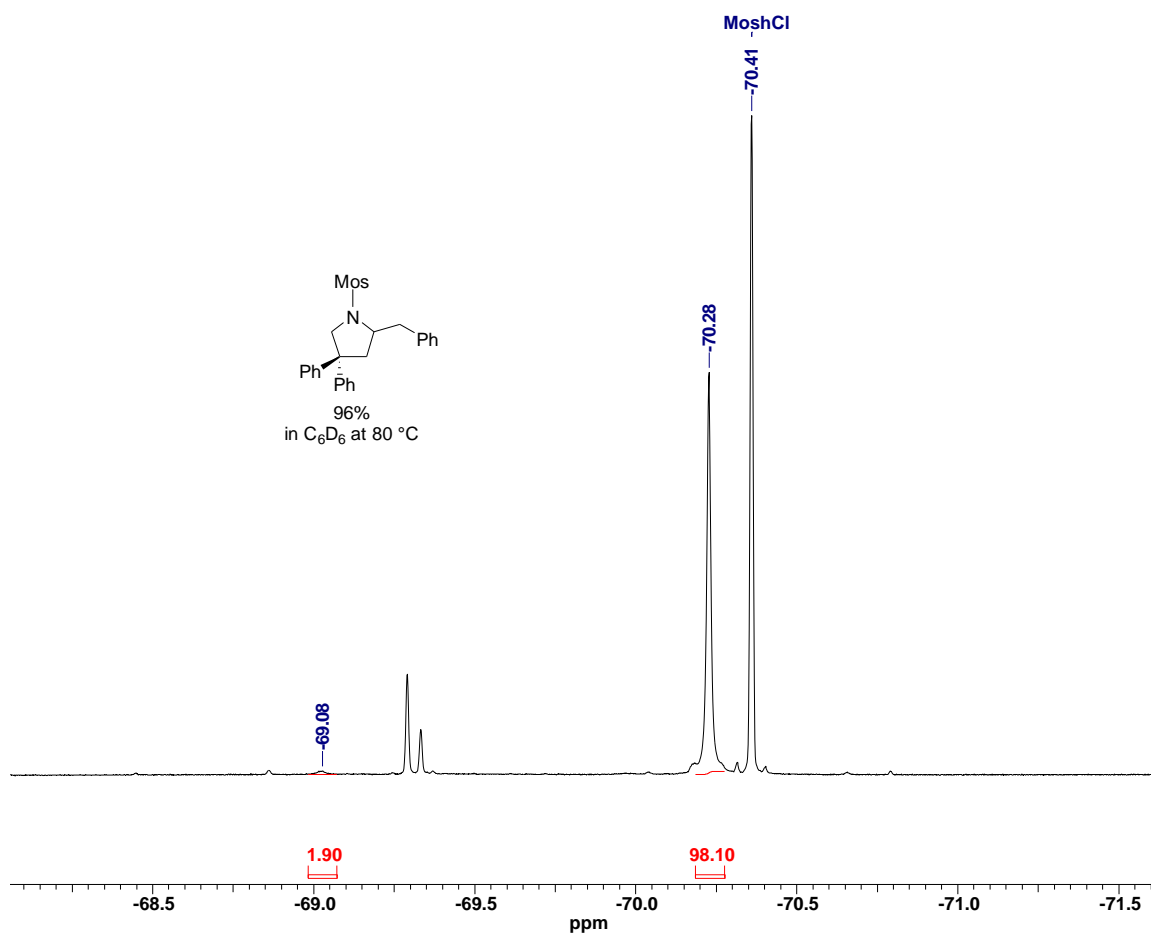
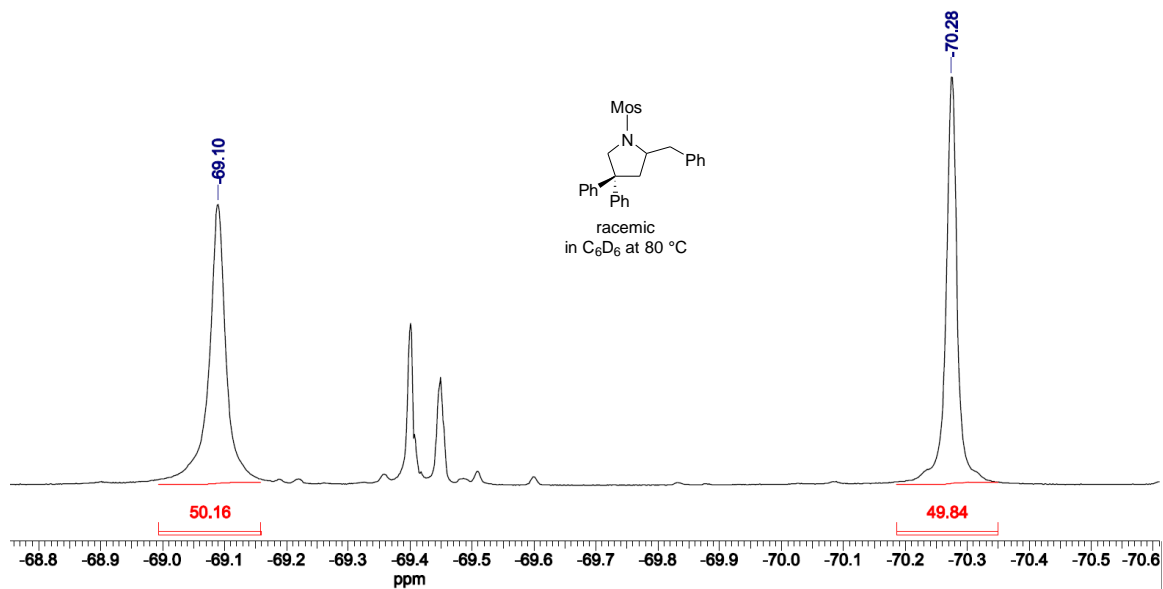






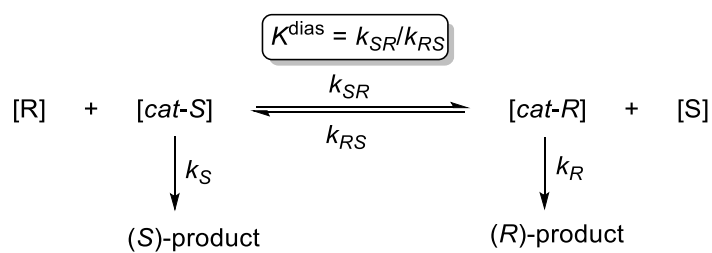






Appendix B: Kinetic Resolution of Aminoalkenes

A Diagram of Kinetic Resolution



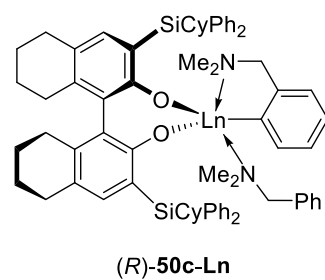
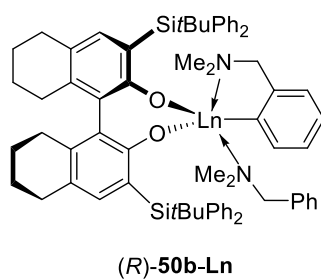
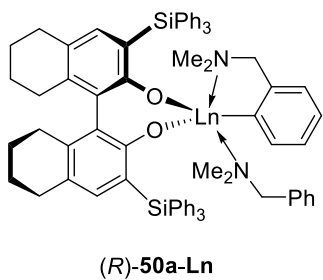
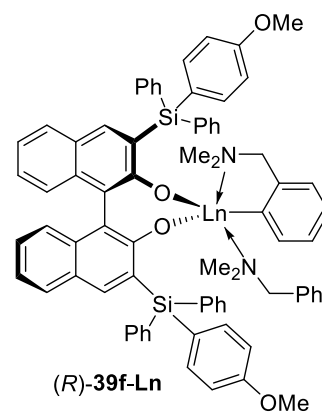
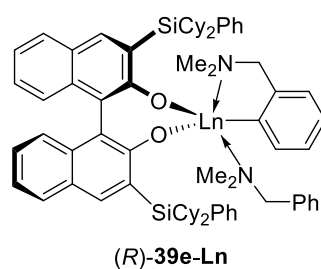
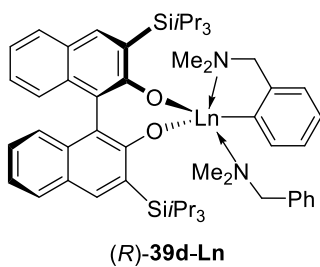
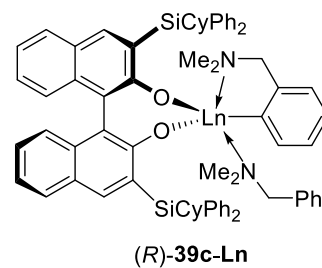
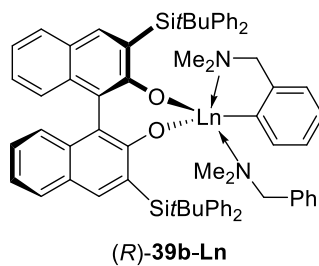
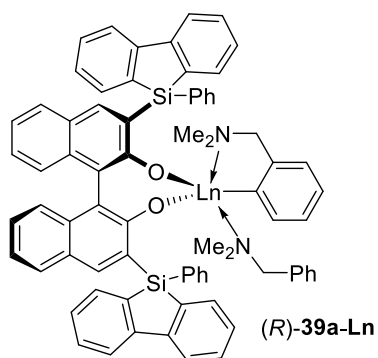
Enantiomeric Excess of Recovered **25a in the Kinetic Resolution using (*R*)-**39c-Y** at 25 °C**

Conversion (%)	% ee of Recovered 25a
7.6	8.0
14.3	16.2
29.1	39.7
38.7	60.4
48.5	88.1
50.3	93.6

Rates Constants for Hydroamination/Cyclization of α -Substituted Aminopentenes using the Binaphtholate Rare Earth Metal Catalysts

Substrate	T (°C)	Cat.	k_{fast} (10^{-3} s^{-1})	k_{slow} (10^{-3} s^{-1})
(S)-25b	25	39b-Y	2.32	0.217
	25	39c-Y	7.35	0.418
	30	39c-Y	10.01	0.744
	40	39c-Y	19.60	1.69
	50	39c-Y	47.24	3.34
	25	39e-Y	3.09	0.343
(S)-25b	40	39b-Y	3.26	0.435
	40	39c-Y	5.38	0.512
	40	39e-Y	2.63	0.540
(S)-25c	70	39b-Y	5.43	0.484
	60	39c-Y	3.76	0.237
	70	39c-Y	6.90	0.459
	70	39e-Y	4.06	0.661
(S)-25d	25	39b-Y	4.47	1.19
	25	39c-Y	3.12	0.797
	25	39e-Y	1.93	1.10

Appendix C: Structures of Binaphtholate and Octahydrobinaphtholate Rare Earth Metal Complexes



Appendix D: Substrates and Hydroamination Products

